The Development of an in vitro 3D Histotypic Model of The Human Eccrine Sweat Gland.

Robles-Munoz, Viviana D

The Development of an in vitro 3D Histotypic Model of The Human Eccrine Sweat Gland

A thesis submitted in accordance with regulations for the degree of PhD

September 2014

Viviana D. Robles-Munoz

Centre for Cutaneous Research

Barts and The London School of Medicine and Dentistry

Queen Mary University

Declaration of Originality of This Research

I hereby declare that the work presented in this thesis is entirely my own.

Viviana D. Robles-Munoz

Abstract

The human eccrine sweat gland is present on most body sites and is crucial for thermoregulation. Yet, little is known on the mechanisms that govern its function and its morphogenesis. The main reason for the lack in research with regards to the human eccrine gland is the difficulty in isolation and maintenance of the glands and cells in vitro. Only one other cell line derived from the human eccrine gland has ever been reported, the NCL-SG3 cell line. NCL-SG3 cells do not however, function like native eccrine secretory coil cells, and thus a better cell model was required. In this project, a human eccrine secretory coil cell line, the EC23 cell line, was developed, along with 8 clones derived from said cell line. EC23 cells and their clones express a panel of markers characteristic of the human eccrine sweat gland secretory coil cells. Furthermore, calcium fluxes can be elicited by cholinergic stimulation of the cells suggesting retention of the native secretory cell phenotype unlike NCL-SG3 cells. The EC23 cell line is also responsive to adrenergic stimuli to a higher degree than NCL-SG3 cells, especially clone 2, however all the cell lines responded significantly less than primary eccrine secretory coil cells upon isoproterenol stimulation.

It was also found that the mesenchyme has a crucial effect in determining the formation of eccrine like down-growths in Matrigel organotypic models seeded with EC23 cells, where organotypics made with adult fibroblasts failed to form down-growths in comparison to neonatal fibroblasts. Furthermore, the co-culture of EC23 cell with keratinocytes enhanced the amount of downgrowth. EC23 cells have the capacity to form branching structures that resemble native eccrine glands in GFR Matrigel supplemented with EGF and EDA, and to

a lesser extent BMP4. In conclusion it was demonstrated that the EC23 cells can be used as a model to study the human eccrine gland, in particular the secretory coil.

Abbreviations

3D	3 Dimensional
AED	Anhidrotic ectodermal dysplasia
ANOVA	Analysis of variance
APC	Allophycocyanin
ATP	Adenosine tri-phosphate
BMP-2	Bone morphogenic protein 2
BMP-4	Bone morphogenic protein 4
Ca^{2+}	Calcium ions
CACC	Calcium activated chloride channels
CAMP	Cyclic AMP
CC1	Coil coil 1
cDNA	Complimentary DNA
CF	Cystic fibrosis
CFTR	Cystic fibrosis transmembrane receptors
Cl^{2-}	Chloride ions
CO_2	Carbon dioxide
CRAC	Calcium release activated channel
DAG	Diacyl glycerol
DAPI	4',6-diamidino-2-phenylindole
DED	De-epidermialised dermis

DMEM	Dulbecco's modified eagles media
DMSO	Dimethyl sulfoxide
ECM	Extracellular matrix
EDA	Ectodysplasin
EDAR	Ectodysplasin Receptor
EDTA	Ethylenediaminetetraacetic Acid
EF-hand	Helix-loop-helix domain
EF-SAM	Helix- loop-helix Sterile α motif
EGF	Epidermal growth factor
EGTA	Ethylene glycol tetraacetic acid
ER	Endoplasmic reticulum
FACS	Fluorescence activated cell sorting
FITC	Fluorescein isothiocyanate
FBS	Foetal bovine serum
FGF	Fibroblast growth factor
GAG	Glycosaminoglycans
GFP	Green fluorescent protein
GFR	Growth factor reduced
GPCR	G-protein coupled receptor
GR	Glucocorticoid receptor
HA	Hyaluronic acid
HESG	Human eccrine sweat gland
HGF	Hepatocyte growth factor
Hh	Hedgehog signalling

HPV	Human papillomavirus
IgG	Immunoglobulin G
IgG1	Immunoglobulin G1
IgG2b	Immunoglobulin G2b
IP_3	Inositol triphosphate
IP_3R	Inositol triphosphate receptor
K^+	Potassium ions
K_{Ca}	Calcium activated potassium channels
MEM	Minimum essential media
Mg^{2+}	Magnesium ions
$MgCl_2$	Magnesium Chloride
MMP	Matrix metalloproteinases
MMP-2	Matrix metalloproteinases 2
MMP-7	Matrix metalloproteinases 7
MSC	Mesenchymal stem ells
Na^+	Sodium ions
NaCl	Sodium Chloride
NaOH	Sodium hydroxide
NS	Not significant
ORAI	Calcium release-activated calcium modulator
P/S	Penicillin streptomycin
PBS	Phosphate buffered saline
PBST	Phosphate buffered saline tween

PLC	Phospholipase C
RPM	Revolutions per minute
RT	Room temperature
RyRs	Ryanodine receptors
SAM	Sterile α motif
SERCA	Sarcoendoplasmic reticulum calcium transport ATPase
Shh	Sonic hedgehog
SOCE	Store operated calcium entry
SR	Sarcoendoplasmic reticulum
STIM1	Stromal interaction molecule 1
STIM2	Stromal interaction molecule 2
TBS	Tris-buffered saline
TBST	Tris-buffered saline tween
TGF-β	Transforming growth factor β
TMB	3,3′,5,5′-Tetramethylbenzidine
TNF	Tumour necrosis factor
TRPC	Transient potential cation channel

List of figures and tables

Table of Contents

Acknowledgements

My PhD was funded under a BBSRC CASE studentship with industrial funding by Unilever.

First I'd like to thank Professor Mike Philpott, for giving me the opportunity to undertake this PhD and for his constant support and encouragement throughout these past 4 years. I would also like to thank my second supervisor, the late Professor Harshad Navsaria for his enthusiasm and guidance, and Dr Mark Harker, my industry supervisor.

Secondly I'd like to thank everyone in the Philpott group especially Dr. Eleni Pantazi – always been happy to answer my questions and for her company in the lab during late evening; Dr. Ros Hannen – who explained all about keratinocytes to me when I first started; Dr. Jamie Upton – who was there for moral support all along; and Miss Zoe Drymoussi – who has been vital during the writing up period.

I would also like to thank all the members of Cutaneous Research for all the help and laughs during my PhD, with special thanks to my bay buddies Dr. Mathew Caley, Dr. Supatra Marsh, Dr. Patricia Costa and Dr. Roanne Jones for their putting up with me these past few months and for the supply of treats. Also I'd like to thank Dr. Mathew Brooke and Dr. Louise Russell for the help.

I would also like to thank Dr. Cleo Bishop for her guidance and technical help when setting up the matrigel model and with analysis troubleshooting and Dr, Kristin Braun who pointed me in the direction of the model.

I would like to thank my friends and family for their understanding, love and support during the last 4 years. Especially my mother who has been invaluable in the process

and I would certainly not be here without her love and encouragement. Finally I would like to thank my grandfather for showing me that I could be anything I wanted.

Chapter 1: Introduction

1.1 Skin

The skin is essential for maintaining homeostasis and forms an essential barrier between internal organs and the exterior environment, providing the first line of defence against pathogens (Freinkel and Woodley, 2001, Tortora and Grabowski, 2003). Other functions include sensory roles, vitamin D synthesis, immune surveillance and excretion of wastes through eccrine glands (Farage et al., 2010). The skin is composed of three main layers: the epidermis, dermis, and hypodermis (Figure 1.1); and a number of appendages: the hair follicle, sebaceous glands and sweat glands (eccrine and apocrine). In the human embryo, the skin begins to develop from the ectoderm at week 4 (Carlson, 2009). By week 11, dermis formation begins. Basal buds start to form, that will eventually become hair follicles, dermal papillae vessels and nerves . The mesoderm is essential in inducing the differentiation of skin appendages, such as the eccrine gland and hair follicle (Blanpain and Fuchs, 2006, McGrath et al., 2008). Rete Ridges form the undulating junction between the dermis and the epidermis that provide mechanical support for the epidermis, but also is a barrier against the exchange of large molecules and cells between the epidermis and dermis (Freinkel and Woodley, 2001, Tortora and Grabowski, 2003). Bellow the dermis resides the hypodermis or subcutis, a layer of adipose tissue. (McGrath et al., 2008).

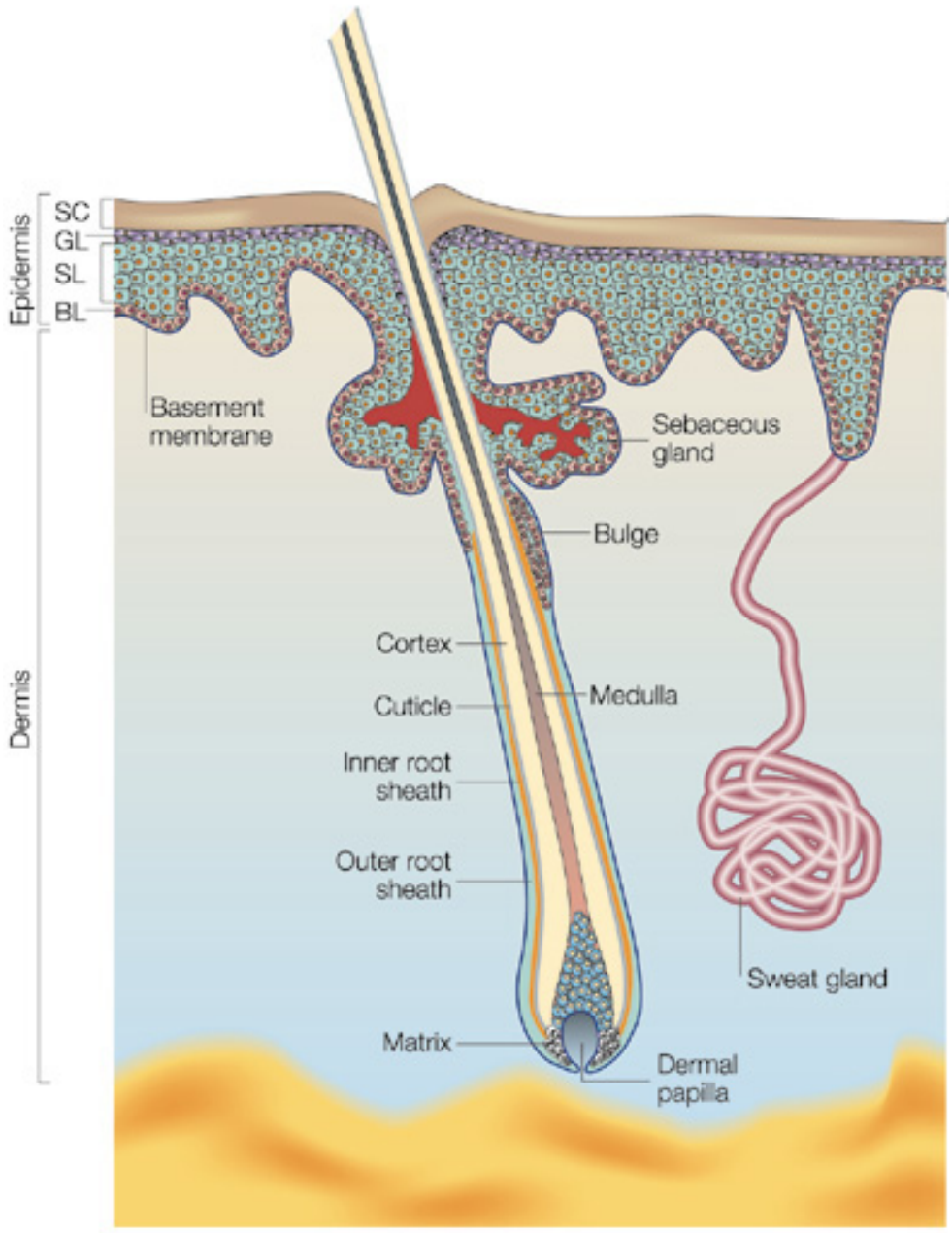

Figure 1.1. Structure of the human skin. (SC) Stratum Corneum; (GL) granular layer; (L) spinous layer; (BL) basal layer (Fuchs and Raghavan, 2002).

1.1.1 The epidermis

The epidermis (figure 1.2), is composed of 4 layers: the stratum corneum, the stratum granulosum (or granular layer), the stratum spinosum (or spinous layer) and the stratum basale (or basal layer)(Freinkel and Woodley, 2001, Tortora and Grabowski, 2003). Epidermal proliferation occurs in the stratum basale, generally composed of a one cell thick layer of 10-14μm cuboidal keratinocytes (characterised by a high composition of keratin 5 and keratin 14) dispersed with melanocytes (Freinkel and Woodley, 2001, McGrath et al., 2008). When dividing, one daughter cell remains on the stratum basale while the other cell migrates upwards towards the stratum spinosum, differentiating in the process whereupon expression of keratins 5 and 14 is down-regulated and keratin 1 and 10 expression is up-regulated (Leigh et al., 1994, Freinkel and Woodley, 2001, Tortora and Grabowski, 2003). Following this differentiation, keratinocytes become polyhedral in shape with tonofil rich cytoplasm providing support (Fuchs, 1990). Langerhans cells can also be found in the stratum spinosum, these are specialised dendritic immune cells (derived from the bone marrow) that express antigen presenting sites and contain a characteristic and unique cytoplasmic organelle, the Birckeck granule (McGrath et al., 2008). As the keratinocytes of the stratum spinosum move upwards to the stratum granulosum, they become more granular and secrete their lipid content to the intracellular space (Leigh et al., 1994, Freinkel and Woodley, 2001). These lipids will provide an important barrier, which aid in maintaining the integrity of the stratum corneum and its adherence to the stratum granulosum (Tortora and Grabowski, 2003).

The stratum corneum, the outermost layer of skin, is composed of corneocytes. Corneocytes are keratinocytes that have terminally differentiated and have lost their nuclei and organelles (Steven and Steinert, 1994, Freinkel and Woodley, 2001). These cells have a flattened appearance with a cytoplasm composed of tonofibrils and keratin fibres that align to form cross-linked macrofibres (Fuchs, 1990, Gawkrodger, 2002, McGrath et al., 2004).

1.1.2 The Dermis and Subcutis

The dermis is the main support for the epidermis and is largely acellular and consists mainly of the extracellular matrix, a complex environment made up of various macromolecules and fibres (Wolff and Fitzpatrick, 2008). The main components of the dermis are collagen fibres, elastin fibres and glycosaminoglycans (GAG) (McGrath et al., 2008). There are two main types of GAGs, non-sulphated - hyaluronic acid (HA) - and sulphated heparin sulphate, chondroitin sulphate, dermatan sulphate and keratin sulphate (Damiano and Cicione, 2011). Even though GAGs only account for 0.1-0.3% of skins' total weight, their ability to retain water accounts for some of the skins' elasticity and volume (Priestley, 1988). The main types of GAGs in skin are HA and chondroitin sulphate, with their concentration being greatest in sub-epidermal regions (Salbach et al., 2011, Papakonstantinou et al., 2012). HA constitutes 75% of GAGs, with its main binding receptors being CD44 and CD168, which are believed to be involved in cell signalling (Penneys, 1993, Salbach et al., 2011). Collagen, the main component of the dermis (70%), provides the dermis with

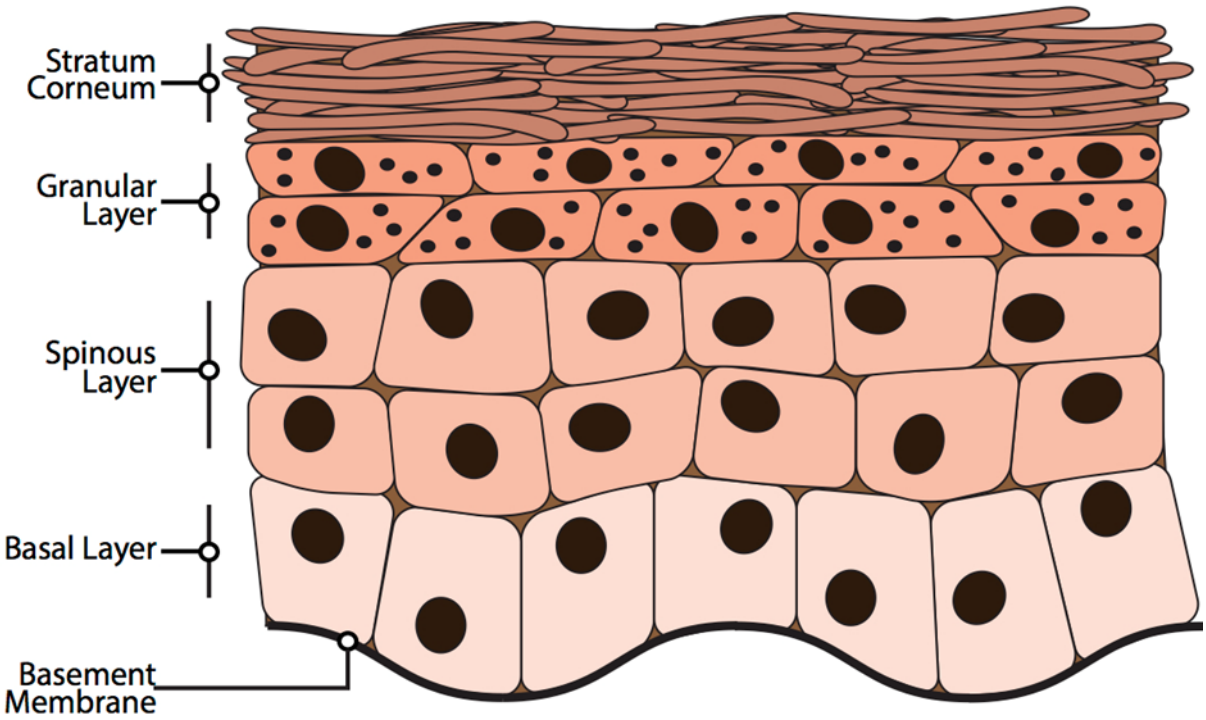

Figure 1.2. Diagrammatical representation of the epidermis showing the main layers.

tensile strength (Salbach et al.). Collagen type I is the most abundant collagen type in the dermis, followed by collagen II and smaller amounts of collagen V and VI (McGrath et al., 2008). Elastin fibres provide elasticity to skin and can be found at much higher numbers in the vicinity of sweat glands and hair follicles (Wolff and Fitzpatrick, 2008).

The main cell type in the dermis is fibroblast (Freinkel and Woodley, 2001). Fibroblasts are mesenchymal cells and a member of the connective tissue family of cells (McGrath et al., 2008). They play a vital role during development of organs such as skin, eyes, lungs, and then later play a supportive and structural role in the body (Burns et al., 2010). Fibroblasts are also important in maintaining homeostasis of adjacent epithelium through the secretion of growth factors (Darby et al., 2014). During processes such as wound healing, fibroblasts are activated and produce matrix degrading enzymes, cytokines and epithelial growth factors (Darby et al., 2014). ECM component such as collagens types I, III, IV and V, fibronectin, GAGs and MMPs are also synthesised by fibroblasts (Bierie and Moses, 2006, Kalluri and Zeisberg, 2006). A small number of dermal dendrocytes can also be found in the dermis. These cells are thought to be involved in immune responses (Headington, 1986). Macrophages, mast cells and lymphocytes are also present in small numbers (McGrath et al., 2008).

The innermost layer of the skin – the hypodermis or subcutis – is composed of lipids and connective tissue, including elastin, and can be up to 3 cm thick, and contains adipocytes, lymphocytes and mast cells (Smith and Dean, 1998). This layer connects the skin to bone and muscle and is important in insulation and nutrient storage (McGrath et al., 2004).

1.1.3 Stem Cells of the Skin

The skin has the ability to regenerate either in normal homeostasis or in response to injury (Blanpain and Fuchs, 2006, Blanpain and Fuchs, 2009b). This ability, which is largely attributed to stem cells and early progenitor basal keratinocytes, has become of great interest in stem cell biology as it could provide a readily accessible source of stem cells for both research and therapies (Kruse et al., 2006, Tiede et al., 2007, Fuchs, 2007, Kajahn et al., 2008). Identifying stem cells, however is difficult and several markers are used for their identification, including integrins (α6, β1), keratin 15, CD34, CD44 and nestin (Jones and Watt, 1993, Alonso and Fuchs, 2003, Nakagawa et al., 2005, Ohyama, 2007, Petschnik et al., 2010a).

The skin's appendages have been studied to great extent in recent years as they are thought to contain adult stem cell niches (Braun and Prowse, 2006, Lu et al., 2012). The hair follicle bulge has been identified as being a source of stem cells (Cotsarelis et al., 1990, Alonso and Fuchs, 2003) and recently the eccrine sweat gland was found to be a rich source of nestin positive cells (Petschnik et al., 2010a). This is an interesting finding as these cells could provide alternative sources for stem cells for both research and therapies (Zhou and Melton, 2008). The capacity of differentiation of these cells still remains to be investigated, however there is evidence that nestin positive cells within the skin (mainly the hair follicle) have the potential to spontaneously differentiate into neural and glial cell lines (Amoh et al., 2012) and that eccrine sweat gland cells can differentiate and reconstitute a stratified epidermis (Biedermann et al., 2010). Researchers have also successfully redirected differentiation of hair follicle stem cells into corneal

epithelial like cells using corneal limbus conditioned media (Blazejewska et al., 2009).

1.2 The Human Eccrine Sweat Gland

The human eccrine sweat gland (HESG) is composed of simple epithelia; it is a tubular structure with a bulbous end. It can be separated into three distinct segments: the accrosyringium – situated in the epidermis and opening directly on the surface of skin – the duct – that passes through the dermis – and the secretory coil, located in the dermis; in some eccrine glands the secretory coils extend to the hypodermis (figure 1.3) (Tortora and Grabowski, 2003, Langbein et al., 2005).

The human eccrine sweat gland is composed of three distinct cells types: the clear cell, which is involved in the secretion of water, ions and solutes; the dark cells, of granular appearance and which are rich in mitochondria, believed to be involved in mucoid secretions; and myoepithelial cells, which are contractile cells aiding the expulsion of secretions (Sato et al., 1991, Saga, 2002). There are 3-5 million sweat glands in the human body, with an uncoiled secretory coil diameter of 30-50 μm and 2-5mm in length (Quinton, 1983). Formation of human eccrine sweat gland (and apocrine glands) begins at foetal week 16 in the feet soles and palms and in week 22 in the rest of the body (Quinton, 1983, Sato et al., 1989).

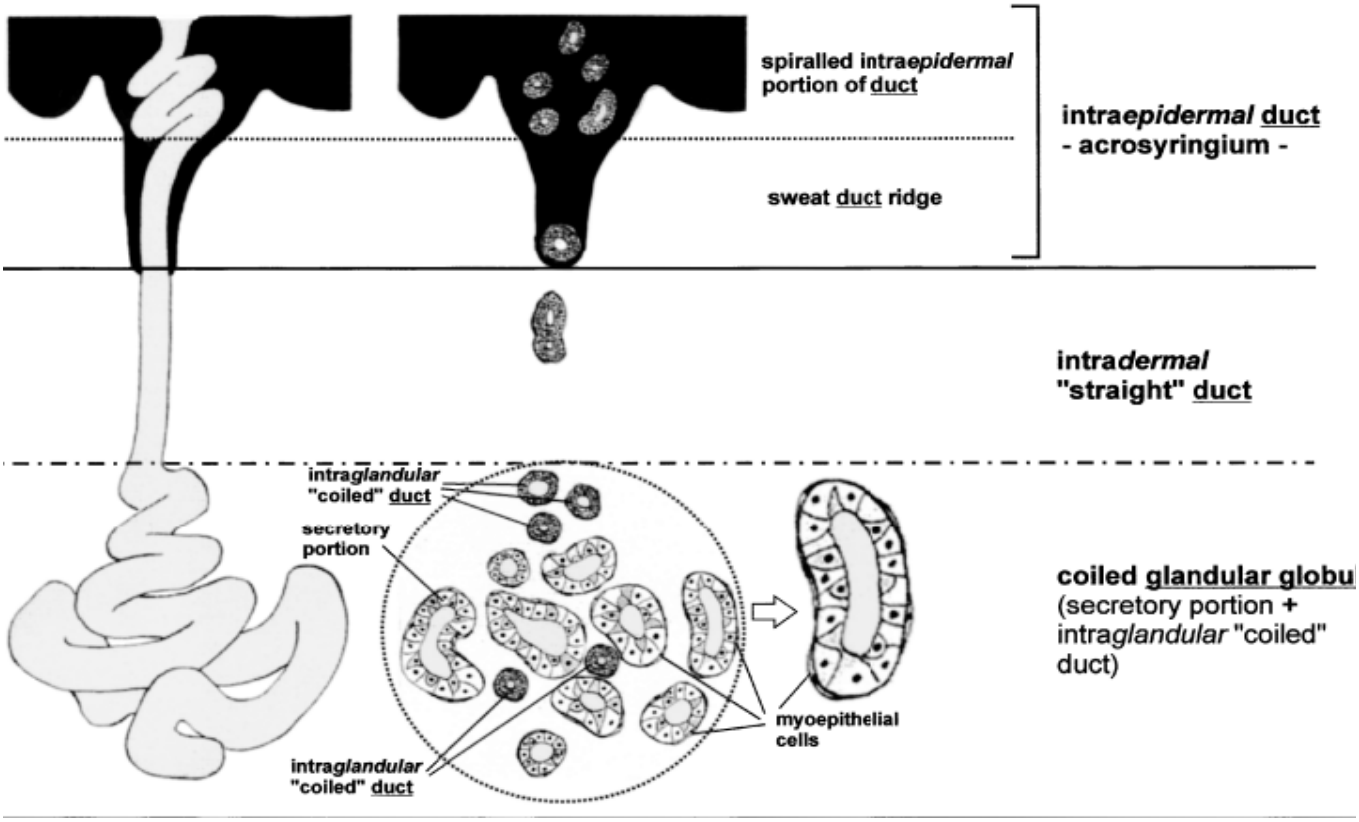

Figure 1.3. Diagramatic representation of the human eccrine sweat gland (Langbein et al., 2005). Showing the three main structures namely: the accrosyrungyum, intradermal duct and secretory coil.

1.2.1 The Development of the eccrine sweat gland.

Little is known about the formation of HESGs, as no *in vitro* model is currently available, and the only reports on sweat gland morphogenesis have been performed on mouse models and these are few (Viallet and Dhouailly, 1994). Eccrine gland development begins from a keratin 14+ progenitor cell rich placode, which grow down into the dermis to develop a sweat duct culminating in the secretory coil (Lu et al., 2012). Epithelial appendage development is composed of three stages, (1) induction, (2) morphogenesis and (3) differentiation. The initial step, induction, is the process by which embryonic cells acquire an organ tissue identity resulting in an ordered pattern of cell activity, in which appendage primordia is formed (Widelitz and Chuong, 1999, Wolpert, 2006). This process is initiated by signalling molecules that affect gene expression (Wolpert, 2006).

For induction to occur there must be at least two interacting components, the inducer, that produces a signal and the responder, that is affected by the signalling molecules produced by the inducer (Gilbert, 2003). In some instances, tissues can have reciprocal interactions in which the previous responder can then become an inducer and affect other tissues, such is the case for the lens, which receives signals from the optic vesicle for normal formation (Ogino and Yasuda, 1998, Zygar et al., 1998). After the lens has fully formed, it becomes an inducer secreting signalling molecules that will affect the optic vesicle which will then differentiate into the optic cup which will give rise to the pigmented and neural retina (Cvekl and Piatigorsky, 1996). These signals can be instructive or permissive. Instructive signalling occurs when a cell or tissue requires signals

from another cell or tissue, and permissive signalling occurs when a cell or tissue is self-sufficient and contains its own potential for development, only requiring an adequate environment to develop, such as laminin or fibronectin, which permit the development of a tissue without altering the cell's fate (Gilbert, 2003). Competence is the ability of a cell to respond to signals from the inducer. Competence is an acquired quality of a cell and can be acquired by synthesizing a receptor to an inducer molecule, by synthesizing a ligand that allows the receptor to function and/or by repressing an inhibitor (Wolpert, 2006).

To study these interactions experiments using epithelial cells adjacent to mesenchymal cells or tissues have been devised. In early experiments Dhouailly, (1975), found that recombining chick epidermis grafted on mouse dermis, mouse epidermis grafted onto chick dermis or reptilian epidermis grafted onto mouse dermis still results in placode development, suggesting the early signals required for appendage development are not species specific. However a mesenchymal condensate failed to form and thus appendages, such as hairs, feathers or scales did not form (Dhouailly, 1975). Similar experiments in which dorsal mouse epidermis was recombined with mouse upper lip dermis resulted in vibrissae follicles and when upper lip dermis was recombined with dorsal skin dermis, pelage follicles were formed, suggesting that the signals from the dermis are responsible for the fate of the resulting appendage (Dhouailly, 1977).

The result of induction is the epithelial placode and a sub-adjacent mesenchymal condensate that make up the epithelial placode (Chuong et al., 2000). At this stage of development, the phenotype of the placode is unstable and can change fate if

subjected to the adequate signals (Dhouailly et al., 1980). During Morphogenesis flat epithelial sheets begin to fold, invaginate, evagenate or branch; processes that are achieved by cell migration, proliferation, or apoptosis (Gilbert, 2003).

Differentiation is the final stage of appendage (or tissue or organ) development. Differentiation, in appendage development is often characterised by a cell becoming committed to its fate to serve a specific function (Carlson, 2009).

Different signalling pathways have been described as being involved in eccrine gland development, Wnt being one of them. It has been suggested that the Wnt/β-catenin/Lef1 pathway is an upstream regulator of the ectodysplasin (EDA) signalling pathway, as the expression of EDA and ectodysplasin receptor (EDAR) are dependent on Lef1, which has been found on the promoter region of the *Eda* gene (Kere et al., 1996, Kobielak et al., 1998, Lu and Fuchs, 2014). Cui et al, studied the involvement of Wnt in eccrine development in mice, observing increased Wnt activity in sweat gland germs and thus is thought to be involved in sweat gland induction (Cui et al., 2014). However Wnt has also been observed to be active later on in eccrine development. Several investigations have also observed that Wnt signalling is observed downstream from EDA during epidermal appendage development. Cluzeau, et al (2011), found that a mutation in the WNT10A gene was involved in the hypohidrotic ectodermal dysplasia (HED) phenotype of 16% of the patients involved in the study, further suggesting the involvement of Wnt in eccrine gland development (Cluzeau et al., 2011).

EDA signalling has been established as being involved in the development of many epidermal appendages. EDA is a member of the tumour necrosis factor (TNF) superfamily. Mutations in the EDA, EDAR or in the EDAR associated death domain protein (EDARADD) genes result in HED or anhidrotic ectodermal dysplasias (AED), characterised by the malformation of hair follicles, exocrine glands, teeth and mammary glands (Kobielak et al., 1998, Srivastava et al., 2001, Gilbert, 2003, Lindfors et al., 2013).

The study of the EDA/EDAR/EDARAAD pathway has been greatly facilitated by the identification of a mouse model that express a *tabby* (*Ta*) gene mutation that is equivalent to a EDA mutation resulting in a phenotype very similar to HEDs (malformations in hair, teeth and absence of sweat glands in foot pads) (Sofaer, 1969). From then on, other mouse mutants that develop a phenotype that resemble HED have been identified, such as *downless (Dl)* a mutation in the gene equivalent to EDAR and *crinkled (cr)* mice, which have a phenotype resembling both the *Ta* and *dl* mutants and is equivalent to a mutation in the human gene for *EDARADD* (Headon et al., 2001).

An investigation of the tabby mouse model Srivastava, et al., (2001), suggested that EDA is involved in sweat gland development. Srivastava et al., (2001) found that mutant EDA mice did not develop sweat glands, and if the EDA pathway is disrupted, even after sweat gland rudiments are formed, gland development is halted, suggesting that for normal sweat gland development a constant level of EDA must be maintained (Srivastava et al., 2001). Interestingly, Cui et al. (2008), found that in mice engineered with a tetracycline inducible Eda-A1 gene, eccrine glands only formed during a discrete window of time during development and that

unless constant EDA signalling was present, mature glands would not form (Cui et al., 2008).

Sonic hedgehog (Shh) is also implicated in epidermal appendage formation, but at a later stage than Wnt and EDA/EDAR, and its induction is dependent on EDA/NF-κB signalling (Tucker et al., 2000). Shh is required for dermal papilla formation in the hair follicle (Chiang et al., 1999) and in branching morphogenesis in the salivary gland (Jaskoll et al., 2004). In the eccrine gland, Cui et al, (2014) found that Shh lacking mice formed normal eccrine ducts but very rudimentary secretory coils suggesting that Shh is required in the late stages of eccrine morphogenesis to form fully functioning complete secretory coils; they also observed that eccrine gland placodes fail to form a dermal condensate, instead forming a connective tissue sheath that (Cui et al., 2014).

Bone morphogenic proteins (BMPs) are a group of 20 secreted signaling molecules, that belong to the TGF-β superfamily (Reddi, 1998, Carlson, 2009). BMPs, are regulators of vertebrate development involved in proliferation, differentiation and apoptosis and after birth, they are involved in tissue remodeling and homeostasis (Li et al., 2003). In the hair follicle, noggin, a BMP antagonist initiates hair follicle developmet by upregulating Lef-1 which in turn stimulated the hair placode and induce hair follicle development (Botchkarev et al., 1999). It is interesting however, how the overexpression of noggin adversely affects the development of the sweat gland. In a mouse model over expressing noggin, Pilkus, at al (2004), found that the eccrine glands that are located on the foot pads of the mice had developed into hair follicles rather than eccrine glands

(Plikus et al., 2004). This suggests that BMP activity is required for eccrine gland development. Wollina et al (1999), studied the presence of BMP-receptor IA, BMP-receptor IB and Smads 1-7. They reported staining for Smad 1 and 3 in the secretory coil of eccrine glands and BMP-receptor IA and Smad 3 in the duct and accrosiringium. This suggests that BMP2/4 may be involved in the development of eccrine glands as their signal via BMP receptor type II and IB to stimulate Smad 1 (Wollina et al., 1999). It has also been noted that BMP2/4 may stimulate BMP-receptor AI signalling to Smad 3 (Heldin et al., 1997, Massaous and Hata, 1997).

Epidermal growth factor (EGF) is also thought to be involved in sweat gland formation. Research performed on tabby mice where sweat gland induction was achieved by injecting the mice with EGF gives evidence that it could be a key factor involved in appendage formation (Blecher et al., 1990). EGF is also thought to be involved in mammary gland formation, tooth and hair follicle development (Partanen and Thesleff, 1989, Richardson et al., 2009, Hynes and Watson, 2010). EGF is also secreted by the HESG, and other ectodermal appendages, possibly for cell maintenance and repair (Saga, 2001).

Spontaneously aborted foetuses from week 11 to 31, have been analysed for EGF and matrix metalloproteinases (MMP) -2 and -7. (Li et al., 2002). This study revealed that EGF and MMP-2 & 7 around sweat gland buds begin to appear at gestational week 14 to 16 (when eccrine gland formation first begins), with levels of MMPs reaching a maximum level by week 22. Expression of MMP-2 was also found on the surrounding mesenchyme suggesting its importance in sweat gland

down growth and epithelial mesenchymal crosstalk. EGF levels however remained constant throughout the duration of eccrine gland morphogenesis (Li et al., 2002).

In another recent study, the effect of hepatocyte growth factor (HGF) on eccrine sweat gland epithelial cell growth was investigated (Lei et al., 2012a). HGF is an important transduction molecule between mesenchymal and epithelial cells and it is implicated in the proliferation of various cells types, such as corneal cells, retinal cells, myofibroblast and many tumour cells (Wilson et al., 1994, Lewis et al., 2004, Colombo et al., 2007). In this study it was found that the addition of 40 ng/ml of HGF significantly increased the proliferation of eccrine epithelial cells (Lei et al., 2012a).

The lack of knowledge on the morphogenesis of the HESG is one of the major barriers to the successful development of an *in vitro* model of the eccrine sweat gland. However, other skin appendages such as the hair follicle, the mammary gland and teeth are derived from the ectoderm and share many similarities of the mesenchymal-epithelial interactions during early development; an example of this are ectodermal dysplasias, where mutations on EDA, its receptor EDAR or its downstream receptor, lead to the absence or malformation of hair follicles, teeth, and eccrine and apocrine glands (Mikkola and Thesleff, 2003).

From the information available about other skin appendages, we can infer that eccrine morphogenesis follows a similar pattern to the hair follicle and mammary gland, in which the epithelium thickens forming a placode as the result of signalling from the dermis (Gilbert, 2003, Chuong et al., 2000). However, eccrine sweat gland development differs significantly from other skin appendages, such as

the hair follicle in that it has been observed that in eccrine gland development, dermal condensate does not form, instead a connective tissue sheath forms around the developing sweat gland and may provide dermal signalling (Cui et al., 2014).

1.2.2 Eccrine Sweat Gland Function

The main function of the eccrine gland is to maintain a constant core body temperature of 37^{o}C. This is achieved by the secretion of an electrolyte rich hypotonic fluid, which together with vasodilation, maintain a constant temperature body temperature (Wilke et al., 2007).

Hyperthermia – body temperatures of 40^{o}C and over – leads to protein denaturation, cell death and organ failure, thus a tightly controlled core body temperature must be maintained (Lepock, 2003). Humans perspire in two ways, thermally (or actively) and emotionally (Sato et al., 1989). Thermal perspiration occurs as a result of an increase in temperature relative to hypothalamic set point, which occurs in hot/warm climate and during exercise, however the HESG can be activated by pyrogens (i.e.: - spicy food), hormones and emotions (Quinton, 1983, Sato et al., 1989). The eccrine sweat gland is innervated by postganglionic non-myelinated C-fibres from the sympathetic nervous system, which appear to be of cholinergic origin (Sato and Sato, 1981b, Quinton, 1983, Shibasaki et al., 2006). The initial signals are sent from the pre-optic hypothalamus, which travel to the pons and the medullary raphe on their way to the spinal cord (Sato et al., 1989). From there, the signals travel to the sympathetic ganglia to stimulate sweat production (Shibasaki et al., 2006, Schlereth, 2009).

The primary neurotransmitter of the HESG is acetylcholine, which is released from cholinergic pseudomotor nerves, and binds to muscarinic receptors on the HESG(Shibasaki et al., 2006). However, stimulation can also be induced by alpha and beta adrenergic agonists *in vitro*, but the response to these agonists is far less than their response to acetylcholine or its analogues (Sato and Sato, 1981b, Quinton, 1983).

The response of eccrine gland to adrenergic agonists *in vivo* is a topic of debate. In one study by Buono, et al., (2011) the effect of sweat secretion was investigated in response to intraepidermal injections of either cholinergic or β-adrenergic agonists, acetylcholine and epinephrine, respectively, in patients that had received localised atropine treatment by iontophoresis (Buono et al., 2011). It was found that neither agonist stimulated sweat secretion in the atropine treated skin, however sweat secretion was observed when a combined injection of acetylcholine and epinephrine was administered. These data could confirm the suspicions of the potentiating role of the adrenergic stimulation (Buono et al., 2011).

Early studies by Sato & Sato (1981) using isolated eccrine glands, demonstrated the need of extracellular calcium ions for sweat production during α-adrenergic and cholinergic stimulation of the eccrine gland. When glands are stimulated with cholinergic agonists in media containing calcium, sweat secretion was observed, however when cells are incubated in calcium-free media, or when EGTA a calcium scavenger is added to media, sweat secretion is inhibited. Sweat secretion was resumed upon further addition of calcium. Similar results were observed upon stimulation with α-adrenergic agonists, however when the glands were

stimulated with β-adrenergic agonists, sweat secretions were still observed, however at lower quantities than those produced with muscarinic stimuli. This suggested the existence of three distinct pharmacological mechanisms for sweat secretion, muscarinic, α-adrenergic and with β-adrenergic secretion being independent of extracellular calcium, with a possible mechanism of action being triggered by intracellular calcium stores in the endoplasmic reticulum (Sato and Sato, 1981b).

When the HESG is stimulated by acetylcholine, a series of responses occur that trigger the release of calcium from the endoplasmic reticulum (Sato and Sato, 1981a, Quinton, 1983, Sato et al., 1989, Reddy and Bell, 1996). This increase makes the cell permeable to chloride and potassium ions, leading to a secretion of an isotonic precursor fluid to perspiration (Quinton, 1983, Cui et al., 2012). After this fluid leaves the secretory coil and enters the duct, reabsorption of electrolytes begins to take place (Quinton, 1983, Reddy and Bell, 1996). The reabsorption of sodium chloride leads to the final secretions being hypotonic compared to plasma (Sato and Sato, 1981a). However, if the rate of secretion is high, the level of reabsorption in the duct decreases, leading to an isotonic secretion which can lead in some cases to dehydration. During extensive exercise or severe heat stress, humans can produce on average 1.5 litres of sweat per hour, however, this rate is greatly reduced after long periods of heat or exercise (~5 hours) (Brake and Bates, 2003). One must bear in mind that the rates of perspiration differ greatly between individuals as variations ranging from gender, physical fitness, circadian rhythm; menstrual cycle and even relative air humidity can affect perspiration (Wilke et al., 2007).

Apart from thermal sweating, as described above, humans can sweat emotionally (Quinton, 1983, Altman and Schwartz, 2002). Emotional sweating differs from thermal sweating in that it is controlled by the neocortical and limbic centres in the brain (Ogawa, 1975). The rest of the mechanism of action is the same as thermal sweating in terms of pre and post ganglionic stimuli, however emotional or stress associated sweating often affect specific sites in the body, such as the face, palms of the hand, soles of the feet and axillary regions (Schlereth, 2009) and is often accompanied by vasoconstriction (Bini et al., 1980, Reisfeld, 2007), which is likely caused by an increase in plasma catecholamines (Robertshaw, 1979).

1.2.3 Calcium Signalling

Calcium signalling is one of the most ubiquitous systems in mammals involved in functions such as cell division, proliferation, differentiation, apoptosis, metabolism and secretion amongst others (Berridge et al., 2000, Bootman, 2012). Most cells maintain a resting cytoplasmic Ca^{2+} concentration between 100-200 nM; this balance is maintained by closely monitoring concentrations and allowing an efflux or influx of calcium via the various Ca^{2+} channels present in cells (Brown, 1989). Calcium is stored in most cells within the endoplasmic reticulum (ER) and in muscle the sarcoplasmic reticulum (SR). In the SR and ER, The sarco/endoplasmic reticulum Ca^{2+} ATPase (SERCA) pumps allow Ca^{2+} to enter into the lumen of the ER/SR and ryanodine receptors (RyRs) and inositol triphosphate receptors (IP_3Rs) to allow Ca^{2+} release from the ER into the cytoplasm (Lanner et al., 2010, Deak et al., 2014). Cells can efflux calcium into

their environment via plasma membrane Ca^{2+}ATPase (PMCA) pumps/channels (Putney, 2010, Soboloff et al., 2012).

In the eccrine gland, during exercise or increased body temperature, acetylcholine binds to muscarinic receptors, members of the G-coupled protein receptors (GPCRs) family, in the cell membrane on clear cells of the secretory coil (Li et al., 2009). The alpha sub-unit of the GPCR then binds to a phospholipase C (PLC) isoenzyme, which then hydrolyses phosphatidylinositol-4, 5-bisphosphate (PIP_2), which is found in the plasma membrane, into inositol triphosphate (IP_3) and diacylglycerol (DAG) (Lewis, 2011). Cytoplasmic IP_3 activates inositol triphosphate receptors (IP_3R) in the endoplasmic reticulum (ER), which opens Ca^{2+} channels on the ER allowing Ca^{2+} to flow into the cytoplasm (figure 1.4) (Parekh, 2008, Lewis, 2011, Soboloff et al., 2012). This increase in cytoplasmic Ca^{2+} then activates several other ion channels that culminate in the production of sweat (Hilgemann et al., 2001, Mikoshiba, 2007, Soboloff et al., 2012).

Apart from IP_3R, the ER also contains ryanodine receptors (RyRs). Ryanodine receptors are sensitive to a variety of compounds and ions and can be modulated by fluctuations in Ca^{2+}, Mg^{2+}, ATP, caffeine, calmodulin, calsequestrin, triadin and juntin, amongst others (Lanner et al., 2010). RyRs are also affected by ryanodine a high affinity ligand for RyRs, and was initially used as an insecticide due to its potent skeletal and cardiac muscle paralytic action (Fill and Copello, 2002). At low nanomolar concentrations Ryanodine locks RyRs in the open state

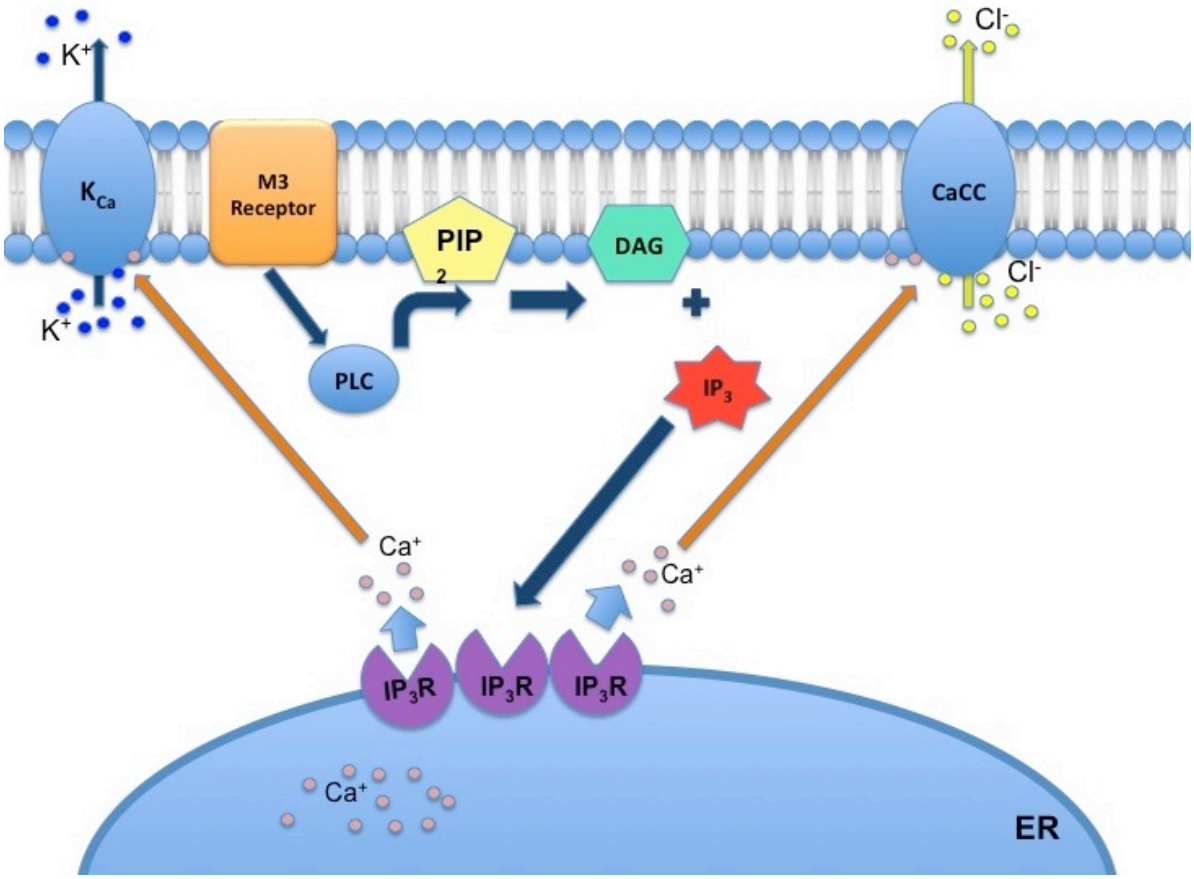

Figure 1.4. Muscarinic activation of IP_3R calcium release. Upon binding of a ligand to the M3 muscarinic receptor, PLC becomes activated and cleaves PIP_2 into DAG and IP_3. IP_3 then binds to IP_3R in the endoplasmic reticulum to release calcium ions into the cytoplasm, calcium them mobilises to the cell membrane, where it activate calcium activated potassium channels (K_{Ca}) and calcium activated chloride channels (CaCC).

and at millimolar concentrations it inhibits the channel. There are 3 isoforms of RyRs. RyR1, mainly found in skeletal muscles and at lower levels in heart muscle, stomach, kidney, adrenal glands, ovaries and testes; RyR2, mainly found in cardiac muscle, cerebellum and cerebral cortex and at lower levels in adrenal glands, ovaries, thymus and lungs (Lanner et al., 2010). The third type of Ryanodine receptor (RyR3), was first identified exclusively in rabbit brain tissue (Hakamata et al., 1992) and later in human brain tissue (Nakashima et al., 1997) and also found in skeletal muscle in neonatal mice and required for proper contraction, however this isoform was not found in adult mice (Bertocchini et al., 1997).

Ca^{2+} also acts on RyRs in a complex manner, as it can activate or deactivate the channel as well as being able to pass through its pore. Low concentrations of Ca^{2+} (1-10 μM) open the channel and high concentrations (1-10 mM) close it. This concentrations are not exact however, as different isoforms of the RyR are affected at different concentrations. Other effectors of RyR activity are Mg^{2+} and ATP, with cytoplasmic ATP opening the channel and Mg^{2+} closing it (Fill and Copello, 2002). It has also been demonstrated that RyRs may also be activated by muscarinic action via the activation of D38, which converts NAD to cyclic ADP ribose, which then activates RYR2 to release Ca^{2+} (Du et al., 2005).

The release of calcium from intracellular stores during sustained stimulation of the cells, such as in prolonged exercise or due to heat, requires the stores to be replenished for proper function of the cells (Clapham, 2007, Lewis, 2011). Store operated calcium entry (SOCE), is defined as the influx of calcium into the cell by activation of calcium release activation calcium (CRAC) channels (Soboloff et al.,

2012). For many years, the main channels for calcium entry were thought to be transient receptor potential channels (TRPCs), however recent investigations using RNAi have identified molecules that trigger and affect the entry of calcium after store depletion (Zhou et al., 2013). Stromal interaction molecules (STIM1 and STIM2) are transmembrane proteins that reside on the membranes of the ER, close to the plasma membrane (Lewis, 2011).

Stim proteins are single transmembrane proteins with a paired EF-hand domain on the N-terminus located on the luminal side of the ER, adjacent to the sterile alpha motif (SAM) (Feske and Prakriya, 2013, Thiel et al., 2013). When the ER Ca^{2+} stores are full, the EF-SAM domain is in the closed position and upon Ca^{2+} store depletion, hydrophobic regions of the EF-SAM motif become exposed, they uncoil and dimerise (Zhou et al., 2013). The dimerization of EF-SAM allows for the coil coil 1 domains (CC1) to become appositioned pushing the STIM ORAI activation region (SOAR) domain of STIM closer to the plasma membrane, where it activates ORAI proteins to form CRAC channels (Lewis, 2011, Feske and Prakriya, 2013, Zhou et al., 2013). STIM 1 is found in much larger quantities in tissues than STIM2 (Soboloff et al., 2012). The difference in the 2 isoforms is their activation. STIM2 is much more sensitive to Ca^{2+} depletion from the ER stores than STIM1, as it senses much lower Ca^{2+} changes. STIM1 activation requires a larger or sustained depletion of Ca_2^+ (Thiel et al., 2013)

1.2.4 Pathologies affecting the Eccrine Sweat Gland

There are a number of diseases that affect eccrine glands and sweat secretion (Quinton, 1983). Abnormal electrolytes can be observed in patients suffering from

Addison's disease, Cushing's syndrome, nephritis congestive heart failure and when undergoing hormone replacement treatments (Sato et al., 1991, Schlereth, 2009). The most severe disease causing defects in eccrine secretions is cystic fibrosis (CF), which is characterised by a mutation on the gene for cystic fibrosis transmembrane conductance regulator (CFTR) protein affecting chloride channels decreasing permeability for Cl^- (Quinton, 1990). Individuals affected by CF have increased electrolyte levels in their sweat, which has become one of the routine tests for the disease (Quinton, 2007). Normal Children have sodium sweat levels of up to 60 mM and affected children have levels of 90 mM and above (Shamsuddin et al., 2008, Coulson, 2010).

Hyperhidrosis, the most common diseases of the eccrine gland, is the over-production of sweat (Schlereth, 2009, Coulson, 2010). It is not a serious condition, however it can cause severe distress to the sufferer (Altman and Schwartz, 2002). This can occur as a result of several triggers and can be grouped accordingly. Generalised thermoregulatory hyperhidrosis occurs when an increase in hypothalamic temperature which induces vasodilation and an increase in perspiration, which can occur due to fever (Quinton, 1983). In some instances, neurological diseases can affect the thermoregulatory centre causing episodic hypothermia (Alty and Ford, 2008). Other conditions affected by generalized hyperhidrosis are diabetic autonomic neuropathy, hyperpituitarism, hyperthyroidism, menopause, substance withdrawal and some medications. (Quinton, 1983, Schlereth, 2009). Palmoplantar and axillary hyperhidrosis, is triggered by emotional or mental stimuli and is often referred to as emotional hyperhidrosis (Altman and Schwartz, 2002). The triggers for this type of sweating can be of a known or unknown emotional cause, it can occur on either sex and

most often affects the axillae, palms and soles (Schlereth, 2009, Quinton, 1983). Asymmetrical hyperhidrosis occurs due to neurological lesions to the parasympathetic nervous system, and it is the only presenting symptom of the lesion, which can affect several sensory segments along a sympathetic grey ramus (Korpelainen et al., 1993, Schlereth, 2009). There are several ways of treating hyperhidrosis however the treatments are in most cases only temporarily successful. These treatments include topical drugs such as muscarinic antagonists (such as atropine) and less often, systemic drug treatments, which are often accompanied by severe side effects such as glaucoma, hyperthermia and convulsions (Thomas et al., 2004, Coulson, 2010). Other treatments include iontophoresis, in which a small electric current is used to affect ion transport within the eccrine glands and thus reduce secretions (Coulson, 2010) and botulinum toxin injections that damage the sudomotor synapses and prevent the release of acetylcholine (Doft et al., 2012). There are also surgical treatments to induce anhydrosis, such as thoracic sympathectomy, in which the sympathetic ganglia Th2/3 is severed, for palmoplantar hyperhidrosis and for axillary hyperhidrosis the removal of sweat glands by axillary curettage (Quinton, 1983).

Granulosis rubra nasi is a rare condition characterised by excessive sweating and facial erythema with small macules and vesicles containing sweat appearing in the affected areas (Kumar et al., 2012, Sonthalia et al., 2012). It is often a disease of childhood, but can in some cases persist in adulthood (Sonthalia et al., 2012). It is a focal type of hyperhidrosis, however it is independent on hypothalamic or emotional stimuli to present itself (Sargunam et al., 2013). Its treatment is rare as it often resolved by puberty, and one of the few treatments reported in the

literature being topical 1% tacrolimus ointments and topical steroids (Kumar et al., 2012).

Anhydrosis, a lack of sweat production during eccrine stimulation (thermal or pharmacological), is rare and when systemic anhydrosis occurs it can be fatal (Quinton, 1983). Its cause is most often due to an underlying condition (Table 1.1) (Quinton, 1983, Dann and Berkman, 1992). In cases of anhidrotic ectodermal dysplasias (AED), an X-linked recessive disorder, where there is a lack or malformation of the eccrine glands, heat exposure can cause severe hyperthermia. AED sufferers must have constant care as chest infections and overheating can be life threatening (Ghosh et al., 2014). Neural lesions, such as spinal cord injury, nerve damage, and neuropathies, can lead to the most severe type of anhydrosis, which causes heat stroke (Quinton, 1983, Dann and Berkman, 1992). This occurs when the central control of temperature responses fails when core temperature increases above 40ºC. Spinal lesions can also affect perspiration, thus high cervical injuries can have detrimental effects which can lead to heat stroke (Quinton, 1983). Peripheral sympathetic nerve damage can lead to regional anhydrosis and it has been noted that the severity and eccrine response to pharmacological stimulation differs depending on whether the injury is pre- or post-ganglionic (Quinton, 1983).

1.3 Mesenchymal Epithelial interaction

Mesenchymal epithelial interactions are essential for maintaining normal organogenesis and tissue development (Gilbert, 2003). Cytokine and growth factor secretion by cells in the mesenchyme or stroma can guide or direct the

development of epithelial cells and *vice versa,* for example urogenital mesenchyme can induce ductal branching morphogenesis and help regulate androgen expression in the urogenital tract (Cunha, 2010). During embryonic development, the ectoderm gives rise to epithelial tissues and the mesoderm to the mesenchymal tissues (Gilbert, 2003, Carlson, 2009); these processes are orchestrated by a vast number of signals including Wnt, sonic hedgehog (Shh), Notch, transforming growth factor- β (TGF-β), bone morphogenic proteins (BMPs), EDA and fibroblast growth factor (FGF) (Li et al., 2003, Yamaguchi et al., 2005, Bazzi et al., 2007, Lu and Fuchs, 2014). These interactions are thought to be (a) permissive - where the epithelium retains its normal phenotype expression despite recombination with heterotypic mesenchyme; and (b) instructive - where the epithelium's phenotype is altered with recombination with the recombination with heterotypic mesenchyme (Aboseif et al., 1999)

In recent years, it has become apparent that the mesenchyme or stroma of tissues can redirect cells to differentiate towards a different cell type than their original phenotype (Merrill et al., 2008, Taylor et al., 2009). Several groups have demonstrated how cells from different origins such as, mammary gland, testicular tissues, urinary bladder, cornea and skin can be redirected to differentiate into different cell types by co-culturing them with mesenchymal/stromal cells (Ferraris et al., 2000, Oottamasathien et al., 2007, Taylor et al., 2009, Wang et al., 2010a). Stem interactions govern their fate by maintaining a balance between self-renewal and terminal differentiation (Fuchs and Raghavan, 2002, Oottamasathien et al., 2007). The ability of the mesenchyme to redirect differentiation of cells is of great cells are also highly dependent upon their microenvironment, as these

Congenital	Physical Damage	Neural Lesions
Ectodermal dysplasia	Eczema	Spinal cord injury
Ichtiosis	Atopic dermatitis	Nerve damage
Sjogren's disease	Psoriasis	Congenital sensory neuropathy
Fabry's Disease	Lichens planus	Autonomic neuropathy
	Miliaria	Organic lesions (i.e.: - Syringomyelia)
	Burns	
	Scars	

Table 1.1: List of pathologies affecting the eccrine gland that can cause anhydrosis.

.

interest as it is can help identify the molecular mechanisms of normal development, malignancies such as cancer and other age related conditions (Takasato et al., 2014). This type of research could also prove useful in development of new therapies and in regenerative medicine.

1.4 Models and Tissue Engineering of Skin and its Appendages

To date, several attempts have been made to develop an *in vitro* model of the human eccrine sweat gland with little progress in the area (Sato and Sato, 1983b). *In vitro* models used to investigate the eccrine gland's function usually involve the use of full glands (human or animal) or cells derived from the glands (grown as a monolayer or 3D culture) which are subjected to electrical input or stimulation by secretagogues to study their effect in electrolyte fluxes, metabolism and receptor changes (Sato and Sato, 1981a, Sato et al., 1990). *In vitro* models devised using whole eccrine glands have several flaws, first, they rely on the isolation of undamaged eccrine glands from skin biopsies, which is a process that in itself can damage the eccrine gland structurally and has the potential to damage cells due to the shearing process and the enzymatic digestion that can affect their function and responses to stimuli (Sato and Sato, 1981a, Kealey, 1983). Also, eccrine glands from different individuals vary in size and functionality, something that is also observed between body sites (Saga, 2002). These models are also of no use when trying to study the morphogenesis of the eccrine gland, but the difficulty of growing eccrine glands in long-term cultures has hindered the development of a 3D *in vitro* model.

Most attempts at developing an eccrine gland model or reconstruction of eccrine gland like structures in vitro have been performed using primary cultures of eccrine cells, mesenchymal, keratinocytes and stem cells seeded on a collagen and/or Matrigel scaffold (Lei et al., 2011, Li et al., 2015, Huang et al., 2010). Matrigel is a protein complex gelatinous material extracted from Englebreth-Holm-Swarm tumour that contains basement membrane proteins (Li et al., 2015). This material has been found to promote growth differentiation and morphogenesis of many cell types. For this reason Lei et al. (2011) used Matrigel in their study, in which they cultured eccrine cells and reported the formation of cyst-like clusters that resemble eccrine glands. However, this study involved only one cell type and the effect that other cells present in the skin exerted on the eccrine cells was not investigated (Groeber et al., 2011). Also as previously mentioned, the isolation of eccrine glands from skin is a delicate process that in itself can harm the cells derived from the glands and because of the difficulty of long term culture of these cells, their integrity cannot be fully established prior to constructing these models. Further, to isolate human eccrine sweat glands you need a supply of human skin. This is often only available to laboratories based within universities and is dependent upon compliant plastic surgeons being prepared to consent patients. Moreover, redundant human skin is becoming difficult to source in the numbers of samples required to maintain an active research programme.

As documented in section 1.2.1 a number of mutations have been identified with defects that affect the eccrine sweat gland and which has lead to the development of useful models to investigate sweat gland biology. An excellent example being the work of Blecher et al (1990) to investigate the effect of EGF on eccrine gland

development in which EGF postnatal treatment of tabby mice (model for ectodermal dysplasia) induced the formation of functional glands (Blecher et al., 1990). Huang et al, (2010) conducted experiments in which eccrine gland derived cells were encapsulated into EGF-containing gelatine microspheres, which were then placed onto a collagen type I/matrigel (2:1) scaffold and implanted onto a mouse model. The eccrine derived cells inoculated onto microbeads formed eccrine like structures, which did not occur with controls that had not been exposed to EGF, and in addition, they measured the rate of wound-healing in their animal model and found it had increased (Huang et al., 2010). The effect of EDA was also investigated using an *in vivo* model in which MSCs were transfected with an EDA expression vector, and injected onto the paws of burned mice. Upon stimulation with adrenaline, the mice injected with these cells showed a sweat response (iodine test), but sites implanted with normal MSCs did not (Cai et al., 2011).

However, using animal models carries with it a number of concern including the fact that mouse skin in particular is very different to human skin both in terms of its epidermal and dermal thickness, cell turnover and wound healing without scar formation and the fact that in mice the epidermis is mainly composed of follicular epithelium while in humans it is mainly inter-follicular (Khavari, 2006) and perhaps most importantly that in most animals the eccrine glands are only found in the paws and unlike in humans they do not play a major thermoregulatory role (Taylor et al., 2012, Wilke et al., 2007). Because of this there is the potential that markers for eccrine function and even stemness may differ when compared to human glands (Ginis et al., 2004). So while animal models have been very useful for many aspects of understanding skin biology in general they are not ideal for

understanding the physiology and function of the human eccrine sweat gland. Moreover, the European Union (EU) Cosmetics Directive provides the regulatory framework for the phasing out of animal testing for cosmetics purposes and specifically established a testing ban and prohibition to test finished cosmetic products and cosmetic ingredients on animals (http://ec.europa.eu/growth/sectors/cosmetics/animal-testing/index_en.htm).

As much eccrine sweat gland research is carried out by companies and there is an increasing need to address the fundamentals of 3R's in research namely animal replacement, refinement and reduction *in vitro* and/or *in silico* models are essential.

The effect of varying concentrations of EGF on eccrine development was investigated by Shikiji et al. (2003). In this investigation it was found that concentrations of 15 ng/ml of EGF in media and above were required to induce the differentiation of primary keratinocytes into eccrine gland like structures in collagen type I gels. This study is the closest to a successful eccrine gland model available to date, however the functionality of these pseudo glands was not investigated (Shikiji et al., 2003).

The current models available, often concentrate on targeting one specific pathway in the hopes on developing eccrine like structures. Even when structures are formed that resemble the eccrine gland visually, such as the work by Shikiji (2003) or Huang's (2010), their functionality has not been studied, which is vital to establish the validity of a model. By using primary cells, the models have the potential of being more like the native eccrine glands, however the isolation process which includes collagenase treatment and mechanical shearing of the

tissue, has the potential of damaging the secretory mechanisms (Lee et al., 1984), and due to the short passage capabilities of primary cells it can be difficult to determine whether or not the basic secretory mechanisms, such as response to cholinergic stimuli are retained by the models. And thus a cell line derived from the eccrine gland that retains its markers and is capable of retaining the ability to respond to cholinergic and adrenergic stimuli would be a major advantage for the development of a 3D model. One cell line derived from the eccrine gland does exist – NCL-SG3 – however the origin of these cells within the eccrine gland (coil or resorptive duct) is unknown, also they cannot be stimulated by cholinergic agonists, thus using them for the purposes of a fully functional model is not possible (Lee and Dessi, 1989).

Ideally a human eccrine gland model, should be reproducible, contain only cells derived from human tissue and be able to respond to cholinergic and adrenergic stimuli in a way that reflects the normal human eccrine gland. In an ideal world such a model would contain all of the cell types required for a functional gland and include light and dark cells as well as myoepithelial cells. Also ideally it would be possible to engineer these cells together to make an intact glandular structure. However, it is also possible to visualise more simplistic models that may in fact only incorporate single cell types e.g. secretory light cells that would still allow significant advances to be made in understanding the biology of these cells and which could then be used to investigate intact glands. Likewise, purified cultures of dark cells and myoepithelial cells would also allow their biology to be studied and from which more precise experiments could be devised that can be carried out on intact glands.

1.5 Summary

In summary although there is a considerable amount of knowledge with regards the pharmacology and physiology of the eccrine gland our knowledge of the precise roles played by the light and dark cells is poor. This is in part due to the lack of good in vitro models and cell lines and this reflects the problems in working with the eccrine gland both with regards its size and the fact it is difficult to isolate but also problems with sourcing suitable human skin from which glands and cells can be isolated and the fact that primary eccrine sweat gland cells are difficult to maintain in culture. The work reported in this thesis describes experiments carried out to characterise an immortalised eccrine secretory cell line (EC23) and investigate its ability to form ductal structures in vitro.

1.6 Background to the project

Due to the difficulty in long term culture of primary eccrine gland cells *in vitro*, our group isolated eccrine glands from redundant skin from face lifts and separated the secretory coil from the rest of the gland for cell isolation using collagenase D. The cells were then immortalised using human papilloma HPV16 E6E7 proteins and are referred to as EC23 cells. Primary eccrine sweat glands were isolated by microdissection and the secretory coil separated from the rest of the gland as described in materials and methods (2.5.1). After primary explant culture the secretory coil cells were transduced using the human papilloma HPV16 E6E7. Both HPV16 E6 and E7 proteins are oncogenes. The HPV E6 protein binds to p53 facilitating its degradation and has been shown to up regulate

the gene and promoter of hTERT, whilst the HPV16 E7 protein acts to inhibit the p16/Rb pathway and degrade Rb (Frippiat et al., 2000; Simbulan-Rosenthal et al., 2002). HPV 16 E6/E7 proteins have been widely used to immortalise human keratinocytes (Storey et al., 1988, Hawley-Nelson et al., 1982).

As the EC23 cell line was derived from the secretory coil of the eccrine sweat gland, it is thought to be heterogeneous and possibly containing both clear and dark cells of the secretory coil as well as myoepithelial cells. In this preliminary work, the cells were only partially characterised according to some secretory coil markers (unpublished data). During this time, 9 clones were derived from the EC23 cell line, with 6 of these clones surviving and will be the subject part of work carried out in this thesis Although detailed characterisation of either the EC23 cell line or the clones was not performed during this preliminary work, early experiments suggest that the EC23 cell line has the ability to form eccrine gland like structures on collagen type I organotypic cultures (Fig 1.5).

1.7 Aims and Hypothesis

We hypothesise that the EC23 cells, an immortalised cell line from the secretory coil of the human eccrine gland retains characteristics and functions of the eccrine secretory coil and can be used in vitro to develop 3D models of the secretory coil. The first aim of this thesis was to characterise the EC23 cells and the clones in order to be certain of phenotype retention of the EC23 cells and being able to identify the phenotype (clear, dark or myoepithelial) of the clones. The second

aim of the project was to assess the ability of the EC23 cell population to react to cholinergic, and β-adrenergic stimuli by assessing calcium fluxes and cAMP levels respectively. The third aim was to attempt to recreate eccrine gland like structures *in vitro*, and the final aim was to assess the possibility of the EC23 cells to contain nestin positive cells.

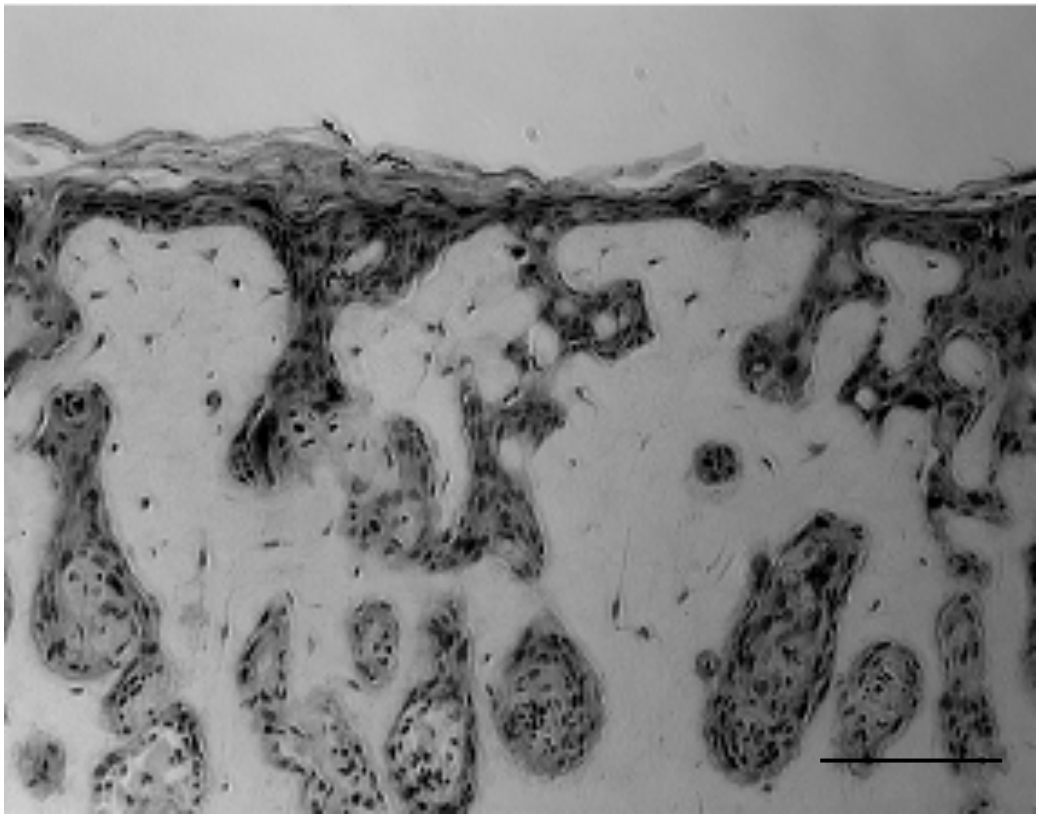

Figure 1.5 Type I collagen gel organotypic model using EC23 cells. Figure shows an initial experiment carried out prior the start of this PhD project, using EC23 cells and illustrating marked ductal structures developing within the organotypic model. Scale bar 200 μM.

Chapter 2. Materials and Methods

2.1 Cell culture methods

Normal whole human skin was obtained from redundant facelift or breast reduction surgeries (ethical committee permission was obtained from East London & The City HA Local Research Ethics Committee 2, ref: T/01/034). All cell culture was performed under aseptic conditions. Sterile flasks, culture dishes, tips and other materials were obtained from Fisher (Leicestershire, UK) unless otherwise stated. Forceps and other instruments were sterilised by autoclaving or with 70% (v/v) ethanol, (Fisher, Southborough, UK). Centrifugation was performed at room temperature (RT) in an IEC Centra-3C Centrifuge (International Equipment Company, Dunstable, UK).

2.1.1 Primary keratinocyte Isolation

Human donor skin was cleaned of excess adipose tissue, cut into 3-5mm squares and incubated overnight at 4°C in 2.5mg/ml dispase in Dulbecco's Modified Eagles Media (DMEM:F12 (3:1)) supplemented with 1% (v/v) Penicillin/Streptomycin (Sigma-Aldrich, Dorset, UK). The dermis was then separated from the epidermis using fine tip forceps and the former incubated at 37°C in trypsin for 1-2 hours, pipetting up and down to detach the keratinocytes every few minutes. The trypsin supernatant containing the cells was removed every 30 minutes and replaced by fresh trypsin. The trypsin removed was neutralised (1:1 v/v) with fully supplemented DMEM:F12, ratio, 3:1 PAA, Yeovil, UK, supplemented with 10% (v/v) FBS, 1% (v/v) PS, 2 mM L-glutamine, and RM+: EGF 10 ng/ml, insulin 5 µg/ml, transferrin 5µg/ml, hydrocortisone 0.4 µg/ml, cholera toxin 0.1nM, lyothyronine 20 pM (keratinocyte media) and

centrifuged at 1000 rotations per minute (RPM) for 5 minutes at RT and processed for cell culture as described below.

2.1.2 Primary Keratinocyte Cell Culture

For routine cell culture primary keratinocytes were cultured on a layer of 3T3 feeder cells as described by Rheinwald and Green (Rheinwald and Green, 1975). The cell suspension was centrifuged at 1000 RPM for 5 min at RT. The supernatant was aspirated and the cell pellet resuspended in 10 ml of keratinocyte media and cells counted using a haemocytometer (see Section 2.1.5) under a Nikon Eclipse Light microscope (TE2000-S with epi-fluorescent attachment, Nikon UK Ltd). Keratinocytes (2×10^6) were seeded onto a pre-prepared feeder layer consisting of 2×10^6 mouse 3T3 fibroblasts in a T75 tissue culture flask. Proliferation of 3T3 cells was halted by gamma irradiation prior to their use (see section 2.1.3). Cells were incubated overnight and the following day the media was changed to remove any dead cells.

2.1.3 Preparation of Mouse 3T3 Feeder cells

3T3s are an immortalised mouse derived fibroblast cell line from Swiss mouse embryo tissue, (Todaro and Green, 1963). These cells are used as a supporting feeder layer for the growth of keratinocytes in culture (Rheinwald and Green, 1975) by secreting nutrients and extra cellular matrix (ECM) that encourage adhesion and proliferation. 3T3s are cultured in fibroblast culture medium consisting of DMEM high glucose (PAA, Yeovil, UK) with supplements (see below for primary fibroblast culture). In order to use these cells in co-culture,

their ability to proliferate needed to be inhibited in order to prevent them from out growing the keratinocytes. To inhibit proliferation Swiss-3T3 fibroblasts were growth arrested by gamma irradiating at 60 Gy for 40 minutes and 11 seconds. Following irradiation cells were seeded at a density of 2 x 10^6 in a T75 tissue culture flask with keratinocyte medium (see Section 2.1.2). This was performed the day prior to the addition of the keratinocytes in order to allow time for the treated 3T3s to secrete nutrients into the medium.

2.1.4 Primary Fibroblast Isolation and Culture

Primary human fibroblasts were isolated from the separated dermis of neonatal foreskins by overnight incubation at 37°C in collagenase D (1mg/ml) (Roche, Welwyn Garden City, UK) in fibroblast growth media which consisted of DMEM supplemented with 10% FBS, 2mM L-glutamine and 1% (v/v) Penicillin and Streptomycin. Cells were collected by centrifugation and expanded until the second passage (see section 2.1.9); at this point stocks of fibroblasts were cryopreserved and stored in liquid nitrogen. For routine culture primary fibroblasts were plated into T175 flasks at a density of 6,000 cells per cm^2 in fibroblast growth media and growth until 70-80% confluent. Sub culturing was performed as described in section 2.1.9 in fibroblast growth media.

2.1.5 Eccrine Sweat Gland Isolation

Face-lift skin was cleaned of excess fat using 3mm blade microdissection scissors (WPI, Hitchin, UK) and cut to 3 x $3mm^2$ pieces and incubated overnight in 5.2 mg/ml at 4°C. The skin was incubated for 30 minutes at RT in 10μM neutral red

solution (Sigma-Aldrich, Gillingham, UK) in PBS to visualise the glands, and then washed with PBS. The skin was visualised using a stereo dissecting microscope (Nikon, Richmond, UK) and using fine tip forceps (WPI, Hitchin, UK) and 3mm blade microdissection scissors, the epidermis was gently disturbed to release the secretory coil of the glands. The glands were gently cut from the skin so they could be and further cleaned from remaining tissue and fat globules. A freshly isolated eccrine gland is represented in figure 2.1. For primary cell isolation the secretory coils were detached from the duct slightly below the end of the duct to ensure the origin of the cells were only from the secretory coil.

The secretory coils were transferred to fresh medium (DMEM: F12, ratio, 3:1 supplemented with 10% (v/v) FBS, 1% (v/v) penicillin streptomycin, 2 mM L-glutamine, and RM+) and incubated overnight at 37°C in a humidified atmosphere of 10% CO_2. The secretory coils from eccrine sweat glands were placed in 12-well plates (Fisher, Loughborough, UK) and covered with sufficient culture medium to form a film over the bottom of the plate and placed in a humidified incubator at 37°C, 10% CO_2. The resulting surface tension was sufficient to hold the dissected coils to tissue culture plastic and allow cells to explant (figure 2.2). After the cells began to explant, a further 1 ml of media was added and it was changed every 2-3 days.

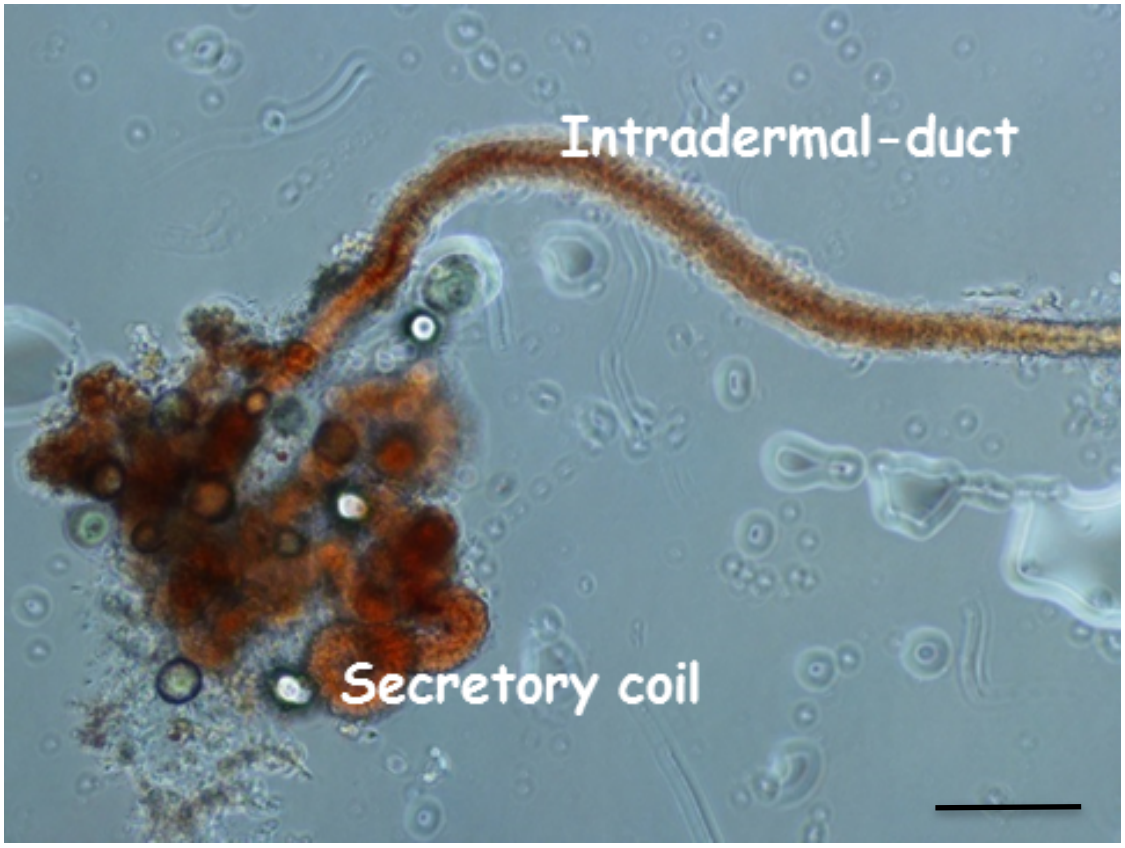

Figure 2.1. Eccrine gland isolated from facelift redundant skin. Scale bar 500 μm.

2.1.6 Primary Eccrine Coil Cell Culture

Primary eccrine secretory coil cells to be used as controls were acquired from Amsbio (Albingdon, UK) and incubated in humidified incubator at 37°C, 5% CO_2 in Eccrine Cell Medium (Amsbio, Albingson, UK). The cells were passaged 1:3 (see section 2.1.9) when they reached 60% confluency.

2.1.7 Immortalisation of human eccrine secretory coil cells using the human papilloma virus (HPV) 16 E6 and E7 proteins.

Immortalisation of primary eccrine gland secretory coil cells was carried out by former post-doctoral member of staff (Queen Mary, University of London, UK) as follows. Cells were transduced using the human papilloma HPV16 E6E7 expressed in the retroviral vector pLXSN. This retrovirus was raised in the NIH 3T3-mouse fibroblast packaging cell line PT67. E6 and E7 are oncogenes of HPV-16; E6 gene product binds to p53 facilitating its degradation and has been shown to up regulate the gene and promoter of hTERT, whilst E7 acts to inhibit the p16/Rb pathway and degrade Rb (Frippiat et al., 2000; Simbulan-Rosenthal et al., 2002).

For retrovirus production, the pLSXNE6E7 retroviral vector plasmid, which contains the HPV16E6E7 cDNA as well as a G418-resistant gene allowing for selection of transfected cells in G418-containing media, was transfected into the PT67 packaging cell line (CloneTech, Saint-Germain-en-Laye, France) by calcium phosphate precipitation, followed by selection with G418 24h later. G418 resistant cells were sub-cultured until 80% confluent. The cells were rinsed once with PBS, fresh medium was added and the cells were incubated overnight at

32°C in a humidified atmosphere of 10% CO_2. Conditioned medium from these cells containing viral particles were collected and stored at -80°C until required to infect primary cell cultures.

For immortalisation, human sweat glands were isolated as described in section 2.1.5. After the cells had explanted and a primary culture established the cells were plated in 6 well plates containing a 3T3 mouse fibroblast feeder layer3T3 (feeders) for amplification. The eccrine coil cells were dissected from the sweat glands and were infected with the pLXSNE6E7 retroviral vector plasmid, which contains the HPV16E6E7 cDNA as well as a G418-resistant gene, allowing for selection of infected cells in G418-containing media. For infection, primary secretory coil cells were incubated with serum free DMEM in the presence of polybrene (8μg/ml) for 15min. The media of each well to be infected was replaced by 1ml of the retroviral suspension containing 8μg/ml of polybrene and the plates were centrifuged for an hour at 32°C at 350rpm. Cells were incubated for an extra hour at 37°C in a humidified environment of 10% CO_2. The supernatant was removed and the cells were washed once in PBS, then incubated at 37°C in a humidified atmosphere of 10% CO_2 for 2-3 days in keratinocyte media followed by 1 week incubation in media containing G418 (400μg/ml) to select for G418 positive cells. Resistant clones were trypsinised (trypsin:versene 1:3) and cultured for amplification. Cultures infected with HPV16E6E7 retained the appearance of control primary sweat gland cultures. By approximately 2 weeks after infection, cells were passaged.

Day 3

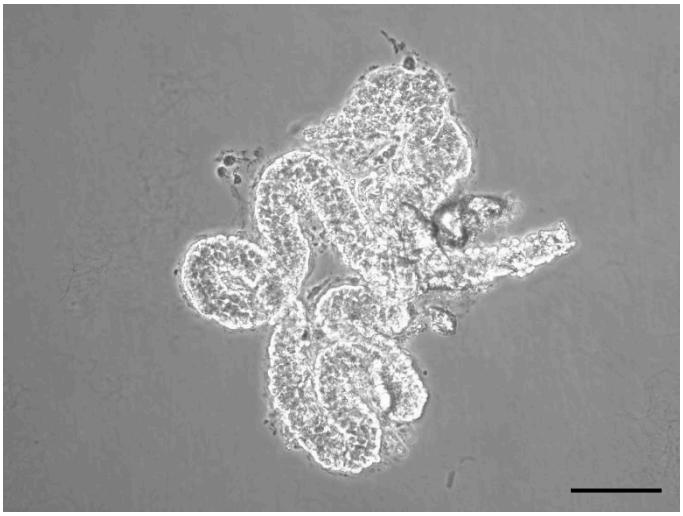

Day 7

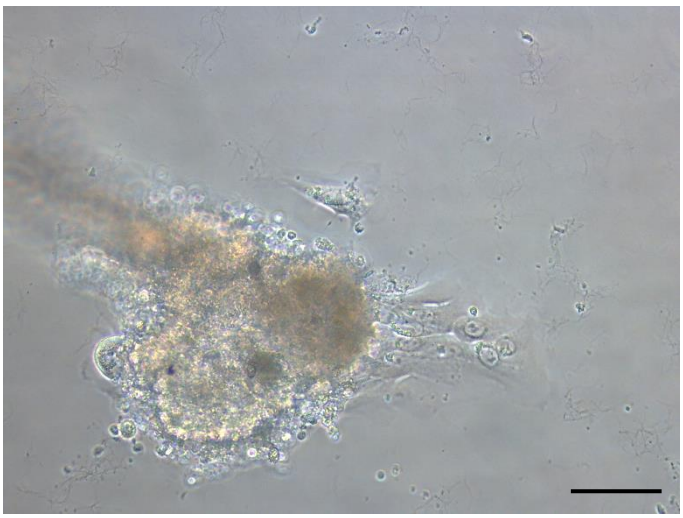

Day 12

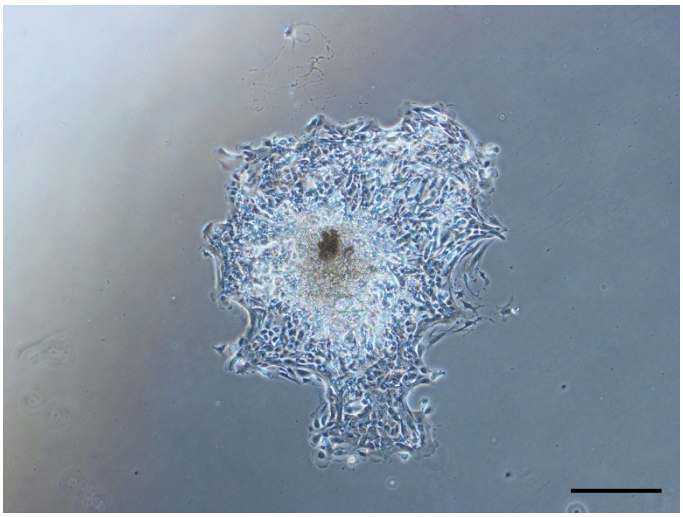

Figure 2.2. Eccrine secretory coils explanted in tissue culture plastic. At day 3 no cells can be observed explanting. At day 7 cells have begun to explant, and at day 12 a colony had begun to form. scale bar 500 μm.

2.1.8 EC23 Cell line and clone culture

EC23 cells, were derived from normal adult human donor facelift skin as described in section 2.1.6. EC23 cells were cultured in standard DMEM/F12 modified media, previously described in primary keratinocyte media (section 2.1.2) in a humidified incubator at 37^{o}C and 10% CO_2. The cells were passaged (see section 2.1.9) when they reached 80% confluency.

2.1.9 NCL-SG3 Cell Culture

NCL-SG3 cells are derived from the human eccrine sweat gland. These cells have been demonstrated to be similar to cells from the eccrine gland, by retaining their ability to react to Beta adrenergic stimuli but not cholinergic stimuli, suggesting their *in vitro* phenotype is more excretory than primary secretory coil eccrine cells (Lee and Dessi, 1989). These cells were cultured in Williams Medium E supplemented with 5% (v/v) FBS, 10ng/ml sodium selenite (Sigma Aldrich), 10ug/ml insulin, 10ug/ml hydrocortisone, 10ug/ml transferrin, 2mM L-glutamine and 10 ng/ml EFG. The cells were incubated in 5% CO_2 humidified incubator at 37^{o}C and passaged (see section 2.1.9) when they reached 80% confluency.

2.1.10 Cell Passaging.

When the cells in culture reached 80% confluency, they were passaged and reseeded at a lower concentration to encourage proliferation and, in primary cultures, to prevent differentiation. The cells were first washed in sterile PBS (Gibco, Paisley, UK) to remove all media from the flask, then incubated in versene (EDTA 0.2 g/L in PBS buffered saline, Gibco, Paisley, UK) for 5 minutes

in a humidified incubator at 37°C and 5% or 10% CO_2 depending on the cells being trypsinised. The versene was removed and the cells incubated with trypsin/EDTA (0.05% 0.02% (v:v) respectively in PBS, Gibco, Paisley, UK) for 5 minutes, at 37°C and 5% or 10% CO_2. After 5 minutes incubation with trypsin/EDTA, the flasks were gently tapped to ensure cell detachment from the tissue culture plastic and an equal amount of tissue culture media containing FBS was added to the cells. The cell suspension was then transferred to a centrifuge tube (Fisher Scientific, Loughborough, UK) and centrifuged at 1000 RPM for 5 minutes. The supernatant was removed and the cell pellet resuspended in fresh complete media and counted (section 2.1.10) and used for experiments, reseeded or cryopreserved (section 2.1.11).

2.1.11 Cell counting – Trypan Blue

Cells were counted and viability numbers calculated using trypan blue (Sigma, Poole, UK) and a haemocytometer (VWR, Leicestershire, UK). Trypan Blue is a non-toxic dye that can only penetrate the cell membrane of cells that have a damaged membrane or are dead. A volume of 10 µl of cell suspension and 10 µl of Trypan Blue 0.4% (v:v) was loaded onto a haemocytometer. The haemocytometer grid, consists of nine large squares and clear cells on five of these squares were counted, averaged, multiplied by two to account for the Trypan Blue dilution factor then multiplied by 1 x 10^4 to get the number of cells per ml.

2.1.12 Cryopreservation of cells

For cryopreservation, 80% confluent cells were detached from the surface of the flask by trypsinisation as described in section 2.1.9, recovered by centrifugation and resuspended in FBS containing 10% DMSO at a density of 2 million cells per ml in aliquots of 1 ml per cryovial. Cryovials were placed in a Mr Frosty container (Fisher, Loughborough, UK) with isopropanol at -80°C for 24 hours to allow a 1°C/min cooling rate required for successful cryopreservation of cells. After 24 hours cells were transferred to liquid nitrogen.

When required, cells were rapidly thawed by immersion in a water bath at 37°C. The cell suspension was then decanted into 10 ml of pre-warmed media containing 10% (v/v) FBS, mixed by inversion, then centrifuged at 1200 rpm for 5 min. The supernatant was aspirated and the cell pellet was resuspended in the appropriate media for cell growth and seeded at the required density for tissue culture for the immunostaining.

2.1.13 Immunocytochemistry

EC23 cells, clones 1-9 and primary eccrine sweat gland cells were cultured on glass coverslips (VWR, Lutterworth, UK) (3:1 DMEM/F12, 37^{o}C, 10% CO_2) and fixed in either ice-cold 4% (v/v) paraformaldehyde or acetone/methanol (1:1 (v/v)) when they reach 50-60% confluency. The fixative used was established during optimisation of the antibodies for each cell type.

The cells were then permeabilised (when paraformaldehyde was used) by adding 0.1% (v/v) Triton-X in PBS for 10 mins followed by three x 5 minute washes with PBS supplemented with 0.1% (v/v) Tween (PBST). The cells were then blocked by the addition of 10% (v/v) animal serum in PBS. Goat serum was used when the secondary antibody was raised in goat or donkey serum was used where the secondary antibody was raised in donkey. After blocking, cells were incubated at 4°C overnight with the primary antibody (see Table 2.1 for full antibody list). The following day, cells were washed three x 5 minutes with PBST, then incubated for 1 hour at RT in the dark with a secondary antibody (see Table 2.2 for specific secondary antibody details). The cells were then incubated for 10 minutes at room temperature in the dark with 4',6-diamidino-2-phenylindole (DAPI) (1:10000 (v/v) in PBST, Sigma, Poole, UK). Finally the cells were washed three times in PBS for 5 minutes and mounted onto microscope slides using VECTASHIELD® Mounting Media (Vector Labs, Peterborough, UK).

2.1.14 Whole-mount immunocytochemistry

Eccrine glands were isolated from the donor skin by collagenase D digestion at 0.5mg/ml in DMEM:F12 (3:1) media (1% (v/v) pen/strep, 2mM L-glutamine, 1% (v/v) RM+) and incubated over night at 37°C and 10% CO_2. The skin was then stained with neutral red diluted in PBS to a concentration of 10 μM so that the glands are visible for dissection with fine forceps as described in section 2.1.5. The glands were then washed in PBS for 1 hour to remove excess dye and fixed in 4% (v/v) paraformaldehyde for 2 hours at RT.

Antibody	Species	Dilution	Location	Source (product code)
Keratin 7 (C-68)	Mouse	1:100	Cells of the secretory coil	ABCAM (ab3973)
Keratin 8	Mouse	1:100	Cells of the secretory coil	CRUK
Keratin 14	Mouse	1:300	Luminal cells of the duct and secretory cells of the coil	CRUK (LL001)
Keratin 18	Mouse	1:200	Cells of the secretory coil	ABCAM (ab7797)
Carbonic anhydrase II	Rabbit	1:300	Cells of the secretory coil	ABCAM (ab6621)
Acetylcholine Receptor -ε	Rabbit	1:100	Secretory and myoepithelial cells	ABCAM (SC-1454)
Sodium potassium chloride co-transporter-I	Rabbit	1:200	Secretory cells	Millipore (AB3560P)
Epidermal Growth Factor Receptor	Rabbit	1:100	Cells of the secretory coil (nuclei and cytoplasm), myoepithelial cells and luminal cells of the duct.	Santa Cruz Biosciences (SC-03)
CD44	Mouse	1:300	Clear cells	BD Biosciences (550392)
Mucin 1	Mouse	1:100	Dark cells	ABCAM (ab15481)
Human Milk fat globulin (SPM291)	Mouse	1:100	Expressed in the apocrine gland, however it has been recently reported in secretory cells of the sweat gland	ABCAM (ab17787-500)
Aquaporin 5 (EPR3747)	Rabbit	1:300	Secretory coil	ABCAM (ab92320)
M3 muscarinic acetylcholine receptor	Rabbit	1:100	Luminal cells of the duct and secretory cells of the coil	ABCAM (ab60981)
Nestin – 10C2	Mouse	1:300	Putative stem cell marker (Petschnik et al., 2010a)	Millipore (MAB5326)
ORAI1	Rabbit	1:50	Calcium Channel Protein	Santa Cruz Biosciences (sc-68895)
STIM1	Goat	1:50	Endoplasmic reticulum calcium signalling protein	Santa Cruz Biosciences (sc-79106)

Table 2.1. Primary antibodies used to characterize EC23 cells clones and primary eccrine sweat gland cells.

This Alexa Fluor® 488 Goat Anti-Mouse IgG (H+L)	Goat	1:500	Invitrogen (A-11029)
Alexa Fluor® 488 Goat Anti-Rabbit IgG (H+L)	Goat	1:500	Invitrogen (A-11008)
Alexa Fluor® 488 Donkey Anti-Goat IgG (H+L)	Donkey	1:500	Invitrogen (A-11055)
Alexa Fluor® 488 Goat Anti-Mouse (IgG_1)	Goat	1:500	Invitrogen (A-21121)
Alexa Fluor® 568 goat anti-mouse (IgG_{2b})	Goat	1:500	Invitrogen (A-21141)

Table 2.2. Secondary antibodies used to characterize EC23 cells clones cells and primary eccrine sweat gland cells.

The glands were blocked in PB Buffer (0.5% (w/v) skimmed milk powder, 0.25% (v/v) fish skin gelatine (Sigma-Aldrich, Poole, UK), 0.5% (v/v) triton X-100 (Sigma-Aldrich, Poole, UK) and 98.75% TBS (Sigma-Aldrich, Poole, UK)) for 30 minutes. The primary antibodies were diluted in PB buffer as described in Table 2.1, added to the glands and incubated overnight at RT with shaking. The glands were washed in TBST for 4 hours, changing the TBST every hour, and incubated in the secondary antibody in PB buffer at RT overnight. The glands were washed again for 4 hours and incubated for 1 hour in DAPI (1:1000 v/v in PBST), the glands were washed for 4 hours and mounted on concave slides (VWR, Lutterworth, UK) for imaging with a Zeiss LSM 710 confocal microscope (Zeiss, Cambridge, UK).

2.1.15 Immunocytochemistry analysis

The images acquired in immunocytochemistry were analysed using Cell Profiler (Broad Institute, www.cellprofiler.org), a software available free online, to determine the degree of fluorescence. For the analysis performed on the EC23 cells and clones in chapter 6 for the analysis of nestin and CD44, the images acquired were split into three channels, red, green and blue. The nuclei were identified in the blue (DAPI) channel, and a minimum and maximum threshold for the nuclei was set, 20 pixels and 55 pixels respectively. Maximum correlation thresholding (MCT) was used to differentiate nuclei from the background and the image intensity was used to declump adjacent objects so that individual cells can be identified. Nuclei outside the diameter range were discarded. Cell staining was analysed using nuclei input objects. Cell outlines were determined using CD44

staining (the red channel). Nestin staining associated with the nuclei was determined using the propagation algorithm with MCT thresholding to quantify the image. The Propagation algorithm is the default approach for secondary object creation, creating each primary object guided by the input image and limited to the foreground region as determined by the chosen thresholding method. The image intensity and the stained area was measured for each cell and the integrated intensity was generated. For all immunocytochemistry images the negative control was also measured and subtracted from the measurements of the fluorescence measurements of the immunocytochemistry fluorescence measurements to gain the real fluorescence measurements for each image.

2.2 Pharmacology

2.2.1 Calcium flux

Calcium flux analysis was performed using a Fluo-4 Direct assay kit (Life Technologies, Paisley, UK). EC23 cells were seeded onto Fluorodish™ cell culture dishes (World Precision Instruments, Hitchin, UK) under standard cell culture conditions (section 2.1) until they were 40-50% confluent. The cells were then incubated in 1:1 solution of phenol red free DMEM/F12 (1:1) cell culture media supplemented with RM+, 1% penicillin/streptomycin, 1% L-glutamine and Fluo-4 reagent (made as specified by the manufacturer) at 37°C in a humidified incubator (CO_2% depended on the cells being assayed) for 40 minutes. After 20 minutes in culture, some dished were treated with 100 nM atropine and others with 10 mM ryanodine, controls dishes received no treatment. The cells were then

place on an inverted Leica DM5000B epi-fluorescence microscope fitted with a timelapse camera. Images were taken for 121 frames (the time between frames was 3 seconds). To stimulate a cholinergic response, at frame 10 (30 seconds), carbachol (Sigma-Aldrich, Poole, UK) was added to achieve a final concentration of 1 mM. To ensure the cells were still able to release their calcium stores from the endoplasmic reticulum, 4 μM of ionomycin (Sigma-Aldrich, Poole, UK) was added at frame 90 (270 seconds).

2.2.2 cAMP metabolism

The EC23 cell line, clones derived from EC23 cells, NCL-SG3 cells and primary eccrine gland cells were seeded on a 96 well plate at a density of $6x10^3$ cells per well and incubated overnight under normal culture conditions that were associated with the specific cell lines. The cells were washed with 200 μl of PBS warmed in a 37°C water bath prior to a 3 minute incubation with 1 μM isoproterenol (Sigma-Aldrich, Poole, UK) in PBS. The cells were then washed three times with ice cold PBS and 100 μl of 1X lysis buffer as supplied in the cyclic AMP XP assay kit (Cell Signalling Technologies, Hitchin, UK) was added to each well and incubated on ice for 5 minutes. The lysates were then transferred to microcentrifuge tubes and stored at -20°C until used.

To assay the level of cAMP, a cyclic AMP XP kit was used following the manufacturers guidelines. Briefly, 50μl of the HRP-linked target solution and 50 μl of the cell lysates were added to the antibody-coated 96 well plate provided by the kit, and incubated in the dark for 3 hours at RT on an orbital shaker. Standards were also prepared and assayed to establish a standard curve. The contents of the

wells were then discarded and washed four times with wash buffer, and 100 µl of TMB substrate was added and incubated for 30 minutes, at which point 100 µl of stop solution was added. The absorbance was read at 450 nm using a Synergy HT plate reader (BioTek Bedfordshire, UK)

2.3 3-D Organotypic Models

2.3.1 De-epidermalized Dermis

Donor cadaveric dermis was obtained from Eurobank, European Tissue Bank (Denmark). The dermis was washed in sterile PBS three times to remove the glycerol in which it was stored and then it was incubated in PBS for 2 weeks. The incubation aided the removal of the epidermis from the dermis so that the epidermis could easily be removed using a No. 10 disposable sterile scalpel (Fisher Scientific, Loughborough, UK) and the dermis cut into 1.5 cm^2 square pieces. A square of the de-epidermialised dermis (DED) was placed in a well of a 6-well Falcon ™ tissue culture plate (Fisher Scientific, Loughborough, UK), reticular side up and a 1 cm diameter metal ring was placed on top. Primary dermal fibroblasts ($5x10^5$) were seeded inside the ring. DMEM/F12 (3:1) RM+ fully supplemented media (as described in section 2.1.1) was also added to the outside of the ring and incubated in a humidified incubator at 37°C, 5% CO_2 for five days, changing media every two days. Then DEDs were then turned so that the papillary side was up the ring was replaced and 5 x 10^5 keratinocytes, EC23 cells or a 1:1 (v/v) mixture of EC23 and keratinocytes, in keratinocyte media were added. Fresh DEMEM/F12 (3:1) RM+ media was also added to the outside of the rings and returned to the incubator. The next day the ring was removed and the

DED was raised to the air-liquid interface using metal grids and cultured for 2 and 3 weeks in a humidified incubator at 37°C, 10% CO_2 , changing media every 2 days.

Following two weeks growth, one half of each DED was fixed in 4% (v/v) paraformaldehyde overnight at 4°C and then placed in 70% (v/v) ethanol for tissue processing and paraffin wax embedding (see Section 2.5.1). The other half was frozen by immersing in cryo-M-bed on dry ice until set and then stored at -80°C until required.

2.3.2 Type I Collagen gels

The following method was obtained from Professor Gareth Thomas (Tumour Biology, Charterhouse Square, Barts and The London, UK) (Nystrom et al., 2006; Nystrom et al., 2005). To make the collagen gels, rat tail collagen type I (BD Biosciences, Oxford, UK) was used. Quantities stated are per gel, which were prepared on ice with pre-cooled pipette tips by adding 7 volumes of collagen type I, 1 volume of 10x MEM (Invitrogen, Paisley, UK). The solution was neutralised to 7.4 pH, measured with litmus paper (VWR, Lutterworth, UK), by drop-wise addition of 0.1 M sodium hydroxide (NaOH) and gently mixed by pipetting up and down, taking care not to incorporate air bubbles. After the collagen solution was neutralised to pH 7.4, $5x10^5$ fibroblast suspended in FBS were added to the collagen and mixed by pipetting up and down. The 2.5ml collagen/fibroblast suspension was then added to each well of a 12-well plate (VWR, Leicestershire, UK) and allowed to solidify for 30 min in a 37°C incubator. After the gels had set, the edges were detached from the plate and filled with fibroblast culture media

and changed every two days. On day five, 5 x 10^5 primary keratinocytes, EC23 cells or a 1:1 (v:v) mixture of both were seeded on top of the gels using a metal ring and allowed to adhere overnight in a 10% CO_2 humidified incubator at 37°C incubator. Meanwhile, gels containing nylon sheets were prepared using the same method above but without the addition of fibroblasts. A gel solution (500 µl) was added to a 1.5 cm^2 nylon sheet (Sefar Ltd, Lancashire, UK) and incubated at 37°C for 30 mins to set. The nylon sheets were then fixed by the addition of 1% (v/v) glutaraldehyde (Sigma-Aldrich, Poole, UK) in sterile water for 2 hr at 4°C. Three times PBS washes were performed and finally media was added. Sheets were incubated at 4°C overnight. The metal ring on the collagen gels was removed after overnight incubation. After two days, the gels were transferred to 6 well plates (Fisher, Loughborough, UK) and raised to the liquid air interface using sterile metal grids, with the nylon sheets in between the gels and the grids. The gels were incubated for 2 and 3 weeks changing media every two days. At the end of the experiment, the gels were removed from the grids, fixed overnight in 4% (v:v) paraformaldehyde at 4°C and then placed in 70% (v:v) ethanol for tissue processing and paraffin wax embedding.

2.3.3 Matrigel Sphere Forming Assay

For this assay growth factor reduced matrigel was used (for full composition see Appendix). Using an ice cold pipette tip, 25 µl of matrigel was used to coat the bottom of each well of a 96 well plate (Fisher Scientific, Loughborough, UK) and

incubated at 37°C for 30 minutes. During this time, EC23 cells were trypsinised and counted using trypan blue as described in section 2.1.10. The matrigel was

then mixed with EC23 cells in suspension (in standard 3:1 DMEM:F12 containing 10% (v/v) FBS, 1% (v/v) penicillin streptomycin, 2mM L-glutamine, and RM-: insulin 5µg/ml, transferrin 5µg/ml, hydrocortisone 0.4µg/ml, cholera toxin 0.1nM, lyothyronine 20pM), to achieve a cell density of 300 cells per well, at a ratio of 2:1 (v:v) respectively and incubated for a further 30 minutes. Media containing 0, 5, 10, 15, 20 and 25 ng/ml of either EGF, BMP, BMP4 or EDA (all recombinant proteins acquired from Cambridge Biosciences, Cambridge, UK) were prepared and 100 µl added to the wells, as depicted in Figure 2.3.

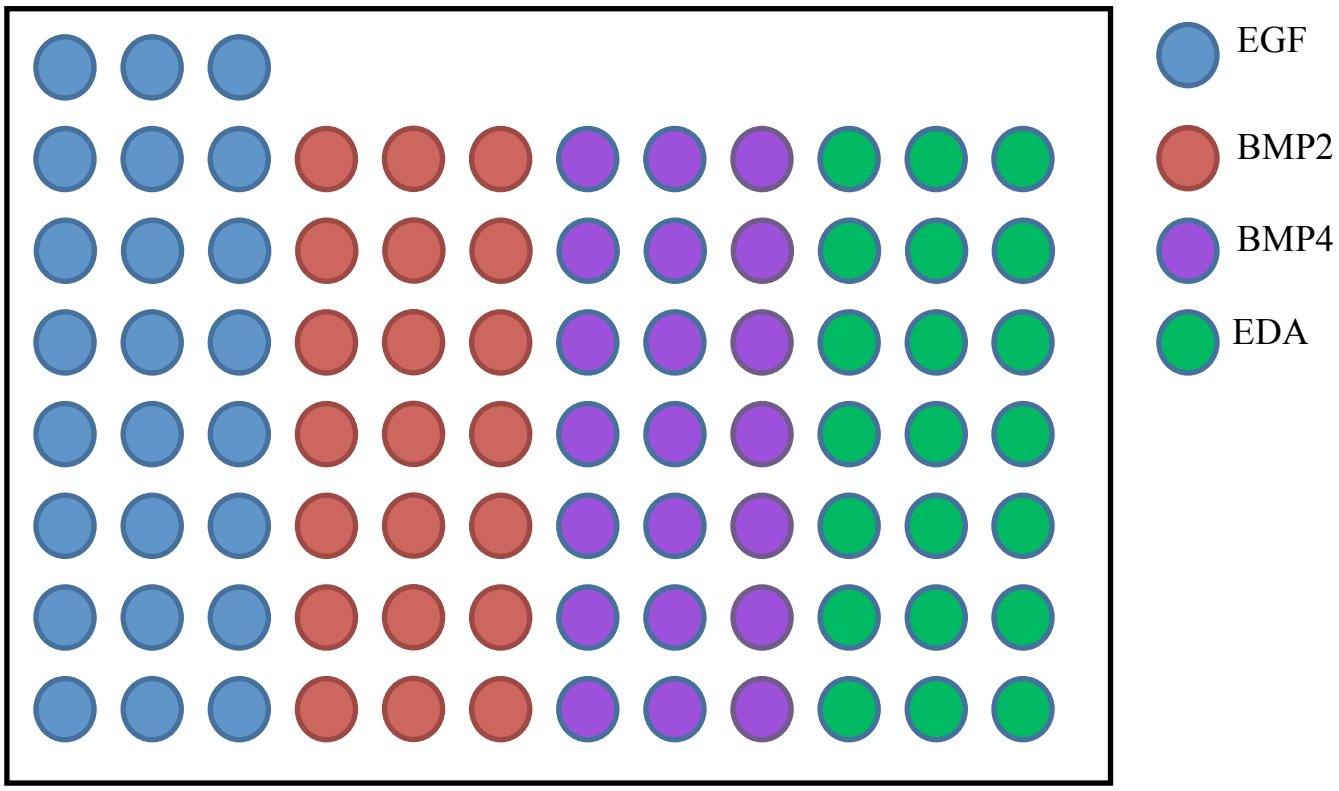

Figure 2.3. Organisation of growth factor treatment of EC23 cells seeded on GFR matrigel.

2.4 High-Content Fluorescence microscopy.

2.4.1 System.

All high-content fluorescence microscopy images were captured using the IN Cell 1000 automated microscope (GE Healthcare, UK) at 4x magnification and analysed using the Developer Tool Version 1.7 (GE Healthcare, UK).

2.4.2 Imaging.

The plates seeded in section 2.5 were imaged under brightfield. For each well, 4 fields were taken with 30 Z stack slices at 100 μm intervals in order to be able to analyse the spheres at their maximum branching. Figure 2.4 depicts the difference between images taken in the same well and field through the Z stack.

2.4.3 Analysis

Images taken for high-content analysis were examined using a protocol designed to determine the degree of branching of the spheroids produced in the experiment at different time points. To remove artefacts and to pick up only spheroids, an acceptance criteria was included in the protocol. For objects to be accepted, they were required to have a density levels of < 900 and an area of > 4000 μm^2. The next step to analyse the organoids was to segment the target sets based on intensity of the density levels. Segmentation parameters were put in place with a minimum threshold of 0 and a maximum threshold of 392 units. Post-processing parameters were then set up to help reduce artefacts and clearly identify individual

spheroids. These including dilation, fill holes, sieve (binary), watershed clump breaking and erosion.

First, a dilation function of a kernel size of 3 was put in place; this operation enlarges the boundaries of bright objects, followed by a fill holes function to fill blank spaces in the object mask so that measurements of whole objects can be made. Following this, a sieve (this function uses a size threshold to filter segmented targets) was set to remove objects with an area smaller than 80 μm^2, and a second dilation was added, this time with a kernel set at kernel size of 6. Next, a watershed clump breaking function was included, in order to separate multiple objects clumped together as a single object e.g. when the targets are so close together that their inter-cellular boundaries are not distinguishable, into segmented objects. A further sieve was set as before, concluding with an erosion function to shrink the boundaries between objects that are too close together in order to differentiate between the two. Figure 2.5 shows a stepwise representation of the steps described above.

After post processing, the data collected was further processed in order to only include objects that were in focus. This was done using excel and the XY position of the objects and their diameter. Only the spheroids that were in focus were used in the analysis of the branching. It is worth noting that it is possible that the spheroids formed were not within reach of the microscope and thus some data was lost. The degree of branching, or branching nodes, was deemed the best measure to be used to study the morphogenesis of eccrine gland like structures as the morphology of the eccrine gland is of a coiled nature and also because we wanted

to study the effect of growth factors on morphogenesis and other parameters would mostly measure size and not shape changes. Furthermore, preliminary staining of the spheroids was compared with wholemount immunohistochemistry of eccrine glands isolated from redundant skin samples, which showed that the branching morphology of the spheroids is comparable to the secretory coil of the human eccrine gland.

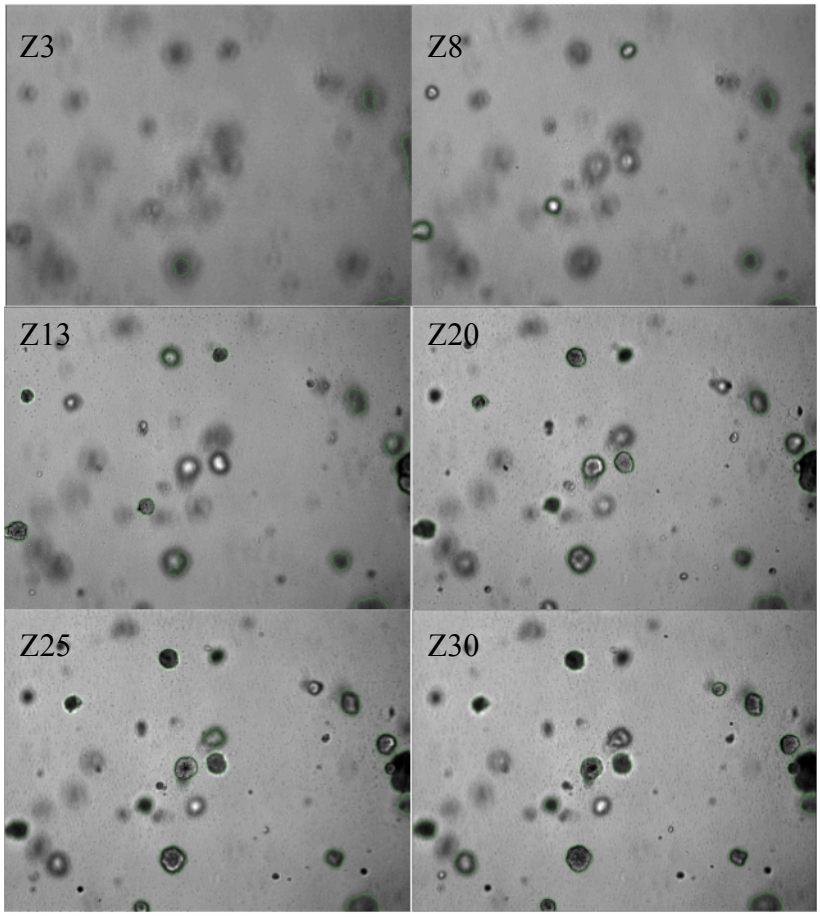

Figure 2.4. Representation of images taken with the IN Cell microscope taken on the same well, same field at different positions within the Z stack. Positions Z3, 8, 13, 20, 25 and 30 are shown. In positions Z3, Z8 it can be seen that the protocol is picking up on objects (Green outline) that are not in focus, as the microscope moves deeper into the gel Z13, Z20 Z25 and Z30 it is observed that the analysis software picks out spheroids that are more in focus. All images taken at 4x magnification.

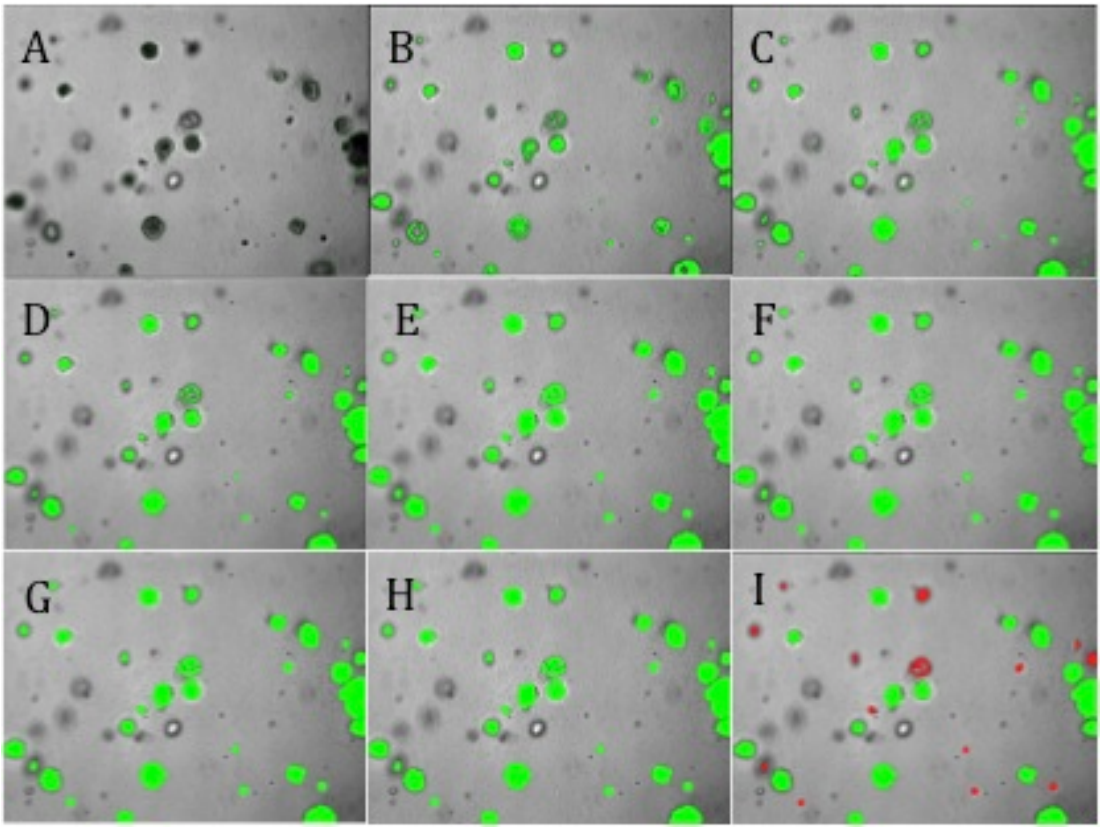

Figure 2.5. Images depict a stepwise representation of the analysis protocol. (A) Shows the original bright field image. (B) shows the initial segmentation step, in which parts of the objects are being picked up and masked in green. (C) shows the dilation function used to fill in gaps in the objects, followed by (D) in which a sieve was applied. In (E) a second dilation was applied followed by a watershed clump breaking (F) to separate objects clumped together into separate segmented objects. (G) shows the effect of a second sieve, followed by the last step of erosion (H). (I) Shows the final result of the post processing steps, with the real objects that will be measured in the analysis in green and the objects that were excluded in red by using the acceptance criteria.

2.5 Histology

Paraformaldehyde fixed paraffin embedded sample sections were cut (5 μM thick) using a microtome (Leica, RM2235), placed on slides and allowed to dry at 37°C overnight. Sections were dewaxed and rehydrated, then stained with haematoxylin and eosin as described in table 2.2. Sections were mounted with DePex mounting medium (Fisher Scientific, UK) and observed using a Leica DM5000B microscope microscopy.

2.6 FACS

2.6.1 FACS Analysis

All reagents used were ice cold. Cells ($5x10^5$) were added to five x 15ml centrifuge tubes (Fisher Scientific, Loughborough, UK), four tubes were to be used to measure CD44, Nestin and IgG (as a control) and one tube was for an unstained control sample. The cells were fixed in 0.01% (w/v) PFA for 10 minutes, then excess PBS was added and samples were centrifuged at 1000 RPM. The supernatant was aspirated to remove the PFA, the cells were then permeabilised for 10 minutes in 0.1% (v/v) Triton X. Excess PBS was added and the cells were centrifuged at 1000 RPM. The supernatant was aspirated and the cells were resuspended in blocking solution (10% (v/v) goat serum in PBST for 30 minutes. The cells were again centrifuged at 1000 RPM, the supernatant removed and the primary antibody (10μg/ml) (table 2.4) was added and incubated for 15 minutes at 4°C. Excess PBST was added and the samples were centrifuged at

Treatment Number	Treatment	Time
1	100% (v/v) Ethanol	1 minute
2	100% (v/v)Ethanol	1 minute
3	70% (v/v) Ethanol	1 minute
4	Tap water	1 minute
5	Haematoxylin	5 minutes
6	Tap Water	3 minutes
7	Acid Alcohol (1% v/v)	6 seconds
8	Scott's Tap Water (until blue)	~5 minutes
9	Tap water	<1 minute
10	Eosin (1% v/v)	5 minutes
11	Tap water	1 minute
12	70% (v/v) Ethanol	1 minute
13	100% (v/v) Ethanol	2 minute
14	Xylene	1 minute
15	Xylene	1 minute

Table 2.3. Stepwise protocol for tissue dewaxing, rehydration and haematoxylin/eosin (H&E) staining, all stages were performed at RT.

1000 RPM. The supernatant was aspirated and the cell pellet was resuspended in the secondary antibody (Table 2.3) at a dilution of 1:2000 in PBST for 15 minutes at 4°C. The cells were washed three times by resuspending in excess PBS and centrifuging at 1000 RPM. The cells were finally resuspended in 500 µl of PBS and analysed using a Canto II cell analyser (BD Biosciences, Oxford, UK).

Type	**Antibody**	**Species**	**Isotype**	**Source (Cat. No)**
Primary	Nestin	Mouse	IgG_1	Millipore (MAB5326)
Primary	CD44	Mouse	IgG_{2b}	BD Pharmingen, UK (550392)
Primary	CD29-Alexa Fluor® 640	Hamster	IgM	BD Pharmingen, UK (561794)
Secondary	Alexa Fluor® 568 goat anti-mouse (IgG_{2b})	Donkey	IgG_{2b}	Invitrogen, UK (A-21144)
Secondary	Alexa Fluor® 488 Goat Anti-Mouse (IgG_1)	Donkey	IgG_1	Invitrogen, UK (A-21121)

Table. 2.4. Antibodies used in FACS analysis.

2.7.2 FACS Sorting

All reagents used were ice cold. After trypsinisation, cells (1 x 10^6) were placed in a 15 ml falcon Fisher Scientific, Loughborough, UK), centrifuged in excess PBS to remove media residues. The cells were resuspended in blocking solution (10% (v/v) goat serum in PBST) for 30 minutes. The cells were again centrifuged at 1000 RPM, the supernatant removed and the primary antibody, CD44 at 10µg/ml in PBS and incubated for 15 mins at 4°C. Excess PBST was added and the samples were centrifuged at 1000 RPM. The supernatant was aspirated and the cell pellet was resuspended in the secondary antibody (Alexa Fluor® 568 goat anti-mouse (IgG_{2b}) at a dilution of 1:2000 in PBS for 15 minutes at 4°C. The cells were washed three times by resuspending in excess PBS and centrifuging at 1000 RPM. The cells were finally resuspended in 500 µl of PBS and sorted using an Aria cell sorting machine (BD Biosciences, Oxford, UK).

2.8 Statistics

Statistical analysis was determined using a one way analysis of variance (ANOVA) followed by a Tukey's post hock test or a two way ANOVA with a Bonferroni post hoc test depending on the number of variables between test samples, i.e.: two or three, respectively. All statistical evaluations were performed using Graph Pad Prism 5.0 software (San Diego, CA, U.S.A). Significance was assessed in all experiments as a probability value of *P<0.05, **P < 0.01, ***P <0.001 or not significant (NS) P > 0.05.

Chapter 3.
Characterisation of the EC23 cell line and its Clones

3.1 Introduction

As previously described in Chapter 1, the human eccrine sweat gland is a unique appendage of the skin, with its main function being thermoregulation. To date, research on the human eccrine gland has been restricted in part due to the limitation of existing in vitro models. Primary cultures of human eccrine sweat gland epithelial cells have several limitations. The limited access to freshly isolated human tissue, the isolation of the glands and preparation of the primary cultures are difficult and with a poor yield leading to insufficient experimental material for studies. For these reasons the generation of immortalized cells would represent an unlimited source of material for routine studies.

Lee and Dessi (1988) have generated an immortalized eccrine sweat gland cell line named NCL-SG3 from a post-mortem skin sample from a 72 years old male using the simian virus 40 (SV40). However these cells appear to have a functional phenotype characteristic of the reabsorptive duct rather than the secretory coil. Buchanan *et al,* (1990) have immortalised 4 sweat gland cell lines from normal individuals and 4 from patients with cystic fibrosis using a chimeric virus Ad5/SV40. However, all the normal sweat gland cell lines were established from the reabsorptive duct and not the secretory coil.

As described in Chapter 2 of this thesis (section 2.1.7) a previous researcher in the laboratory developed an immortalised cell line (EC23) derived from the secretory coil of human eccrine glands (unpublished data) and 8 clones from the EC23 cell

line, clone 1, clone 2, clone 3, clone 4, clone 5, clone 7, clone 8 and clone 9. Clone 6 did not survive.

The aim of the work presented in this chapter was to characterise the EC23 cell line and clones developed from this cell line using markers that are associated with the eccrine gland. These include the keratins 7, 8, 14, 18, (Sato et al., 1991, Li et al., 2009, Tao et al., 2010), sodium potassium co-transporter I (Nejsum et al., 2005, Cui et al., 2012), carbonic anhydrase II, aquaporin 5 (Nejsum et al., 2002, Ma et al., 2007, Bovell et al., 2011), acetylcholine receptor epsilon, muscarinic receptor M3 (Grant et al., 1991, Schiavone and Brambilla, 1991), epidermal growth factor (Saga, 2001, Li et al., 2002), CD44 (Penneys, 1993, Wilke et al., 2006, Bovell et al., 2007), mucin 1 (Kim do et al., 2006), and milk fat globulin (Wilke et al., 2006, Bovell et al., 2007). Emphasis was placed on the functional markers carbonic anhydrase II, sodium potassium co-transporter I, muscarinic receptor M3 and Acetylcholine receptor epsilon. The presence or absence of these markers can help determine the likelihood of retention of a secretory phenotype as well as aid in the identification of the clear and dark cells within the EC23 cell line and its clones.

3.2 Characterisation of the EC23 cell line and clones using a panel of markers characteristic of the human eccrine secretory coil.

EC23 cells, clones derived from the EC23 cell line, and primary sweat gland cells were cultured on cover slips, fixed and stained by IF for a panel of keratins and sweat gland specific protein markers. In addition where possible a control cell line

that is known to express the marker in question as a positive control was used in the staining. EC23 cells and all clones showed positive staining for keratins K7, K8 and K18 which are expressed in the secretory coil cell of the eccrine sweat gland (Li et al., 2009, Tao et al., 2010) and keratin K14 which is expressed in secretory cells and luminal cells of the eccrine duct (figures 3.1 to 3.4)(Li et al., 2009).

Keratin K7 (figure 3.1) was expressed in the EC23 cells although expression in individual cells did show considerable variability with some cells having very strong K7 expression and others very weak. This may reflect the heterogenic nature of the original cell line. This heterogeneity was further seen in the individual clones. Clone 1 showed weak expression of K7 as did clones 3, 4, 8 and 9. Clone 2 distinctively expressed very low levels of K 7. In contrast clones 5 and 7 showed strong K7 expression and this was comparable with the HELA control cells. In contrast the primary eccrine sweat gland coil cells weakly expressed K7. In both the primary EC23 cell line and in the clones K7 was expressed in the cytoplasm although in some clones strong perinuclear staining was detected.

Keratin K8 (figure 3.2) was expressed very weakly in the EC23 cell line and in many cells appeared negative. In contrast strong expression was detected in clones 1, 4, 5 and 9. Weaker staining was detected in clones 2, 3, 7 and 8. K8 was not detected in primary eccrine sweat gland coil cells. K8 was expressed in HepG2 control cells.

Keratin K14 (figure 3.3) was expressed in both the EC23 cell line and in all clones as well as control keratinocytes. In the EC23 cell line expression was variable with some cells showing strong K14 expression and others weaker expression. All clones showed similar patterns of expression with the clonal lines also showing marked perinuclear expression of K14. This was also seen in the primary eccrine sweat gland coil cells, which showed much weaker levels of K14 expression.

Keratin K18 (figure 3.4) was expressed in the EC23 cell line and showed variable expression in the clones. In particular clones 1, 4, 5, 7 and 8 showed very weak staining for K18. Clone 2 also very weak to negative. In contrast clones 3 and in particular clone 9 showed very strong K18 expression. Control HepG2 cells also showed variable levels of K18 expression. Primary eccrine sweat gland coil cells were also only very weakly stained.

Carbonic anhydrase II (figure 3.5) was expressed in all cells investigated. Strong cytoplasmic staining was observed in the EC23 cell line as well as in clones 2, 5, 7 and 8 as well as in the primary eccrine sweat gland coil cells. Weaker but still pronounced staining was seen in clones 1, 3 and 9 as well as HEK293 control cells. In addition to the cytoplasmic expression of carbonic anhydrase II punctate nuclear expression was also observed.

CD44 (figure 3.6) was expressed in the EC23 cell line where expression was mainly membranous with some cytoplasmic staining. Considerable variation was detected across the clones. In particular clones 2, 4, 7 and 9 strongly expressed

CD44 in clone 2 expression was strongly cytoplasmic and also perinuclear although not in all cells. In clone 4 and 7 CD44 was predominantly cytoplasmic although some strong cytoplasmic staining was also seen. In clone 9 strong cytoplasmic staining was seen. In contrast clone 2, 3, 5 and 8 expressed much weaker staining for CD44 and this was generally cytoplasmic. Human keratinocytes also expressed strong cytoplasmic CD44 and in the membrane. Primary eccrine sweat gland coil cells were also positive for CD44 although again staining was variable with both membranous and cytoplasmic expression observed.

The acetylcholine receptor subunit epsilon (AChR-ε) showed variable expression in all cells investigated (figure 3.7). EC23 cells appeared to express AChR-ε evenly throughout the cytoplasm, however clones 1 and 2 seem to have higher expression of the receptor but expression was within the cytoplasm and in some cells perinuclear. Similar expression was also seen in HepG2 control cells. Clone 3 was very weakly stained for AChR-ε and clone 4 showed very distinct but punctate expression in the nucleus. Clones 5 and 8 strongly expressed AChR-ε but mainly cytoplasmic. AChR-ε was also detected in clones 7 and 9 but this was much weaker cytoplasmic expression. Primary eccrine sweat gland coil cells also expressed AChR-ε but this was very weak and cytoplasmic.

Epidermal growth factor receptor (EGFR) can be found on the membrane of secretory cells of the coil, myoepithelial cells and to a lesser extent on luminal ductal cells, and more recently it has been reported in the nuclei of secretory cells (Li et al., 2009, Li et al., 2002) . On EC23 cells as well as clones 3, 4, 5, 7, 8 and

9 EGFR was found both in the membrane and the cytoplasm (figure 3.8). The staining pattern was similar in primary cells, however it was much fainter in primary cells compared to the EC23 cell line and clones (figure. 3.8). Clone 2 appears to form clusters of cells that strongly express the EGFR whereas clone 1 did not show any EGFR expression.

Muscarinic receptor M3 is found on secretory cells of the coil and luminal cells of the duct (clear cells) (Sato et al., 1989, Lei et al., 2008). In figure 3.9, all cells showed expression of the M3 receptor, mainly in the nuclei. Expression does seem to vary between clones, with clone 3, 8 and especially 9 having high levels of expression and this was similar in the control HepG2 cells. In contrast in clones 1, 2, 4 and 7 expression in the nucleus was much more punctate. Primary eccrine sweat gland coil cells showed very weak cytoplasmic staining.

Sodium potassium chloride co-transporter I (NKCC1) is important in the secretions of Na^+, K^+ and Cl^- in the coil and their reuptake in the duct (Nejsum et al., 2005, Bovell et al., 2011). EC23 cells, clones 4, 5, 7 and 9, and primary sweat gland cells show expression of NKCC1 (figure. 3.10). Clones 1, 2, 3, and 8 do not appear to express this transporter, suggesting these cells may not have retained their secretory phenotype. In EC23 cells expression is distinctly punctate in the nucleus whereas in clones 7 and 9 expression is more diffuse. NKCC1 was weakly cytoplasmic in Primary eccrine sweat gland coil cells and was detected in the nuclei our control HEK293 cells.

Mucin 1 (MUC1) is thought to be a marker specific to the sweat gland dark cells (Li et al., 2009). Expression of this marker (figure.3.11) was found in EC23 cells, clones 3, 4, 5, 7, 8 and 9. However levels of expression varied considerably and mucin-1 was mainly punctate and nuclear in EC23 cells and in clones 3, 7 and 8. Expression in clones 4 and 5 was very weak and mainly cytoplasmic and in clone 9 extremely weak. In keratinocytes expression was cytoplasmic. In clone 1 and primary sweat gland cells, expression was also very weakly cytoplasmic.

Human milk fat globulin (HMFG) has been described as a marker for distinguishing between the eccrine and apocrine glands, however it has recently also been reported to be expressed by the secretory cells of the eccrine glands (Bovell et al., 2007). EC23 cells, clones 3 and 7 showed weak expression of HMFG where it was mainly cytoplasmic, with clone 9 expressing very low levels and only few cells of clones 1 and 5 expressing HMFG1. Clones 2 and 3, and primary cells were negative. HELA cells were positive for HMFG1, with varied levels of cytoplasmic staining.

Aquaporin 5 is expressed in secretory cells of the sweat gland and was detected in all cells investigated although with varying levels of expression (figure 3.13). In EC23 cells aquaporin 5 was perinuclear and also punctate in the nucleus. Clone 2 was very weakly cytoplasmic. In the other clones aquaporin was mainly cytoplasmic and perinuclear. Primary eccrine sweat gland coil cells were only very weakly stained as were HEK293 cells.

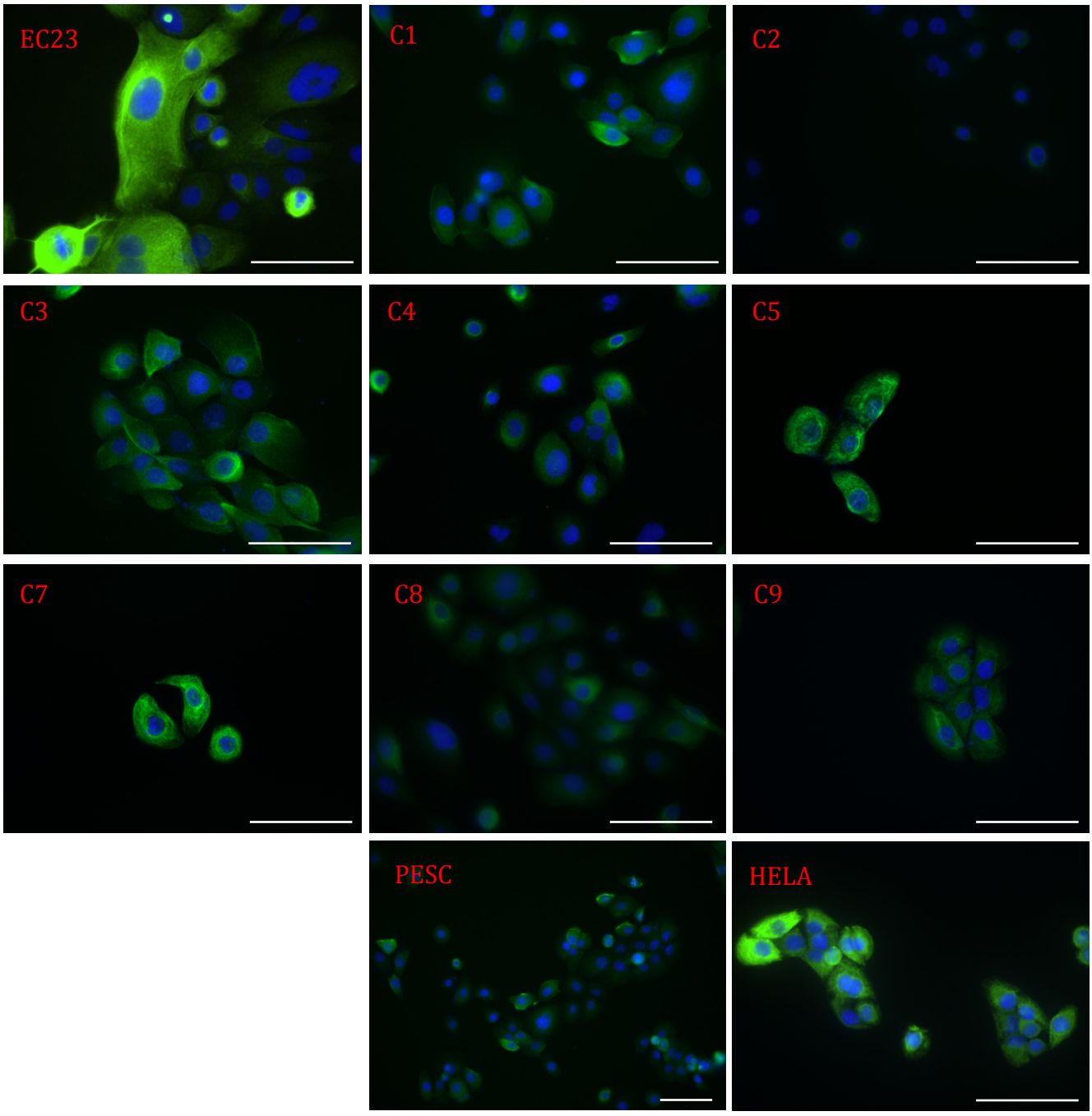

Figure 3.1. Immunocytochemistry showing expression of keratin K7 in the EC23 cell line and in clones derived from the EC23 cell line as well as in primary eccrine gland secretory coil cells (PESC) and HELA cells (positive control). Scale bar 100 µm.

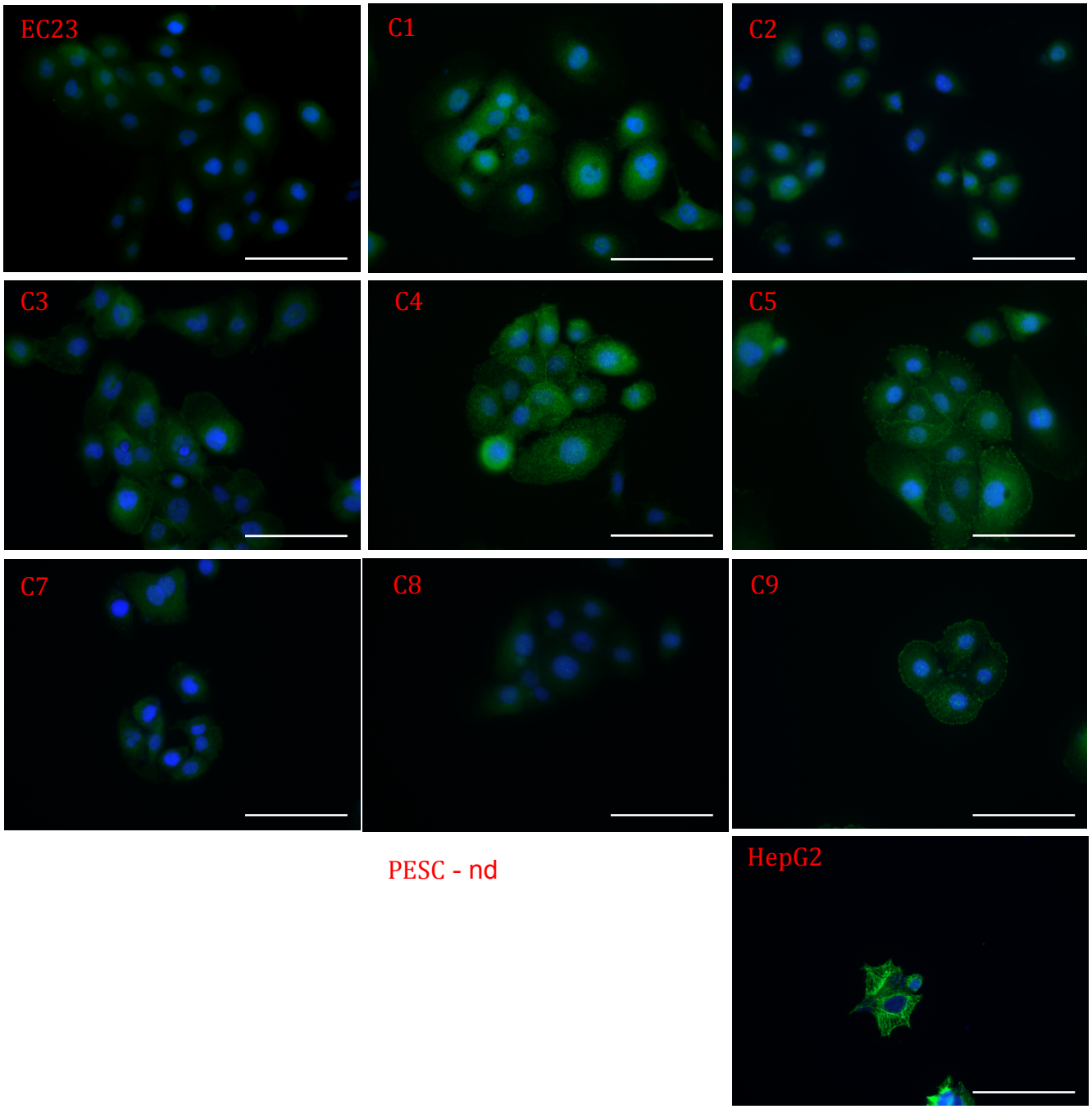

Figure 3.2. Immunocytochemistry showing expression of keratin K8 in the EC23 cell line and in clones derived from the EC23 cell line as well as in primary eccrine gland secretory coil cells (PESC) and HepG2 cells (positive control). Scale bar 100 µm.

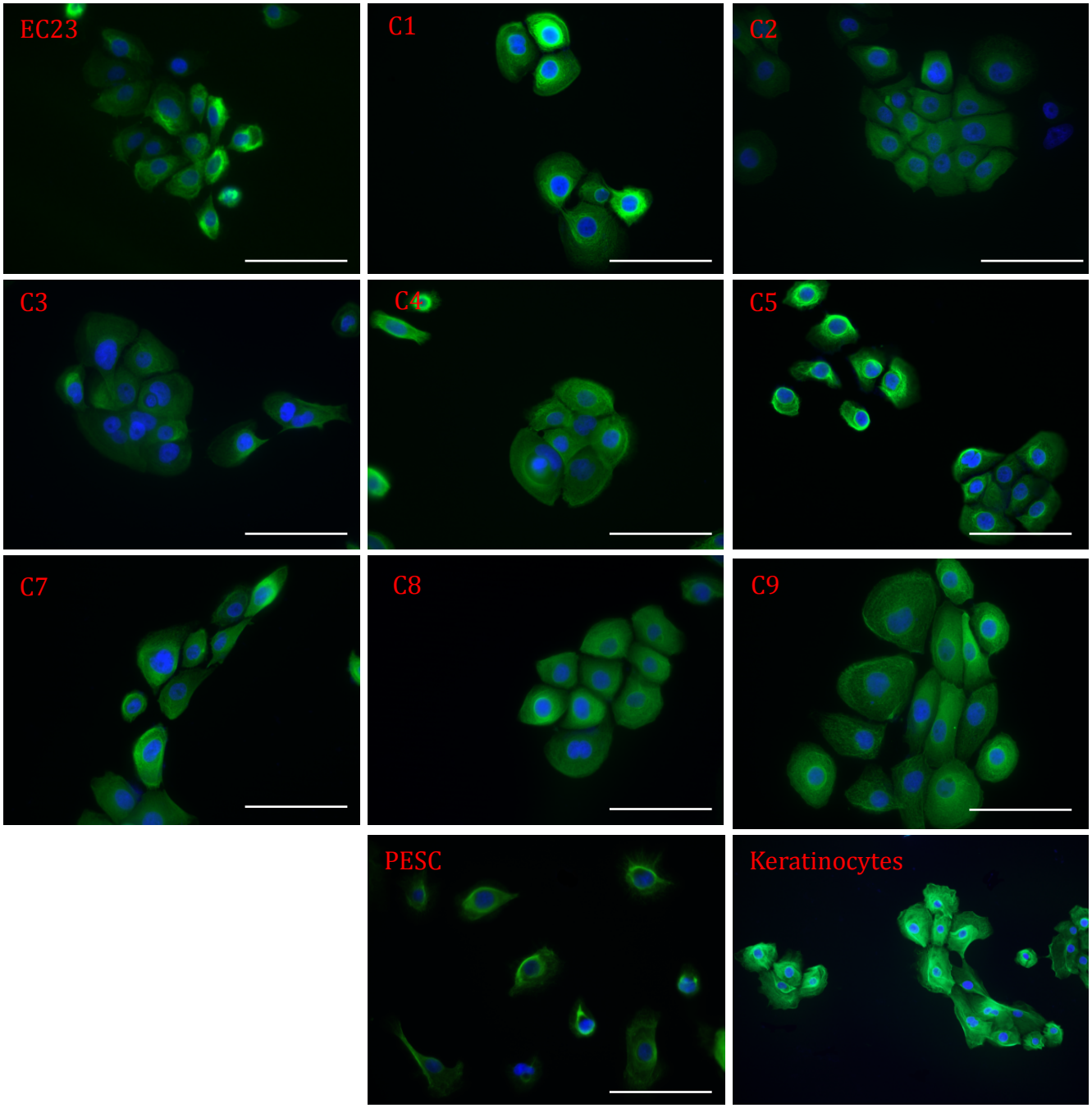

Figure 3.3. Immunocytochemistry showing expression of keratin K14 in the EC23 cell line and in clones derived from the EC23 cell line as well as in primary eccrine gland secretory coil cells (PESC) and keratinocytes cells (positive control). Scale bar 100 µm.

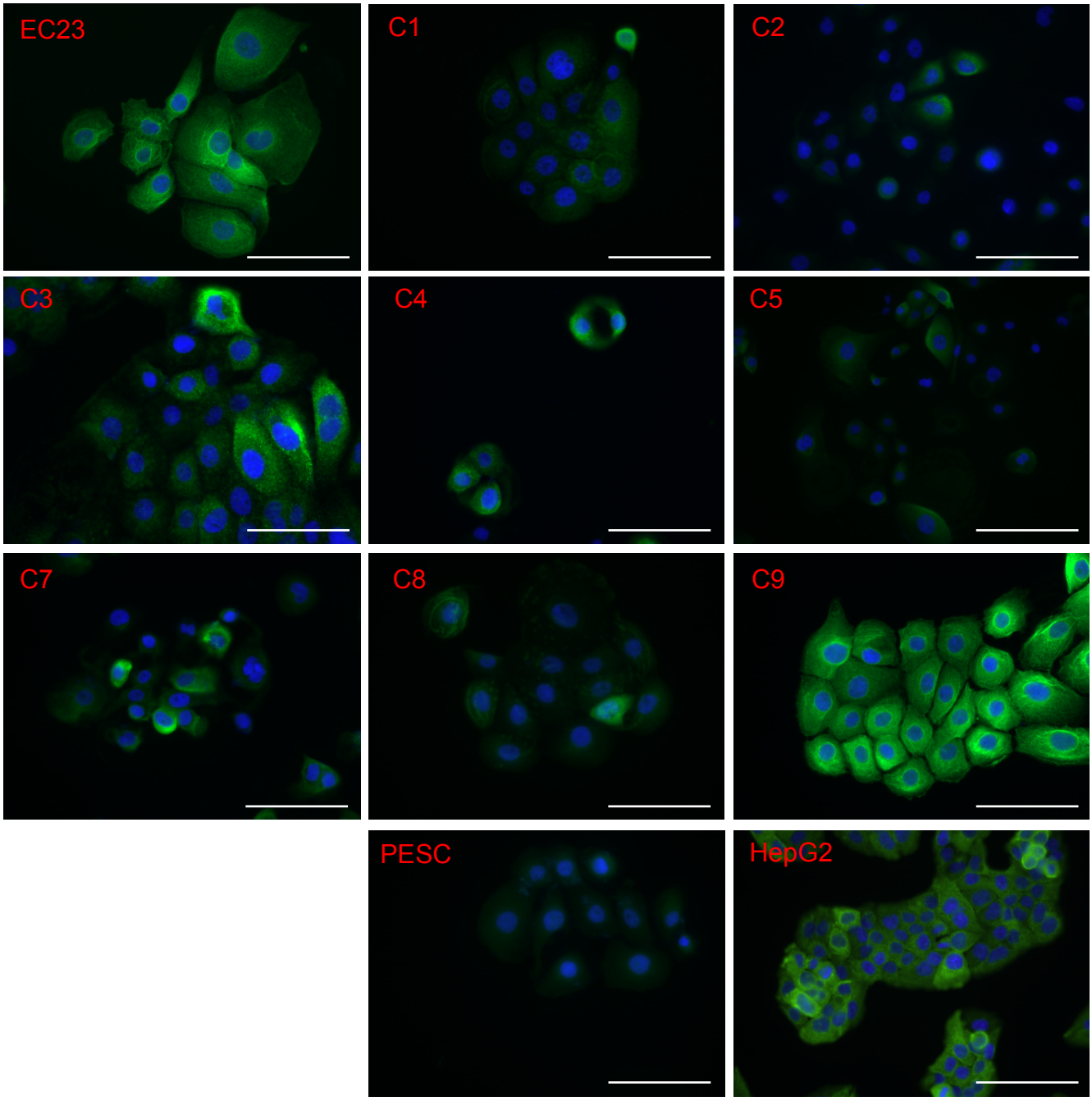

Figure 3.4. Immunocytochemistry showing expression of keratin K18 in the EC23 cell line and in clones derived from the EC23 cell line as well as in primary eccrine gland secretory coil cells (PESC) and HepG2 cells (positive control). Scale bar 100 µm.

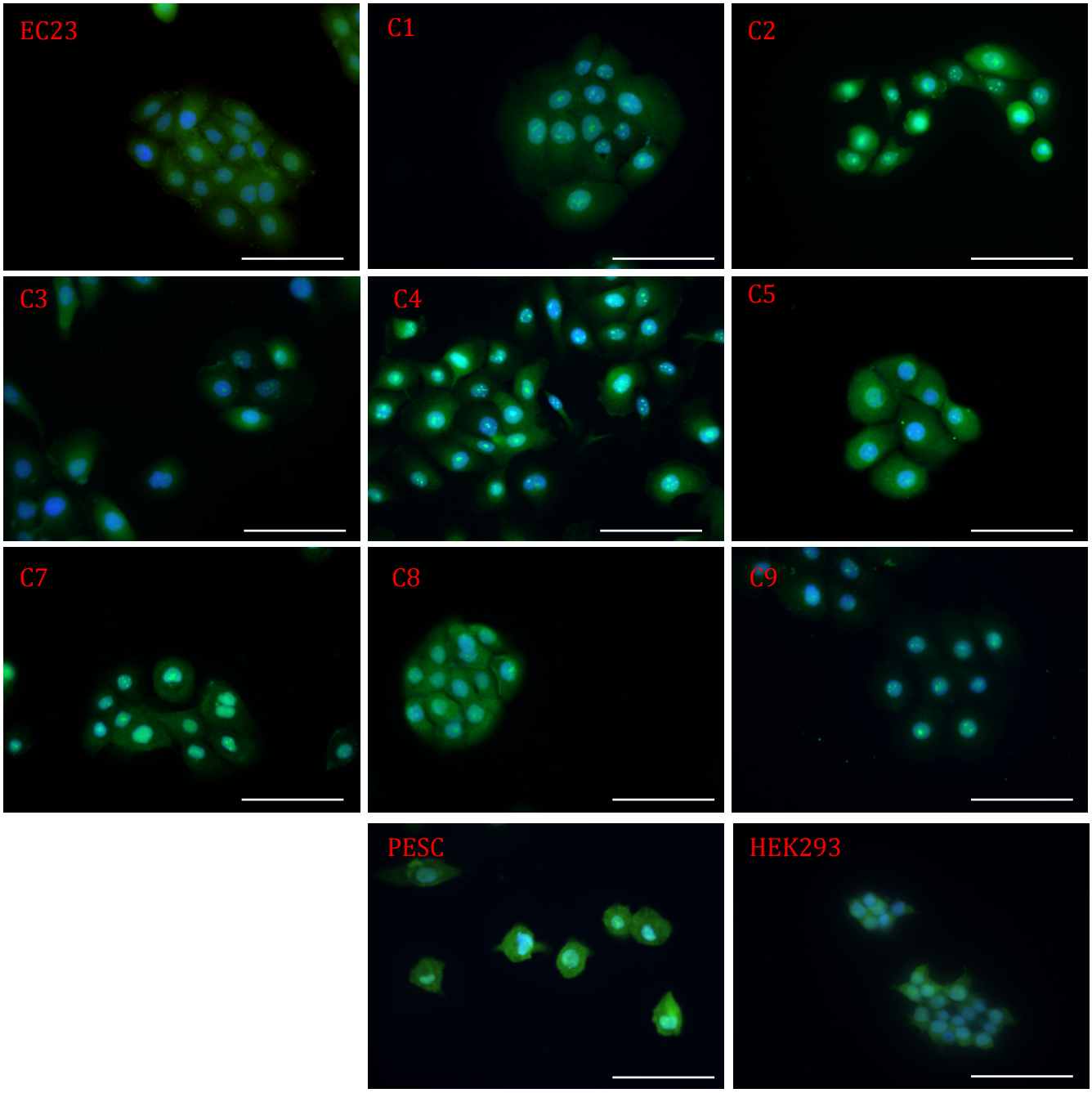

Figure 3.5. Immunocytochemistry showing expression of carboonic anhydrase II in the EC23 cell line and in clones derived from the EC23 cell line as well as in primary eccrine gland secretory coil cells (PESC) and HEK293 cells (positive control). Scale bar 100 µm.

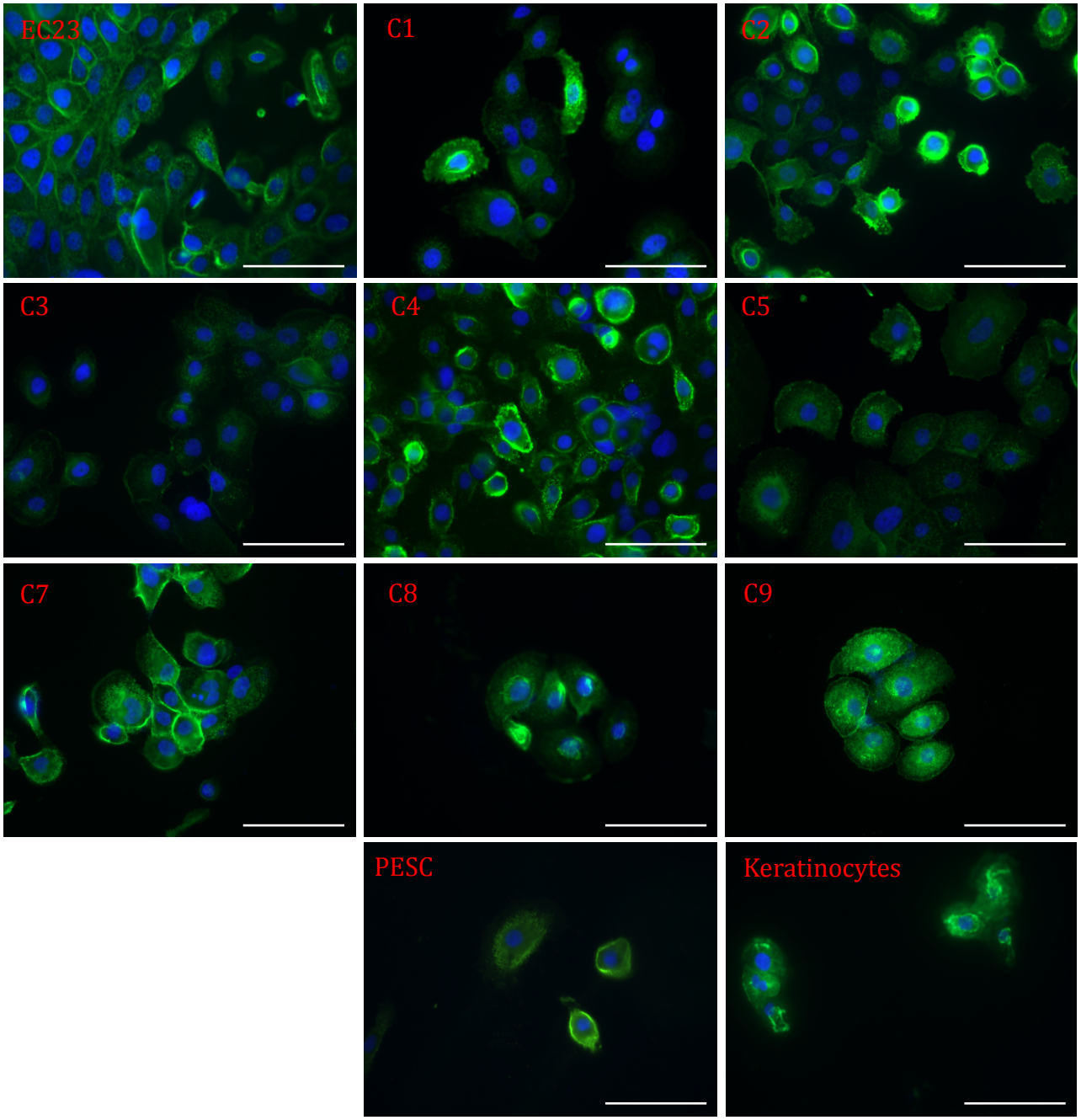

Figure 3.6. Immunocytochemistry showing expression of CD44 in the EC23 cell line and in clones derived from the EC23 cell line as well as in primary eccrine gland secretory coil cells (PESC) and keratinocytes cells (positive control). Scale bar 100 μm.

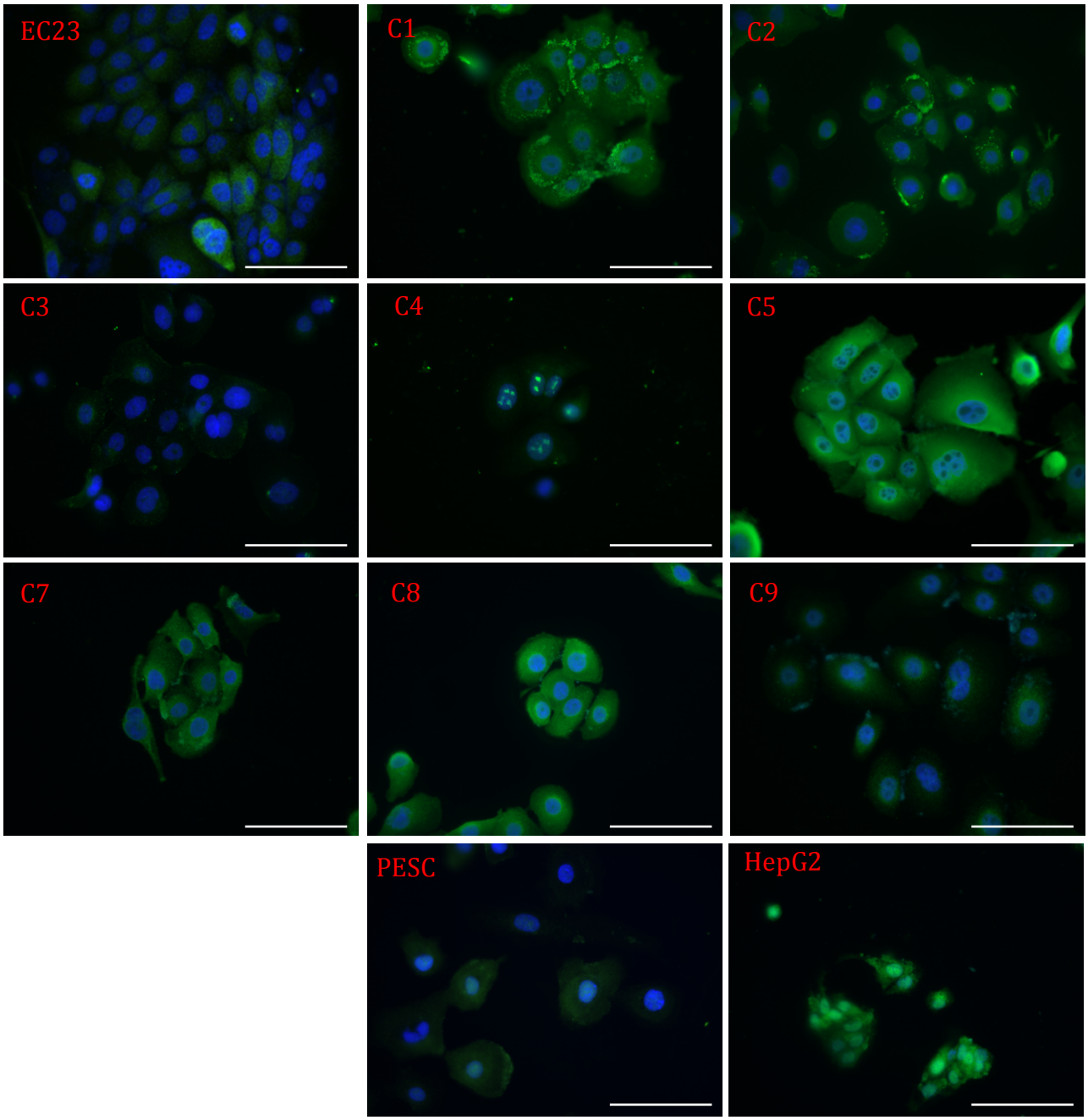

Figure 3.7. Immunocytochemistry showing expression of AChR-ε in the EC23 cell line and in clones derived from the EC23 cell line as well as in primary eccrine gland secretory coil cells (PESC) and HepG2 cells (positive control). Scale bar 100 µm.

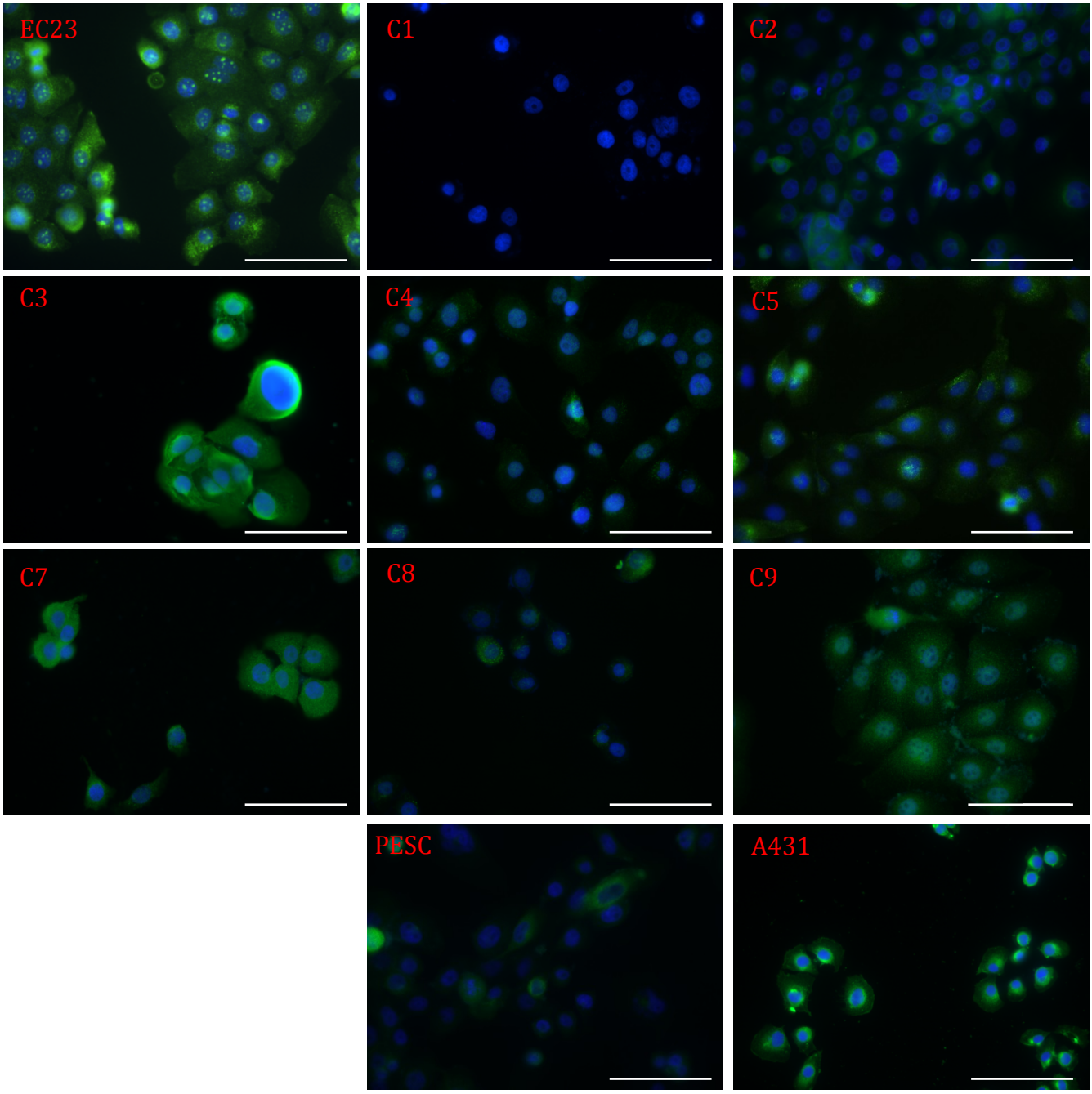

Figure 3.8. Immunocytochemistry showing expression of EGFR in the EC23 cell line and in clones derived from the EC23 cell line as well as in primary eccrine gland secretory coil cells (PESC) and A431 cells (positive control). Scale bar 100 µm.

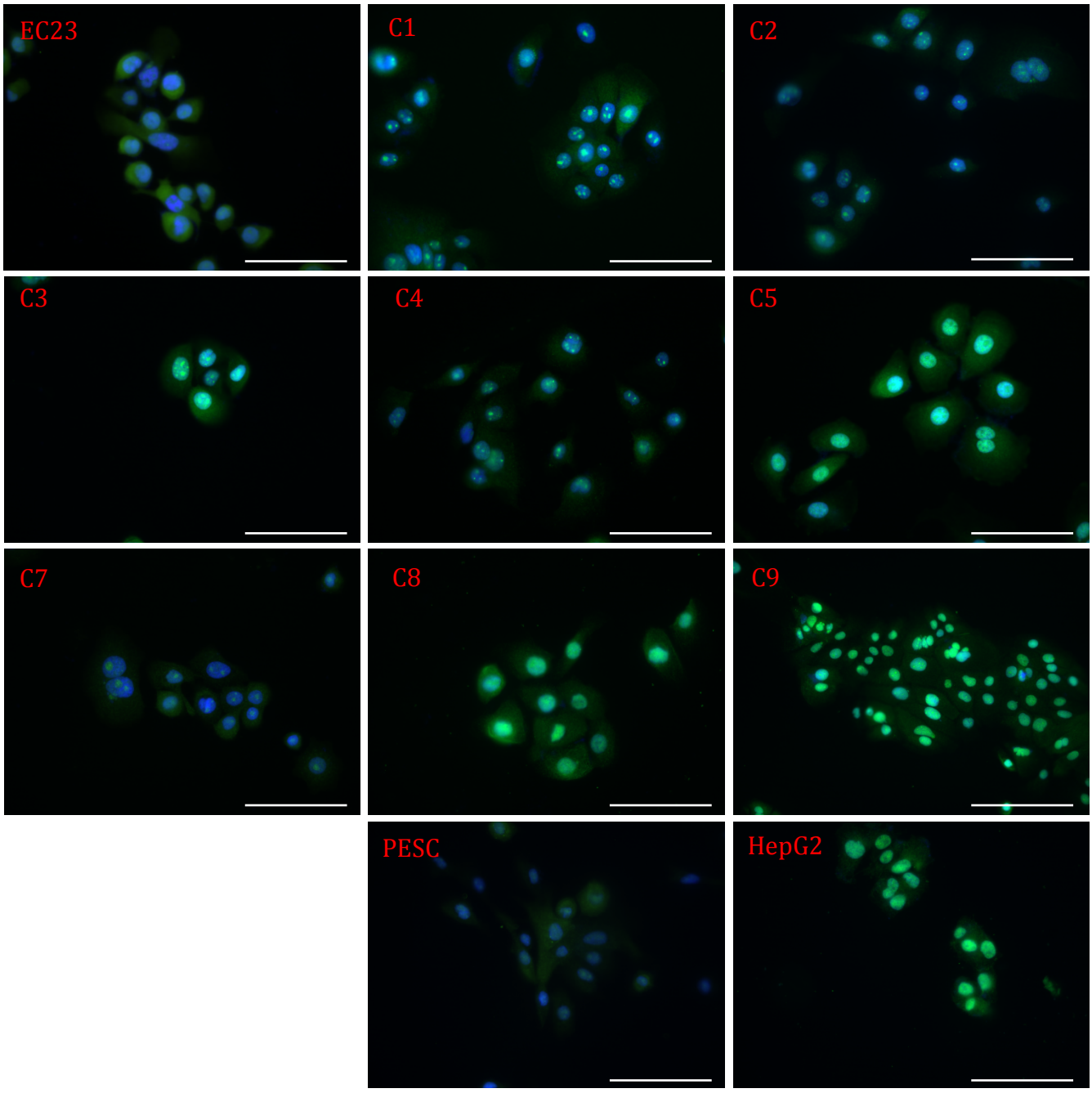

Figure 3.9. Immunocytochemistry showing expression of Muscarinic M3 receptor in the EC23 cell line and in clones derived from the EC23 cell line as well as in primary eccrine gland secretory coil cells (PESC) and HepG2 cells (positive control). Scale bar 100 µm.

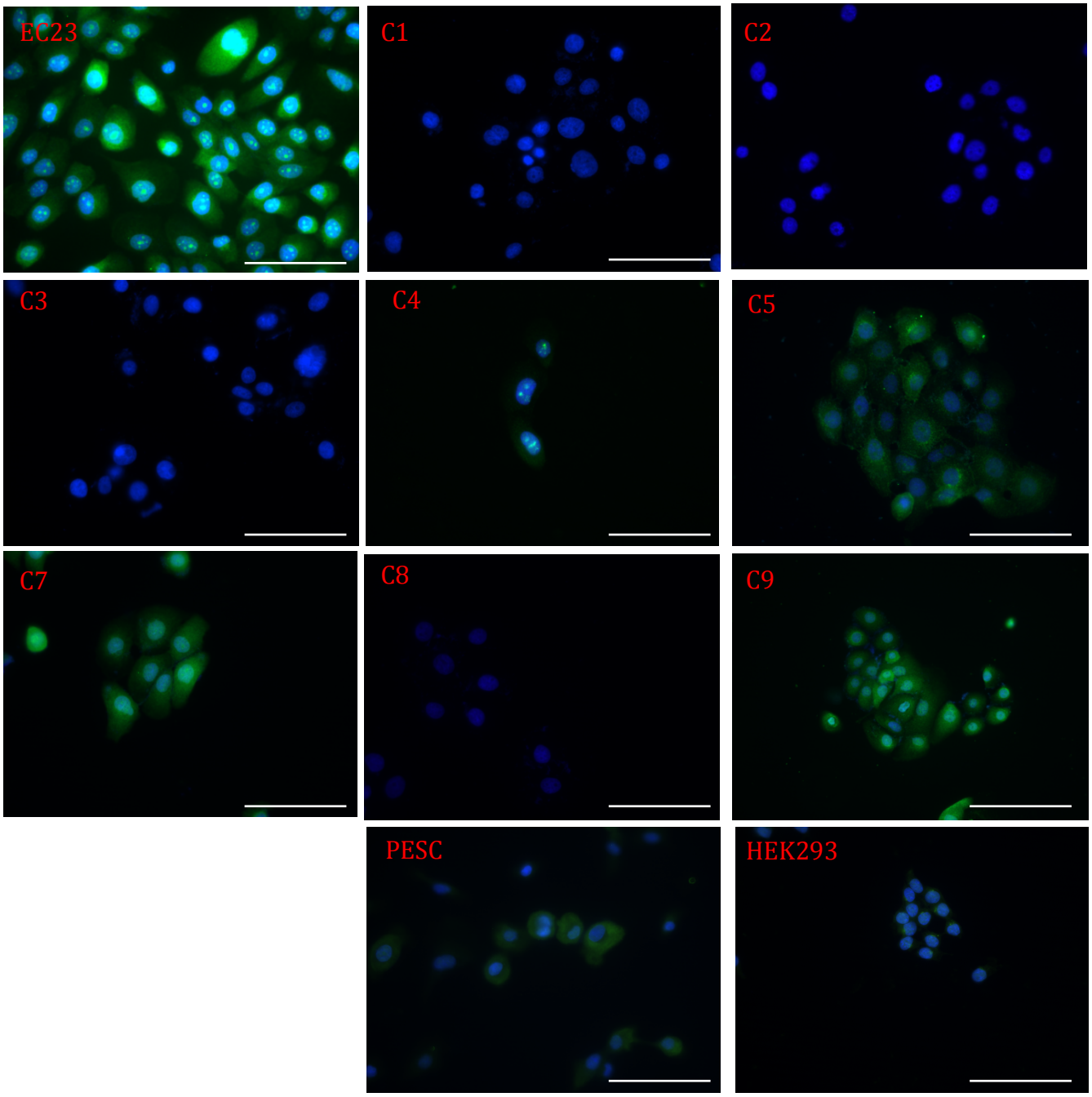

Figure 3.10. Immunocytochemistry showing expression of NKCC1 in the EC23 cell line and in clones derived from the EC23 cell line as well as in primary eccrine gland secretory coil cells (PESC) and HEK293 cells (positive control). Scale bar 100 µm.

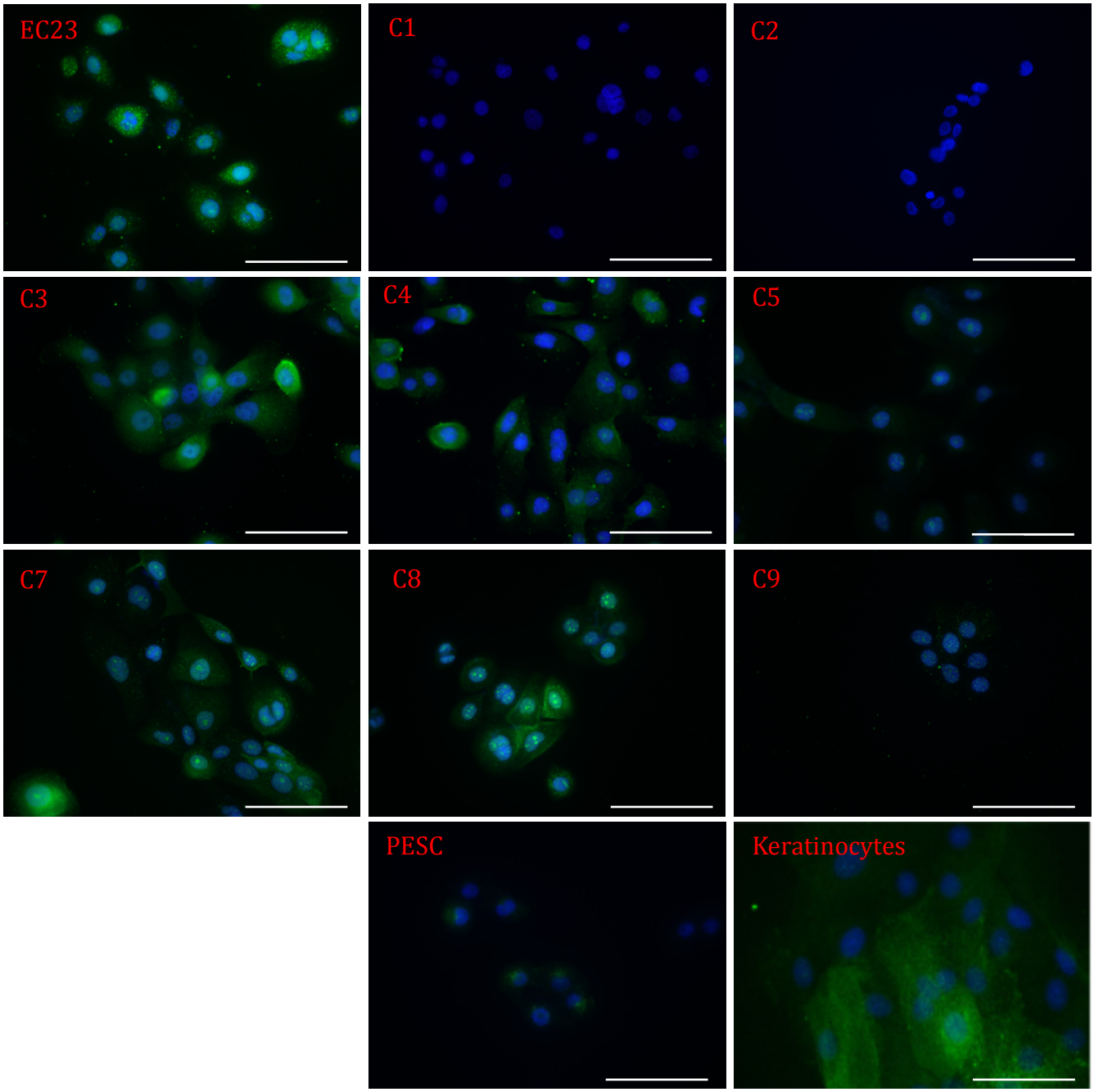

Figure 3.11. Immunocytochemistry showing expression of MUC-1 in the EC23 cell line and in clones derived from the EC23 cell line as well as in primary eccrine gland secretory coil cells (PESC) and keratinocytes cells (positive control). Scale bar 100 µm.

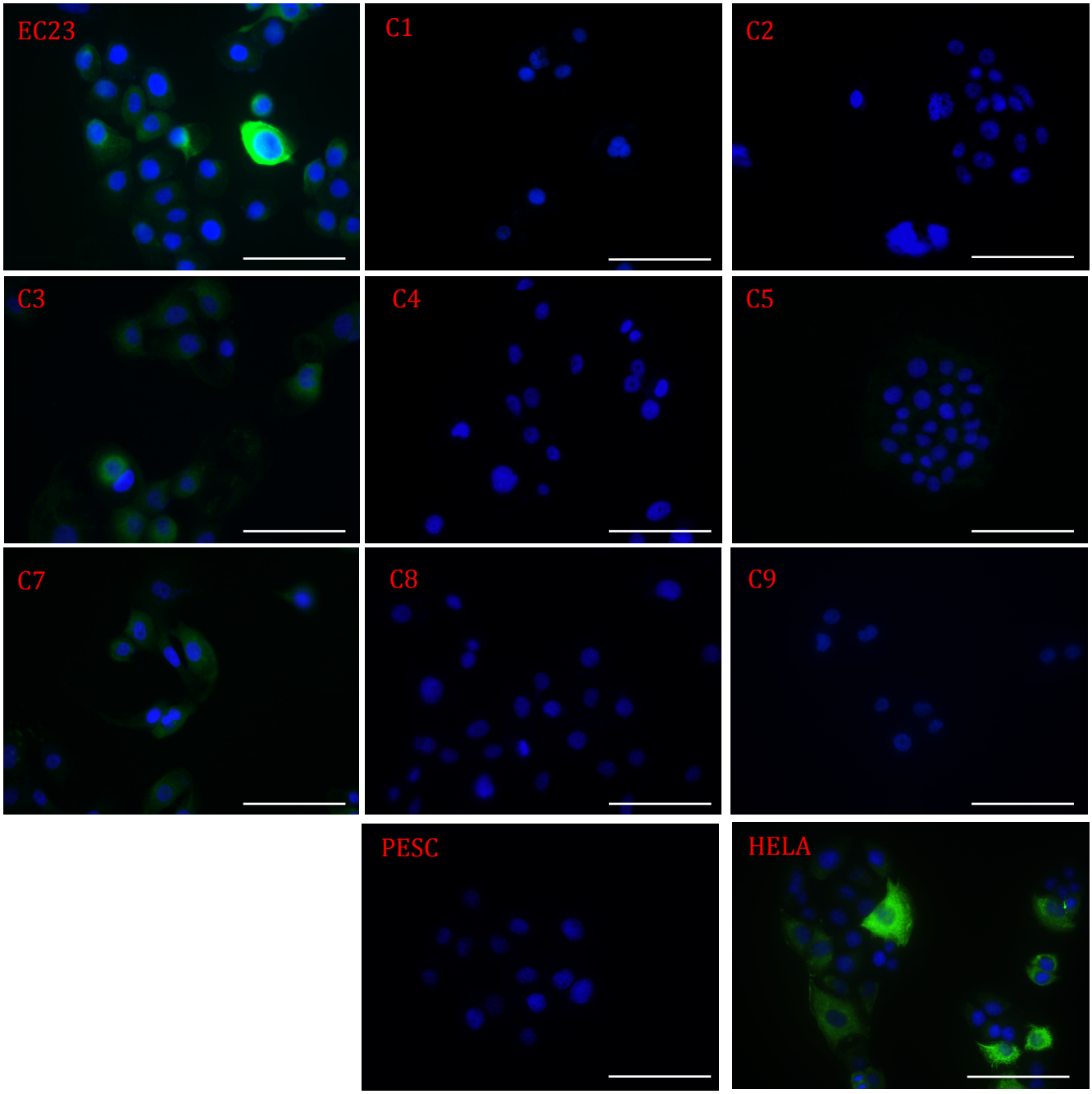

Figure 3.12. Immunocytochemistry showing expression of HMFG1 in the EC23 cell line and in clones derived from the EC23 cell line as well as in primary eccrine gland secretory coil cells (PESC) and HELA cells (positive control). Scale bar 100 µm.

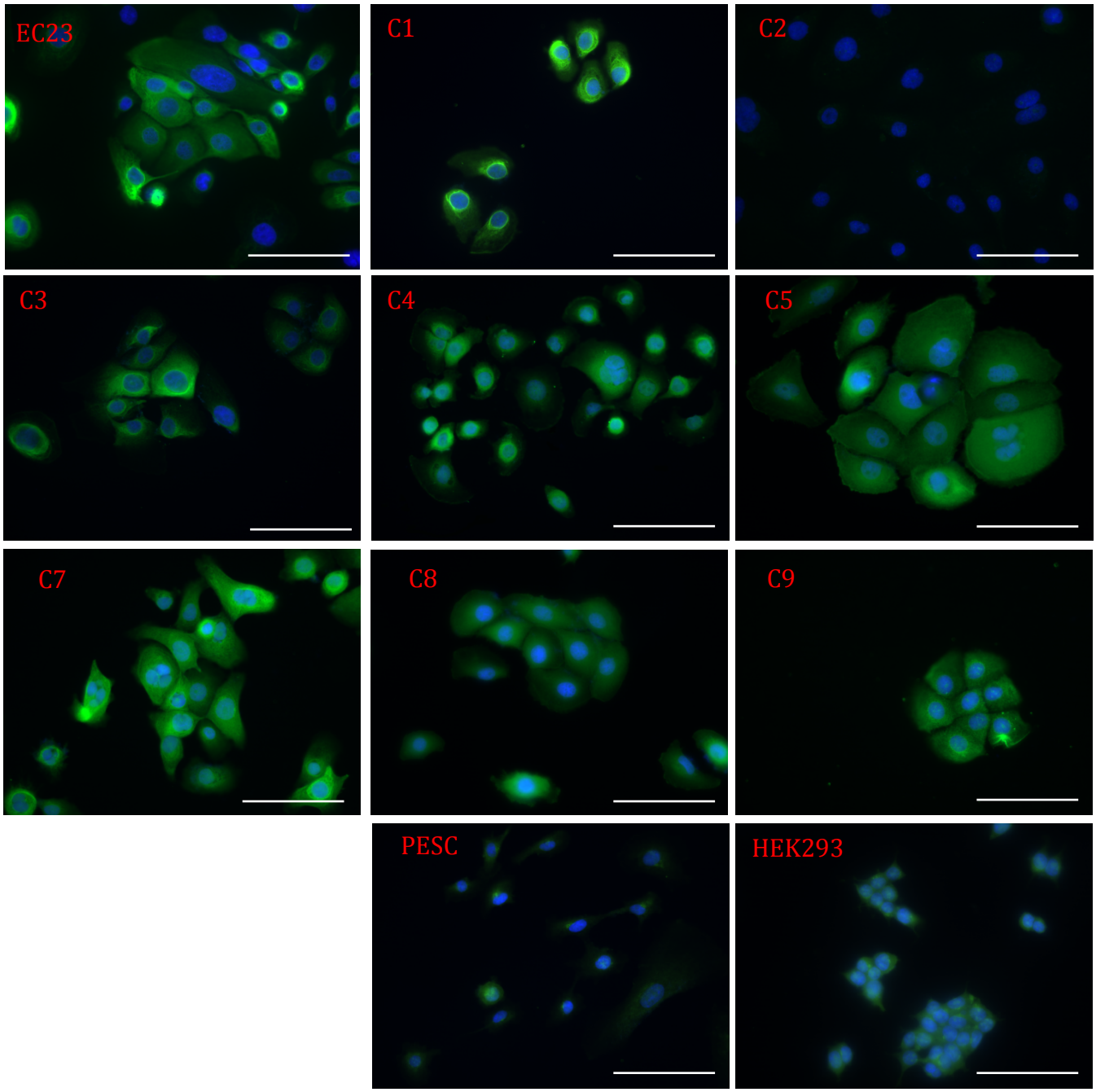

Figure 3.13. Immunocytochemistry showing expression aquaporin 5 in the EC23 cell line and in clones derived from the EC23 cell line as well as in primary eccrine gland secretory coil cells (PESC) and HEK293 cells (positive control). Scale bar 100 μm.

	PESC	EC23	Clone 1	Clone 2	Clone 3	Clone 4	Clone 5	Clone 7	Clone 8	Clone 9
Keratin 7	+	+	+	+	+	+	+	+	+	+
Keratin 8	nd	+	+	+	+	+	+	+	+	+
Keratin 14	+	+	+	+	+	+	+	+	+	+
Keratin 18	+	+	+	+	+	+	+	+	+	+
CD44	+	+	+	+	+	+	+	+	+	+
Aquaporin 5	+	+	+	+	+	+	+	+	+	+
Muscarinic Receptor M3	+	+	+	+	+	+	+	+	+	+
Acetylcholine Receptor	+	+	+	+	+	+	+	+	-	+
NKCC1	+	+	-	-	-	+	+	+	-	+
EGFR	+	+	-	+	+	+	+	+	+	+
Carbonic anhydrase II	+	+	+	+	+	+	+	+	+	+
Mucin	+	+	-	-	+	+	+	+	+	+
H.Milk fat globulin	-	+	-	-	+	-	+	+	-	-

Table 3.1. Summary of the characterisation of the EC23 cell line and clone 1, 2, 3, 4, 5, 7, 8, and 9 compared to primary eccrine sweat gland cells (PESC).nd= not determined.(+) Expression. (-) no expression.

3.3 Discussion

To characterize the EC23 cell line and clones derived from the EC23 line, a panel of proteins previously described to be expressed by the secretory coil of the eccrine gland were chosen for analysis (See Chapter 2, Table 2.1). From the data generated in this chapter, we can see that the expression of cell markers expressed by EC23 cells is very similar to that of primary eccrine cells derived from the secretory coil. However, we did observe considerable variation in the levels of expression of the relative markers both within EC23 cells and also the various clones derived from the EC23 cells. In addition we found that expression of these markers on primary eccrine sweat gland coil cells was generally very weak. We also observed considerable variation in membrane, cytoplasm and nuclear expression and these are discussed below.

To distinguish between clear cells and other cells found in the eccrine sweat gland secretory coil namely, dark cells and myoepithelia cells particular emphasis for comparison was placed on proteins that were considered as markers known to be involved in secretory functions of the coil, such as sodium potassium co-transporter 1 (NKCC1), carbonic anhydrase II, Muscarinic receptor M3 and acetylcholine receptor epsilon (AChR-ε) (Quinton, 1983, Sato et al., 1991, Nejsum et al., 2005).

Keratins K7, K 8 and K18 are simple epithelial keratins and as a result are typically expressed in many gland ducts and simple epithelia (Saga and Jimbow, 2001). In my experiments I observed that keratins K6, K8 and K18 showed marked differences in expression between some of the clones, thus they could be

important in the classification of the clones retaining secretory phenotype, as these keratins are reported to be markers for the secretory coil (Langbein et al., 2005). It is to be noted that there is heterogeneity in the expression of K7, K8 and K18 in the EC23 cells and some of the clones. The reasons behind this could be due stress to the cells, mitosis or apoptosis (Oshima, 2002, Toivola et al., 2002). During apoptosis, keratins such as K18 are cleaved into granular components (Caulin et al., 1997). During cell division, cells undergo major structural changes, where keratins are phosphorylated followed by keratin solubilisation terminating in reorganizations of the keratin cytoskeleton (Ku et al., 1999, Toivola et al., 2002). Weak expression of keratins K7 and 18 in the primary eccrine sweat gland coil is difficult to explain but as these cells are very difficult to grow and maintain in culture this may reflect a loss of differentiation away from that of a simple epithelium. However, although these keratins are considered as markers for the secretory coil; they are usually expressed in most simple epithelium and their actual function is not known (Langbein et al., 2005). However, the fact that both the EC23 cells and the clones express these keratins suggests they may be derived from the primary eccrine sweat gland coil. Although these simple keratins are thought to be predominantly involved in maintaining the structure of simple epithelium there is also some evidence that they may play a role in vesicular trafficking (Casanova ML, 2006, Planko et al., 2007). Planko, et al, identified Hsc70 as a protein that interacts with the head domain of K5, which could relate to a role of K5 in the uncoating of clathrin coated vesicles and thus be involved in vesicular transport (Planko et al., 2007), however the involvement of keratins in vesicle trafficking in the eccrine gland remains unclear.

Keratins are also involved in other cell functions such as cell signalling, proliferation, differentiation and apoptosis (Owens and Watt, 2003). Keratin 10, is found in the spinous and granular layers of the epidermis and it inhibits proliferation of keratinocytes and enhances differentiation promoting stratification (Burns et al., 2010). Keratin 8 and 18, are a pair of keratins which are mostly expressed in simple epithelia, and are the first keratins to be expressed in development (Casanova ML, 2006). From work performed on knockout mice, we

know keratin 8 to be indispensable during development. The same is not observed for keratin 18, where the mice survived until shortly after birth (Oshima, 2002). Also the keratin 8/18 pair has been demonstrated to be involved in Fas and TNF induced apoptosis. (Moll and Moll, 1992, Oshima, 2002). It is likely that in the eccrine gland this keratin pair function is mainly structural, but there is the possibility that they are also involved in functions such as apoptosis but to establish this knockout experiments would be necessary.

Carbonic anhydrases are zinc metalloenzymes that catalyse the reaction of carbon dioxide and bicarbonate (Lindskog, 1997). There are 15 identified isotypes of carbonic anhydrases in humans, classified depending on their tissue distribution and their differences in selectivity, catalytic activity and sensitivity (Chengwidden et al., 2000). Their mode of action is indispensable for physiological activities such as carbon dioxide (CO_2) transport from tissues to the lungs, glucogenesis and ureagenesis, by regulating acid/base balances during these processes. For example, CO_2 is not very soluble in blood and in order to mobilize it towards the lungs it must be converted to bicarbonate (HCO_3^-) by carbonic anhydrase II (CAII). CAII, has a high catalytic efficiency rate amongst the carbonic anhydrases (Chengwidden et al., 2000, Lindskog, 1997). Its mode of action is a two-step process, shown below:

Enz: $Zn\text{-}OH^-$ + CO^2 $\longleftrightarrow$ Enz: $Zn - H_2O$ + $HCO3^-$

The first step is the hydration reaction, where the hydroxide molecule bound to zinc acts as a nucleophile reacting with the CO2, forming HCO3-. The second step of the reaction involves reversing the zinc to being bound with a hydroxide

instead of a water molecule, by a proton transfer mechanism (Berg JM, 2002). Carbonic anhydrase II has a high catalytic efficiency and is found in the cytoplasm of many cells and organs, including the clear cells of the human eccrine gland, which helps to remove HCO3- from the body by secreting during perspiration (Chengwidden et al., 2000). We found all the clones and the EC23 cells to express high levels of carbonic anhydrase in the cytoplasm; however there appear to be slightly lower levels of expression in clones 9 and 3. Carbonic anhydrase, has recently been described as being a marker exclusively for the eccrine gland and to be absent from the apocrine gland (Bovell et al., 2011), thus its presence in the EC23 cells and the clones further suggests an eccrine phenotype. Furthermore, CAII has been described as an enzyme only found in the clear cell (Bovell et al., 2011), however this is controversial, as recent research suggests that the dark cell of the eccrine is also being involved in the production of secretions, where HCO3- is transported (Cui and Schlessinger, 2015), and it is possible that CAII is present in the dark cells.

In addition to the expression of carbonic anhydrase in the cytoplasm we also observed expression in the nuclei of cells. Although classically considered to be a cytoplasmic protein nuclear carbonic anhydrase has previously been reported in C elegans where it is thought to play a role in the regulation of nuclear pH and may be involved in signalling (Sherman et al., 2012). In mammalian tissues a nuclear carbonic anhydrase identified by its binding to a carbonic anhydrase II antibody was shown to be identical to nonO/p54(nrb), a previously cloned and characterized RNA and DNA binding nuclear factor whose function is also believed to be regulation of nuclear pH (Karhumaa et al., 2001, Sherman et al.,

2012). Thus, it is possible that CAII is indeed present in the nuclei of eccrine cells, however western blotting of nuclear cell fractions would be required to confirm this.

CD44 is a cell surface glycoprotein that is a receptor for hyaluronic acid (HA), a component of the ECM, however it can also interact with other ligands such as osteopontin, metalloproteinases and collagen (Goodison et al., 1999, Ponta et al., 2003). In the eccrine gland CD44 is present in the secretory cells of the coil, and it has been used to it distinguish between the eccrine and apocrine glands (Wilke et al., 2006, Bovell et al., 2011). In this investigation, CD44 was found to be present on all the EC23 cells, the clones and the primary eccrine secretory coil cells. CD44 is an ubiquitous transmembrane protein with various isoforms and can elicit a variety of responses (Lopez et al., 2005). Its physiological functions include cell adhesion, aggregation, migration and activation of cells. Hyaluronic acid, the main ligand for CD44 can influence intracellular signalling when binding to CD44. When high molecular weight hyaluronic acid binds to CD44, it can inhibit angiogenesis and has shown anti-inflammatory faculties and binding of low molecular weight hyaluronic acid to CD44 can induce angiogenesis and promote cell migration (Feinberg and Beebe, 1983, West et al., 1985, Sugahara et al., 2003, Louderbough and Schroeder, 2011).

There are however several isoforms of CD44, with CD44s being present on most vertebrate cell membranes and CD44v being present on several types of carcinoma cells (Zöller, 2011). CD44v has also been found to be present in metastatic tumours (Gunthert et al., 1991), and there is evidence that interaction

between CD44v and HA has an anti-apoptotic effect in cancer stem cells (Yu and Toole, 1997, Zöller, 2011). It would be interesting to further investigate which isoform of CD44 is present in the EC23 cells and its clones, as mutations in the CD44 structure from the normal CD44 structure found in primary eccrine gland cells could have occurred. A mutation in the structure could affect the cells in several ways, from affecting cell migration, its interaction with the ECM and even made the cells tumorigenic. Therefore, knowing which isoform of CD44 is present in our immortalised cells would give us clues as to whether immortalization had transformed our cells.

Acetylcholine, is one of the main neurotransmitters involved in eccrine secretions, thus its expression in eccrine cells is essential for functionality. AChR-e was expressed at different levels across the clones. EC23 and clones 1 and 2 cells expressed AChR-e in the membrane and clone 4 expressed it in the nuclei. Nuclear expression of certain receptor such as G-protein coupled receptors, and EGFR, has been reported in the nuclear membrane of several cell types (Tadevosyan et al., 2012). These receptors in the nuclear membrane are thought to be involved in transcription and gene activation. For example, nuclear EGFR has been found in tumour cells, regenerating liver cells and proliferating hepatocytes (Wang et al., 2010b).

Clones 3, 4 and 9 showed low levels of AChR-e. Primary cells show varied expression, however this could be due to the cells being used at passage 5 and reflecting loss of differentiation also it has been demonstrated that eccrine glands isolated with collagenase tend to respond less to stimuli than when isolated by

shearing (Sato and Sato, 1981b). Although the cells used in these experiments have been under cell culture and therefore, any adverse effects of collagenase used in their isolation may have worn off the fact these cells have undergone a number of passages may explain the reduced expression of AChR-e. Moreover, it is possible that at passage 5 these primary cells may have begun to senesce (Freund et al., 2012). However, as we were using the primary cells for comparative purposes with regards expression of cell specific markers the varied expression in primary cells is not a major problem.

Muscarinic receptor M3 is also involved in the cholinergic activation of the eccrine gland, which lead to the increase on intracellular calcium ions (Ryer et al., 1995, Schiavone and Brambilla, 1991). M3 receptor is expressed on the secretory cells of the coil and luminal cells (clear cells) of the duct (Grant et al., 1991). We found the expression of this receptor to be mainly located in the nuclei of cells (Figure. 3.8), with levels of expression varying between clones. As mentioned above, nuclear G-protein coupled receptors, such as the muscarinic receptors, have been identified in several tissues, such as corneal epithelial cells and endothelial cells (Tadevosyan et al., 2012). The function of muscarinic receptors in these tissues is to up regulate of DNA and RNA polymerases and increase cGMP in the nuclei, and thus, it is possible that similar effects are occurring in the cells expressing these nuclear markers (Lind and Cavanagh, 1995, Tadevosyan et al., 2012). The presence of acetylcholine receptors in the EC23 and the clonal cell lines is vital for phenotype retention, as without them the cells would not be able to perform their basic function of sweat production.

NKCC1 is essential for the function of the eccrine gland as it tightly controls the levels of secretions of Na^+, K^+ and Cl^- in the secretory coil and their reuptake in the resorptive duct (Nejsum et al., 2005). When acetylcholine binds to the muscarinic receptors in the clear cell, an influx of calcium is triggered which activates inositol polyphosphates (IPPs). These in turn open chloride ion channels in the apical membrane and potassium ion channels on the basolateral membrane of the secretory coil clear cells, allowing an efflux of calcium ions to occur. This causes a change in polarity of the cell membrane, sodium ions diffuse towards the lumen of the gland to form sodium chloride, thereby mobilising water to the lumen. The data collected shows that clones 1, 2, 3 and 8 do not express NKCC1, suggesting that these cells are not of a secretory phenotype or that they have lost its expression during the immortalization process. Of interest is the apparent nuclear location of NKCC1 in the EC23 cells and clone 4. To date no reports of nuclear NKCC1 have been described in the literature, nevertheless it is possible that NKCC1 can translocate to the nuclei in the eccrine gland and EC23 cells. Further experiments would be required to confirm the nuclear localization of NKCC1, such as western blotting of subcellular fractions (Alberts et al., 2008).

EGFR is predominantly present on the luminal cells of the eccrine gland and also on the myoepithelial cells (Saga and Jimbow, 2001) . When EGFR binds to EGF, it dimerises, and activation of tyrosine kinases occurs which then results in phosphorylation, activating downstream signalling proteins which modulate transcription, DNA synthesis, cell migration, adhesion, proliferation, and in some cases immune responses (Yu et al., 2002). EGFR, has been reported on the membrane of secretory cells of the coil, myoepithelial cells and to a lesser extent

luminal cells of the duct (Saga and Jimbow, 2001). Although EGFR is typically expressed on the cell membrane (Saga and Jimbow, 2001), there is now increasing evidence that nuclear EGFR is not an artefact and that nuclear EGF has important signalling roles (Brand et al., 2011). It is also possible that the location of EGFR expression within cells could also be influenced by the confluence of the cells; in figure 3.8, clone 9 cells are more confluent than some of the other clones, such as clone 1, and it can be observed that clone 9 cells show much more membranous EGFR expression. However further experiments are required in which all clones should be grown to similar level of confluence. Western blot analysis would also be useful in determining whether the EGFR antibody was picking up the correct molecular weight protein.

Mucin, is thought to be a marker of eccrine sweat gland secretory coil dark cells, in contrast human milk fat glibulin-1 (HMFG1), has been used to distinguish between apocrine and eccrine cells in the past, however there have been reports of HMFG1 being expressed in eccrine clear cells (Bovell et al., 2007).

Mucin 1 (MUC1) is a high molecular weight glycoprotein, expressed in a cell and tissue specific pattern common in glandular epithelial tissue, and are present in most epithelial tissues (Constantine and Mowry, 1966). In the eccrine gland it is present in the secretory coil. It is also thought to be present in the dark cell luminal membrane (Yoshii et al., 2002). In my experiments MUC1 was detected in primary eccrine secretory coil cells, EC23 cells, and clones 3, 4, 7 and 8. These findings suggest clones 3, 4, 7 and 8 have features of dark cells, and confirm the

mixed population of cells present within the EC23 population. The expression of this marker was relatively low in comparison to other markers, thus it could be possible that the immortalization process may have enhanced expression of the marker on clear cells or that the antibody used was not specific or expression is switched on in response to cell culture. In most simple epithelial cells, mucins are abundant and often concentrated to the apical surface and they can extend up to 500 nm above the cell membrane, which are useful in providing protection for the cell (Brayman et al., 2004). Another feature of MUC1 that is vital for its function is its high degree of glycosylation, which provides lubrication and prevents dehydration. Also the high level of steric hindrance prevents microbial access to the cell (Brayman et al., 2004).

Aberrant expression of MUC1, has been found to be present in roughly 64% of all the tumours diagnosed in the United States each year (Kufe, 2009). MUC1 is overexpressed and under-glycosylated in most of all human epithelial adenocarcinomas and has been reportedly found in salivary and mammary gland tumours (Hamada et al., 2004, Singh and Bandyopadhyay, 2007). The main changes that occur in adenocarcinomas, is the loss of structure in tissues. The amino acid sequence of MUC1 in normal tissue and in tumours is identical, with the only marked differences is the level of expression and the under glycosylation that is present in tumours.

The expression of MUC1 on the EC23 cells and clones 3, 4, 5, 7, 8 and 9 is not unexpected as this transmembrane glycoprotein is known to be present in most glandular epithelia (Singh and Bandyopadhyay, 2007) never the less it would be

advantageous to further study MUC1 to establish whether the cells retain the normal level of glycosylation and expression that is present in normal eccrine secretory coil cells. This would be important as stated above, changes in levels of glycosylation may indicate the EC23 cells have been transformed by the immortalisation process.

HMFG1, is found in the luminal membranes of secretory cells of the apocrine glands (de Viragh et al., 1997, Saga, 2001) and has been used in the past to differentiate between the eccrine and the apocrine gland, however Bovell, 2007 found that human milk fat globulin -1 was also expressed in the eccrine gland, suggesting there could be expression of the protein in the eccrine gland also, possibly at lower levels (Bovell et al., 2007). The EC23 cells and clones 3 and 7 showed low levels HMFG1 expression. Although HMFG1 is more highly associated with the apocrine gland it is possible that lower levels of HMFG1 expression are present in the eccrine gland. We are confident that the EC23 cell line and derived clones are indeed from the eccrine gland, as these were isolated from facial skin where no apocrine glands are present and also morphologically were typical of the coiled eccrine gland rather than the lobed apocrine gland.

Efficient water transport is essential for eccrine gland function, for this, simple diffusion across the plasma membrane is insufficient, thus specialised water transport channels such as AQP5 are present (Nejsum et al., 2002). This family of channels are proteins no larger than 30kDa and are members of major intrinsic protein family with a main function of transporting water across the cell membrane (Ishikawa and Ishida, 2000). In the parotid gland, AQP5 levels have

been noted to be increased upon stimulation of muscarinic and adrenergic agonists. AQP5 levels are later lowered and an increase in vesicle-associated AQP5 is observed, suggesting translocation of the protein within the cell. Aquaporin 5 was also detected on all the clones and the EC23 cell line providing further evidence of phenotype retention. Interestingly, AQP5 can be seen, in clone 9 and a few cells on other clones, in the nuclei. Until recently, no reports of AQP5 in the nuclei had been reported, but Cho et al (2015) reports that upon muscarinic receptor activation in rat parotic acinar cells, induces the translocation of AQP5 to the nuclear membrane (Cho et al.,2015). Because of the similarities between the function of the parotic and eccrine glands it is likely that a similar mechanism occurs in the eccrine gland.

In conclusion although the immunocytochemistry data generated in this chapter shows marked variation in the patterns and intensity of expression of some of the markers investigated, we can be confident that the EC23 and the clones were derived from the EC23 cell line show overall characteristics expected from cells derived from the secretory coil of the eccrine gland. However, in some instances high levels of heterogeneity in the single clonal populations were observed for some markers, which we suspect is due to the cells being at different stages in the cell cycle, and thus in future experiments synchronising the cells using serum starvation or by using drugs such as nocodazole (Davies, 2001). What is more difficult to dissect is whether any of the clones show distinct characteristics of dark cells as we find expression of both dark and light cells markers. The data does show that clone 1, 2 and 3 do not express NKCC1 suggesting these cells are not secretory cells or that their secretory mechanisms have been severely

compromised. Also the presence of MUC1 on clone 3 and 5 and the absence of NKCC1, could be interpreted as this cells having more of a dark cell phenotype. The presence of MUC1 on clones 3 to 9 however, leads us to think that during the immortalisation process, expression of this glycoprotein was induced, as all other markers of the clear cell are also present on clone 4, 7 and 9. Interestingly all the clones express CAII, an enzyme thought to be found only in the clear cells (Bovell et al., 2011), and we identified it in every clone, yet we also found MUC1 on clones 3-9. From this data, we can conclude that a secretory coil retaining cell line, EC23 was successfully immortalised, and that we have derived 8 clones from this line and produced some that appear to express dark and clear cell specific cell markers. Unfortunately we could not determine with certainty if any of the clones were of dark cell origin, as at the time the work was performed no other markers for the dark cell existed, however this year FoxA1 (Cui and Schlessinger, 2015) has been identified as a possible marker for the dark cell and future experiments should be carried out in using FoxA1 in hopes of identifying dark cells in the clonal cell lines. However, to establish for certain the phenotype of these cells we need to carry out functional studies and these are presented in Chapter 4.

Chapter 4. The effect of cholinergic and beta adrenergic stimulation of EC23 cells on calcium flux and cyclic AMP

4.1 Introduction

In Chapter 3 the expression of a range of biomarkers that are considered to be expressed on cells of the secretory coil of the eccrine sweat gland were investigated on the EC23 cell line. Although the data generated in Chapter 3 showed that the EC23 cell line and clones derived from this line did express secretory coil markers there was marked heterogeneity between the clones. Therefore, although these cells were derived from micro dissected secretory coil and so unlikely too be contaminated by non secretory coil cells *per se* it cannot be ruled out that the changes in expression of secretory coil markers may reflect de-differentiation of secretory coil cells and although they may express secretary coil markers these do not necessarily indicate they retain secretory coil function.

The function of the eccrine gland in humans is to produce secretions that aid thermoregulation of the body. The mechanism, by which perspiration is initiated, occurs via the cholinergic and/or the adrenergic pathways (Quinton, 1983, Sato and Sato, 1981b). Thermal regulation, however, is mostly regulated by the cholinergic pathway, initiated by the secretion of the neurotransmitter acetylcholine (Lei et al., 2008). When acetylcholine is released from nerve endings it binds to acetylcholine muscarinic receptor M3, which activates PCL to cleave PIP_2 into DAG and IP_3. IP_3 then travels to the ER where it binds to the IP_3R, resulting in a release of calcium (Ca^{2+}) from the ER (Mikoshiba, 2007, Hilgemann et al., 2001). This increase in Ca^{2+} is the key effector for sweat production. It triggers ionic efflux by opening luminal membrane chloride channels and basolateral potassium channels within the clear cell membrane (see

figure 4.8). The efflux of chloride into the lumen generates a negative potential in the lumen, inducing the movement of sodium towards the lumen. This in turn mobilises water towards the lumen, producing isotonic to plasma secretions (Quinton, 1983, Lei et al., 2008, Reddy and Bell, 1996).

The aim of the experiments carried out in this chapter was to investigate functional aspects of the eccrine secretory coil and in particular to investigate whether or not EC23 cells retain Ca^{2+} transport ability when stimulated with the muscarinic agonist carbachol and the ionophore ionomycin. We also investigated the effect of the β-adrenergic agonist isoproterenol in increasing intracellular cAMP levels in the EC23 cells and clones, in comparison to primary eccrine secretory coil cells and NCL-SG3 cells.

4.2 Results

4.2.1 Effects of the Muscarinic Agonist Carbachol and Ionophore Ionomycin on Ca^{2+} Transport by EC23 Immortalised Eccrine Secretory Coil Cells.

To establish whether the EC23 cell line retains the pharmacological characteristics of the secretory coil and hence the potential for the production of sweat, experiments were carried out to assess whether the EC23 cell line is capable of effectively mobilising Ca^{2+} into and out of the cell. To study these fluxes, the Fluo-4 Direct™ assay kit was used. Fluo-4 Direct™ offer a method of detecting calcium fluxes in cells by means of fluorescence. Fluo-4 Direct™ offers a large window of time in which to perform the assay, and contains a background suppressing quencher. In its normal untreated state, Fluo-4 Direct™ remains unreactive within the cell with low levels of fluorescence being observed. Upon stimulation, Ca^{2+} is either released from the ER calcium stores or influxes via membrane bound calcium channels. Ca^{2+} then binds to the FLUO-4 Direct™ creating a highly fluorescent complex.

In these experiments, EC23 and NCL-SG3 cells were treated with atropine or ryanodine in order to inhibit the muscarinic pathway and ryanodine channels in the ER respectively. Experiments in which the EC23 cells were left untreated with atropine or ryanodine were also conducted in order to better determine if muscarinic and ryanodine receptors were being targeted correctly by carbachol and ionomycin. Atropine (figure 4.1A) is a naturally occurring compound found in some plants (*Atropa belladonna, Datura stramonium and Mandragora*

officinarum), and is a competitive agonist acting on muscarinic receptors of the parasympathetic nervous system (Rang and Dale, 2007). Ryanodine (figure 4.1B) is a compound found in *Ryania speciosa*, and it has a very high affinity for ryanodine receptors found in the ER of cells (Sorrentino, 1995). Ionomycin (figure 4.1D) is an ionophore that triggers the release of calcium from the ER without interacting with G coupled proteins (Yoshida and Plant, 1992, Morgan and Jacob, 1994).

To assess whether EC23 and NCL-SG3 cells were capable of effectively mobilising Ca^{2+} in response to cholinergic stimulation, the cells were seeded onto glass bottom dishes and allowed to reach ~40-50% confluency. When the cells reach this confluency, they were incubated in FLUO-4 direct™ assay reagent. The experiments were conducted in two stages. Stage 1 consisted on two sets of dishes, with one set being incubated in the absence of atropine and the other set in the presence of atropine. The second stage involved a separate two sets of dishes containing cells, in which one set was incubated in the presence of ryanodine and the other in the absence of ryanodine. The reason for the two stages was purely because conducting all sets at one time would be too lengthy. After incubation, with either atropine or ryanodine or in their absence of either inhibitor, the cells were then stimulated with the muscarinic agonist carbachol and the change in fluorescence was recorded using a time-lapse microscope. After 270 seconds (frame 90), the cells were treated with ionomycin and the change in fluorescence was recorded. The results are shown in figures 4.2, 4.3, 4.4, 4.5 and table 4.1.

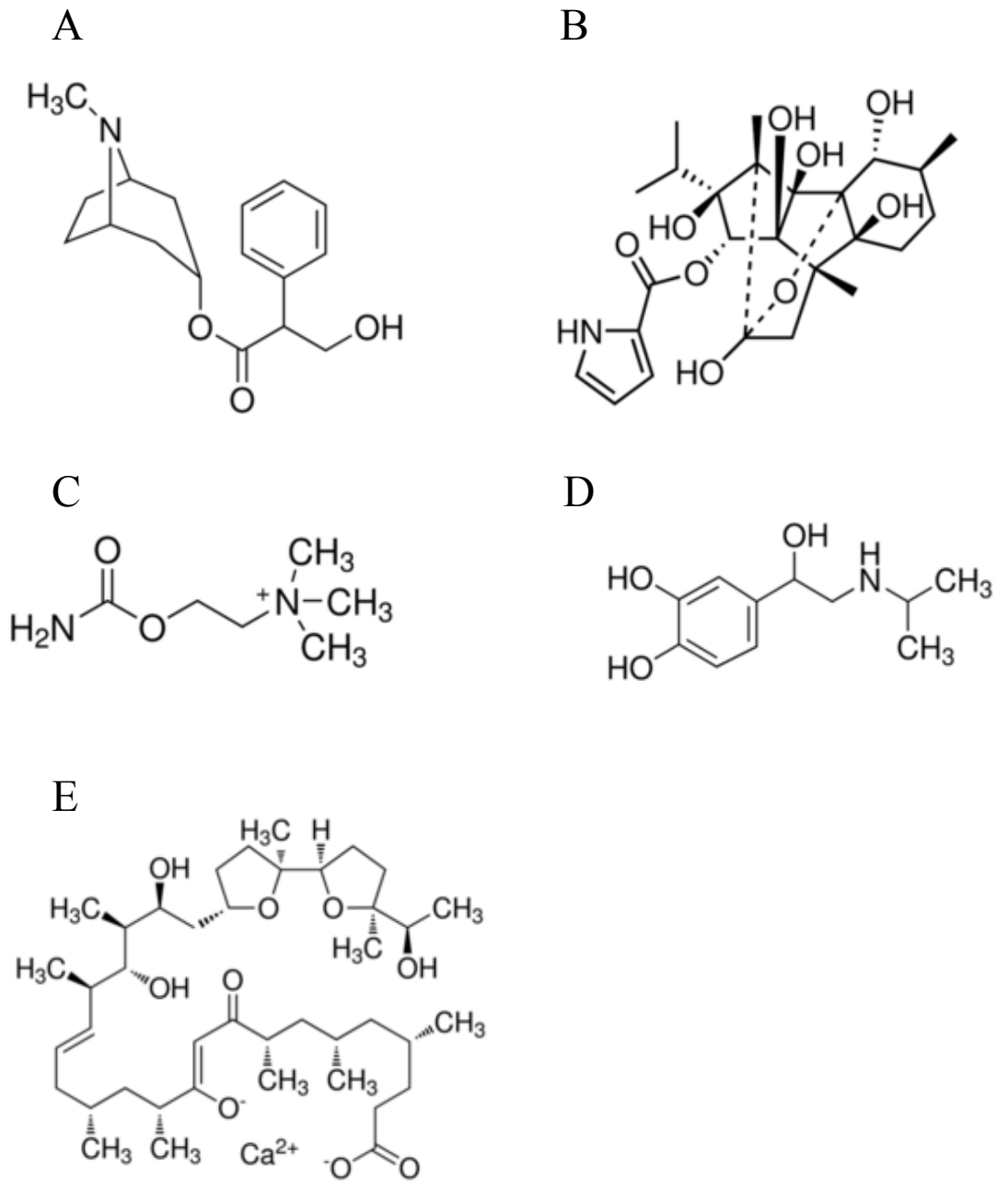

Figure 4.1. Chemical structure of (A) atropine; (B) ryanodine; (C) isoproterenol ;(D) carbachol and (D) ionomycin.

EC23 cells stimulated with carbachol averaged a calcium flux of 0.45 ΔRFU (figure 4.2). After carbachol stimulation of the EC23 cells that were incubated in atropine, calcium flux was significantly ($P<0.05$) lower at 0.09 ΔRFU. When the EC23 cells (not incubated in atropine) were stimulated with ionomycin the fluorescence registered was much higher, at 0.99 ΔRFU, compared to the set of EC23 dishes that had been incubated with atropine, which exhibited significantly ($P<0.05$) lower level of calcium flux, 0.14 ΔRFU. Thus showing that atropine was able to block calcium flux stimulated by both the muscarinic agonist carbachol and ionomycin, which release calcium from the ER.

In a second set of experiments the effect of ryanodine on calcium flux were studied in a similar way to that used to investigate the effects of atropine. When EC23 cells were incubated with ryanodine and then stimulated with carbachol the cells were observed to have a fluorescence change (0.49 ΔRFU) similar to that of EC23 cells that were not incubated with ryanodine and carbachol stimulated (0.44 ΔRFU) (figure 4.3). EC23 cells stimulated with carbachol and then ionomycin without ryanodine incubation displayed a much higher calcium flux at 0.99 ΔRFU when compared to the stimulation with carbachol. This was significantly ($P<0.05$) inhibited in cells that were treated with ryanodine and then stimulated with carbachol and ionomycin, which had a calcium flux of only 0.04 ΔRFU after ionomycin stimulation. This data showed that while ryanodine had no effect on carbachol stimulated calcium flux, it had a major and significant effect on calcium flux in cells stimulated by both carbachol and ionomycin, and that the inhibition of calcium flux was significantly lower than both Carbachol stimulated cells alone and carbachol and ionomycin stimulated cells.

In NCL-SG3 cells, no significant difference was observed in calcium flux between the two groups; atropine incubated and non-atropine incubated upon carbachol stimulation, 0.11 ΔRFU and 0.08 ΔRFU, respectively. There was also no significant difference observed between atropine incubated (0.38 ΔRFU) and non-atropine incubated (0.39 ΔRFU) NCL-SG3 cells upon stimulation with ionomycin (figure 4.4). This data suggests that the NCL-SG3 cells are not responsive to carbachol but retain responsiveness to ionomycin.

In the set of experiments in which NCL-SG3 (Figure 4.5) cells were not incubated with ryanodine, carbachol stimulation resulted in a calcium flux of 0.10 ΔRFU, which was not significantly different from the results obtained for the cells treated with ryanodine and stimulated with carbachol (0.17 ΔRFU). However when ryanodine was used to inhibit ryanodine receptors in the ER, we observed a significantly lower calcium flux ($P<0.05$) in NCL-SG3 cells incubated with ryanodine and then stimulated with ionomycin (0.08 ΔRFU) compared to the non-ryanodine incubated cells (ΔRFU 0.38). These data suggest that NCL-SG3 cells have a very weak response to carbachol that is unaffected by atropine. However ryanodine is able to block calcium influx stimulated by ionomycin.

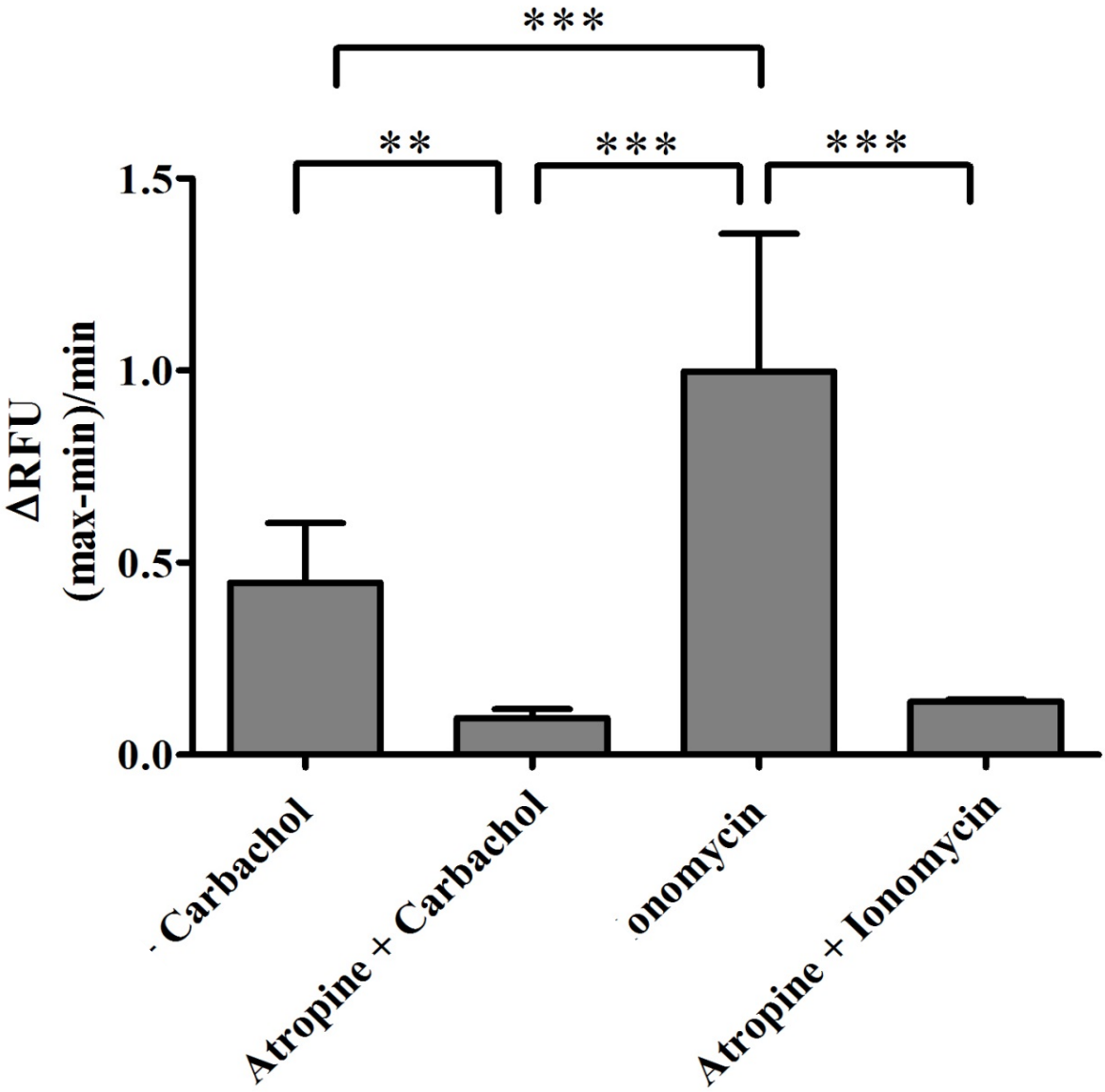

Figure 4.2. Effect of atropine on calcium influx of EC23 cells treated with carbachol and ionomycin. Cells with or without atropine treatment were stimulated with carbachol and ionomycin, and show that atropine was able to block calcium flux stimulated by the muscarinic agonist carbachol and ionomycin. Results are expressed as the mean +/- SEM change in fluorescent units (ΔRFU) for n = 3 separate experiments. Statistical analysis was carried out using a one way ANOVA with post hoc Tukey's multiple comparison test (*P<0.05; **P<0.01; ***P<0.001).

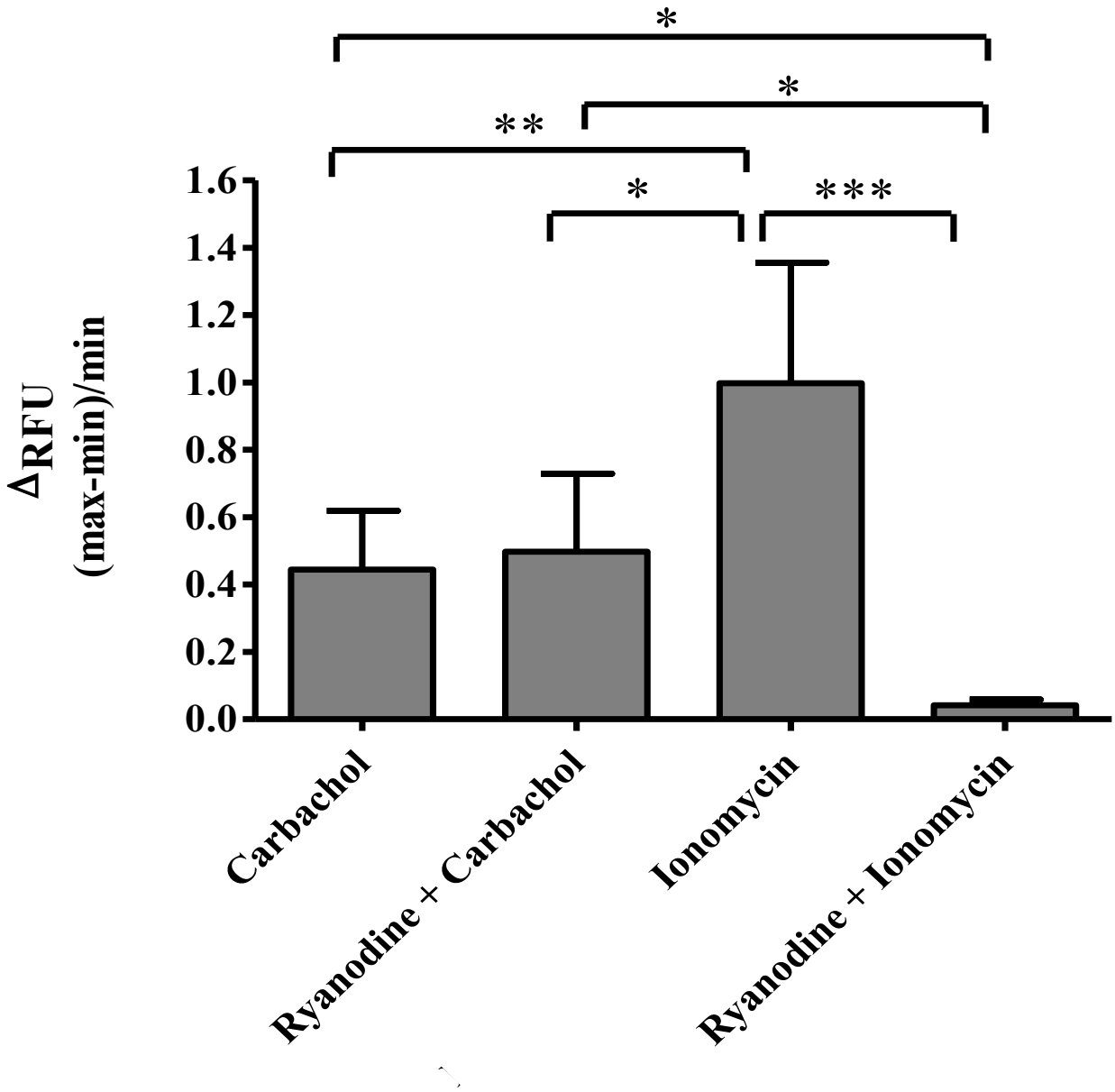

Figure 4.3. The effect of ryanodine on calcium influx of EC23 cells treated with carbachol and ionomycin. EC23 cells with or without ryanodine treatment, were stimulated with carbachol and ionomycin and show that ryanodine had no effect on calcium flux stimulated by carbachol and it was able to block calcium flux stimulated by ionomycin. Results are expressed as the mean +/- SEM change in fluorescent units (ΔRFU) for n = 3 separate experiments. Statistical analysis was carried out using a one way ANOVA with a post hoc Tukey's multiple comparison test (*P<0.05; **P<0.01; ***P<0.001).

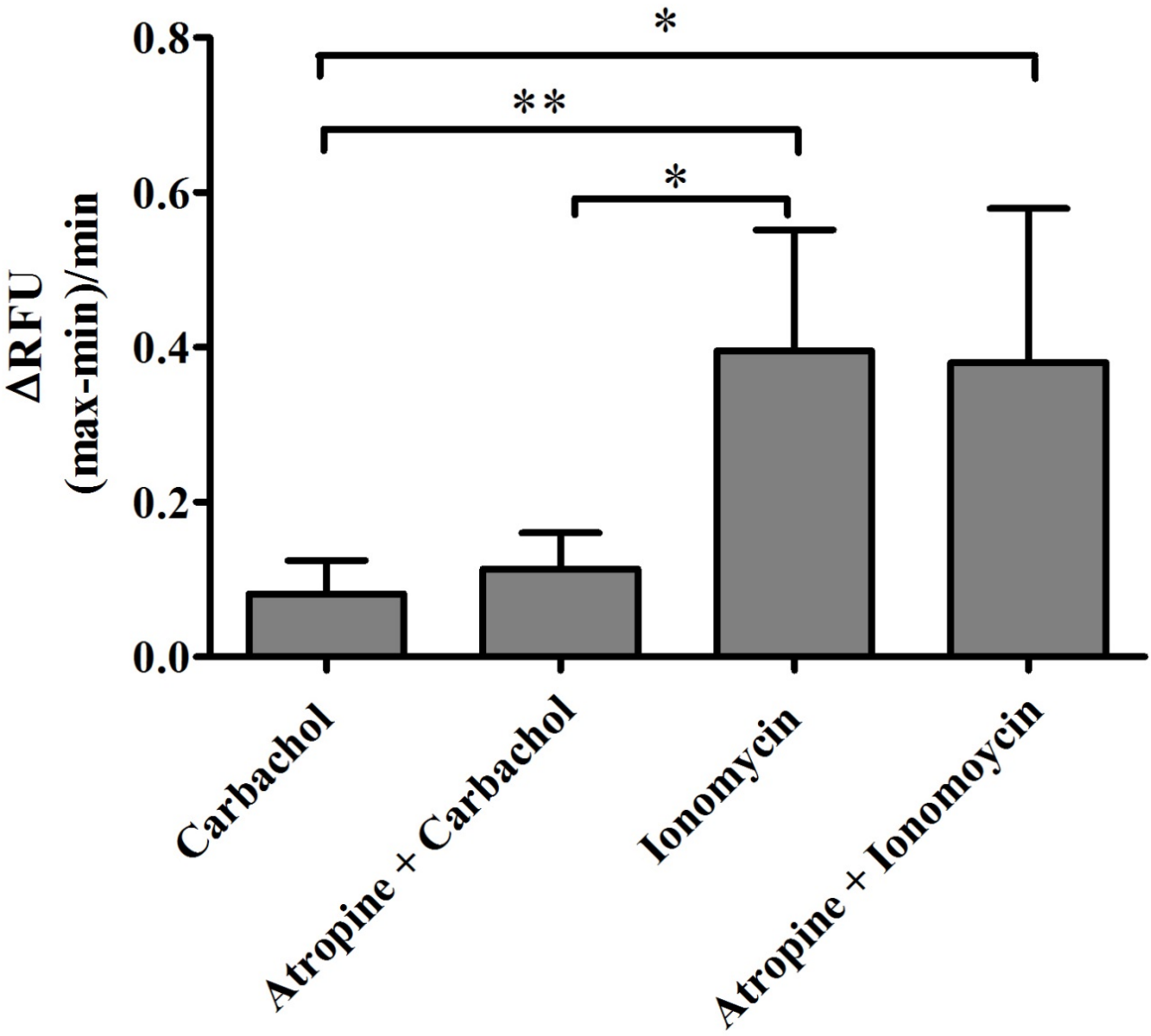

Figure 4.4 Effect of atropine on calcium influx of NCL-SG3 cells treated with carbachol and ionomycin. Cells with or without atropine treatment were stimulated with carbachol and ionomycin. And show that atropine was unable to block calcium flux stimulated by ionomycin Results are expressed as the mean ± SEM change in fluorescence units (ΔRFU) for n=3 separate experiments. Statistical analysis was carried out using a one way ANOVA with a post hoc Tukey's multiple comparison test (*P<0.05; **P<0.01).

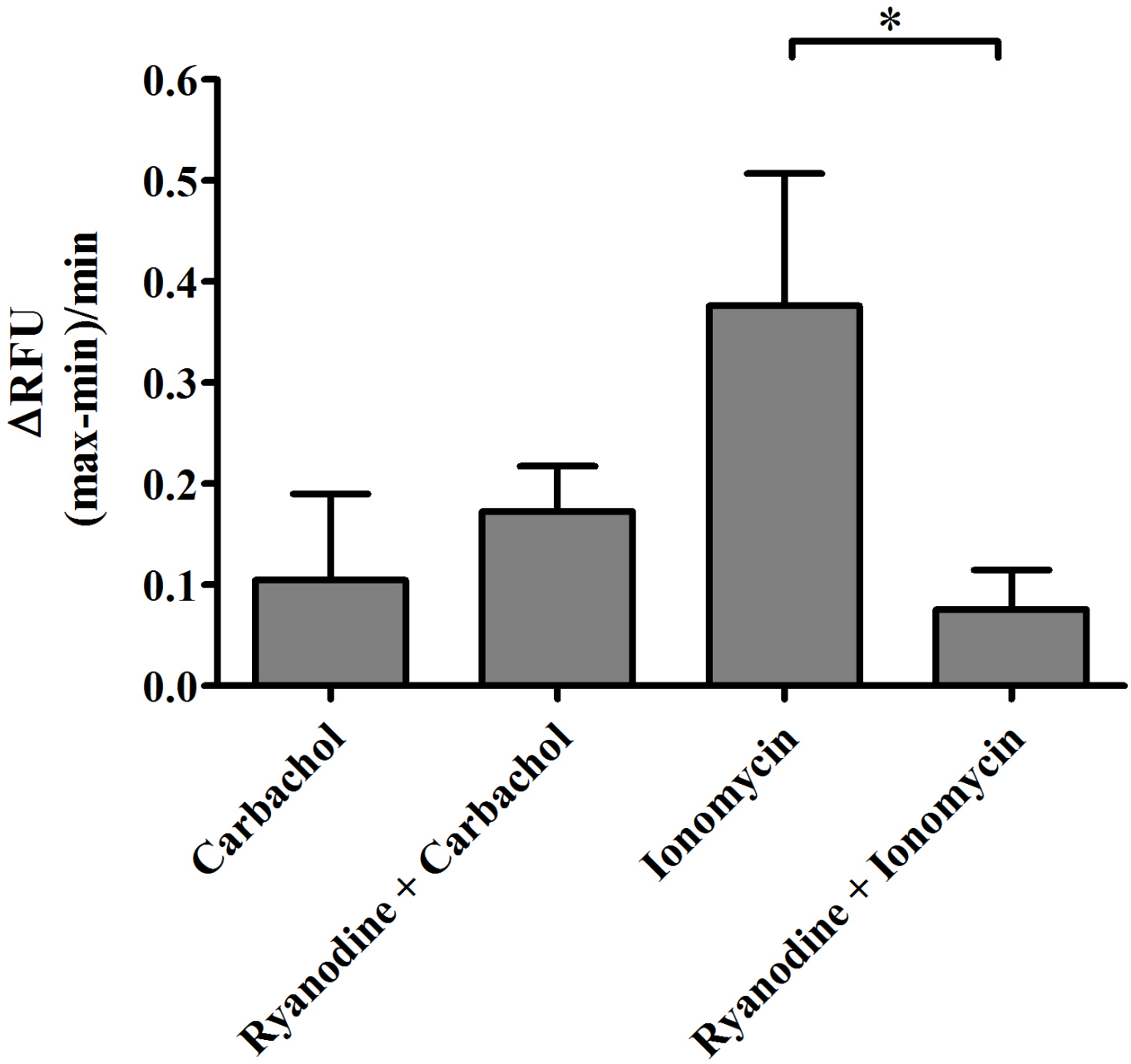

Figure 4.5 Change in relative fluorescent units (ΔRFU) of NCL-SG3 cells treated with ryanodine and stimulated with carbachol and ionomycin. Results are expressed as the mean ± SEM for n=3 separate experiments. Statistical analysis was carried using a one way ANOVA with a Tukey's multiple comparison test as post hoc test ($P<0.05$).

Treatment	EC23 (ΔRFU)	NCL-SG3 (ΔRFU)
No Atropine + Carbachol	0.45 ±0.15	0.08 ± 0.04
Atropine + Carbachol	0.09 ± 0.02	0.11 ± 0.05
No Atropine + Ionomycin	0.99 ± 0.36	0.39 ± 0.16
Atropine + Ionomycin	0.14 ± 0.01	0.38 ± 0.19
No Ryanodine + Carbachol	0.44 ± 0.17	0.11 ± 0.08
Ryanodine + Carbachol	0.49 ± 0.23	0.17 ± 0.04
No Ryanodine + Ionomycin	0.99 ± 0.35	0.38 ± 038
Ryanodine + Ionomycin	0.04 ± 0.01	0.08 ± 0.04

Table 4.1. Summary showing changes in calcium flux as measured by ΔRFU for EC23 and NCL-SG3 cells upon stimulation with carbachol and Ionomycin**.** Results are expressed as the mean ± SEM for n=3 separate experiments.

4.2.2 Effects of the Adrenergic Agonist Isoproterenol on Cyclic AMP Levels in EC23 Immortalised Eccrine Secretory Coil Cells

Levels of cellular cyclic AMP are also very important in assessing the functionality of secretory coil cells, as stimulation from the β-adrenergic pathway can also elicit a sweat response (Martinez et al, 2012; Quinton, 2012). The mode of function of this pathway, however, differs from that of the cholinergic pathway in that it is calcium independent (Sato and Sato, 1981b, Quinton, 1983). Instead it depends on the responses produced upon stimulation of the prostaglandin I_2 receptor, which triggers an increase in cAMP that in turn activates CFTR receptors that release chloride ions (Reddy and Bell, 1996). These secretions cannot be sustained over long periods of time and are roughly 20% of those produced by the cholinergic pathway (Sato, et al 1988; Martinez et al., 2012). This could be explained by the fact that in the adrenergic pathway, the production of cAMP only activates CFTR, mobilizing Cl^- out of the cell and not K^+, thus preventing full electrolyte fluxes and water diffusion through the membrane to produce a larger volume of secretion (Reddy & Bell, et al 1996). The purpose of adrenergic-induced secretion remains unclear, but to fully study the retention of the eccrine phenotype of the EC23 cells and their possible use as a model for the study of cystic fibrosis, we have studied the response of the EC23 cells and clones to the β-adrenergic agonist isoproterenol in comparison to primary eccrine secretory coil cells and NCL-SG3 cells.

To study the response of EC23 cells to the β-adrenergic agonist isoproterenol, EC23 cells and clones were stimulated with 1μM isoproterenol for 3 minutes,

following which a commercially available kit for measuring intracellular cAMP concentration was used (see Materials and Methods). The results of these experiments are shown in Figure 4.6 and summarised in Table 4.2. EC23 cells, clone 1, clone 3, clone 4, clone 7 and clone 8 cells responded to β-adrenergic stimuli with similar increases, in cAMP between 13.6 nM and 23.8 nM of cAMP (see table 4.2 for values). Clone 8 responded to β-adrenergic stimulation slightly higher concentration of cAMP at 34.3 nM. Of the clones, clone 2 had the highest response to isoproterenol at 58.7 nM cAMP, which was significantly higher ($P<0.05$) than that of NCL-SG3 cells. The NCL-SG3 cells responded to a lesser degree to isoproterenol than all the cells tested, with a cAMP concentration of 4.3 nM. The primary eccrine secretory coil cells had the largest response to stimulation, with a concentration of 93.5 nM of cAMP, a value that was significantly higher ($P<0.05$) than all other cell types.

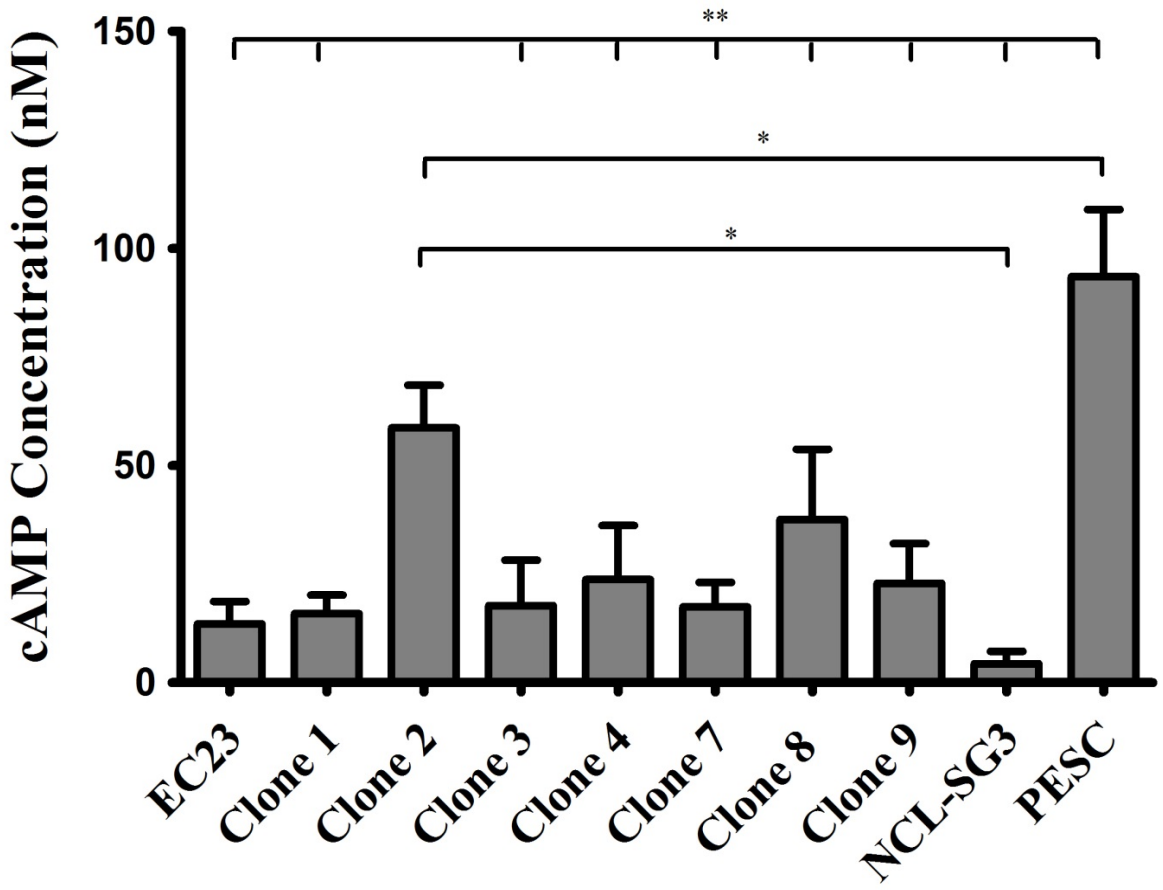

Figure 4.6. Intracellular cAMP concentrations (nM) in EC23 cells as well as clones derived from the EC23 cell line, NCL-SG3 cells and primary eccrine secretory coil (PESC) cells, after stimulation with 1µM isoproterenol. PESC cAMP concentrations were significantly higher than all other cell lines. Clone 2 cAMP concentration was significantly higher than NCL-SG3 Data is shown as the mean ± S.E.M for n = 3 separate experiments. Statistical analysis was carried out using a one way ANOVA with a post hoc Tukey's multiple comparison test (*P<0.05; **P<0.01).

Cell Type	cAMP Concentration (nM) in stimulated cells	Control cAMP Concentration (nM) in unstimulated cells
EC23	13.55 (5.17)	1.82 (0.10)
Clone 1	15.95 (4.28)	2.18 (0.59)
Clone 2	58.71 (9.82)	2.90 (0.29)
Clone 3	17.78 (10.45)	1.99 (0.05)
Clone 4	23.76 (12.43)	2.14 (0.36)
Clone 7	17.49 (5.61)	2.21 (0.29)
Clone 8	34.27 (18.08)	2.45 (0.06)
Clone 9	22.90 (9.14)	1.94 (0.24)
NCl-SG3	4.36 (2.33)	1.98 (0.40)
PESC	93.50 (12.63)	1.82 (0.24)

Table. 4.2. cAMP concentration of EC23, Clones, NCL-SG3 cells and primary eccrine secretory coil (PESC) cells after stimulation with 1μM isoproterenol. Control cAMP values are for cells without stimulation with isoproterenol. Data is shown as the mean ± S.E.M (brackets) for n=3 separate experiments.

4.2.3 Identification of calcium release modulator 1 (Orai1) and stromal interaction molecule 1 (Stim1).

Stim1 is an important protein that resides in the endoplasmic reticulum of some cells (Lewis, 2011).Stim1 detects decreases in Ca^{2+} in the lumen of the ER at which point it changes conformation, allowing it to reach the plasma membrane (Liou et al., 2005). Once it reaches the plasma membrane, Stim1 activates the calcium channel pore protein Orai1. After activation Orai1 forms hexamers forming a channel that allows the entrance of Ca^{2+} (Srikanth and Gwack, 2012, Zhou et al., 2013).

In a 2009 study by McCarl, et al, it was found Orai1 expression in normal eccrine sweat glands and other tissues such as thymus, spleen and adrenal glands (McCarl et al., 2009). It was also noted that mutations in Orai1 deficiency leads to severe defects in immunity, congenital myopathies and ectodermal dysplasias, which affect eccrine gland development and function often causing anhydrosis. McCarl also found that all the patients that had Stim1 deficiencies also presented with anhidrosis (McCarl et al., 2009). Because Orai1 deficiencies seem to lead to eccrine gland developmental problems, it is unclear if Orai1 is required for proper eccrine function (Lewis, 2011). More recently, Robertson and Bovell (2014), demonstrated that the inhibition of Stim1 can lead to anhydrosis in equine eccrine cells, suggesting an important role of Stim1 in anhidrosis (Robertson and Bovell, 2014). With this in mind, it was important to establish the presence of Stim1 and Orai1 in the EC23 cell line, as it appears to be required for proper eccrine function.

To establish the presence of Stim1 and Orai1 in the EC23 cell population, the cells were cultured on cover glass and immunocytochemistry was performed. Figure 4.7 shows that both Orai1 and Stim1 expressed in EC23 cells. Interestingly Orai1 appears to be present in the nuclei of cells in both EC23 cells and in primary eccrine secretory coil cells, however it has only ever been reported in the plasma membrane (Henke et al., 2013).

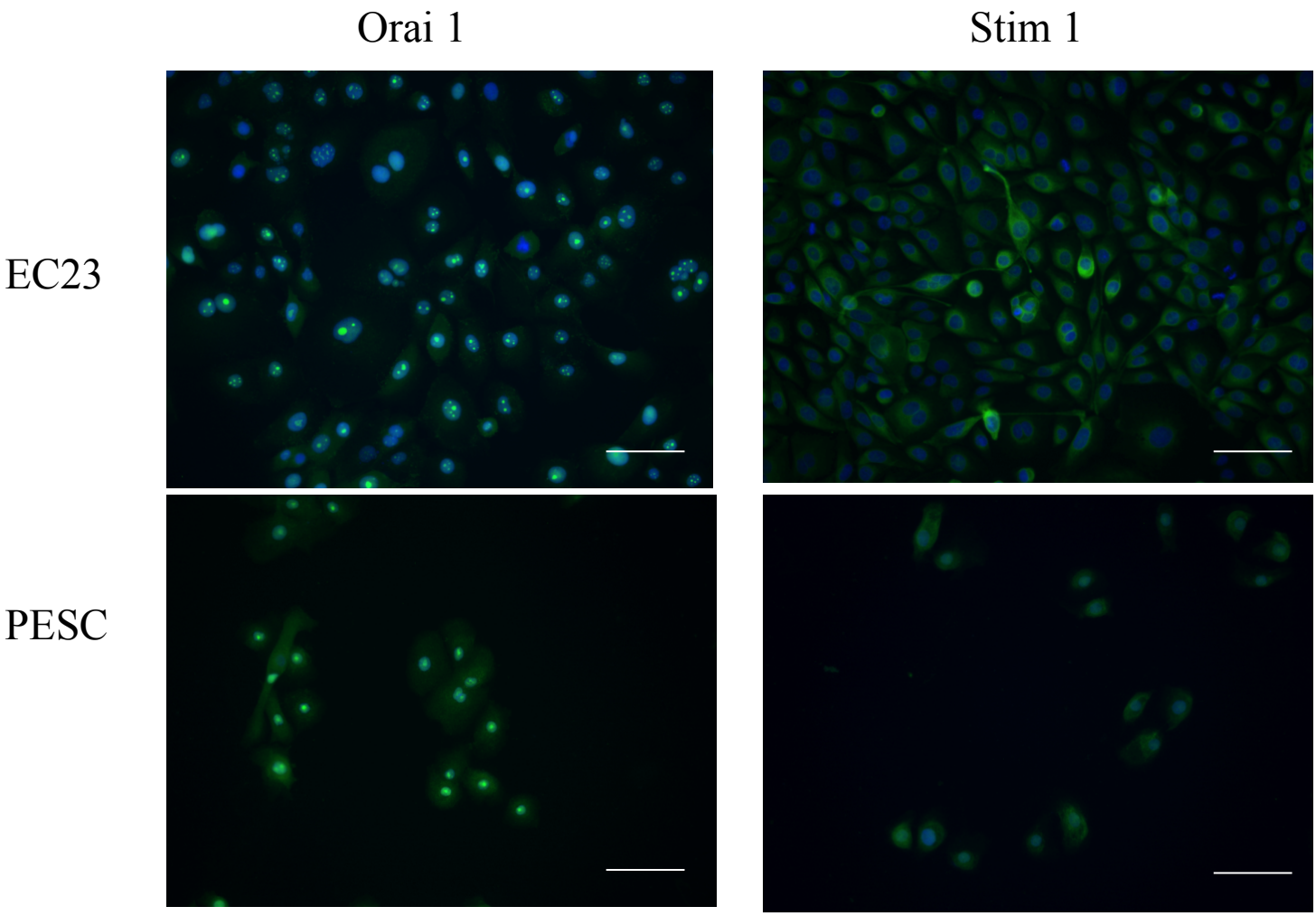

Figure 4.7. Immunocytochemistry identifying Orai1 and stim1 in EC23 cells and primary eccrine secretory coil cells. Showing expression of Orai1 on EC23 cells and primary eccrine secretory cells, including their nuclei and or Stim1 in the cytoplasm of the cells. n=3 separate experiments. Scale bars = 100 μM

4.3 Discussion

The EC23 cell line is, to our knowledge, the only other immortalised cell line derived from the eccrine gland apart from the NCL-SG3 cells. Lee and Dessi, (1989) derived the NCL-SG3 cell line from human eccrine glands using SV40 to immortalise primary cells cultures. The NCL-SG3 cell line was described as being sensitive to the beta-adrenergic agonist isoproterenol, but not to the cholinergic agonist carbachol (Lee and Dessi, 1989). In the experiments carried out in this chapter we aimed to study the effect of the cholinergic agonist carbachol and the adrenergic agonist isoproterenol on calcium flux and intracellular cAMP concentration in the EC23 cell line and clones derived from this cell line and where possible compare with both the NCL-SG3 cell line and primary eccrine sweat gland secretory coil cells. For the latter this was not always possible as the PESC cells are difficult to grow and it was not always possible to generate enough cells for pharmacological assay.

During the course of this project, clone 5 became increasingly apoptotic and thus was not used in these experiments. The cholinergic experiments were only performed on EC23 cells and NCL-SG3, as it was felt that using the EC23 cell line mixed population of cells of would give a good overview of the secretory coil derived cells' response to cholinergic stimuli in comparison to the NCL-SG3 cell line. Attempts were made to use primary secretory coil cells in the calcium flux (cholinergic) experiments, however the cells were too sensitive to the reagents and became apoptotic very rapidly and thus no usable data was collected.

The initial stimulation of the EC23 cell line with carbachol resulted in an increase in intracellular calcium, represented as 0.45 ΔRFU, but when the cells were pre-treated with atropine a much lower calcium flux was observed, 0.09 ΔRFU. The increase in intracellular calcium in non-atropine treated cells suggests that the EC23 cells have retained the ability to respond to cholinergic stimuli and activate ER calcium store IP_3R receptors and open channels to release calcium into the cytoplasm. Interestingly, the cells appear to influx calcium even when the cholinergic pathway was blocked by atropine. This influx, which is low (0.09 ΔRFU), could have been caused by entry of Ca^{2+} via a different pathway such as receptors tyrosine kinase (RTKs) or by one of the many other calcium channels present in the cell membrane, such as receptor operated channels (ROCs) or transient receptor activated potential cation channels (TRCPs) (Berridge et al., 2003). RTKs work in a similar way to G-protein coupled receptors, however PCL-γ –which contains a tyrosine residue- is phosphorylated upon RTKs activation, cleaving PIP_2 into DAG and IP_3 and then IP_3 can activate IP_3Rs to induce calcium release from the ER. DAG can activate TRPCs (Albert et al., 2007) and can be calcium store depletion independent, unlike Orai channels that are store operated calcium channels (Ma et al., 2000), and thus could also have also been activated by cholinergic stimuli to further increase cytoplasmic calcium. ROCs, which are often present in the membranes of cells can be stimulated by various ligands such as ATP, glutamate or acetylcholine and as could be responsible for the small calcium flux as the reagents used in the experiments were dissolved in media which contains glutamine and calcium chloride.

The results of carbachol treatment of NCL-SG3 cells after atropine pre-treatment were nearly identical to those for the cells that remained untreated with atropine. A much lower response than that elicited in EC23 cells under the same conditions (untreated with atropine) was seen, but the response was similar to both cell types after pre-treatment with atropine, 0.09 ΔRFU for EC23 cells and 0.11 ΔRFU for NCL-SG3 cells. These data again could support Lee and Dessi's (1989) work, in which NCL-SG3 cells were found to be non-responsive to cholinergic stimuli. The NCL-SG3 cells, however, do release calcium from stores upon stimulation with ionomycin, with or without pre-treatment with atropine. This suggests that only the initial activation of calcium secretion via cholinergic stimuli is impaired in the NCL-SG3 cells.

To further study the mechanisms of calcium movement within the EC23 and NCL-SG3 cells, the cells were treated with ionomycin. Upon administration of ionomycin, the non-atropine incubated EC23 cells again exhibited an increase in cytoplasmic calcium (0.99 ΔRFU) compared to a lower increase for the atropine incubated cells (0.14 ΔRFU). Stimulation of the cells with ionomycin was performed 4 minutes after the addition of carbachol. The low ΔRFU observed on cells treated with atropine and ionomycin is unexpected, as the blockade of the muscarinic pathway by atropine should not have affected the ER, and therefore should not influence the effect of ionomycin. One explanation of this could be that the large calcium flux observed in the non atropine treated cells is partly due to the release of calcium ions from the ER and the rest is due to the activation of CRAC channels eliciting a larger influx of calcium, and it is possible that the atropine may have had an effect on the CRAC channels. Another possible

explanation could be that the stores had already been depleted in order to counteract any effect the atropine may have had on the cells, or that the atropine was too toxic to the cells, thus preventing further calcium fluxes.

In another set of experiments, we used ryanodine to block ryanodine receptors, in an attempt to study the function of both IP_3R and ryanodine receptors. After incubation with ryanodine, the cells were treated with carbachol, and as expected, there was no significant difference in the response between ryanodine treated and untreated EC23 cells.

The response of the EC23 cells to ionomycin when pre-treated with ryanodine was negligible in comparison to the response of the cells to ionomycin without ryanodine treatment, which was significantly higher than that of the treated cells. The near equal response to carbachol by the EC23 cells with and without ryanodine treatment suggests that carbachol activates the muscarinic receptors in the cell membrane of the cells resulting in production of IP_3 and thus the activation of the IP_3R receptors in the ER resulting in the release of Ca^{2+} into the cytoplasm. On the other hand, the vast difference in the response to ionomycin after treatment with ryanodine suggests that ionomycin activates the ryanodine receptors of the ER in EC23 cells. This contradicts some studies performed in muscle cells, where it has been hypothesised that cholinergic activation of IP_3R in turn activates ryanodine receptors (White an McGeown, 2002; Boittin et al 1999). Thus, our data suggests that two separate mechanisms of activation may exist for calcium release from internal stores in the EC23 cells, one in which muscarinic receptor activation results in a release of calcium from the ER via IP_3R activation and other by the sole activation of s RyRs.

In the NCL-SG3 cell line, calcium influx responses were much lower overall than for the EC23 cells. After pre-treatment with ryanodine, NCL-SG3 cells still responded to carbachol to a minimal extent (0.17 ΔRFU). The strength of this response was similar to their response to carbachol after atropine pre-treatment (0.11 ΔRFU), and to carbachol without atropine treatment (0.08 ΔRFU). This is surprising, as the NCL-SG3 cells have previously been reported to be non-reactive to carbachol (Lee & Dessi, 1989), but as mentioned previously, other calcium channels may be present that are activated by the PIP_2 product DAG (Albert et al., 2007). There is also a significant difference between ryanodine pre-treated NCL-SG3 (0.08 ΔRFU) cells and untreated cells (0.38 ΔRFU) with ionomycin stimulation. Interestingly, the response of the NCL-SG3 cells to ionomycin when pre-treated with ryanodine is higher the response of the EC23 cells (0.041 ΔRFU), which could be interpreted as a dual mechanism of activation of IP_3R and ryanodine receptors in the NCL-SG3 cells. The response to carbachol for the NCL-SG3 cells after incubation with ryanodine was larger than expected, for both ryanodine pre-treated and untreated cells. This could again be due to influx via non-cholinergic receptors taking place.

Overall the calcium flux experiments suggest that EC23 cells have retained the phenotype of normal human eccrine secretory coil cells. However, this cannot be fully confirmed by these results alone, as there are a number other downstream pathways that need to be functioning properly in order for sweat production to occur, such as the movement of K^+ and Cl^- ions (Sato et al., 1989) . The initial step in the production of sweat secretions is the activation of the muscarinic

receptor M3, which activates the cleavage of the membrane bound PIP_2 by phospholipase C into IP_3 and DAG. IP_3 then translocates to the ER where it activates IP_3R receptors to release Ca^{2+} from the ER stores. In our experiments, only this initial step of activation was investigated, with results suggesting that the EC23 cells' muscarinic receptors can be successfully activated by the cholinergic agonist carbachol to activate the release of Ca^{2+} from the ER.

In the eccrine gland secretory cells, calcium is the key to initiating sweat secretions. The release of Ca^{2+} into the cytoplasm activates the opening of Cl^- and K^+ channels (figure 4.8), allowing these ions to exit the cell towards the lumen of the gland and the interstitium respectively. The increase in Cl^- concentration in the lumen creates an electrochemical gradient that drives the movement of Na^+ from the interstitium into the lumen via tight junctions, forming NaCl. The increase in solutes in the lumen of the gland drive the movement of water into the lumen via AQP5 (Roomans, 1999, Quinton, 1990). The chemical potential created by the movement of Cl^- and K^+ out of the cell activates NKCC1 to pump Na^+, K^+ and $2Cl^-$ back into the secretory cells to maintain an electrochemical balance. Na^+ is pumped out of the cell in exchange for K^+ via the Na^+/K^+ ATPase. Finally, K^+ ions diffuse from the cytoplasm back into the interstitium via K^+ channels to maintain the negative potential of the cell membrane (Sato et al., 1989, Lei et al., 2008). In a study to investigate sweat secretion in response to cholinergic and β-adrenergic stimulus, Reddy *et al*., (1996), found that the treatment of primary cells with barium ions (Ba^+) – a known K^+ channel blocker - after the muscarinic agonist methacholine was added only reduced K^+ conductance slightly. This suggests the existence of 2 (or more) K^+ channels in the membranes of secretory cells of the eccrine gland, barium sensitive and insensitive (Reddy and Bell,

1996). As we can see, the function of the clear cells of the secretory coil is dependant of a vast array of channels for proper function, and to fully study the functionality of the EC23 cells an array of further experiments must be conducted. These experiments should include the study of Cl^- and K^+ fluxes, with and without the inhibition of NKCC1.

To study whether the EC23 cells and clones retained the ability to react to the beta adrenergic agonist isoproterenol, a commercially available kit, Cyclic AMP XP® was used, and the results obtained were compared with data acquired from primary eccrine secretory coil cells and NCL-SG3 cells. The cells were incubated overnight (all cell types at the same seeding density), and the cells were treated with isoproterenol. After 3 minutes the cells were washed in PBS and lysed (section 2.4). The data gathered in these experiments suggest that the EC23 cells and all the clones maintain their ability to react to β-adrenergic stimuli. Clone 2 responded to isoproterenol at levels close to that of primary secretory coil cells, and clones 4, 7 and 8 had the largest responses after stimulation. When compared to the NCL-SG3 cells, the EC23 cells and all the clones yielded higher levels of cAMP after isoproterenol stimulation. This suggests that the EC23 cells and the clones are potentially better cell models for the study of the β-adrenergic pathway in the eccrine gland than the NCL-SG3 cell line.

The existence of dual innervation of the eccrine gland is well known (Sato and Sato, 1983a). However, only the cholinergic mode of action of the eccrine gland is fully understood. The specifics of the adrenergic mode of action are still open for debate. One hypothesis suggests that the adrenergic innervation of the eccrine

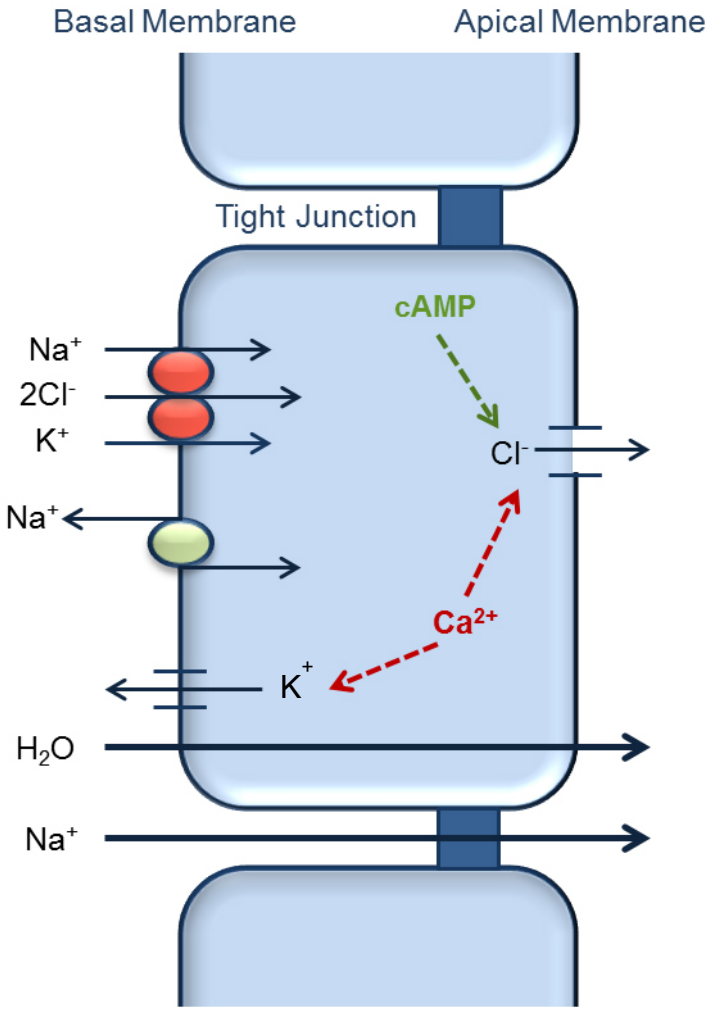

Figure 4.8. Schematic diagram of Eccrine gland secretory cells, depicting electrolyte and fluid secretion. Calcium, which is secreted into the cytoplasm upon cholinergic stimuli, activates Cl^- efflux from the apical membrane and K+ from the basolateral membrane, triggering the cascade of ion transport across the cells' membrane. Another initial activator of Cl^- is cAMP, however this stimuli does not K^+ efflux and activates CFTR, a non Ca^{2+} operated calcium channel (Adapted from (Roomans, 1999).

gland exists to facilitate heat acclimation, in which increased periods of perspiration occur (Sato et al., 1990, Martinez et al., 2012). However, *in vivo* experiments in which beta adrenergic responses were blocked by propranolol, topically applied via iontophoresis, found no effect of inhibition on heat acclimation compared to the control (Martinez et al., 2012). It is has also been established that the response to β-adrenergic stimuli is of lower magnitude than that caused by cholinergic stimuli; roughly 20% of the secretions produced by cholinergic stimuli (Sato and Sato, 1981b, Harker, 2013). It has also been postulated that adrenergic innervation exists to potentiate cholinergic sweating. A study by Mack, et al. (1981) found that sweat rates during exercise were decreased when subjects were administered propranolol, a β-adrenergic receptor blocker. Buono et al., (2010) found that after fully inhibiting the cholinergic responses by administration of atropine – to block the cholinergic pathway - and aminophylline – to amplify the β-adrenergic signal transduction pathway, there was no sweat induced after exercise. In an *in vitro* study, Sato and Sato 1981, found that isoproterenol enhanced sweat responses after stimulation with methacholine. These studies and others suggest that adrenergic sweating could indeed be a way to potentiate cholinergic sweating (Mack, 1986, Ohara et al., 1984, Buono et al., 2010, Buono et al., 2011, Sato and Sato, 1981b). However, the opposite has also been suggested, namely that cholinergic stimuli, potentiates β-adrenergic sweating. Sato and Sato 1983, found that the levels of cAMP induced by isoproterenol were increased upon stimulation with methacholine (Sato and Sato, 1983a).

In the experiments carried out in this chapter, it was found that all the cells tested were capable of reacting to isoproterenol (figure 4.5), with all control cells – untreated with isoproterenol – measuring between 1.19 and 3.19 nM of intracellular cAMP. The levels of cAMP found in the NCL-SG3 cells after stimulation (4.36 nM) was much lower than for most of the other cells used in this study, however they were only significantly lower than the concentrations found for the primary secretory coil cells and clone 2. This supports the findings by Lee and Dessi (1989) where they found that addition of isoproterenol to NCL-SG3 cells induced a multiphasic response in electrophysiology experiments. When stimulated, primary eccrine secretory coil cells responded with increased concentration of cAMP (93.49 nM), which was significantly higher ($p<0.05$) than all the other cells in the assay. This confirms that we were able to isolate and culture over a short time frame cells from the secretory coil and that they retained some of their expected pharmacological responses.

The decreased response of the EC23 cells and the clones in comparison to primary eccrine secretory coil cells suggests that the EC23 cell line and clones derived from this cell line have either had a decreased in number of beta adrenergic receptors, or have had some of the functionality compromised in the immortalisation or cell culture process. However, they do still retain a response to isoproterenol. Reddy et al., (1991), described the identification of a subclass of clear secretory coil cells: the β-adrenergic sensitive (β-S) and the β-adrenergic insensitive (β-I) cells, which are both sensitive to cholinergic stimuli (Reddy and Bell, 1996). The existence of these cells could explain the lower response of the EC23 cells and clones to isoproterenol. This could explain the differences

between the primary and EC23 cells and most of the clones, as there could be a much higher proportion of β-adrenergic insensitive cells within the EC23 cell population, and it is possible that the clones with the lowest responses to isoproterenol may be of the β-adrenergic insensitive phenotype. This could be investigated in the EC23 cells and clones by designing an experiment based on Reddy and Bells paper, in which the electrophysiology of the cells (membrane polarisation and depolarisation) measured after cholinergic stimuli and for β-adrenergic stimuli. In particular it would be interesting to know whether clones 2 and 8 which had the highest response to isoproterenol could be classified at β-adrenergic sensitive.

It would also be of extreme interest to investigate further which clones exhibit the highest responses to cholinergic stimuli and compare the data to the characterisation data acquired in chapter 3. Also it is interesting that the data collected from chapter 3 suggests that clones 2 and 8 do not retain full functionality as they lack NKCC1 that is essential for function; yet they responded with the greatest intensity of all the clones and EC23 cells when stimulated with isoproterenol. This is interesting as these cells may only react to β-adrenergic stimuli, and could have a role in potentiating the response to cholinergic stimuli, as suggested by Buono et al (2011). Due to the lack of understanding of the function of the dark cells in the eccrine gland and the lack of definitive markers, it remains difficult to device conclusive tests that differentiate between the clear and the dark cells. However recent studies suggest that FoxA1 may be exclusively present in the nuclei of dark cells, this study also suggests that the dark cell is also involved in the production of secretions, which makes

differentiating between the clear and dark cells by their differences in response to stimuli difficult (Cui and Schlessinger, 2015).

The presence of Stim1 and Orai1 (figure 4.6) within the EC23 cell population was also identified, providing further evidence that the cells may retain most if not all of the phenotype of primary secretory coil cells. Stim1 is highly important in facilitating calcium reuptake in cells, which in the eccrine gland is essential for function. This could suggest that the EC23 cells retain the ability to reuptake Ca^{2+} by store operated calcium channels. Furthermore, the presence of Stim1 and Orai1could make the EC23 cell line a good candidate for the study of store operated calcium channels in the eccrine glands and secretory cells in general. The expression of Orai1 in the nuclei of both the EC23 cell line and the primary eccrine secretory coil cells however is unexpected. Orai1 is located in the nuclear membrane and becomes activated by Stim1 upon calcium store depletion (Srikanth and Gwack, 2012, Zhou et al., 2013), and thus its expression in the nuclei is puzzling. To date there have not been any reports of Orai1 in the nuclei of cells, however the discovery of Orai1 is recent (Prakriya et al., 2006) and there is yet much to discovered about its mechanisms of function, and thus it is possible that Orai1 has a nuclear function. To confirm its location in the nuclei and to further study Orai1 in future, subcellular fractionation and subsequent western blotting experiments would be ideal.

It is highly likely the EC23 cell line is a heterogeneous population of cells and the different clones derived from this mixed population may represent different cells present in the eccrine gland (clear, dark, etc). It is possible that there are cells with

a dark cell phenotype within the EC23 cells in addition to β-adrenergic insensitive and sensitive cells. Our data also suggests that clone 2 may be a beta sensitive cell, as it had the largest response from all the cells to isoproterenol. The same could be true for clone 8 even though the response was lower, which could be due to a reduction in β-adrenergic receptors and decreased function.

The experiments carried out to investigate the responsiveness of the EC23 cell line and the clones suggest that the cells retain much of the phenotype of primary cells of the secretory coil of the eccrine gland. The calcium flux experiments suggest that the cells are indeed responding to cholinergic stimuli by activation of IP_3R and ryanodine receptors. However, the initial responses to cholinergic and β-adrenergic agonists were the only ones investigated, and thus it is not possible to be sure that the phenotype is fully retained. To fully study this, electrophysiology experiments would be ideal, in which membrane potentials in response to stimuli can be measured. With these experiments one would be able to determine K^+ and Cl^- conductance in order to determine K^+ and Cl^- channel function in response to stimuli. Finally, it is clear that there is significant heterogeneity in the cell types derived from the EC23 cell line, the reasons for this are not clear, however, as these are clonal lines and based on the acknowledged difficulty in culturing and maintaining primary eccrine secretory coil cell it is very likely that the clones derived from the EC23 cell line may represent the range of different states of differentiation and de-differentiation in the EC23 line. Further experiments could be carried out with a view to screening for further clones that exhibit even closer characteristics to the secretory coil phenotype.

Chapter 5. Development of a 3D Organotypic model of the Eccrine Gland

5.1 Introduction

Skin is a complex organ composed of several layers, Dermis, epidermis and subcutis, with the epidermis being composed of keratinocytes in an undifferentiated state in the basal layer, which differentiate as they move up the epidermis until they fully lose their nuclei and become stratified and form the stratum corneum. The human eccrine gland, and other skin appendages such as the hair follicle, sebocyte and apocrine glands, transverse these epidermal layers and the dermis. The eccrine gland's secretory coil rests within the dermis with the duct traveling through the dermis towards the epidermis, where the accrosyringium opens up towards the surface of the skin.

The development of the human eccrine sweat glands begins in the third gestational month in the soles of the feet and the palm of the hands followed by the development of eccrine glands in the rest of the body at the fifth gestational month (Saga, 2002). The eccrine gland is composed of three cell types, the clear cell, the dark cell and the myoepithelial cells, with the clear cell being the main fluid secreting cell of the gland. Eccrine glands vary in size from individual to individual, however the secretory coil is about 60-80 μm in diameter and two to five mm in length (Sato et al., 1989, Saga, 2002). The duct (the intradermal duct and accrosyringium) is composed of two layers of cells, the luminal and basal cells. The secretory coil on the other hand, is composed of a single cell layer of clear and dark cells, which are then surrounded by myoepithelial cells. The secretory portion of the eccrine gland appears to be globular due to its coiled conformation (Quinton, 1983, Sato et al., 1989).

2D cell culture systems cells often differ in morphology, cell matrix and cell-cell interactions compared to those found in cells grown in 3D environments. In 2D culture cells often lose their polarity, which can affect their function, the formation of branching structures often found in glands is compromised in 2D culture (Griffith and Swartz, 2006; Nelson and Bissell, 2006, Yamada, 2007). Animal models offer another option for the study of tissues and disease, however there are many issues to consider before using an animal model, from ethical reasons to molecular interactions in the animal that may influence the experiment in ways that would differ from humans rendering them inadequate (Fisher et al., 2009). Three dimensional modelling can be a useful tool in understanding tissue morphogenesis, cell-cell interactions and molecular mechanisms in which 2D modelling falls short.

When considering 3D modelling, there are many factors to consider, starting from the scaffold material to be used in the experiment. This is highly important as stiffness, tensile strength, porosity and the composition (proteins, cytokines and growth factors) of the matrix can affect the outcome of the experiment (Yamada and Cukierman, 2007, Chan and Leong, 2008, Watt and Huck, 2013). It is well documented that the stiffness of the material can affect the way cells behave (Breuls et al., 2008, Watt and Huck, 2013). The material the scaffold is made from can affect the experiment to a great extent. The use of decellularised tissue has great advantages in modelling of some organs as the scaffold retains extracellular matrix that signal cells to organise in a particular pattern (Crapo et al., 2011), however this is not a suitable material for all experimental models,

such as the eccrine gland. There are also synthetic materials available such as, poly-lactic acid, polyglycolic acid to name a few and some scaffolds from natural materials such a silk and chitosan. These materials have the advantage that they are very malleable and can be made into sponges, hydrogels and electrospun fibres, which can be useful in models of whole organs or tissues such as bone (Chan and Leong, 2008)

Other natural materials that have been widely used for 3D cell culture and tissue modelling include collagen and matrigel, the two materials that were used in this project. Collagen is abundant in skin and has been widely used to make 3D models of human skin (Navsaria et al., 1995) as well as keratinocytes, fibroblasts and cancerous cells for example to model melanoma (Smalley et al., 2006) and squamous cell carcinoma (Ng et al., 2012).

Recently matrigel has been used in the study of the morphogenesis of organs such as the mammary gland, parotid gland and small intestine crypts. The use of matrigel in 3D modelling has been extensively documented. Lo et at., (2012) described a protocol in which matrigel was being used to study the branching morphogenesis of the mammary gland (Lo et al., 2012). In the mammary gland much of the research has been focused on understanding morphogenesis with implications in cancer development. In the small intestine, it has been used in the development of organoid 'mini guts'. The mini guts were developed with the focus of identifying stem cells in the intestinal crypts to study intestinal epithelial homeostasis and regeneration (Sato et al., 2009). This intestinal organoids have opened the doors to a vast array of investigations, from understanding intestinal

regeneration and the stem cells present in intestinal crypts, to models of disease (Barker et al., 2007). The intestinal organoid model in matrigel consists of the isolation of Lgr5+ slender crypt base columnar (CBC) cells which are cultured in matrigel supplemented with R-spondin, EGF and noggin, which are the essential growth factors required for stemness maintenance. The organoids produced are then passaged by matrix disruption and reseeded in matrigel weekly in order to maintain culture for up to 1.5 years (Sato et al., 2009, Sato and Clevers, 2013).

Initial work performed in our laboratory demonstrated that the EC23 cell line could form eccrine like structures in collagen type I organotypic cultures (Figure 1.5). The aim of the following experiments was to further investigate these structures in more detail and to further develop a model of the human eccrine sweat gland that could be used to study its development and the effects of pharmacological agents on the gland. In matrigel experiments the degree of branching (branching nodes) was examined in spheroid structures formed by EC23 cells. Branching is not necessarily an eccrine gland feature but it's the most adequate way of studying coil like formation that was available at the time especially as we were investigating the effect of growth factors on morphogenesis and the other parameters that could be measured could only give information about size changes in response to the growth factors.

5.2 Results

5.2.1 Organotypic raft cultures of EC23 cell seeded De-epidermialised dermis.

Organotypic models were made using de-epidermialised dermis EC23 cells, keratinocytes and fibroblast, with different combinations to assess the properties of each model. DED organotypics seeded with keratinocytes at two weeks also show some degree of down growth. The DEDs seeded with keratinocytes and EC23 cells show a good level downgrowth and a possible formation of a glandular structure at 2 weeks of culture; this was not observed in the 3 week culture. Furthermore, there was little stratification and no cornification of the keratinocytes. On organotypics seeded with EC23 cells no cornification is observed, however there appears to be cell down growth on all DEDs apart from week 3 DED seeded keratinocytes (figure 5.1). Organotypics seeded with keratinocytes at two weeks, seem to form uncharacteristic ‘buds’, which is especially pronounced on keratinocytes seeded on DEDs without fibroblast. In week 3 keratinocyte organotypics, it appears as if all the cells have become differentiated.

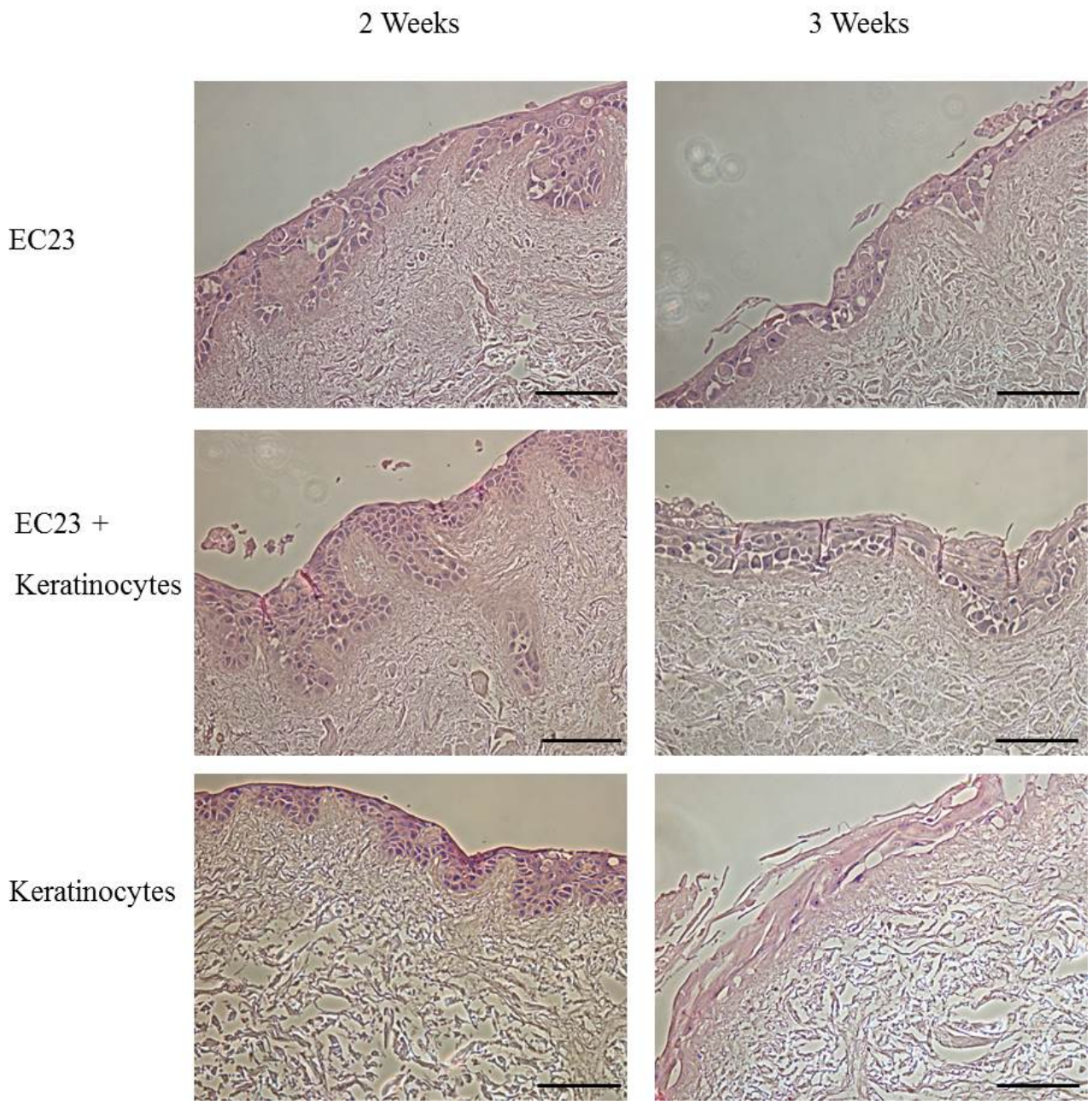

Figure 5.1. DED organotypic cultures using EC23 cells. EC23 cells and primary human keratinocytes were cultured in a DED organotypic model and after 2 and 3 weeks processed for histology. Figure shows at 2 weeks EC23 cells form a layer of cells on top of the DED with cells appearing to begin to form down growths. Similar results are observed on 2 week gels seeded with only keratinocytes, and with DEDs seeded with both keratinocytes and EC23 cells there appears to be further invasion. Scale bars = 200 μM.

5.2.2 EC23 Cell Seeded Collagen Type I Organotypic Raft Cultures Using Adult and Neonatal Fibroblasts.

Collagen gels were made containing either adult dermal fibroblasts (Figure 5.2), or neonatal foreskin fibroblasts (Figure 5.3). EC23 cells seeded on collagen gels with adult fibroblasts developed a thin stratified epidermis approximately 3 cell layers thick at 2 weeks of culture and a thicker stratified epidermis roughly 7 cells thick at 3 weeks of culture with a few layers of cornified cells at the surface. The gels seeded with EC23 cells and keratinocytes, formed a 5 cell thick epidermis with cells beginning to become more differentiated on the upper layers at 2 weeks. At 3 weeks, in the EC23 and keratinocyte gels, the cells had become more differentiated on the upper layers with cornification developing. The gels seeded with just keratinocytes formed a thin layer of cells at 2 weeks with a few differentiated cells scattered on the top. At 3 weeks the keratinocytes formed 3-4 layers of cells with cells differentiating on the top layers and a defined cornified layer.

Collagen gels made with neonatal foreskin fibroblasts (figure 5.3), developed overall better than with adult fibroblasts. Gels with EC23 cells seeded on the gels, showed 3 – 4 cell layers developing on the gel with a cluster of cells that had migrated into the gel at 2 weeks of culture. At 3 weeks, the EC23 gels had formed a thick epidermis with undifferentiated cells at the basal layer, with cells becoming differentiated on the upper layers and a thin cornified layer but no downgrowths. The gels seeded with both keratinocytes and EC23 cells formed a thin 1-2 layer of cells with cornification visible and cells migrating into the gel.

At 3 weeks, there is a similar pattern as in the 2-week gels, but there is a much greater level of down growth into the gels. The gels seeded with only keratinocytes formed a thin 3-4 layer of cells with slight cornification at 2 weeks. At 3 weeks the keratinocytes had formed a slightly thicker layer of cells that had all become differentiated and begun to cornify.

At no time during the course of these experiments did we see the formation of glandular structures similar to those initially seen in work performed prior to the start of this project (figure 1.5).

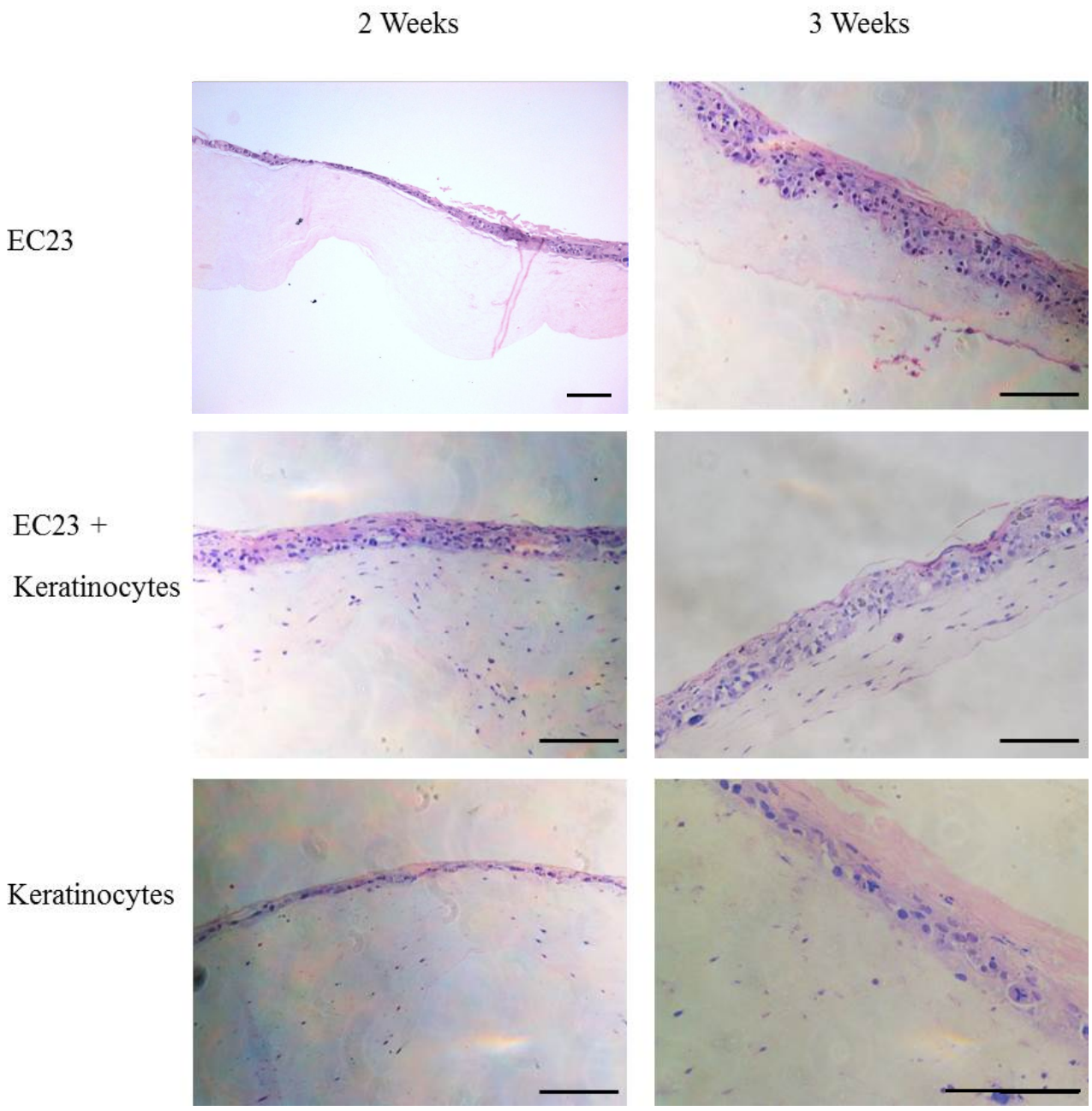

Figure 5.2. Collagen type I organotypic cultures of EC23 cells. Collagen type I organotypic culture containing adult human fibroblasts seeded with EC23 cells and primary keratinocytes and processed for histology at 2 and 3 weeks, showing a 3 cells thick layer of cells at 2 weeks for gels seeded with only EC23 cells, seeded only with keratinocytes showed only 1-2 cell thick layer and gels made with both EC23 cells and keratinocytes show a 5 cell thick layer on the surface of the gels. At 3 weeks all gels show several layers of cells forming an epidermis however gels containing only keratinocytes show the most cornification of all . Scale bars 200 μM

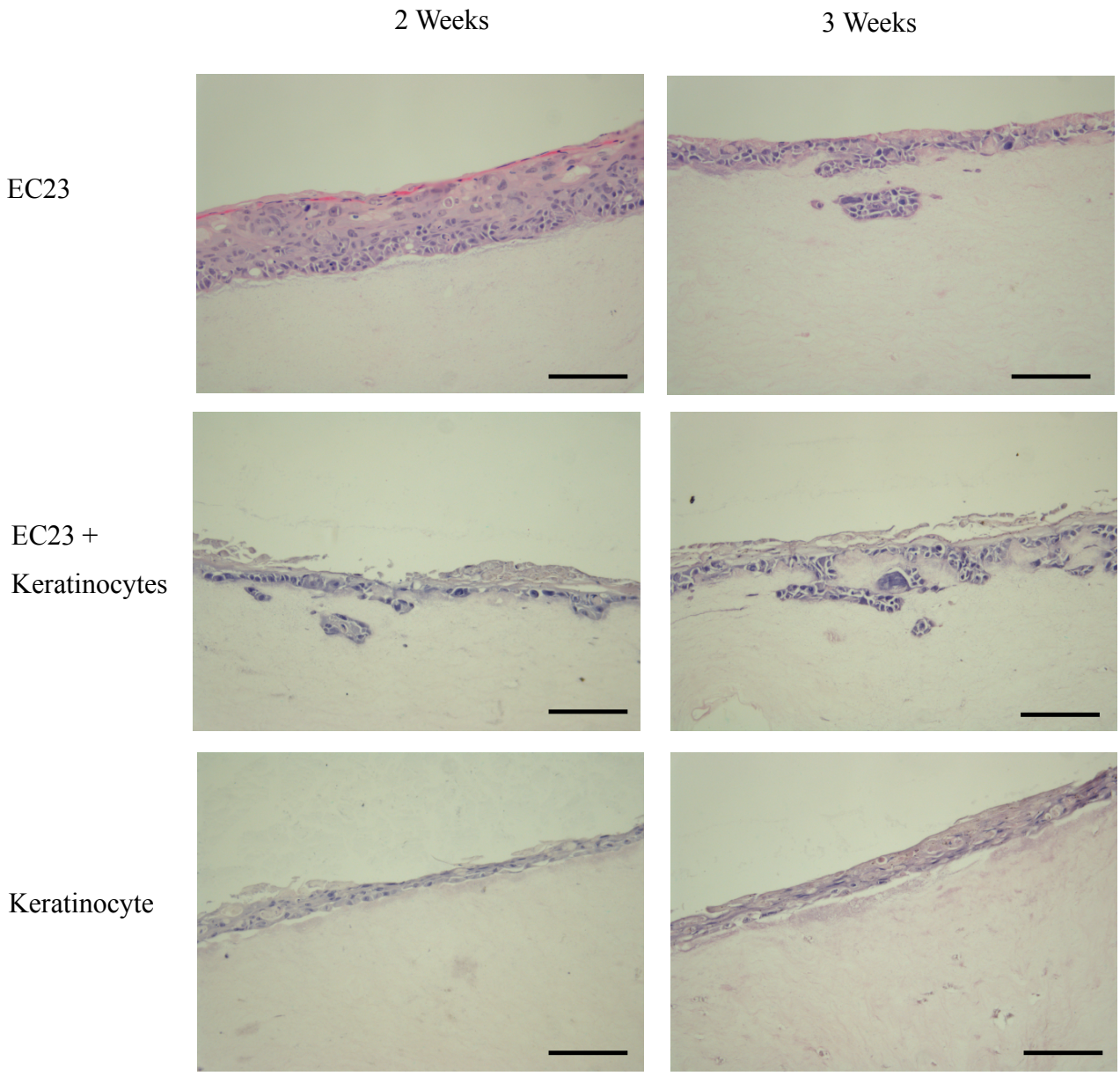

Figure 5.3. Collagen type I organotypic cultures made with neonatal fibroblasts, seeded with EC23 cells. Collagen type I organotypic cultures containing neonatal fibroblasts seeded with EC23 cells and primary human keratinocytes and processed for histology after 2 and 3 weeks. Showing a thicker epidermis with EC23 cells at 3 weeks compared to keratinocytes alone that appear to be differentiating. But also shows some ductal structures forming at 3 weeks of co-culture with EC23 cells and keratinocytes. At 2 weeks the beginnings of the formation of ductal structures can be seen for co-cultures of EC23 cells and keratinocytes. For gels seeded only with EC23 cells a thick epidermis can be is observed and on gels seeded with only keratinocytes at 2 weeks a very thin layer of cells can be seen. Scale bars 200 μM

5.2.3 Effect of Epidermal Growth Factor on Branching Morphogenesis of EC23 Spheroid structures seeded on Matrigel

Because we were unable to replicate the original glandular structures observed in preliminary work performed before the start of this PhD project, it was decided to focus on a simpler model involving matrigel to see if we could develop eccrine organoids. Branching morphogenesis of EC23 cell spheroid structures formed on matrigel were studied using an In Cell automated microscope system and analysed using the developer tool software compatible with the microscope. The analysis software measures the spheres and gives a value of 0 to objects that are round, objects that are more branched are designated a higher value, all values referred to as arbitrary units (A/U). In these set of experiments, no supplementation of EGF yielded a low level of branching that was consistently lower than all other treatments (figure 5.4 and table 5.1). At day 6 of culture, 25 ng/ml of EGF appears to yield the highest degree of branching of all the treatments, interestingly followed closely by 5 ng/ml of EGF, followed closely by 15 ng/ml and then 20 ng/ml.

At day 12, the degree of branching of the spheroids for most of the treatments appears to decrease slightly, apart from for structures treated with 20 ng/ml of EGF which appear to have nearly doubled in branching from (4.91 to 7.94 A/U). Branching in EGF untreated cells, appears to increase ever so slightly too.

By Day 18, branching of the structures again appears to have decreased this time for all the treatments. At day 24 there is a further decrease in the branching in wells with 5 ng/ml of EGF, but an increase in branching can be observed in all

other wells, it what appears to be a dose dependent manner, with 25 ng/ml exhibiting the highest degree of branching and with 15 and 20 ng/ml being lower but very similar to each other, and 10 ng/ml level of branching being bellow 15 ng/ml but higher than 5 ng/ml. In figure 5.6, we can clearly see the increase in branching with an increase in concentration of EGF at day 24. All cells that were supplemented with 25ng/ml of EGF were significantly different ($p<0.05$) to cells that were not supplemented with EGF at every time point.

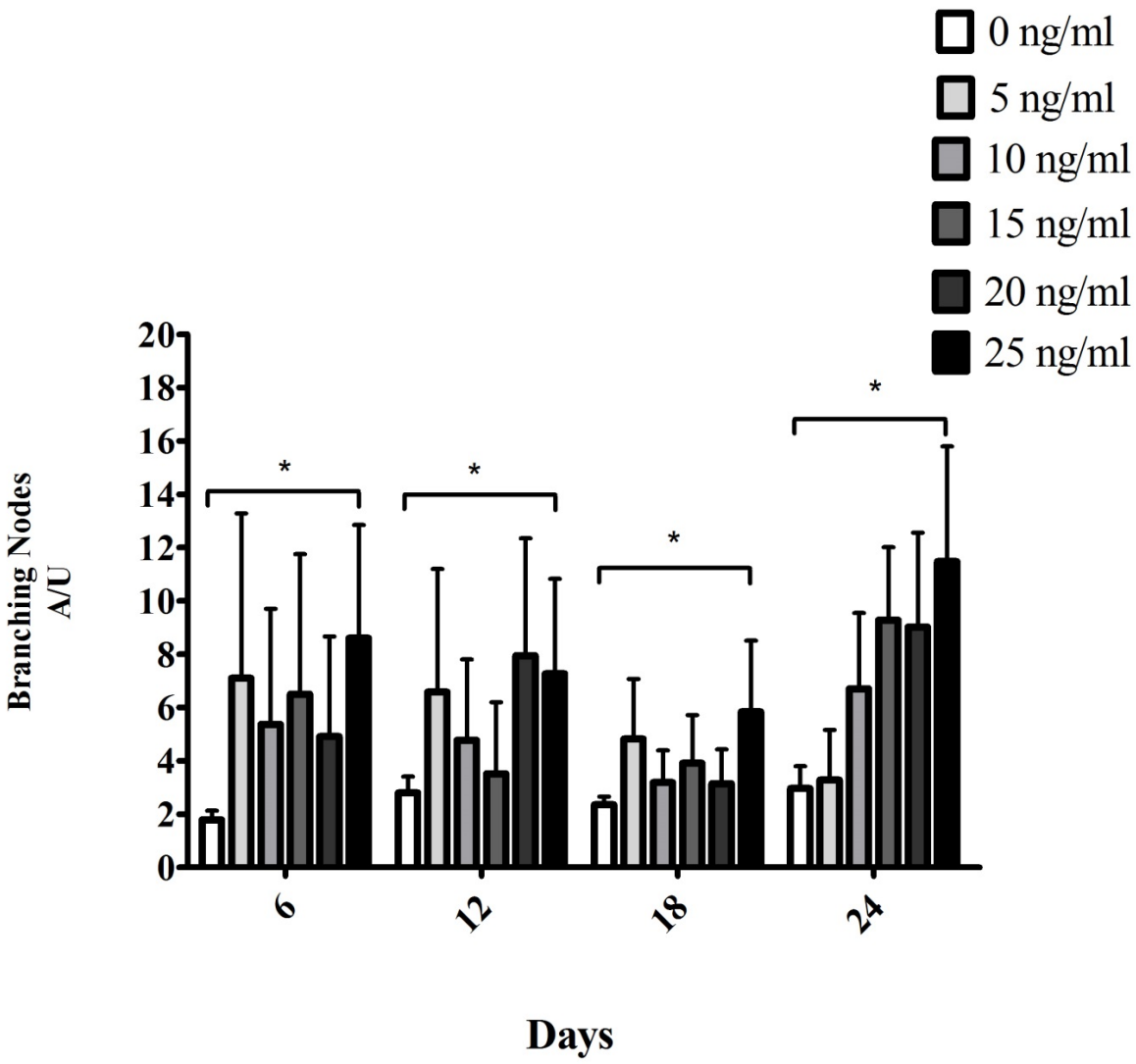

Figure 5.4. Effect of varying doses of epidermal growth factor on branching nodes of EC23 spheroid structures cultured in growth factor reduced matrigel. Data presented as the means ± SEM for n=3 separate experiments. Statistical analysis was carried out using a 2 way ANOVA with a Bonferroni post hoc test. * $p<0.05$

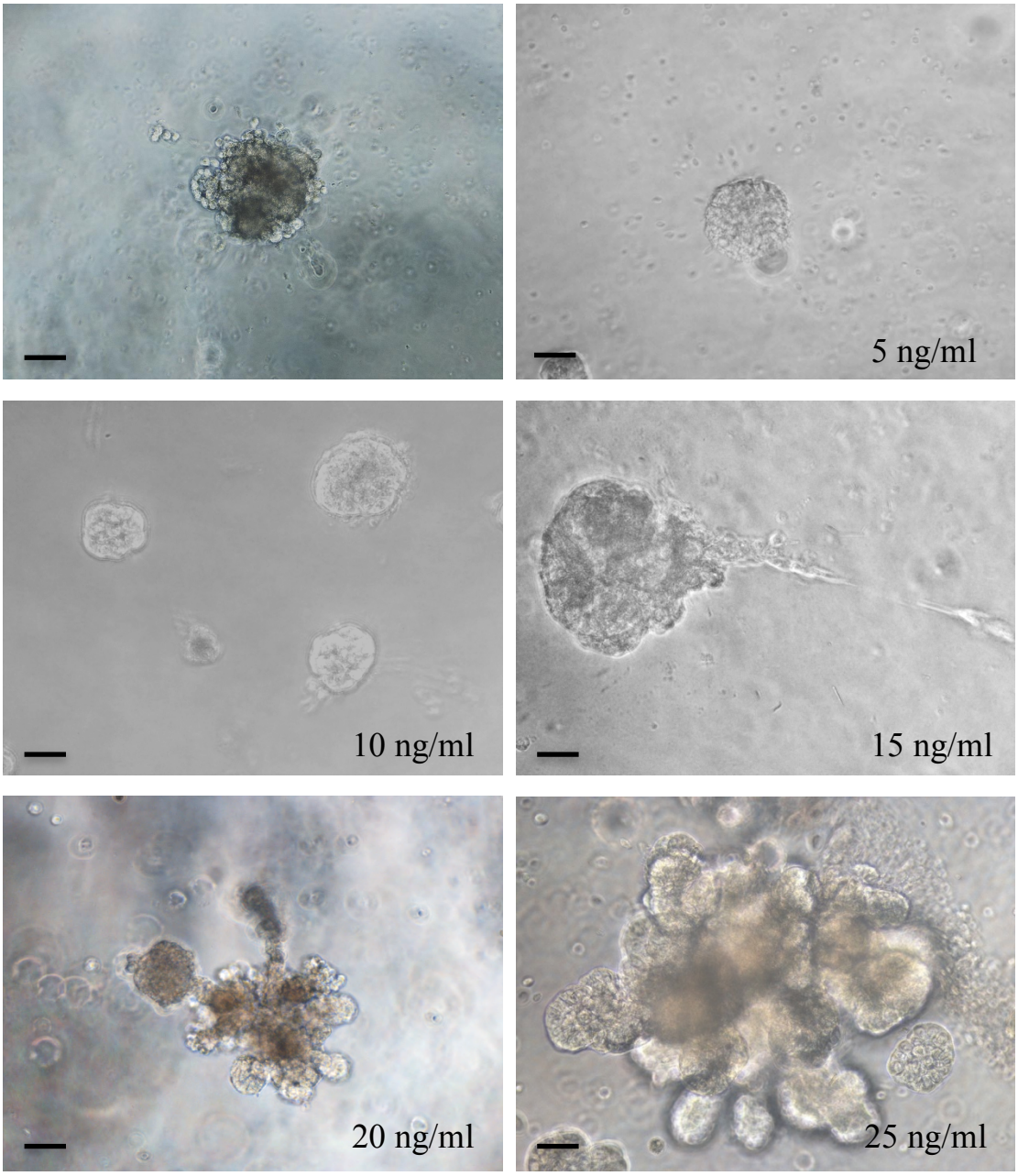

Figure 5.5. Spheroid formation by EC23 cells cultured in growth factor reduced matrigel supplemented with epidermal growth factor, showing the effects of EGF on spheroid branching after 24 days. All images acquired at 10x magnification using a tissue culture microscope.

Concentration of EGF		Days			
		6	12	18	24
0 ng/ml	Mean	1.79	2.80	2.35	2.96
	SEM	0.34	0.61	0.31	0.83
	N	3	3	3	3
5 ng/ml	Mean	7.10	6.58	4.82	3.27
	SEM	6.18	4.61	2.25	1.89
	N	3	3	3	3
10 ng/ml	Mean	5.36	4.77	3.19	6.70
	SEM	4.34	3.03	1.21	2.85
	N	3	3	3	3
15 ng/ml	Mean	6.50	3.51	3.91	9.27
	SEM	5.26	2.69	1.81	2.73
	N	3	3	3	3
20 ng/ml	Mean	4.91	7.94	3.14	9.02
	SEM	3.76	4.41	1.29	3.54
	N	3	3	3	3
25 ng/ml	Mean	8.60	7.27	5.84	11.48
	SEM	4.25	3.56	2.67	4.32
	N	3	3	3	3

Table 5.1. Results of branching nodes of EC23 spheroids supplemented with epidermal growth factor. Showing values for the mean branching node and SEM for each condition and time point for n=3 separate experiments.

5.2.4 Effect of Bone Morphogenic Protein 4 on Branching Morphogenesis of EC23 Spheroid structures seeded on Matrigel

EC23 cells were seeded onto matrigel and treated with 0, 5, 10, 15, 20 and 25 ng/ml of BMP4 over a period of 24 days, and data was collected every 6 days, with the first time point being day 6 (figure 5.6 and table 5.2). Data was not collected on day 0 or day 1 as the parameters which were used to measure structures were incapable of measuring single cells in the matrigel. At day 6 however, there were some spheres beginning to form in the matrigel with all treatments. With 0 ng/ml of BMP4 having the least branching of all the treatments, and 20 ng/ml of BMP4 having the highest value for branching nodes for this day. For day 12, only wells supplemented with 15 ng/ml of BMP4 appear to have greater branching; however the SEM was rather large for this concentration of BMP4. All other concentrations appear to have a similar range in branching nodes, with 10 ng/ml treated spheroids having the lowest branching nodes.

By day 18, the higher concentrations of BMP4 had peaked slightly, especially for 25 ng/ml of BMP4, which was at (1.63 A/U), interestingly, 5ng/ml of BMP4 was also higher at this time point, at 1.46 A/U. At the final time point, day 24, there was a large increase in branching nodes for the wells supplemented with 25 ng/ml of BMP4 (2.6 A/U). The wells with other 0, 5 and 10 ng/ml of BMP4 supplementation, remained at similar levels to each other between 1.10 and 1.22 A/U. With 15 and 20 ng/ml of BMP being slightly higher, 1.63 and 1.36 A/U respectively. At day 24, supplementation of 25ng/ml of BMP4 was significantly different to cells supplemented with 10ng/ml of BMP4 ($p<0.05$).

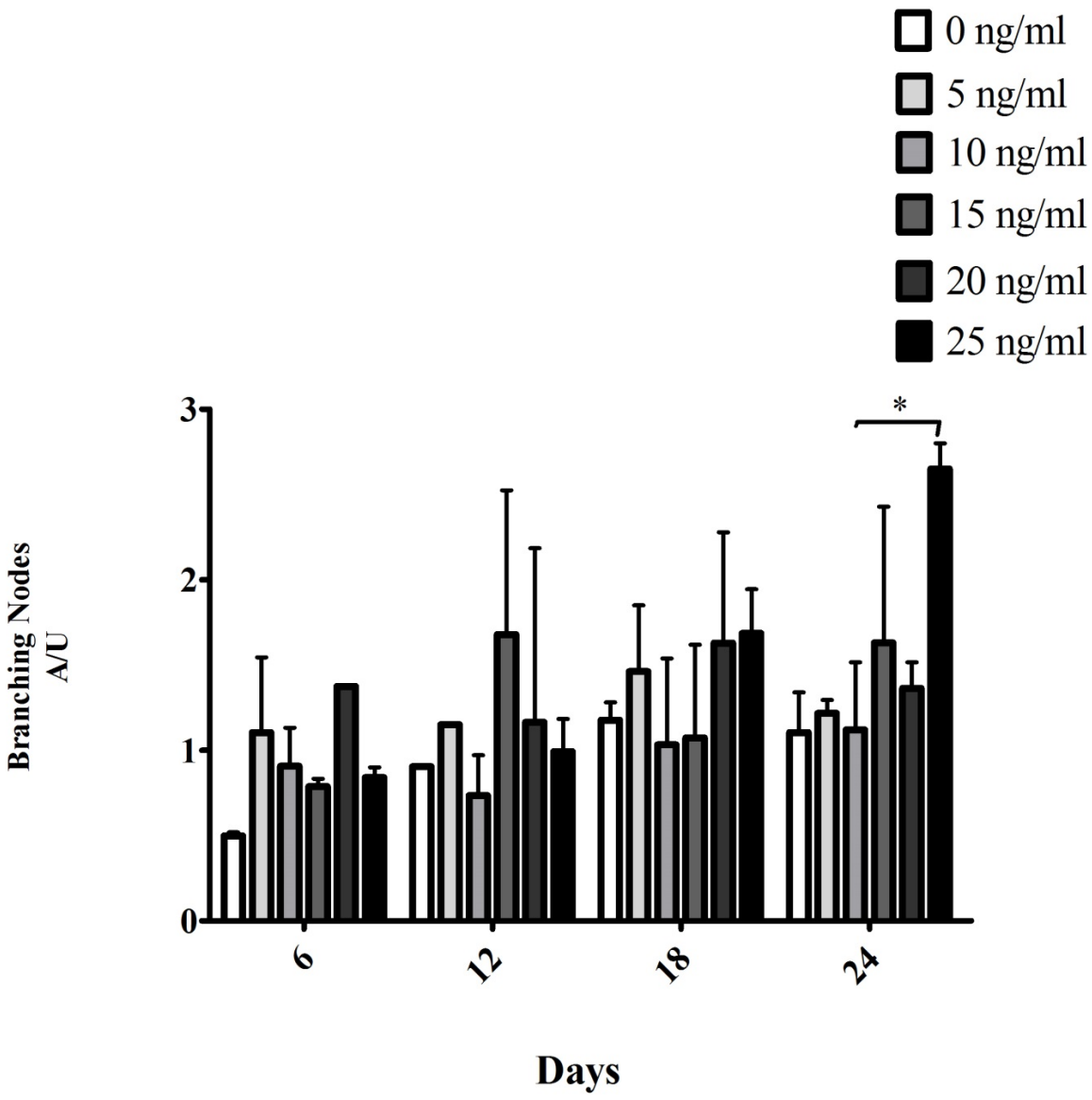

Figure 5.6. The effect of bone morphogenic protein 4 on branching nodes of EC23 spheroid structures cultured in growth factor reduced matrigel. Data is presented as the mean ± SEM for n=3 separate experiments. Statistical analysis was carried out using a 2 way ANOVA and a Bonferroni post hoc analysis. *P<0.05

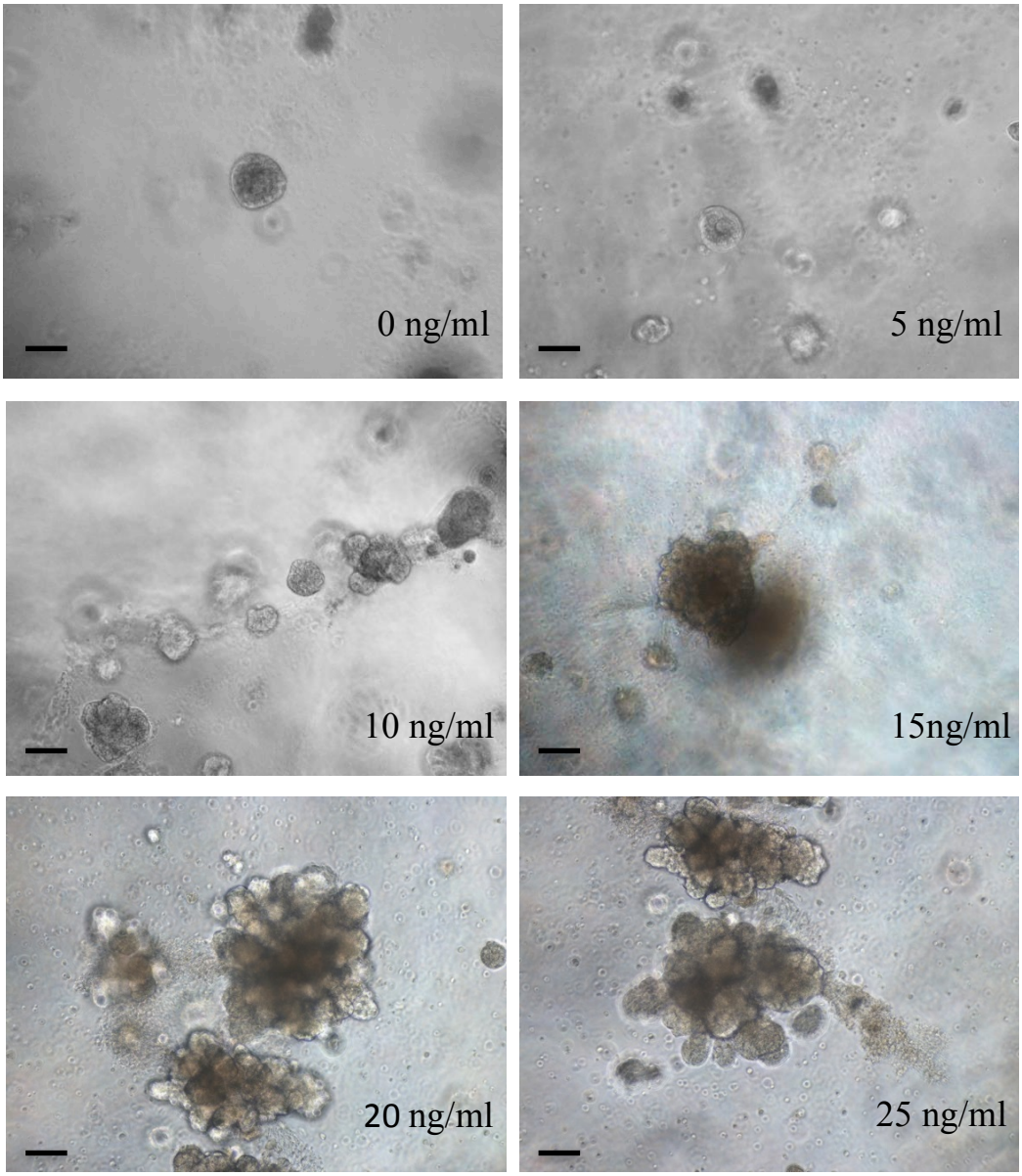

Figure 5.7. Spheroid formation by EC23 cells cultured in growth factor reduced matrigel supplemented with bone morphogenic protein 4. Showing the effects of BMP4 on spheroid formation at 24 days of culture. Scale bar 500 μm.

Concentration of BMP4		Days			
		6	12	18	24
0 ng/ml	Mean	0.50	0.90	1.18	1.10
	SEM	0.02	0.00	0.10	0.24
	N	3	3	3	3
5 ng/ml	Mean	1.10	1.15	1.46	1.22
	SEM	0.44	0.00	0.39	0.08
	N	3	3	3	3
10 ng/ml	Mean	0.91	0.74	1.03	1.12
	SEM	0.23	0.24	0.51	0.40
	N	3	3	3	3
15 ng/ml	Mean	0.79	1.68	1.07	1.63
	SEM	0.05	0.85	0.55	0.80
	N	3	3	3	3
20 ng/ml	Mean	1.38	1.16	1.63	1.36
	SEM	0.00	1.02	0.65	0.15
	N	3	3	3	3
25 ng/ml	Mean	0.84	0.99	1.69	2.65
	SEM	0.06	0.19	0.26	0.15
	N	3	3	3	3

Table 5.2. Results of branching nodes of EC23 spheroid supplemented with bone morphogenic protein 4. Showing values for the mean branching node and SEM for each condition and time point for n=3 separate experiments.

5.2.5 The Effect of Ectodysplasin on Branching Morphogenesis of EC23 Spheroid structures seeded on Matrigel

In experiments in which EC23 cells seeded in GFR matrigel (figure 5.8 & table 5.3) at day 6, the branching nodes number was low for cells that were not supplemented with EDA. However the level of branching at day 6 was similar for all concentrations of EDA. The degree of branching at day 12 decreased for cells supplemented with 5 and 10 ng/ml of EDA. The level of branching remained similar to that of day 6 for 15 ng/ml and 20 ng/ml of EDA. There was, however an increase in the branching nodes for 25 ng/ml at day 12.

At day 18, the cells left untreated with EDA still exhibited low branching, and interestingly cells treated with 5 ng/ml of EDA appear to markedly increase branching at this time point (10.79 A/U) – an increase was also observed for 10 ng/ml EDA, but this was less than that of 5 ng/ml EDA. The cells treated with 20 ng/ml of EDA, remained at a similar level as that of previous time points with the largest branching being observed for 25 ng/ml of EDA.

At the final time point, day 24, a small increase in the branching was seen for no growth factor treatment. The level of branching for 5 ng/ml of EDA remained stable from the previous time point at 10.18 AU. Spheroids supplemented with 15 ng/ml of EDA increased in branching to 12.20 A/U. With 15 ng/ml of EDA, an increase to11.15 was also observed. There was also a large increase in branching nodes for 20 ng/ml of EDA, but a decrease in branching nodes for 25 ng/ml.

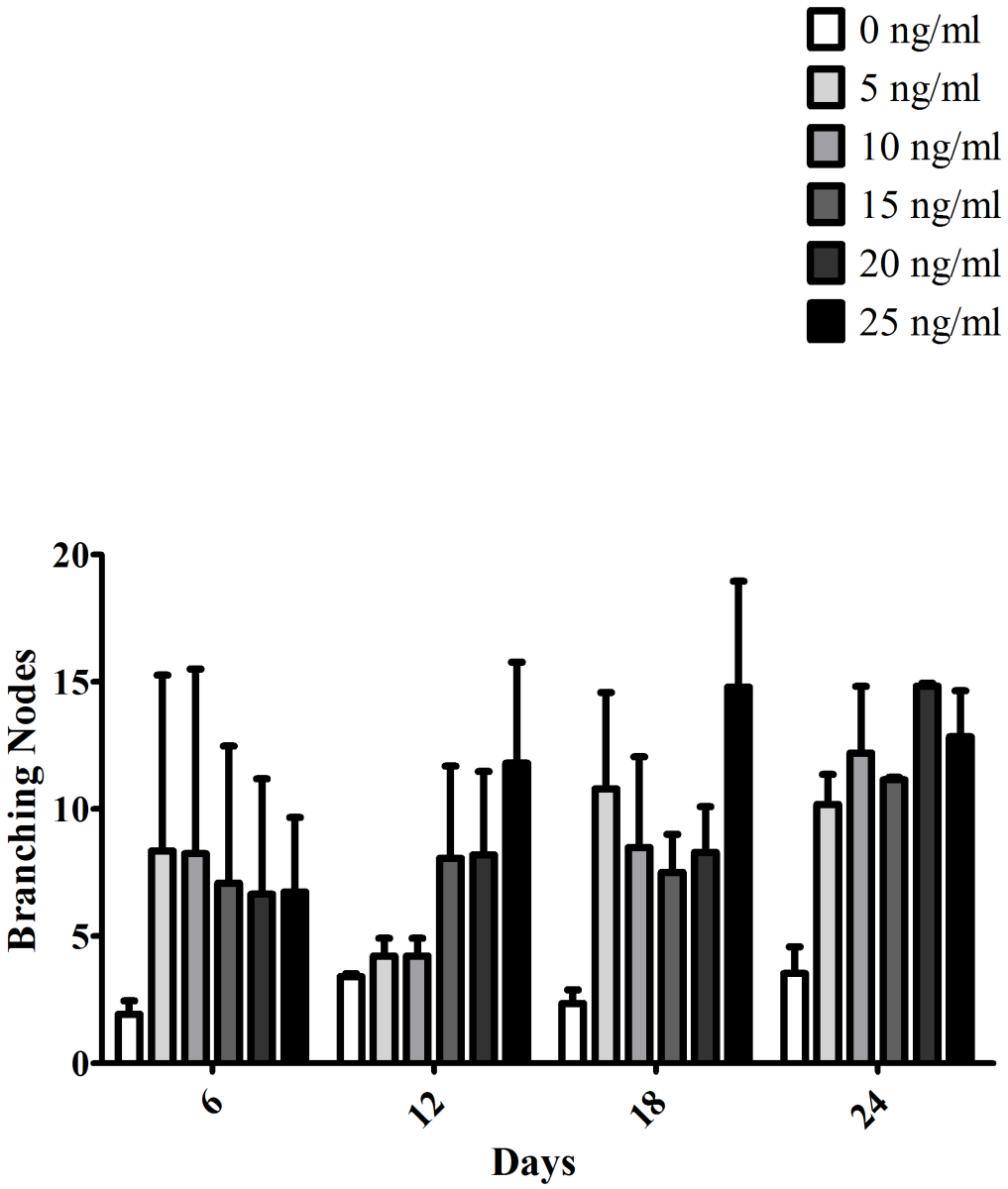

Figure 5.8. The effect of ectodysplasin on branching nodes of EC23 spheroid structures cultured in growth factor reduced matrigel. Data presented as the mean ± SEM for n=2 separate experiments.

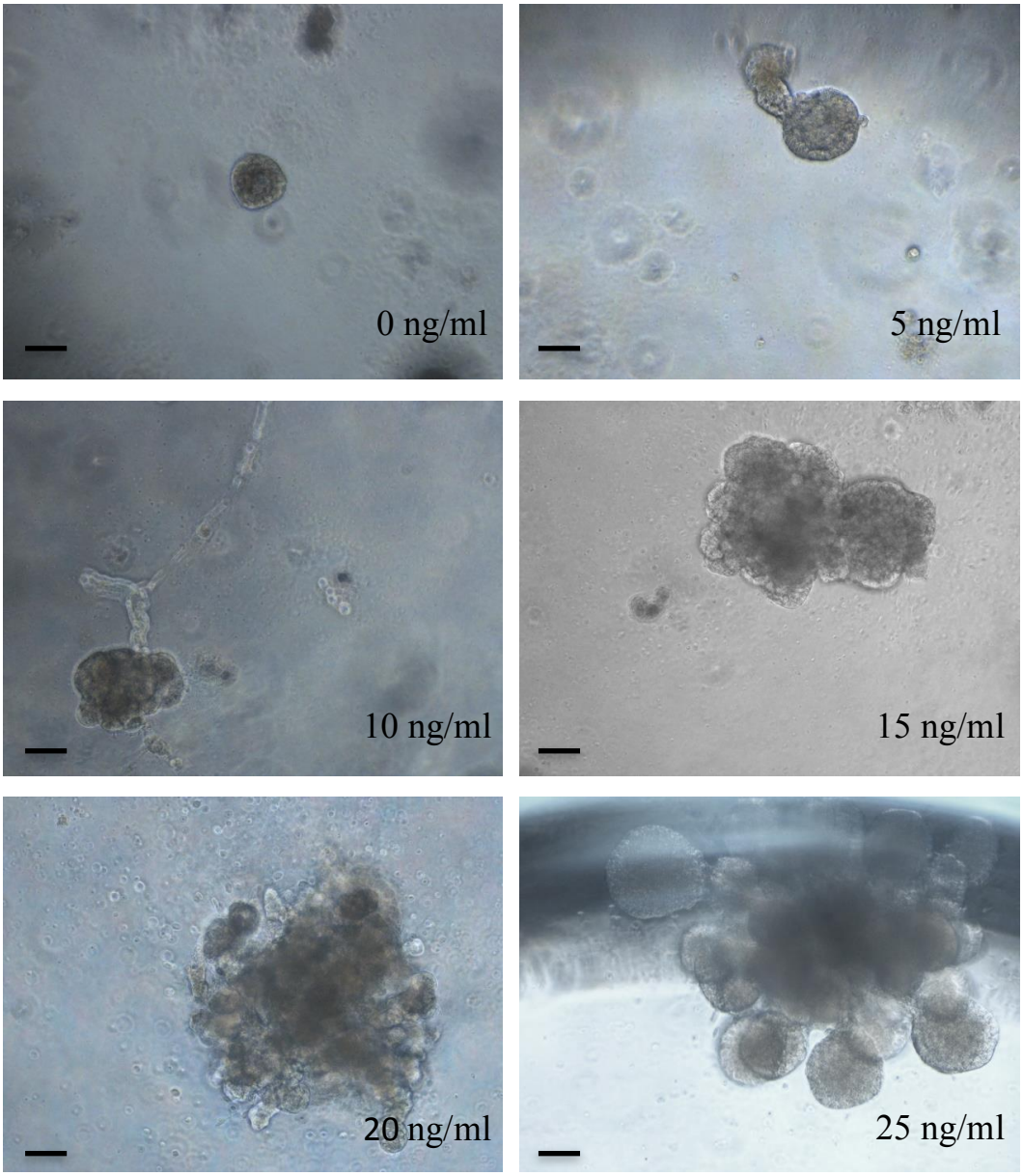

Figure 5.9. Spheroid formation by EC23 cells cultured in growth factor reduced matrigel supplemented with Ectodysplasin, showing the effect of ectodysplasin on spheroid branching at 24 days of culture. Scale bar 500 μm.

Concentration of EDA		Days			
		6	12	18	24
0 ng/ml	Mean	1.93	3.41	2.35	3.54
	SEM	0.53	0.11	0.54	1.04
	N	2	2	2	2
5 ng/ml	Mean	8.35	4.22	10.79	10.18
	SEM	6.91	0.70	3.79	1.18
	N	2	2	2	2
10 ng/ml	Mean	8.24	4.22	8.49	12.20
	SEM	7.26	0.70	3.57	2.63
	N	2	2	2	2
15 ng/ml	Mean	7.08	8.06	7.50	11.14
	SEM	5.39	3.63	1.50	0.10
	N	2	2	2	2
20 ng/ml	Mean	6.65	8.20	8.29	14.83
	SEM	4.54	3.28	1.79	0.12
	N	2	2	2	2
25 ng/ml	Mean	6.74	11.81	14.79	12.85
	SEM	2.93	3.97	4.17	1.80
	N	2	2	2	2

Table 5.3. Results of branching nodes of EC23 spheroid supplemented with ectodysplasin. Showing values for the mean branching node and SEM for each condition and time point for n=3 separate experiments.

5.2.6 Effect of Bone Morphogenic Protein 2 on Branching Morphogenesis of EC23 Spheroid structures seeded on Matrigel

EC23 cells seeded onto matrigel supplemented with BMP2 (figure 5.10) did not survive for the whole duration of the experiment; by day 18 most of the cells had become apoptotic. At day 6 of culture, there is little difference in branching nodes between most of the concentrations of BMP2, with 15 ng/ml of BMP2 having the largest effect at a mere 1.6 AU. By day 12, samples treated with no BMP2, 5, 10 and 25 ng/ml of BMP exhibiting similar branching as in day 6, all bellow 0.9 AU. The degree of branching increase for samples treated with 15 and 20 ng/ml to 3.83 AU and 4.62 AU respectively. At day 18, only data for the untreated samples could be collected, with branching remaining at a similar level as in previous time points.

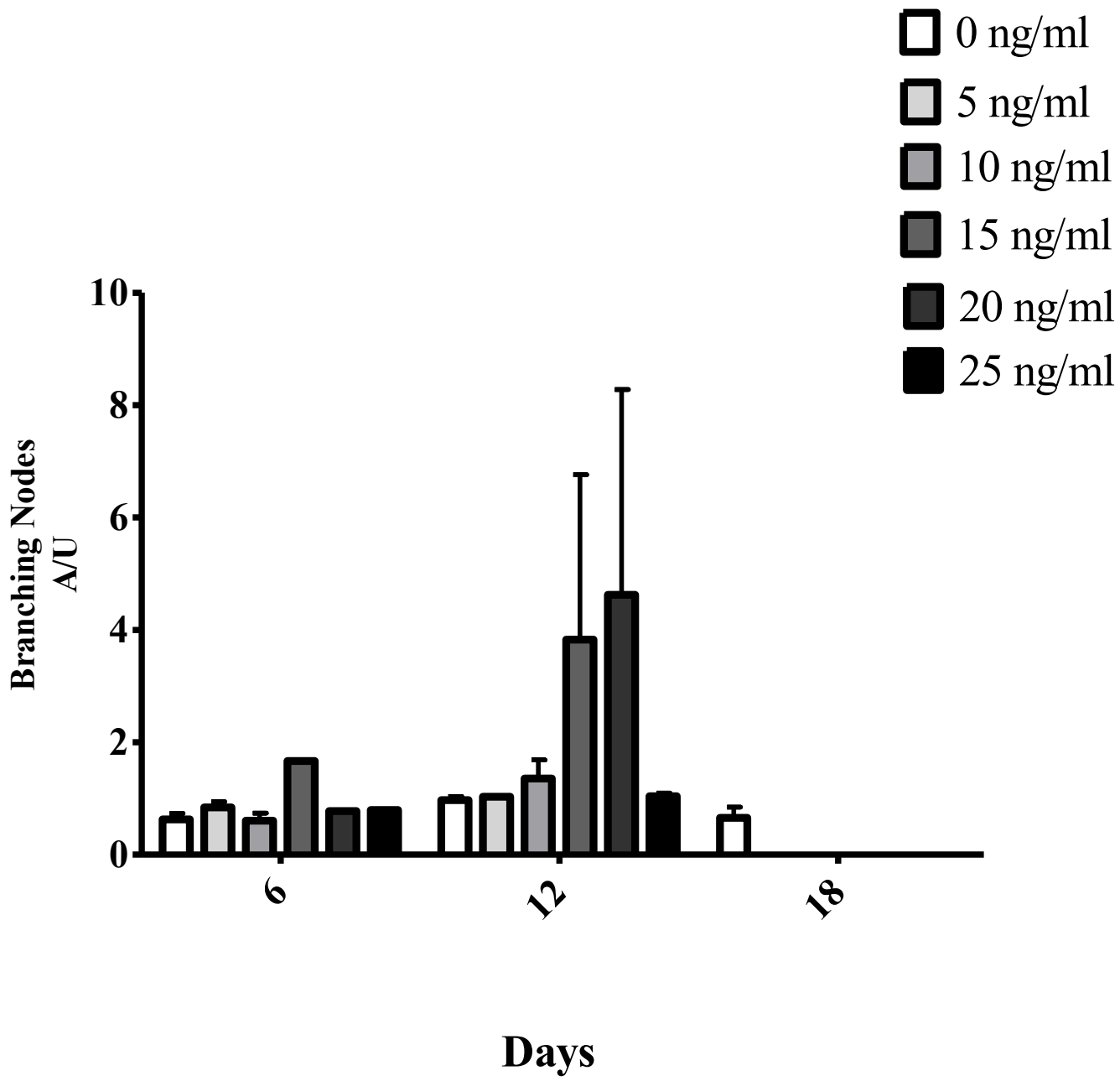

Figure 5.10. Effect of bone morphogenic Protein 4 on branching nodes of EC23 Spheroid structures seeded on Matrigel. Data is presented as the mean ± SEM for =2 separate experiments.

5.2.7 Comparison between the structure of EC23 Spheroids and Whole Human Eccrine Sweat Glands.

In order to investigate the structure of the EC23 spheroids, wholemount immunohistochemistry on human eccrine glands and EC23 spheroids after 24 day of culture supplemented with 20 ng/ml of EGF was performed. Staining for keratin K14 (figure 5.11) shows both the pattern of expression and staining of both eccrine gland (A) and EC23 cell spheroid (B). From these data it can be seen that the EC23 spheroids appear to be forming ductal 'like' structures.

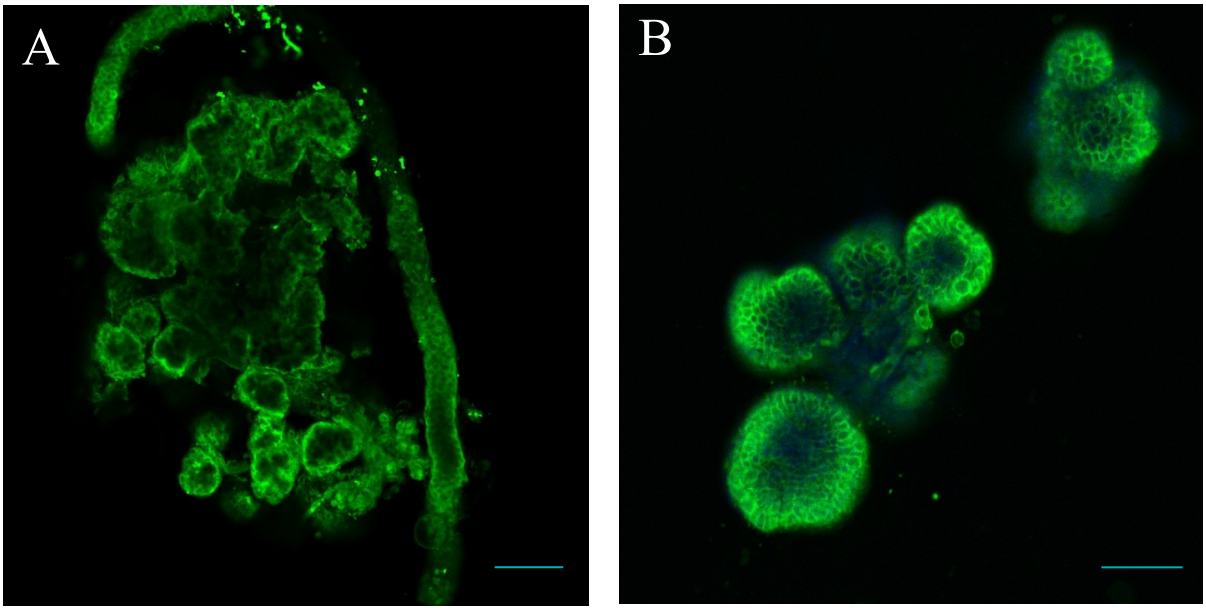

Figure 5.11. Immunocytochemistry using keratin 14 antibody of (A) an isolated human eccrine sweat gland and (B) EC23 cell derived spheroids at day 24 supplemented with 20 ng/ml. Scale bars 100µm.

5.3 Discussion.

In this chapter a number of different number organotypic models were investigated in order to asses the ability of the EC23 cell line to form eccrine sweat gland like structures *in vitro*. Initial work performed in our lab by the postdoctoral researcher who developed the original EC23 cell line and the clones investigated in this thesis had indicated that the EC23 cell line had the capacity of forming gland like structures on collagen gels (See Figure 1.5). Unfortunately the details of the experiment carried out by this person, such as the source of fibroblasts (foetal, neonatal or adult), contraction of the gels or concentration of the gels were not available and attempts to repeat these experiments were not successful.

With normal cell culture on tissue culture plastic, it is difficult to study organ systems fully. Cells in 2D cultures tend to lose some of their in vivo characteristics, with keratinocytes in normal cell cultures losing the expression of higher molecular weight keratins over time (Prunieras 1983). DED models utilise de-epidermialised cadaveric dermis, where the laminal side is seeded with primary fibroblasts, that provide essential nutrients and possibly cues that maintain the keratinocytes (Prunieras et al., 1983, El-Ghalbzouri et al., 2002). In organotypic cultures, the skin equivalents are raised to the liquid air interface to induce terminal differentiation of the keratinocytes so that the cells can form layers that resemble the epidermis.

In experiments carried out using DEDs (figure 5.1) it became apparent that this model was not suitable for the generation of an in vitro eccrine gland model. We initially hoped that the EC23 cells would repopulate the de-cellularised eccrine ducts and coil space of the DEDs, however, we could not see this happening. Also, any indication that the cells may form epidermal buds and invade the dermis to form eccrine gland like structures could not be assessed as it was not really possible to distinguish between the skin papillae and epidermal buds. In addition the organotypics developed using DED very rarely formed a multi-layered epidermis and seemed to show premature terminal differentiation. The terminal differentiation of the keratinocytes on the 3 week DEDs could have occurred due to the fibroblasts not laying down enough ECM components, as the fibroblasts were only allowed to attach over-night prior to seeding of the keratinocytes and EC23, which probably did not allow enough time for the secretion of ECM.

Apart from DED, Collagen type I gels have been routinely used in skin research to study skin regeneration, wound healing and many diseases affecting the skin (El-Ghalbzouri et al., 2002, Egles et al., 2010, Oh et al., 2013). In this study, collagen type I organotypics were constructed to see whether they would be better able to recreate eccrine like structures *in vitro*. Collagen fibres are present in vast quantities in the epidermis with collagen type I being of the highest proportion 80% of the total collagen fibres, thus they were used in these experiments (O'Toole, 2001). Collagen type III and IV are also present and have been used in organotypic cultures alone or as mixtures (McGrath et al., 2008). In this types of culture, the fibroblasts are mixed in with the collagen and allowed to polymerise overnight (Gangatirkar et al., 2007).

Collagen gel experiments were performed using adult (figure 5.2) and neonatal fibroblasts (figure 5.3). In the collagen gels in which adult dermal fibroblasts were used, we can see a very good epidermis being formed at 3 weeks culture with EC23 cells alone, EC23 cells and keratinocytes as well as the stratification of keratinocytes alone on gels at 3 weeks. The epidermis formed using collagen gels appears much healthier for collagen gels with EC23 cells than in the collagen gels at 3 weeks seeded with keratinocytes only. This decrease in stratification when keratinocytes alone were seeded onto collagen gels could be attributed to the length of the experiment and that the keratinocytes were reaching a later passage by the end of the experiment, never the less, there is still a visible basal layer with some more differentiated cells on the top layers. Interestingly, the gels at 3 weeks with just EC23 cells have a cell layer that is very similar to that on the gels with both cell types and the gels with just keratinocytes. This supports findings by Biedermann, et al (2010), in which eccrine gland cells were seeded on hydrogels and found to form a stratified epidermis with markers resembling those of normal epithelia (Biedermann et al., 2010). Rittié, et al (2013), in a human in vivo study, found that eccrine gland cells, after injury expressed high levels of Ki67, in comparison to uninjured skin. Suggesting that the eccrine gland may make a major contribution to reepithelialisation in response to skin injury (Rittie et al., 2013). In yet another investigation, by Böttcher-Haberzeth, (2013), human eccrine gland cells were found to interact with melanocytes in organotypic cultures by incorporating melanin, thus possibly achieving photoprotection (Bottcher-Haberzeth et al., 2013).

My data therefore suggests that cells from the secretory coil of the eccrine sweat gland are able to form a stratified epidermis and this confirms the data of Biedermann, (2010) and Bottcher-Haberzeth, (2013). However, no down growth of cells into the collagen were observed when using adult fibroblasts, suggesting that the cells were not receiving the correct signals from the fibroblasts or were not competent to form down-growths.

In the set of experiments where collagen gels were made using neonatal fibroblasts (derived from foreskins), it was observed that at 2 weeks the gels made with only EC23 cells developed an epidermis with a large number of layers in comparison to the week 3 gels that had fewer stratified cells. However, the cells on the top layers of the week 2 gels were rather disorganised. Therefore it is possible that by 3 weeks the more differentiated cells may have sloughed off either during the harvesting of the gels or while in vitro.

However, the most important feature of these gels is the formation of a cluster of cells within the gel, especially when EC23 cells and keratinocytes were co-cultured. From these experiments it is not possible to determine whether these down growth are EC23 cell, primary keratinocytes or a mixture of both. This could be investigated by labelling the EC23 cells with a fluorescent label and monitoring their invasion (Jung et al., 2002). It is known that there are marked differences between growth factor secretion and the composition and amounts of ECM laid down between foetal and adult fibroblasts, which is thought to be involved in scarless wound healing in utero (Gosiewska et al., 2001). Foetal fibroblasts lay down more collagen III and V than adult fibroblasts, and also carry

on secreting HA, even after reaching confluency. Also, Foetal fibroblasts secrete a higher proportion of TGF-β3 than adult fibroblasts. Higher levels of VEGF have been observed in scarless healing (Bullard et al., 2003). However, acquiring foetal fibroblasts is difficult and costly, thus neonatal fibroblasts were used. Neonatal fibroblasts are also thought to differ from adult fibroblasts, they grow faster and can reach higher passage number in cell culture (Plisko and Gilchrest, 1983). Glass, et al. (2010), demonstrated that after stress adult fibroblasts secreted increased amounts of TGF-B than stressed neonatal fibroblasts, which showed no change in secretions compared to non-stressed controls. Glass also found higher expression of TGF-RII receptors in adult fibroblasts compared with neonatal fibroblasts (Glass et al., 2010).

For these experiments, only neonatal foreskin keratinocytes were used as they can be maintained in culture for a longer number of passages than keratinocytes from adult skin, never the less they were always seeded onto the organotypics at passage 3 as a maximum. The reason for the low number of layers in the epidermis formed in some of the organotypics is not known. It is possible that variability may be attributed to number of the fibroblasts used. The number of fibroblasts per ml of collagen in the experiments conducted was of 2.5 $x10^5$ a number thought to be sufficient for the development and maintenance of an epidermis (El-Ghalbzouri et al., 2002). Keratinocytes and fibroblasts contribute to producing components that constitute the basement membrane. The Basement membrane is a layer of collagen IV, and VII, laminin, proteoglycans and glycosaminoglycans (Iozzo, 2005). Fibroblasts and also secrete TGF-β, which

stimulates the production of collagen IV and VII by keratinocytes (O'Toole, 2001, Brohem et al., 2011).

However we cannot exclude the possibility that the fibroblasts may have been damaged in some way in the process of making the gels, for example by pH changes – especially for DEDs, where the fibroblasts were seeded overnight inside metal rings with a small amount of media available for that period of time - to stress that could have occurred when the gels were raised to the air liquid interface. However, we think this unlikely as such organotypic models are routinely made without problems.

It is also possible that the fibroblasts did not lay down enough ECM in the collagen gels. Several studies have demonstrated the importance of the ECM in developing skin 3D organotypic models (Cooper et al., 1991, Chioni and Grose, 2008). The ECM is highly important for the maintenance of epidermal homeostasis. The fibroblasts and keratinocytes secrete ECM components, which constitute the microenvironment in which the cells reside. The ECM is also essential in regulating signalling pathways and influences tissue regeneration, cell growth, and differentiation (Brohem et al., 2011).

Also allowing the collagen gels to contract has an effect on the fibroblasts. Contractibility is dependent upon the number of fibroblasts that have been seeded onto the collagen gels. In an experiment in which a non-contractile matrix made out of hyaluronic acid, Stark, at al (2006), found that the epidermis formed in these experiments was much more like the native epidermis, with improved cell

growth and differentiation (Stark et al., 2006). When the collagen gels are allowed to contract, fibroblasts become dendritic and quiescent. When the gels are left attached to a solid support, not allowing them to contract, they become lamellar and remain in a proliferative state. In normal skin, fibroblasts are in a quiescent state, only becoming proliferative after injury to the skin (Grinnell, 2008, Brohem et al., 2011).

In conclusion previous work performed in our lab suggested that the EC23 cells have the capacity of invading collagen gels in a way that resembles eccrine glands in the skin however, we could not reproduce this data using DED. The collagen gel experiments, demonstrated that the mesenchyme, has a strong influence in the behaviour of eccrine derived cells in a 3D in vitro environment. The collagen gels constructed with adult fibroblasts did not develop any down-growth of cells into the collagen gel as was observed in collagen gels that were constructed with neonatal fibroblasts. Also the collagen gels with neonatal fibroblasts, seeded with EC23 cells and primary keratinocytes, contained a much higher number of down-growths than the collagen gels seeded only with EC23 cells, suggesting that there may be some cytokines produced by keratinocytes that can influence the degree of down- growth of the cells. Further experiments would be required to investigate this in more detail. However, collagen gel organotypic models are expensive to produce and time consuming. Therefore we decided to investigate other more simple models that could be used to investigate whether the EC23 cells had the ability to form eccrine like structures..

Skin begins to form early in gestation, producing fully formed and functional skin and appendages at birth apart from the apocrine gland that becomes functional during puberty. The human eccrine sweat gland begins to develop in the soles of the feet and palms of the hand, being apparent there at the week 16 of gestation, with eccrine glands becoming apparent in the rest of the body by gestational week 22 (McGrath et al., 2008). Skin appendages derive from the embryonic ectoderm in a process that is closely regulated by the crosstalk between the ectoderm and the mesenchyme derived from the mesoderm. The cells of the ectoderm, begin to cluster at different locations in the embryo to produce different primary placodes, that go on to become hair follicles, eccrine glands, apocrine glands, and teeth (Mikkola, 2007, Headon, 2009). There are a small number of pathways that govern the signals for placode development, including Hedgehog (Hh), Wnt, transforming growth factor β (TGF-β), tumour necrosis factor (TNF) and their downstream transcription factors. Because of this close-knit regulation, conditions arise when these systems malfunction that have a broad effect in malformation amongst appendages, such as ectodermal dysplasias, which affect the hair follicle, teeth and eccrine glands. (Mikkola and Thesleff, 2003, Cui et al., 2008, Headon, 2009).

During this time in development, it is known that there are spikes in the levels of a number of growth factors including BMPs (Wollina et al., 1999, Headon, 2009) EGF and EDA (Cui et al., 2008). In a study performed using mouse model, Cui, et al (2008) demonstrated, by removing EDA signals in their model at different points, that the hair follicle requires sustained EDA signalling for full development and that the eccrine gland develops slightly later than the hair

follicle (Cui et al., 2008). BMPs are also involved in initial hair placode development, with noggin inhibiting BMP4 signalling for further development of the hair follicle and are found in interfollicular epidermis during development, thus it is possible that they are involved in the development of eccrine glands also (Li et al., 2003, McGrath et al., 2008). Therefore, we were interested in developing a simple model that could be used to investigate the effects of some of these signalling molecules on our EC23 cell line and their potential to form eccrine structures.

Matrigel is a heterogeneous material composed of various ECM proteins, such as collagen IV, laminin and entactin and is extracted from Englebreth-Holm-Swarm mouse sarcomas. The presence of ECM and basement membrane proteins makes Matrigel ideal for cell culture of difficult to grow cells. Also, Matrigel it also contains an array of growth factors that can influence cell growth and morphogenesis such as, fibroblast growth factor (FGF), EGF, insulin-like growth factor 1 (IGF-1), TGF-β, platelet derived growth factor and nerve derived growth factor (Vukicevic et al., 1992, Hughes et al., 2010). In the experiments conducted in this chapter, growth factor reduced (GFR) Matrigel was used, as it is a modified version of the original matrigel with much lower levels of growth factors (see appendix for full composition) that allows for a more defined control of the growth factors that affect the cells.

Matrigel has been used in many studies to investigate morphogenesis of organs. One of the main areas of research employing matrigel is mammary gland development a breast cancer. Krause, et al, used a matrigel-collagen model to

study the stromal-epithelial interactions involved in breast cancer (Krause et al., 2008). Lo, *et al,* (2012), used matrigel to study branching morphogenesis and differentiation of the mammary gland (Lo et al., 2012). In a study by Sato, *et al* (2009), matrigel was used to study Lrg5 positive cells in the gut and their retention of stem cell like properties. It was found that these cells had the potential to form crypt like structures that resemble the native gut (Sato et al., 2009).

In the GFR-Matrigel experiments carried out in this thesis, the EC23 cells were seeded at a low density (300 cells per well) and cultured for 24 days in media containing varying concentrations of EGF, BMP-2, BMP-4 and EDA. Many measurements can be made using the system used to image and analyse the spheroids, such as diameter, density area, perimeter and branching. Even though the eccrine gland is not a branched structure, but rather a tubular structure with a coiled end, it was decided that branching was the most adequate measure to analyse. This is because we wanted to investigate the effect of growth factors in the morphogenesis of the eccrine gland and all the other measurements available would only give information with regards to size and density. Branching nodes is a measure of the bifurcations within a single object, an object that is a perfect round shape is allocated a value of 0 with the value assigned increasing depending on the degree of branching.

Morphogenesis of the eccrine gland is not well understood and much of what is known has been through studies of anhidrotic ectodermal dysplasia (AED), a condition that is characterised by the absence or malformation of the hair follicle, teeth and eccrine glands (Cui and Schlessinger, 2006, Mikkola, 2009). AED

arises from a mutation in the EDA gene or a mutation in EDA receptor and its association adaptor protein. Research into the involvement of EDA in morphogenesis using transgenic mice engineered to express EDA upon tetracycline, has shown that EDA is necessary for eccrine gland initiation and early morphogenesis for normal gland formation (Srivastava et al., 2001, Cui et al., 2008).

In this study, it was found that EDA appeared to have a marked effect in EC23 with regards to formation of branching structures. In experiments it was found that EDA generally yielded higher branching at all concentrations in comparison to no EDA treatment. However, due to time restrictions and availability of reagents we were only able to carry this experiment out on two separate occasions. However, from these two experiments the data indicate very clearly that EDA appears to promote growth and branching of EC23 cells. Further experiments are of course required to validate this data.

BMPs are members of the TGF-β family present in the mesenchyme and regulate the development of ectodermal appendages. BMPs are known to be involved in hair follicle formation, being active at the initial placode formation (Aubin-Houzelstein, 2012). This signalling is then inhibited by noggin, to stimulate lymphoid enhancer-binding factor 1 up regulation that promotes hair follicle formation (Botchkarev et al., 1999). Interestingly, *in vivo* mouse model experiments where noggin was overexpressed, eccrine glands in the paws of the mice were replaced by hair follicles (Plikus et al., 2004), which suggests that active BMP signalling is involved in eccrine gland development. Also BMPs are

found to be present in interfollicular epidermis, further suggesting their involvement in eccrine gland morphogenesis (McGrath et al., 2008). BMP 2 and BMP4 are present in embryonic mesenchyme (Blanpain and Fuchs, 2009b) and they have been found to be involved in the development of skin appendages (Srivastava et al., 2001). Also because of the involvement of BMP2 and BMP 4 in hair follicle development (Wollina et al., 1999) these growth factors to were chosen for the matrigel experiments.

In experiments in which the EC23 cells were supplemented with BMP4, the degree of branching was a lot lower than those for EGF and for EDA, only reaching a maximum of 2.65 A/U in branching nodes. In these experiments, only at day 24 did we observe a noticeable increase in branching nodes for cells treated with 25 ng/ml of BMP4. In all other time points data sets there does not seem to be much correlation between concentration and branching apart from at the final time point. There is higher branching for 20 and 25 ng/ml of BMP4 at day 18, however there is also an increase for 5 ng/ml, thus suggesting considerable variability in response of cells to growth factors or in our ability to accurately measure branching (see below).

Unfortunately, in the experiments in which BMP2 was used, the cells became apoptotic after day 12 and the experiment had to me stopped. The degree of branching in these experiments at day 6 is minimal, something that is also observed at day 12 for the cells left unsupplemented with BMP2 at 5, 10 and 25 ng/ml of BMP2. There is an increase in branching nodes for 15 and 20 ng/ml treated cells, however the SEM on these samples is rather high making it difficult

to infer that there is a real response by the cells to these concentrations of BMP2. We can however infer that BMP2 alone is not sufficient to maintain EC23 cells in culture for more than 2 weeks of culture. It must be noted that in other experiments spheroids that received no growth factor supplementation did result in some spheroids remaining viable until the final time point, however these structures were few and branching was minimal.

EGF has also been implicated in eccrine gland formation. A study by Shikiji, et al (2003) demonstrated that keratinocytes supplemented with EGF had the ability to form eccrine duct like structures on collagen gels when supplemented with 15 ng/ml of EGF (Shikiji et al., 2003). Interestingly, in the experiments performed in the current study, it was found that neonatal fibroblasts when co-cultured with EC23 and keratinocyte also formed rudimentary down growths in the prescience on 10ng/ml of EGF. Another study by Li, et al (2002) demonstrated that EGF and MMP7 were involved in eccrine gland formation in utero by studying spontaneously aborted foetuses at different stages throughout development. Furthermore Blecher, *et al* (1990), demonstrated that administration of EGF to tabby AED model induced sweat gland formation (Blecher et al., 1990).

In experiments in which the EC23 cells were supplemented with EGF, there appears to be a correlation between the concentration of EGF used and the degree of branching at the 24-day time point. Even though treatment of the cells with 25 ng/ml of EGF yielded the most branching for day 6 and day 18, these levels showed considerable variability with branching being high (8.60 A/U) at day 6, then decreasing slightly at day 12 (7.27 A/U), with a further decrease at day 18

(5.35 A/U). Similar patterns were observed across the experiment for all other EGF concentration treatments, in which the cells initially branched upon EGF treatment followed by a decrease in Branching. At day 24 an increase in branching was observed at all EGF concentrations with the exception of cells maintained in the absence of EGF and those maintained with 5 ng/ml EGF. This data suggests that EGF in important in branching morphogenesis of the human eccrine gland. It also implies that EGF is required at different time points in eccrine gland development for proper structural formation.

We can conclude that growth factor reduced Matrigel appears to be a good model for investigating the effects of growth factors on the growth and branching of EC23 cells. However, it was also clear that we observed a significant amount of variability in the data and this did make analysis difficult. Matrigel plates were imaged using an in cell microscope that can image multi-well plates in an automated manner. Images were captured at varying X and Y positions to image the maximum number of structures formed as possible. The images were then analysed using the In Cell Developer Toolbox software V.1.8 to quantify specific parameters, such as branching, sphere form factor, area and diameter. The main interest in these experiments was the level branching of the structures formed upon treatment with varying concentrations of EGF, BMP2, BMP4 and EDA.

The data collected in these experiments suggests there is a requirement for these growth factors in the development of the eccrine gland. However, it must be taken into consideration that by using an automated microscope, imaging at particular levels within Y position, focus may have been compromised, due to small bubbles

in the matrigel, debris from cells, or dust on the objective or plate, resulting in out of focus images in some occasions which could not be analysed. Because of this, some degree of accuracy in the data may have been lost, as some larger or more branched structures in some cases could not be analysed, which could account for the high degree of variability between some time points. Also, there were several instances in which the microscope would not focus properly on the gels due to small bubbles or improper alignment within the wells. It was attempted to correct for such discrepancies, however due to the time that was taken in the imaging of the individual wells, it was not possible to do this as a matter of routine, as imaging was carried out under atmospheric conditions and this would have involved keeping the plates out of culture for long periods of time. This would have resulted in the loss of buffering capacity of the tissue culture medium and death of the spheroids.

A number of issues with the model may also have influenced the focusing of the automated microscope system. One of them is the possibility that enzymatic degradation of the matrigel will occur over extended periods of culture in 3D culture systems. This degradation affects the composition of the matrix changing the way it absorbs and refracts light where degradation has occurred. These changes, can make it difficult for an automated system to pick an area to focus on and thus the images acquired can be blurry making it very difficult to analyse.

Another possible reason for the lack of focus in our images is cell debris from dead cells that have become apoptotic during the course of the experiment. This is likely, as the issue with unfocused images was far more pronounced on latter time

points during the experiments. The reason behind this could have been due to normal cell terminal differentiation or because of a lack of nutrients reaching the cells located further inside the spheroids/furthest from the Matrigel, that may have received fewer nutrients, oxygenation and may have been unable to remove toxic metabolites efficiently. This is a problem in many 3D experiments, as cell aggregates, spheroids or pseudo tissues grow larger and thicker, there is less nutrients and oxygen available for the cells deep within the objects being cultured as there is a lack of vasculature (Yamada and Cukierman, 2007b). However we cannot at this point confirm if this was the situation in our organoid experiment as further investigations into this matter were not conducted.

Even though Sato et al (2009), managed to culture intestinal epithelial cells for over a year without much cell death, his team's experiments differ from ours in 2 key points. Firstly, they used cells thought be adult stem cells that express the Lgr5-CBC phenotype and have the potential to be maintained for longer periods of time in culture. Secondly, they disrupted the spheroids weekly in order to passage them, which means their organoids had fresh Matrigel at each passage (Sato, et al., 2009). Given our results, it might be advantageous to incorporate this part of the protocol to future investigations using the EC23 cell line.

Another factor that may have affected the results collected, was the automated system used for the analysis of the data. Although we attempted to optimise the automated system in order to acquire high quality of data there were instances where the system did not pick up objects correctly and some data may have been lost. Nevertheless, these problems were mainly restricted to capturing data for

quantification, with the images themselves showing clearly the growth and branching of the EC23 cells, and clearly show that EGF, BMP-4 and EDA affect the branching morphogenesis of the EC23 cells.

It will also be of great interest to perform immunofluorescence experiments on the organoid structures developed to asses their retention of eccrine gland markers such as NKCC1, muscarinic M3 receptor, carbonic anhydrase, mucin and FoxA1 (as mentioned in chapter 4). Immunocytochemistry of the matrigel organoids was attempted, initially by removing the organoids from the matrigel and attempting to embed in cryopreservative however it became clear that removing the spheroids from the matrigel damages their structure and thus initial attempts at staining in the wells were performed. A preliminary experiment as can be seen in figure 5.11, in which the sphere was stained for K14 however there was not enough time too further develop the technique. This staining was performed by gently washing the wells 5x in PBS order to remove all excess media and fixing the spheres overnight in 10% paraformaldehyde. The wells were then gently washed 5 times in PBS, the protocol used after these washes is the same used for all the immunocytochemistry performed in chapter 3, the protocol is described in section 2.2.1.

In conclusion, in this chapter it was demonstrated that the EC23 cell line has the potential to form rudimentary eccrine gland structures in collagen gels that have been constructed with neonatal fibroblasts. Furthermore, these eccrine gland like structures, are more prevalent when the EC23 cells have been co-cultured with keratinocytes. Furthermore we have shown that growth factor reduced Matrigel

can be used to investigate the effects of growth factors on the ability of EC23 cells to form spheres and branching structures. Moreover, our data using this model indicate that our EC23 cells are responsive to EGF, BMP-4 and EDA and this correlates with reported roles for these growth factors on eccrine sweat gland biology in vivo.

Chapter 6. The Identification of cells within the EC23 cell line that expresses stem cell markers.

6.1 Introduction

The skin is a dynamic organ, in which the epidermis in constant self-renewal. Keratinocytes multiply in the basal membrane and migrate to the upper layers of the skin whilst differentiating as they move up from layer to layer of the epidermis. The cells responsible for the renewal of the skin are epidermal stem cells that reside on the basal membrane of the epidermis. Stem cells are cell types capable of extensive self-renewal and unlimited replicative potential throughout adult life, which also have the ability to produce daughters that undergo terminal differentiation and thus differentiate into a diverse range of specialized cell types (Lajtha, 1979). Most epithelial tissues, including skin, self-renew throughout adult life. The renewal capacity of the skin is dependent on proliferation of a subpopulation of keratinocytes, known as epidermal stem cells (Lavker and Sun, 2000, Blanpain and Fuchs, 2006, Watt et al., 2006, Blanpain et al., 2007). Thus, epidermal stem cells are responsible for renewing the epidermis throughout adult life giving rise to the differentiating cells of the interfollicular epidermis, hair follicles and sebaceous glands (Watt, 2001, Watt, 2002, Blanpain et al., 2007).

There are at least three distinct niches of skin epidermal stem cells, the follicle bulge, the base of the sebaceous gland and the basal layer of the epidermis. Moreover, it also seems that these three progenitor populations share a few common expression markers such as K5, K14, p63, E-cadherin, $\alpha_3\beta_1$ and $\alpha_6\beta_4$ integrins as well as reduced levels of desmosomes and increased levels of adherens junctions (Fuchs, 2008).

More recently putative adult stem cell niches have been identified within the eccrine sweat gland, with work by Petshnik, et al., suggesting the presence of a nestin rich population within the eccrine gland (Petschnik et al., 2010b). Nestin is a class VI intermediate filament protein that was originally identified in neuroepithelial stem cells (Lendahl et al., 1990) and is believed to play an important role during early embryogenesis although it has also been found to be expressed in neural stem cells during tissue repair (Matsuda, et al. 2013). Nestin is also found in other tissues, such as skin, heart, blood vessels and muscle cells, and it is generally thought to be expressed in regenerating tissues and rapidly proliferating progenitor cells (Frojdman et al., 1997, Humphrey et al., 2003, Ishiwata et al., 2006) (Matsuda et al., 2013). Nestin can form homodimers and heterodimers with other intermediate filament proteins such as vimentin, desmin and alpha-anexin (Sjorberg, et al., 1994), which act as scaffolds anchoring proteins, such as the glucocorticoid receptor, which regulates growth and differentiation (Reimer et al., 2009, Matsuda et al., 2013). The ability of nestin to tether cell surface receptors such as the GR receptor has been shown to play an important role in regulating cell proliferation as down-regulation of nestin results in enhanced nuclear translocation of GR to the nucleus and inhibition of cell proliferation via irreversible G1/S phase cell cycle arrest (Reimer et al 2009).

The aim of the work presented in this chapter was to investigate whether it was possible to identify stem cells in our EC23 cell line based on expression of nestin and whether co-localisation with the cell surface marker CD44, another putative stem cell marker would allow me to isolate a population of eccrine sweat gland

stem cells that could be used in three-dimensional organotypic models as demonstrated in Chapter 5.

6.2 Results

6.2.1 Identification of Nestin positive cells.

Immunocytochemistry was carried out on EC23 cells using a commercially available antibody to nestin. Figure 6.1 shows that within the general population of EC23 cells it was possible to identify cells that were nestin rich, with nestin filaments clearly visible at higher magnifications.

Because nestin is an intracellular protein it could not be used to select for live nestin expressing cells using FACS sorting, thus a cell surface stem cell marker that is co expressed with nestin positive cells would be required.

CD44 is a cell surface protein that has been reported to be a marker for epidermal stem cells (Szabo, et al, 2013) and has been used successfully by other researchers within the Centre for Cutaneous Research to select for putative cancer stem cells that can be cultured (Biddle, et al, 2013). I therefore carried out a series of experiments to determine whether CD44 would co-localise with nestin bright cells. Figure 6.2 shows that some cells did appear to be CD44 high and nestin high although there was not complete overlap by immunocytochemistry and many nestin bright cells did not express high levels of CD44.

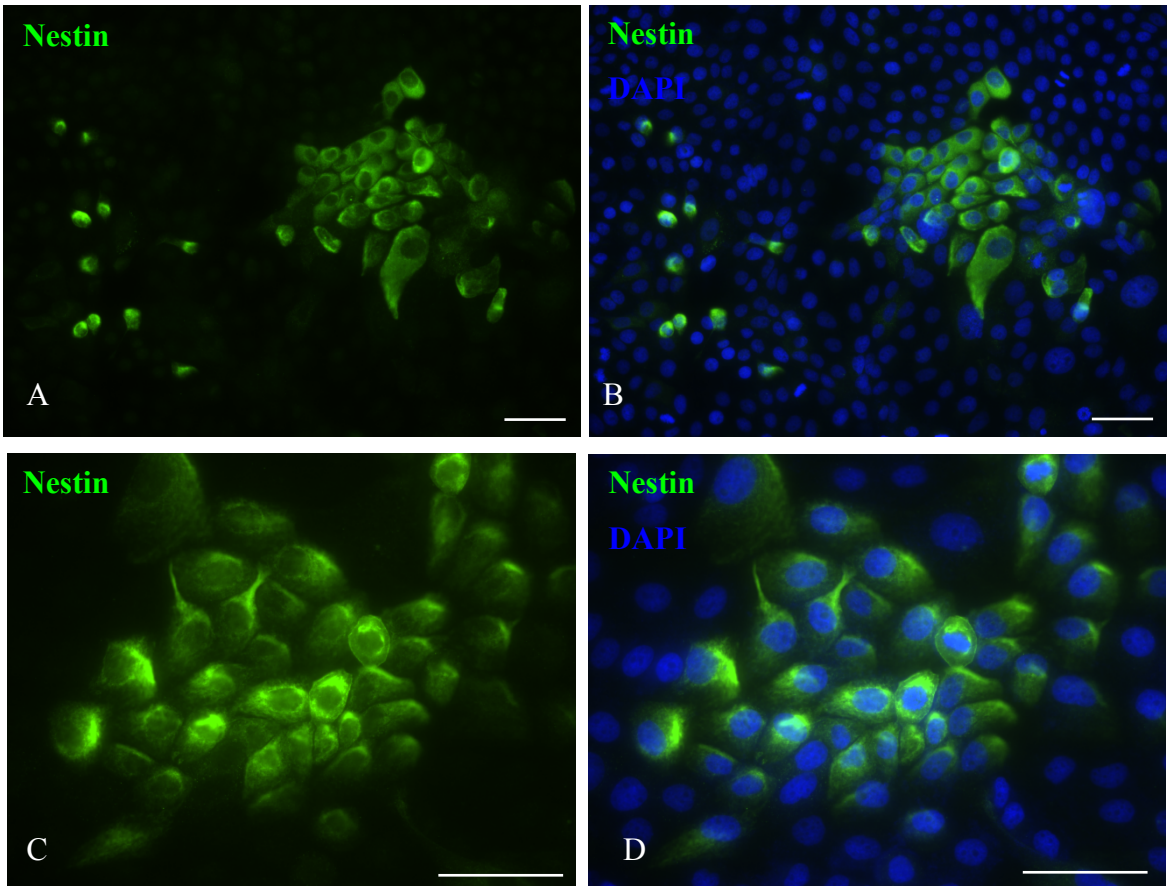

Figure 6.1. Identification of nestin positive cells within the EC23 cell line population. Showing under both X20 (A) Nestin & (B) nestin and DAPI merged cells; and X40 (D) Nestin & (C) nestin & DAPI merged cells. DAPI stained cells clearly show that the nestin positive cells form a sub population of the total number of cells present. Scale bars 100μm.

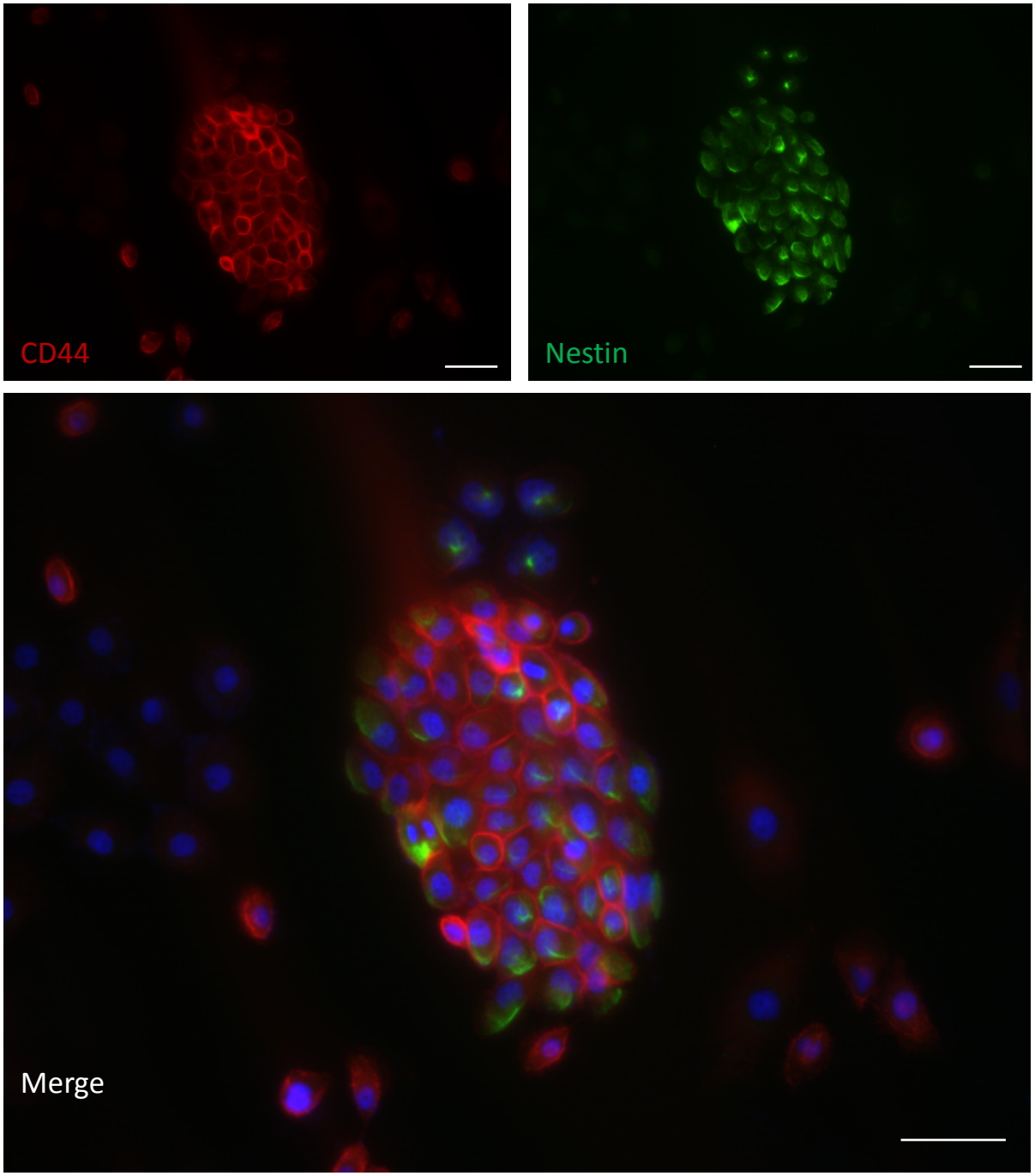

Figure 6.2. Colocalisation of nestin and CD44 in EC23 cells. Showing (A) expression of CD44 and (B) nestin. Panel (C) shows overlap in expression between CD44 and nestin and clearly shows that not all CD44 bright cells are also nestin bright. Scale bars 100µm.

6.2.2 Isolation of CD44 high and CD44 low cells within the EC23 cell line population and assessment of co-localization between CD44 high and low cells.

Having shown by immunocytochemistry that a sub population of EC23 expressed both nestin and CD44 (section 6.1), further experiments were carried out to investigate this co-localisation using FACS analysis. The data presented in figure 6.3 is representative of two separate experiments. As can be observed in figure 6.3 (A), CD44 expressing cells can be seen in quadrant 1 (Q1). Interestingly, it was found that there are 2 populations of CD44 bright cells within the EC23 cell line, as can be seen in Q1 in figure 6.3A: CD44 high, the cluster of cells that is furthest from the *x* axis, and a further population of CD44 bright cells that are closer to the *x* axis intersect. The cells were then analysed for their expression of Nestin, figure 6.3(B). The expression of nestin appears to be broad, with cells in quadrant 3 (Q3) expressing very little or no nestin, and cells in quadrant 4 (Q4) expressing increasing levels of nestin depending on their position along the x axis.

Figure 6.3 (C) shows the analysis of EC23 cells stained with both Nestin and CD44, in which we can still see two populations of CD44 bright cells in quadrant 2 (Q2) that also express high levels of nestin. The positioning of the cells in Q2 signifies that there are cells that express both CD44 and Nestin, with 78.1% (15,620 events; figure 6.3 D) of the total number of cells assayed being positive for both nestin and CD44. Out of the 15,620, 98.3% of the cells were located on Q2. The gates P2 and P3 were placed in an adequate position to analyse the two populations of cells found for CD44 (Figure 6.3A). CD 44 high cells, P2, account for 30% of the total number of cells expressing both CD44 and nestin, and CD44

low cells (P3), account for a much larger proportion of 60.8% of the total number of cells expressing both markers.

The CD44 high and CD44 low cell populations were then isolated using FACS sorting and the cells were seeded onto cover slips. Immunocytochemistry was carried out with CD44 and nestin, in order to determine if the CD44 high cells expressed higher levels of nestin than the CD44 low cells. After analysis, it was found that there was no correlation between the expression of CD44 and nestin in either the CD44 high or CD44 low EC23 cells (Figure 6.4 and 6.5).

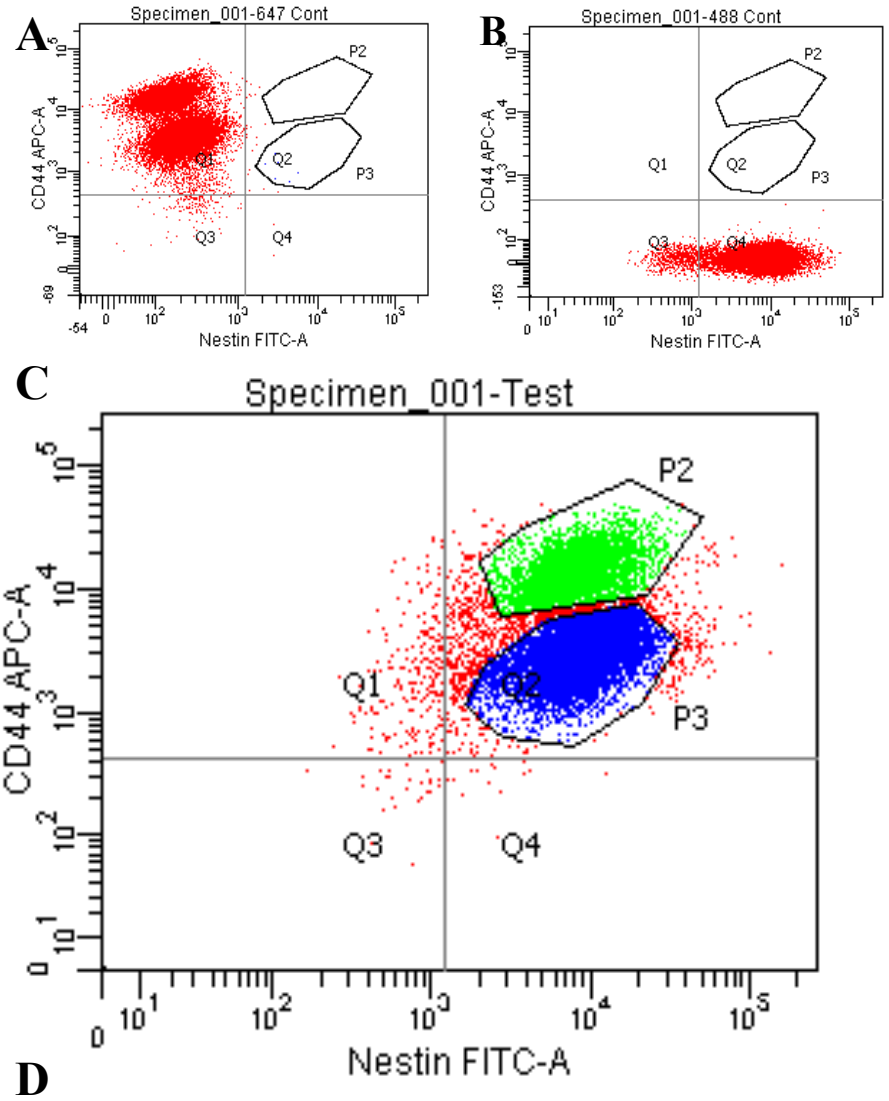

D

Tube Name: Test

Population	#Events	%Parent	Nestin Fl... Mean	Nestin F... Median	CD44 A... Mean	CD44 A... Median
P1	15,620	78.1	9,979	8,849	6,746	3,805
Q1	211	1.4	833	869	3,275	1,952
Q2	15,354	98.3	10,135	8,943	6,817	3,843
Q3	36	0.2	744	749	280	276
Q4	19	0.1	2,894	2,378	311	318
P2	4,685	30.0	9,359	8,194	14,714	13,472
P3	9,502	60.8	10,214	9,510	3,031	2,865

Figure 6.3.FACS analysis of EC23 cells for CD44 (APC) and nestin (FITC). (A) Analysis of CD44 ; (B) analysis of nestin; (C) analysis of nestin and CD44 (D) events recorded for CD44 and nestin analysis, showing (A) 2 populations of cells Q1 that express CD44; (B) a population of cells expressing varying levels of nestin from no expression on Q3 to cells expressing nestin in Q4;(C) shows cells expressing both CD44 and nestin and P2 gating for cells expressing a highest expression of CD44 and P3 gating the population of cells that express low CD44 expression (D) shows the events per gate with P2 having roughly half the number of cells of P3.

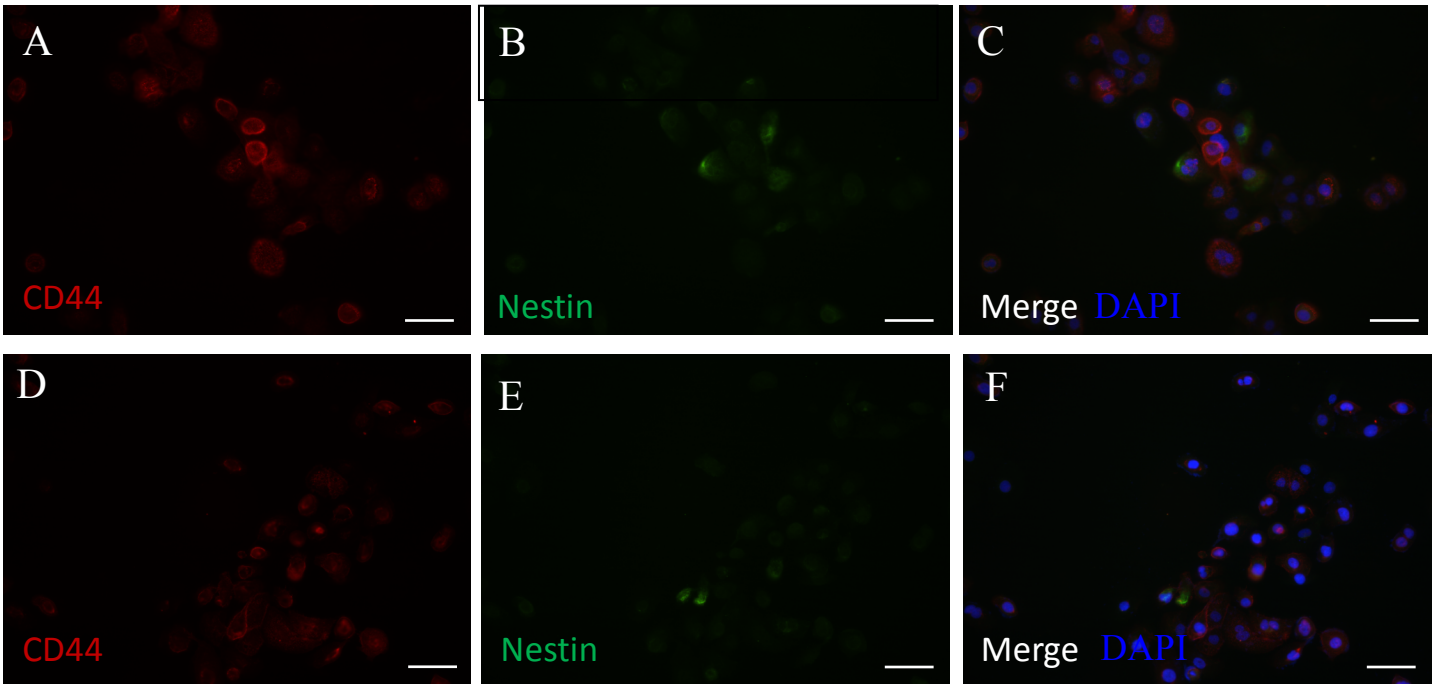

Figure 6.4.Immunocytochemistry of experiments on CD44 and Nestin in CD44 low EC23 cells. (A&D) CD44; (B&E) Nestin; (C) Merge of A and B with DAPI; (F) Merge of D and E with DAPI. Showing cells varying levels of CD44 expression with few cells expressing nestin with no overlap between the highest CD44 expressing cells and nestin or the lowest expressing cells and nestin. Scale bar 100µm.

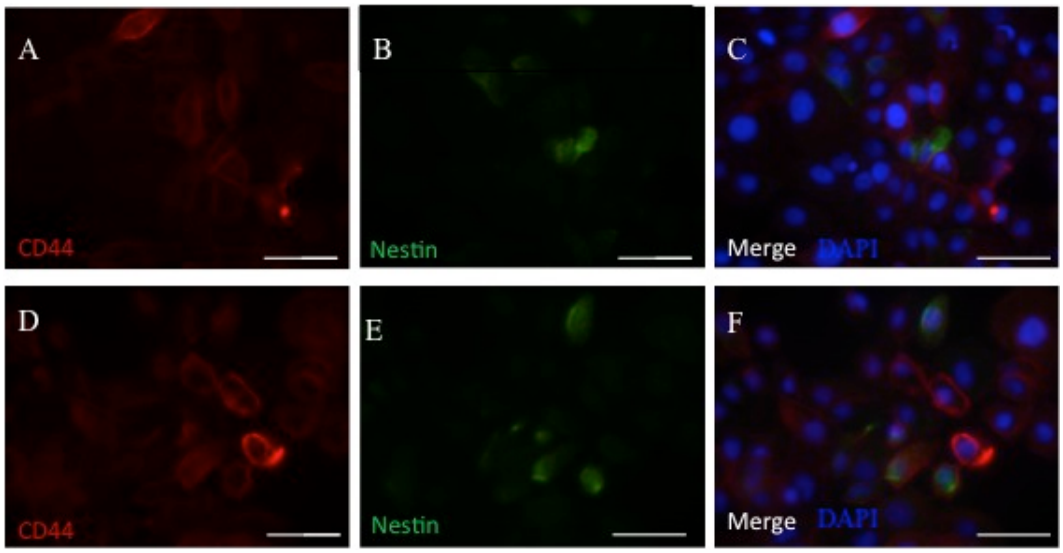

Figure 6.5 Immunocytochemistry for experiments of CD44 and Nestin in CD44 high EC23 cells. (A&D) CD44;(B&E) Nestin; (C) Merge of A and B with DAPI; (F) Merge of D and E with DAPI. Showing most varying levels of expression of CD44, with a few cells expressing nestin but no overlap between the highest CD44 expressing cells and nestin or the lowest expressing cells and nestin. Scale bar 100µm

6.2.3 Study of nestin expression in EC23 cells and clones.

Because no correlation was found between the expression of CD44 and the expression of nestin, I decided to analyse the levels of expression of nestin in the clones derived from the EC23 cell line to determine whether some clones may express higher levels of nestin than others. To do this, immunocytochemistry was performed using nestin and CD44 antibodies as described above and analysis of fluorescent intensity was performed using Cell Profiler. The intensity was quantified and the maximum fluorescence expressed by the cells was determined for each of the clones. DAPI and CD44 staining were used to identify single cells so that accurate analysis could be made.

The analysis of the maximum fluorescence (Figure 6.6 & Table 6.1) shows that the EC23 population of cells exhibit the highest levels of fluorescence intensity of all the cell lines, the next cell lines with maximum fluorescence after EC23 were clone 2 (1575AU), and clone 7 (1491AU), neither of which was significantly different from the fluorescence of the EC23 cells. EC23 cells were significantly different from clones 3 and 8 to $p<0.05$, these cells had a maximum fluorescence of 952AU and 989AU respectively. The EC23 cells were also significantly different to clones 4 and 9, which had fluorescence values of 691AU and 845AU respectively, to $p<0.01$. The maximum difference in fluorescence was between EC23 cells and clone 1 also being significantly different to $p<0.001$.

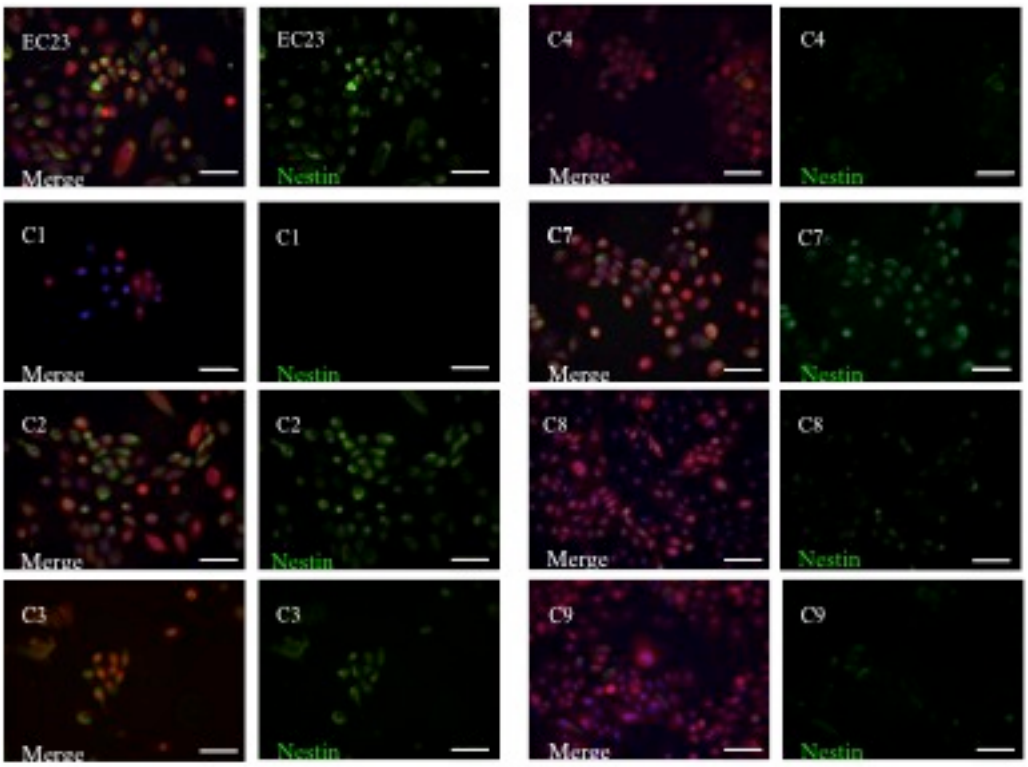

Figure 6.6. Immunocytochemistry analysis of EC23 cells and clones depicting cells expressing CD44 (red), nestin (green) and DAPI (blue). Showing that even among the clonal cells we still see different levels of expression although clones 2, 3 and 7 appear to express similar levels of nestin to the EC23 cell line. Scale bar 100um.

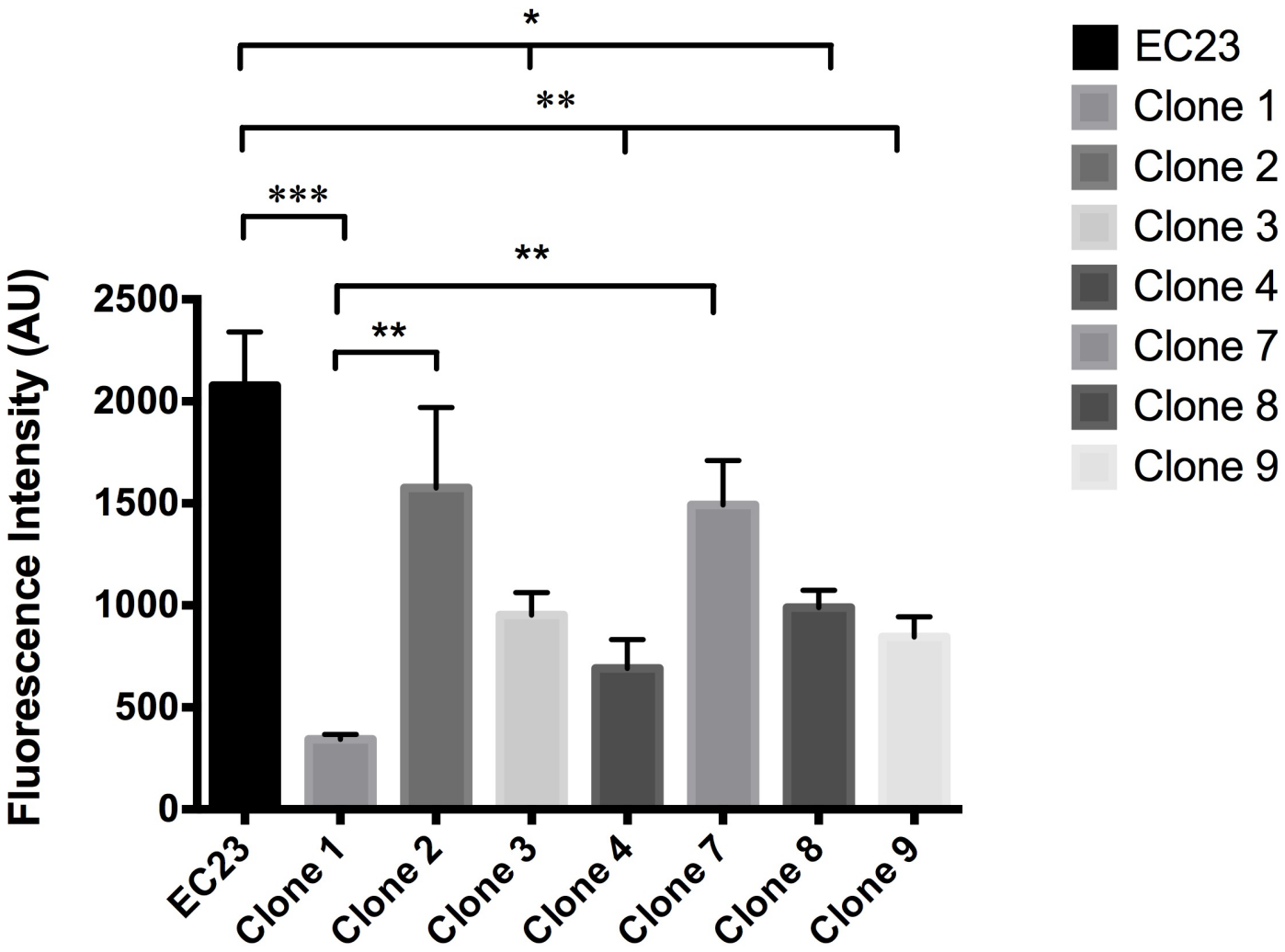

Figure 6.7.Graph showing the mean maximum nestin fluorescence intensity recorded for each cell line. Data shoes that EC23 cells that had the highest nestin fluorescence followed by clones 2 and 7. Results are expressed as the ± SEM for n=3 separate experiments. Statistical analysis was carried out by ANOVA with a Tukey's post hoc test. Error bars show SEM, *P<0.05 and ** P< 0.01 and ***P<0.001

	Mean Maximum Intensity (SEM)	Percentage of cells expressing Nestin (SD)
EC23	2077 (263)	38.28 (14.97)
Clone 1	342.6 (24)	58.75 (7.59)
Clone 2	1576.0 (395.2)	55.49 (42.14)
Clone 3	952 (110.1)	49.87 (28.58)
Clone 4	691 (141)	55.56 (33.13)
Clone 7	1491 (218)	54.1 (39.11)
Clone 8	989 (84)	19.64 (3.46)
Clone 9	845 (99)	23.88 (10.85)

Table 6.1. Showing the mean maximum levels of nestin immunofluorescence intensity for the EC23 cells and its clones, and the percentage of cells that positive for nestin.

6.2.4 Identification of CD29 and CD49f within the EC23 cell line.

Stem cell identification and isolation is a challenging task, due to the lack of reliable markers. CD29 (β1 integrin) and CD49f (α6 integrin), are markers that have been used to identify epidermal, spermatogonial and prostate stem cells (Shinohara et al., 1999, Alonso and Fuchs, 2003, Yamamoto et al., 2012), and thus these markers were investigated to see whether they may be suitable candidates to isolate a population of cell that could retain stem like qualities from the EC23 cell line.

The EC23 cells were stained using a CD29 APC conjugated antibody and with nestin in order to perform FACS analysis (figure 6.8). The analysis showed, as previously described in section 6.1, levels of nestin expression that ranged from low to high (see figure 6.6 A for previous data). EC23 cells showed expression of

CD29 (figure 6.9 B). When the cells were analysed for expression of both nestin and CD29, it was found that 60.2% (P1, ~12,000 cells) of the total EC23 cell population expressed either nestin alone or nestin and CD29 (figure 6.9 C&D). Off these 12,000 (PI) cells 50.6% expressed both CD29 and nestin (Q2) while 49.4% of the 12,000 (PI) cells only expressed nestin (Q4), suggesting that all the CD29 expressing cells also express nestin. Immunocytochemistry was also carried out on EC23 cells to investigate expression of CD49f (α-6 integrin) and is shown in Figure 6.10. This figure shows that EC23 cells expressed α6 integrin at high magnification (figure 6.9 B), filopodia can be observed in the EC23 cells. Because of time restraints I did not have time to further investigate expression of α1 and α6 integrin.

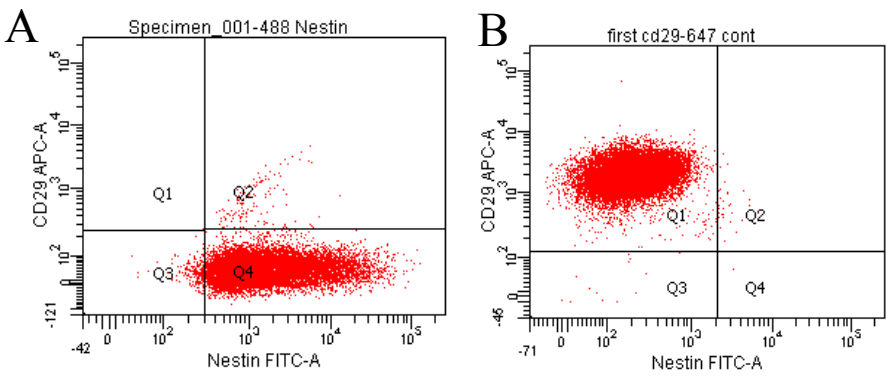

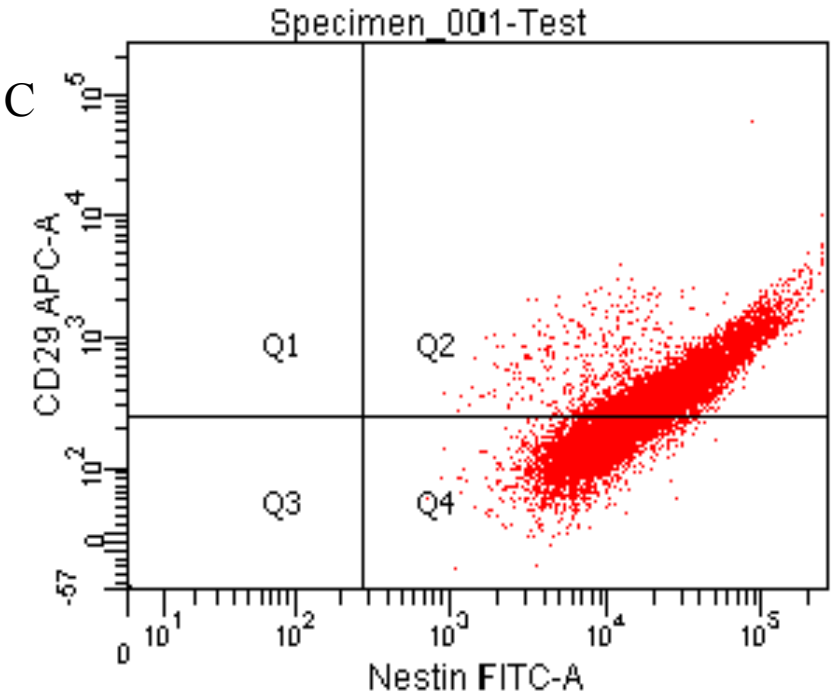

D

Tube: Test

Population	#Events	%Parent	%Total
All Events	20,000	####	100.0
P1	12,033	60.2	60.2
Q1	0	0.0	0.0
Q2	6,093	50.6	30.5
Q3	0	0.0	0.0
Q4	5,940	49.4	29.7

Figure 6.8. FACS analysis of EC23 cells for (A) nestin; (B) CD29; showing that EC23 cells express both CD29 and nestin (C) shows analysis of EC23 cell for CD29 and nestin; this data is also shown (D) as a table of events for CD29 and nestin analysis. Showing in (A) most cells expressing nestin in Q4; (B) shows cells expressing CD29 in Q1;(C) shows cells most cells expressing nestin with only cells in Q2 (6093 events) expressing both nestin and CD29. Data is representative of n=2 separate experiments.

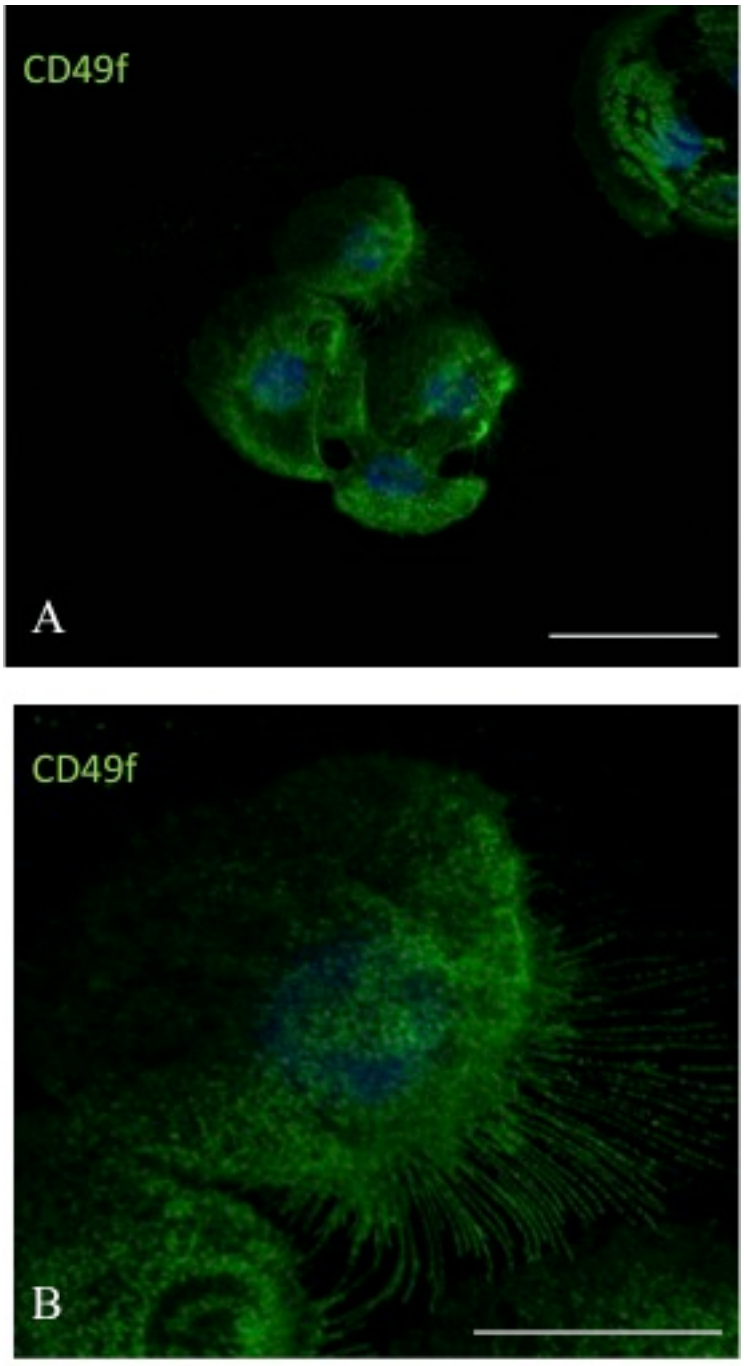

Figure 6.9. Expression of CD49f in EC23 cells. Immunocytochemistry was carried out for CD49f on EC23 cells, showing (A) EC23 cells expressing CD49f (scale bar 50μm); and (B) EC23 cells expressing CD49f, where filopodia can be observed, (scale bar 20μm).

6.3 Discussion

In the previous chapter I showed that EC23 cells could be placed in growth factor reduced Matrigel and that in response to certain growth factors formed branching structures. In order to investigate this further and as the data from previous chapters indicated very strongly that the EC23 population was a heterogeneous population of cells I wanted to know whether it was possible to identify a stem cell population within the EC23 cell line and further whether this cell line could be isolated and whether if placed in growth factor reduced matrigel would form enhanced branching structures.

Adult stem cells are defined as cells that maintain their ability to undergo self-renewal throughout an organism's lifespan and are able to produce daughter cells that terminally differentiate (Watt, 1998). In skin, such stem cells are essential for the maintenance of homeostasis and wound repair. In interfollicular epidermis, epidermal stem cells are located in the basal layer, where they are thought to divide with some cells remaining behind, retaining their stem cell qualities and others entering a transient amplifying state (Lavker and Sun, 2000, Blanpain and Fuchs, 2006, Watt et al., 2006, Blanpain et al., 2007). Transient amplifying cells are capable of a limited number of cell divisions, and the daughter cells exit the cell cycle in order to begin migrating towards the stratum corneum, differentiating further through every layer (Watt, 1998). The hair follicle bulge, has also been identified as a source of epidermal stem cells, with cells of this region contributing to regenerating the inner root sheath and the hair shaft (Blanpain and Fuchs, 2009a). However, unless the skin is wounded, bulge cells only function in

hair follicle homeostasis and are not essential for maintenance of the interfollicular epidermis, which instead depends on its own resident stem cell population (Claudinot et al., 2005, Ito et al., 2005, Levy et al., 2005, Watt et al., 2006).

Nestin, is an intracellular filament, originally identified as a marker of neural tube associated neural stem cells (Tsujimura et al., 2001). However, recently nestin has been found in progenitor cells in a range of tissues including neuroectodermal cells, skeletal muscle cells and islet progenitor cells (Lechner et al., 2002). In the skin nestin rich cells have been found in mesenchymal compartments of skin appendages (Kruse et al., 2006, Tiede et al., 2009, Petschnik et al., 2010a). Nestin positive cells from hair follicles can be directed to differentiate into melanocytes, keratinocytes, neurons, glia and smooth muscle cells in vitro (Amoh et al., 2005, Amoh and Hoffman, 2010, Najafzadeh et al., 2015). Nestin mRNA has been found in the eccrine sweat gland (Tiede et al., 2009) and Petschnik, et al, (2010) identified nestin expressing cells within isolated eccrine glands, furthermore, other markers associated with stem cells, Oct-4, NANOG and CD9, were also identified in these cells (Petschnik et al., 2010a).

More recently nestin positive stem cells have also been identified in the stroma of both eccrine and apocrine glands (Nagel et al., 2013). Nagel et al (2013) found that isolated cells from the eccrine gland stroma contain a population of nestin rich cells that co-express α-6 integrin, which is involved in cell migration, survival and signal transduction and is thought to maintain pluripotency due to its

role in regulating SOX2 and Oct-4 (Yu et al., 2012). They also provided evidence that these cells retain their multipotency.

Following experiments in which the EC23 cell line was able to form glandular like structures in collagen gels and the formation of branching structures in Matrigel, it was postulated that stem cell 'like cells' could be responsible for generating these structures, as it is possible that they may have been immortalised during the process of developing the EC23 cell line. Therefore, immunocytochemistry aimed at identifying nestin expressing cells was conducted and nestin positive cells were identified (figure 6.1). From this it was hypothesised that if it were possible to isolate these cells, a much higher yield of eccrine like structures could be achieved in 3D matrigel experiments.

However, because nestin is an intracellular filament protein, these cells could not be isolated by FACS sorting. Thus other epidermal stem cell associated markers that are expressed on the cell membrane and that may be useful in isolating stem cells from the EC23 cell line were investigated. Initially, CD44 was studied, as it was already known to be present within the EC23 population. In FACS analysis results (figure 6.3), 2 populations of CD44 cells were present, and a range of nestin expression from low to high expression was also identified. From this it was decided that the cells expressing the highest 20% and the lowest 20% of CD44 would be isolated using FACS sorting, to see if there was any correlation between the co-expression of nestin positive cells and either CD44 high or CD44 low cells. The CD44 high and CD44 low cells were seeded onto cover slips and immunocytochemistry using nestin and CD44 was performed. In these

experiments (figure 6.4) no defining co-localisation could be observed in either the CD44 high or the CD44 low cells, suggesting that CD44 may not be the best marker for the isolation of nestin positive cells.

Due to the lack of co-expression of nestin and CD44 in the EC23 cell line, it was decided that analysing the degree of expression of nestin in the clones could provide a better cell line to further study and possibly use in the generation of an improved 3 dimensional model. To do this the cells from the various clones were stained as before, for the EC23 cells, with nestin, CD44 and DAPI. From the data generated from the clones, it is clear to see that there are marked and significant differences in nestin expression by each of the clones with in particular clones 1 and 4 expressing low levels of nestin and clones 2 in particular but also clone 7 expressing high levels of nestin that were not significantly different to levels of nestin expressed in the founder EC23 cell line. In addition I also observed varied degrees of expression within each clone with some cells expressing very low or no expression of nestin, to some very bright nestin positive cells distributed within the various clonal populations. Overall, the percentage of cells expressing nestin was very similar for clones 1, 2, 3, 4 and 7, with between 49.87% and 58.75% of the cells being positive. However, in clones 8 and 9 only 19.64% and 23.88% of the cells were positive for nestin. Therefore from the 7 clones I investigated there are a range of levels of expression and percentage of nestin positive cells both between different clones and within clones.

The variations observed in the levels of nestin expression within the same clones (figure 6.6) and the variations in maximum fluorescence (figure 6.7) may be due

to the expression of nestin being cell cycle dependent. A number of proteins are expressed at different levels during the cell cycle including p53 (Sunabori et al., 2008) and Vimentin (Ferrari et al., 1986). The expression of the nestin gene *Nes* has been found to be up-regulated during the G1-S phase of the cell cycle followed by a sharp decrease in Nes expression in the G2-M phases of the cell cycle, which is thought to be due to the phosphorylation of its upstream regulator Brn2, a class II POU protein (Sunabori et al., 2008, Matsuda et al., 2013). Also the intermediate filament network in cells depolymerises in the M phase of the cell cycle, which requires a twisting process to occur during the G1 stage, the point when *Nes* transcription is it its highest (Sunabori et al., 2008).

In the experiments carried out in this chapter I did not synchronise the cell cycle of either EC23 cells or their clones and this may explain why within the clones I also saw variability in expression of nestin. The cell cycle of cultured cells can be synchronised by using a double thymidine block to arrest and, subsequently, release the cells at the G1/S boundary (Pena-Diaz et al., 2013) or by serum starvation or using drugs such as nocodazole and colcimid (Davis et al., 2001). Once synchronised, we could then investigate whether there is greater homogeneity in levels of expression within clones.

The maximum nestin fluorescence recorded was for the EC23 cells, followed by clones 2 and 7. From this data it could be suggested that the EC23 cells in addition to clones 2 and 7 should be used for future experiments when investigating nestin expression. However, as clone 2 and 7 do not express all of the expected secretory coil markers (see Chapter 3), EC23 cells would be the best

cell choice for further studying nestin and its possible role as a stem cell marker in the human eccrine gland. Nevertheless, only a percentage of the cells express nestin even within the clones and because the expression of nestin is associated with highly proliferative cells in embryonic development and may well be cell cycle dependent it will be important to synchronise the cell cycle prior to further nestin analysis. This experiment would allow nestin expression to be analysed at different stages of the cell cycle allowing us to build a clear view of the pattern of expression of nestin during the cell cycle and which may prove invaluable for the better isolation of nestin positive cells by means of a cell surface receptor marker. Interestingly, it has been found that glucocorticoid receptor co-localises with nestin in embryonic mouse tissue (Reimer, et al., 2009), and thus it would be interesting to see if this is the case for EC23 cells.

Because of problems identifying a clear population of cells that retained expression of both nestin and CD44, we further investigated the presence of another marker that is thought to be present in epidermal stem cells, CD29 (β-1 integrin). CD29, is the β1 subunit of many integrins that are transmembrane receptors for ECM components. CD29 is a widely used marker for stem cells of the basal layer of the human skin and hair follicle bulge (Alonso and Fuchs, 2003). It has been found that CD29 expressing cells attach to tissue culture plastic, form larger colonies and proliferate for longer than CD29 null cells (Watt, 1998). Also, high levels of CD29 (and CD49f) have been described as stem cell markers for mammary gland (Wang and Li, 2006, Pontier and Muller, 2009). Furthermore, Kurata et al (2014), has recently reported that isolated CD29 high and CD49f high myoepithelial cells isolated from eccrine glands have high self-

renewal capabilities a high proliferative potential in sphere forming assays (Kurata et al., 2014). Because of its expression in stem cell compartments of the epidermis and hair follicle as well as localisation in the eccrine sweat gland we decided to investigate its expression in our EC23 cell line.

Analysis of EC23 cells for CD29 and nestin using FACS showed that there are CD29 expressing cells within the EC23 cell population and some degree of co-localization with nestin. In addition immunocytochemistry analysis showed that a portion of the EC23 cell population expressed CD49f. This experiment was only a preliminary assessment and thus further analysis of CD29, CD49f and nestin would be required for future studies. The fraction of EC23 cells expressing nestin CD29 and CD49f could then be isolated to investigate whether they retain stem cell-like qualities, including whether they are able to differentiate along other cell lineages. Experiments could include seeding them in Matrigel and in collagen gels, then examining their capacity to develop eccrine sweat gland like structures.

In conclusion in this chapter I have shown that EC23 cells and the clones express both nestin and CD44 as well as CD29 and CD49F. This data suggests that there are potential stem cells within the cell populations being investigated. However, the degree of stemness within these cells is not clear and nestin and CD44 expression do not necessarily indicate these are stem cells. To investigate this further we could investigate the ability of these cell lines to form holoclones as the stem cell fraction of both normal epithelial cells and cancer cell lines when seeded at low density in vitro, generate proliferating colonies termed holoclones that can be distinguished from differentiating cells or paraclones (Locke et al., 2005). However, as the main focus of the experiments in this chapter was to

identify whether stem cells were retained within the EC23 population or whether one or more of the clones were enriched for potential stems or that we could isolate these cells by FACS. Then the next step with these experiments would be to investigate the ability of clones 2 and 7 to form branching structures in vitro. It would also be worth investigating the CD44 high population of cells.

Chapter 7. Final Conclusions and Future Work

The aim of this project is to develop and characterise an immortalised cell line derived from the secretory coil of the eccrine sweat gland and also to see if such a cell line could be used to develop a functional 3D *in vitro* model of the eccrine sweat gland. The main problems with existing models of the eccrine sweat gland, is that they are based on the culture of primary cells from isolated eccrine glands (Huang et al., 2010, Lei et al., 2011, Lei et al., 2012b, Li et al., 2015). These glands in themselves are difficult to isolate and depend on a ready supply of human tissue. Furthermore, primary cell cultures from the eccrine gland are very difficult to maintain in culture, they are highly variable and when grown as monolayer cultures they do not take into account the three-dimensional nature of the intact gland.

To circumvent problems with sourcing redundant human skin and problems with maintaining primary cell cultures we have previously generated an immortalised cell line from an explant culture of human eccrine gland secretory coil cells. This cell line is called the EC23 cell line and from this were derived a further 8 clonal cell lines. The EC23 cell line is thought to contain eccrine secretory coil clear cells and possibly dark cells. The clones were derived in hopes to isolate a population of only clear and/or dark cells to develop a 3D model that can be used to further understand the eccrine gland and to be used in pharmaceutical research.

The first aim of this project was to confirm the cells' phenotype, all immortalised cells were characterized by immunocytochemistry using a panel of antibodies to proteins that from a review of the literature were considered to be potential markers of eccrine sweat gland clear cells and dark cells.

The data shown in Chapter 3 suggests that the EC23 cell line contains all the markers of the eccrine gland clear and dark cells. The data however does not clearly point to one clone being from a clear or dark cell origin, as all the cells are all positive for the clear cell marker carbonic anhydrase II and clones 3, 4, 5, 6, 7, 8 and 9 also express MUC1, which is thought to be a marker of the dark cell (Bovell et al., 2007, Bovell et al., 2011). However clones 4, 7 and 9 retain all the markers of the eccrine gland necessary for function. In a recent paper it has been found that FoxA1 could possibly be used to distinguish between the dark and clear cells, thus in future experiments it would be essential to investigate the present of FoxA1 in the clones (Cui and Schlessinger, 2015). During the course of the experiments presented in Chapter 3, significant variability in expression of markers both with regards to levels of expression and cellular localisation was observed. These are discussed in Chapter 3 with regards sub cellular localisation. It would be important to carry out western blot analysis especially where proteins were detected in compartments where they were not expected to confirm initial findings.

As discussed in Chapter 6 for nestin the fact that clones showed different levels of protein expression within the same clone may reflect differences in cell cycle stage. it would therefore be important to synchronise the cells by cell cycle block

and then release the synchronised cells to determine whether we se more homogeneity of expression within the same clones. Differences in expression of markers between clones may reflect the nature of the cells immortalised and stages of differentiation. It would also be worth investigating different types of tissue culture medium. In our experiments we have focussed on culturing cells in DMEM/D12 modified media (see section 2.1.1. for full composition). It is possible that differences in expression of secretory coil markers may reflect the medium in which they are maintained and that different tissue culture medium may be better at maintaining expression of specific markers.

In Chapter 4, I carried out experiments to investigate whether the EC23 cell would respond to cholinergic and adrenergic stimuli and to determine whether they maintained characteristic secretory coil response. In addition I also compared the response of the EC23 cell line with that of the only other cell line that is available, namely the NCL-SG3 cells, which are believed to have been derived from the excretory duct. In the experiments conducted it was found that the EC23 cell line does respond to cholinergic stimuli and that NCL-SG3 cells responded minimally to the same stimulation. It was also established that the EC23 cells have functioning RyRs, providing further evidence of normal function. However, further experiments must be conducted as only the initial response to a cholinergic agonist was studied and the response of magnesium and chloride channels must be assessed in order to establish whether the EC23 cells retain all eccrine clear cell functionality. Also by performing these same functionality experiments on the clones derived from the EC23 cell line we could further assess their response to cholinergic and adrenergic stimuli. This may help improve our understanding of

the phenotype of the various clones and help further define which clones are more characteristic of the clear cell of the secretory coil and which may reflect dark cells. If we were able to gain a greater understanding of the various clones and be more certain about whether we have both clear and dark cells this would be a significant advantage especially if we were able to confirm we had an immortalised cell line from the dark cells as their biology is poorly understood.

The EC23 cells were then subjected to further experiments to determine their response to adrenergic stimuli. It was found that the EC23 cells and all clones responded to isoproterenol to a higher degree than the NCL-SG3 cells. However, the response was much lower than that of primary eccrine secretory coil cells, which is a possible consequence of the immortalization of the cells. From these experiments we provide evidence that the EC23 cells are a better model for the study of the human eccrine sweat gland than the NCL-SG3 cells. However, further pharmacological analysis of both the EC23 cells and especially the clones is required. Patch clamping has been widely used on primary eccrine cells (Saga et al., 1988, Joris et al., 1989, Wilke et al., 2007) and this would be very important in establishing the phenotype of the clones investigated in this project. Unfortunately during my PhD it was not possible to either carry out a more detailed pharmacological investigation of the clones or do any patch clamping.

After confirming that the EC23 cell line does express the main protein markers of the human eccrine gland secretory coil and these cells appear to retain the cholinergic and adrenergic functional qualities of the human eccrine gland, we

then carried out the experiments described in Chapter 5 to investigate their ability to form 3D models of the eccrine gland. Since the start of this project we had preliminary evidence provided by work completed before the start of my PhD (figure 1.5) that the EC23 cells could be cultured in organotypic models that resembled the appearance of glandular structures. EC23 initially cultured on DEDs, yielded no down-growths or any resemblance of glandular structures. Because of the inherent variability in DEDs as a result of spaces left by skin glands and appendages, it was decided to continue my experiments using collagen gels. When the EC23 cells were seeded onto collagen type I gels containing adult fibroblasts the EC23 cells were not capable of forming down-growths, however they were able to grow and organise as an epidermis; this agrees with Rittee (2013) who's research suggests that the eccrine gland can repopulate the epidermis following wounding. Nevertheless, the EC23 cell line was capable of forming down growths in collagen type I gels that were made using neonatal fibroblasts. A feature that was accentuated by the co-culture of keratinocytes with the EC23 cells. This may indicate that signals provided by the mesenchyme and keratinocytes may be important in the formation of eccrine glands. However, as the down-growths were not very convincing and time consuming, taking at least one month for each experiment, it was decided to look for a more simple but robust model that could be used to investigate glandular formation by the EC23 cells.

To further develop the 3D model we looked at the recent advances in bioengineering in fields like the gut, eye, mammary gland and brain. A lot of these advances in bioengineering have involved stem cells, and it has been noted

that the microenvironment in which the stem cells are seeded is highly important in determining the fate of the stem cells (Gjorevski et al., 2014). Matrigel has been crucial for much of the recent work in organoid formation as it provides a good microenvironment and specific signalling molecules that complement organoid formation (Sato et al., 2009, Lo et al., 2012).

The eye is a very interesting organ to study in relation to bioengineering, it is composed of several tissues, such as the retina, cornea, optic nerve, macula, sclera, and the cilliary muscle amongst others, with these tissues having very different compositions and densities which can be very challenging when trying to develop an engineered tissue. Eiraku et al., (2011) demonstrated that mouse ESCs can self organise into optic cup like structures in culture. Firstly, mouse ESCs aggregates were cultured in matrigel and low growth factor media conditions, followed transient activin treatment that directed the cells to differentiate into a retinal lineage. Matrigel was incorporated into the culture system and within 6 days spherical hollow structures began to express the retinal marker Rx. By day 10 the cells had acquired a two tailed cup morphology which closely resembles the morphology of the *in vivo* optic cup (Eiraku et al., 2011).

Another important breakthrough in tissue engineering has been the creation of 'mini guts'. The major breakthrough in this field was done by Barker et al., (2007), who identified the Lgr5, a marker of intestinal stem cells (Barker et al., 2007). Sato et al., (2009) describes a model of the small intestine that can maintain primary adult cells in culture over long periods of time (1.5 years). This

was achieved by culturing slender crypt columnar cells that express Lgr5 in matrigel supplemented with R-spondin, that augments Wnt signalling, EGF and Noggin (Sato et al., 2009).

The creation of brain organoids is yet another example of advances in the field. Lancaster et al., (2013) developed a technique to culture brain organoids by initially generating embryoid bodies from human ESCs or induced pluripotent stem cells by culturing the cells in embryonic stem cell medium containing low levels of bFGF and ROCK inhibitor. Neural induction of the embryoid bodies was directed by using media containing specific growth factors that ensure cell lineage all while maintaining the cells in suspension. After this the embryoid bodies were seeded onto Matrigel and to introduce oxygen the culture system was agitated, which they found to greatly increase the viability of the organoids produced. The organoids produced in this experiments contain parts of various brain regions such the midbrain, hindbrain, meninges, choroid plexus, hippocampus and retina and can be maintained for over a year (Lancaster and Knoblich, 2014)

This advances in bioengineering offer many insights into the requirements for building a 3D organ model. It is evident that the use of Matrigel is key in these experiments, as it provides a microenvironment that allows for the formation of organoids that with the correct signals resemble and express markers of the tissues that are being studied. With this in mind it was decided that Matrigel was a superior matrix, compared to collagen type I, to investigate the ability of the EC23 cells to form eccrine like structures. From the literature, it was established that

EGF, EDA, BMP2 and 4 would be used to supplement the spheroids culture media as these have previously been reported to be associated with eccrine sweat gland development (Blecher et al., 1990, Wollina et al., 1999, Srivastava et al., 2001, Cui et al., 2008)). The data shown in Chapter 5 suggests that EGF and EDA play important roles in morphogenesis and growth of ductal structures, as higher concentrations induced a higher degree of branching, however there were problems with the quantification of the images generated especially with regards the formation of branching structures.

The problems with the focusing in the imaging system are thought to be due to debris from dead cells. This however could in future be resolved by incorporating the use of a spinning bioreactor such as the one used by Lancaster et al., (2013). It is also possible that these growth factors are required at different times throughout the formation of eccrine spheroids and it is also possible that they are required at different concentrations at times; which is something that should be investigated further in future works.

A number of papers have been published suggesting that the eccrine gland has a stem cell niche (Biedermann et al., 2010, Petschnik et al., 2010, Lu et al., 2012). It was therefore decided to investigate whether our EC23 cell line contained stem cells and whether living stem cells could be isolated. If it were possible to isolate stem cells from the EC23 population it would be important to place these into matrigel and see whether they were able to produce improved glandular structures. In order to investigate the presence of stem cells in the EC23 cell

population and clones, a nestin antibody was used as nestin has previously been reported in eccrine sweat glands (Nagel et al., 2013, Petschnik et al., 2010) and to be a putative stem cell marker (Hoang et al., 2009, Sellheyer et al., 2011, Amoh et al., 2012). The experiments shown in Chapter 6 show that the EC23 cells expressed the highest levels of nestin fluorescence compared to the clones. However clones 2 and 7 also expressed high levels of nestin and could be used in further experiments although clone 2 does not express NKCC1 or mucin, suggesting these cells have lost their ability to function like eccrine gland secretory coil cells.

We also established that CD29 (β1-integrin) is expressed in some of the EC23 cells, and there seems to be a correlation between nestin expression and CD29, where the cells with higher levels of nestin expression also show higher levels of nestin expression. We also performed staining for CD49f (α6-integrin), which showed that the EC23 cells also express this integrin. The expression of nestin, CD29 and CD49f, suggests that the EC23 cells contain some stem like cells. In future it would be beneficial to attempt to isolate cells within the EC23 cell line that express stem cell markers, such as nestin or β1 integrin or α6 and incorporate these cells in the matrigel model as this could provide better morphogenesis.

However, while isolation of stem cells is one potential route by which to engineer eccrine glands in vitro it is important to remember that eccrine glands are made up of both clear and dark cells and that using a mixed population of cells such as present in the EC23 cell line may in fact be the optimum way to go forward with

regards gland formation. Perhaps of more importance that identifying specific cell markers will be establishing more robust functional assays both to measure pharmacological response but also whether the glandular structures formed in matrigel are capable of sweat formation.

In conclusion, we have analysed the EC23 cells and its clones for a panel of markers present in the normal human eccrine gland and determined that the EC23 cells retain all the markers of the native eccrine gland. It was hoped that the analysis of the clones would result in the identification of a clones that could be clearly identified as a clear cell and dark cells as these would be a unique. However the data remains inconclusive as there appears to be no clear distinction between clear or dark cells, and further work with a new dark cell marker should be conducted. However, it is also important to note that in a recent publication, Pontiggia et al., (2014) also reports a high degree of heterogeneity between cells of the secretory coil of the human eccrine gland. They also attempted to identify clear and dark cells in their secretory coil cultures by immunocytochemistry with markers reported in the literature, but due to the instability of the markers *in vitro* conditions they found it impossible to discern between clear and dark cells (Pontiggia et al., 2014).

From the data collected from the pharmacological studies we conclude that the EC23 cells retain their cholinergic pathway of action and that all the clones and EC23 cells also retain the ability to react in a β-adrenergic manner to stimuli. In the experiments reported in this thesis it has also been shown that EC23 cells form

glandular like structures in matrigel and this should form the basis of future work in this area. However a better imaging system would help considerably if we are to continue quantifying images. Finally, we identified a population of cells within the EC23 cell line and the clones that express nestin as well as CD29 and CD49f. Further work should be carried out on the basis of cells expressing these markers to see whether it is possible to purify stem cells from the EC23 cells and that could be further used in the matrigel model.

Appendix

Composition of growth factor reduced Matrigel

Growth Factor	Typical Growth factor in GFR Matrigel
EGF	< 0.5 ng/ml
bFGF	0-0,1 pg/ml
NGF	< 0.2 ng/ml
PDGF	< 5 pg/ml
IGf-1	5 ng/ml
TGF-β	1.7 ng/ml
Collagen IV	30%
Entactin	7 %
Laminin	61 %

Bibliography

ABOSEIF, S., EL-SAKKA, A., YOUNG, P. & CUNHA, G. 1999. Mesenchymal reprogramming of adult human epithelial differentiation. *Differentiation,* 65**,** 113-8.

ALBERT, A. P., SALEH, S. N., PEPPIATT-WILDMAN, C. M. & LARGE, W. A. 2007. Multiple activation mechanisms of store-operated TRPC channels in smooth muscle cells. *J Physiol,* 583**,** 25-36.

ALBERTS, B., WILSON, J. H. & HUNT, T. 2008. *Molecular biology of the cell,* New York, Garland Science.

ALONSO, L. & FUCHS, E. 2003. Stem cells of the skin epithelium. *Proc Natl Acad Sci U S A,* 100 Suppl 1**,** 11830-5.

ALTMAN, R. S. & SCHWARTZ, R. A. 2002. Emotionally induced hyperhidrosis. *Cutis,* 69**,** 336-8.

ALTY, J. E. & FORD, H. L. 2008. Multi-system complications of hypothermia: a case of recurrent episodic hypothermia with a review of the pathophysiology of hypothermia. *Postgrad Med J,* 84**,** 282-6.

AMOH, Y., AKI, R., HAMADA, Y., NIIYAMA, S., ESHIMA, K., KAWAHARA, K., SATO, Y., TANI, Y., HOFFMAN, R. M. & KATSUOKA, K. 2012. Nestin-positive hair follicle pluripotent stem cells can promote regeneration of impinged peripheral nerve injury. *J Dermatol,* 39**,** 33-8.

AMOH, Y. & HOFFMAN, R. 2010. Isolation and Culture of Hair Follicle Pluripotent Stem (hfPS) Cells and Their Use for Nerve and Spinal Cord Regeneration. *In:* TURKSEN, K. (ed.) *Epidermal Cells*. Humana Press.

AMOH, Y., LI, L., CAMPILLO, R., KAWAHARA, K., KATSUOKA, K., PENMAN, S. & HOFFMAN, R. M. 2005. Implanted hair follicle stem cells form Schwann cells that support repair of severed peripheral nerves. *Proc Natl Acad Sci U S A,* 102**,** 17734-8.

AUBIN-HOUZELSTEIN, G. 2012. Notch signaling and the developing hair follicle. *Advances in experimental medicine and biology,* 727**,** 142-60.

BARKER, N., VAN ES, J. H., KUIPERS, J., KUJALA, P., VAN DEN BORN, M., COZIJNSEN, M., HAEGEBARTH, A., KORVING, J., BEGTHEL, H., PETERS, P. J. & CLEVERS, H. 2007. Identification of stem cells in small intestine and colon by marker gene Lgr5. *Nature,* 449**,** 1003-1007.

BAZZI, H., FANTAUZZO, K. A., RICHARDSON, G. D., JAHODA, C. A. B. & CHRISTIANO, A. M. 2007. The Wnt inhibitor, Dickkopf 4, is induced by canonical Wnt signaling during ectodermal appendage morphogenesis. *Developmental Biology,* 305**,** 498-507.

BERG JM, T. J., STRYER L 2002. *Biochemistry,* New York, W. H. Freeman.

BERRIDGE, M. J., BOOTMAN, M. D. & RODERICK, H. L. 2003. Calcium signalling: dynamics, homeostasis and remodelling. *Nat Rev Mol Cell Biol,* 4**,** 517-29.

BERRIDGE, M. J., LIPP, P. & BOOTMAN, M. D. 2000. The versatility and universality of calcium signalling. *Nat Rev Mol Cell Biol,* 1**,** 11-21.

BERTOCCHINI, F., OVITT, C. E., CONTI, A., BARONE, V., SCHÖLER, H. R., BOTTINELLI, R., REGGIANI, C. & SORRENTINO, V. 1997. Requirement for the ryanodine receptor type 3 for efficient contraction in neonatal skeletal muscles. *The EMBO Journal,* 16**,** 6956-6963.

BIEDERMANN, T., PONTIGGIA, L., BOTTCHER-HABERZETH, S., THARAKAN, S., BRAZIULIS, E., SCHIESTL, C., MEULI, M. &

REICHMANN, E. 2010. Human Eccrine Sweat Gland Cells Can Reconstitute a Stratified Epidermis. *J Invest Dermatol,* 130**,** 1996-2009.

BIERIE, B. & MOSES, H. L. 2006. TGF-beta and cancer. *Cytokine Growth Factor Rev,* 17**,** 29-40.

BINI, G., HAGBARTH, K. E., HYNNINEN, P. & WALLIN, B. G. 1980. Thermoregulatory and rhythm-generating mechanisms governing the sudomotor and vasoconstrictor outflow in human cutaneous nerves. *The Journal of Physiology,* 306**,** 537-552.

BLANPAIN, C. & FUCHS, E. 2006. Epidermal stem cells of the skin. *Annu Rev Cell Dev Biol,* 22**,** 339-73.

BLANPAIN, C. & FUCHS, E. 2009a. Epidermal homeostasis: a balancing act of stem cells in the skin. *Nat Rev Mol Cell Biol,* 10**,** 207-17.

BLANPAIN, C. & FUCHS, E. 2009b. Epidermal homeostasis: a balancing act of stem cells in the skin. *Nat Rev Mol Cell Biol,* 10**,** 207-217.

BLANPAIN, C., HORSLEY, V. & FUCHS, E. 2007. Epithelial stem cells: turning over new leaves. *Cell,* 128**,** 445-58.

BLAZEJEWSKA, E. A., SCHLÖTZER-SCHREHARDT, U., ZENKEL, M., BACHMANN, B., CHANKIEWITZ, E., JACOBI, C. & KRUSE, F. E. 2009. Corneal Limbal Microenvironment Can Induce Transdifferentiation of Hair Follicle Stem Cells into Corneal Epithelial-like Cells. *Stem Cells,* 27**,** 642-652.

BLECHER, S. R., KAPALANGA, J. & LALONDE, D. 1990. Induction of sweat glands by epidermal growth factor in murine X-linked anhidrotic ectodermal dysplasia. *Nature,* 345**,** 542-544.

BOOTMAN, M. D. 2012. Calcium Signaling. *Cold Spring Harbor Perspectives in Biology,* 4.

BOTCHKAREV, V. A., BOTCHKAREVA, N. V., ROTH, W., NAKAMURA, M., CHEN, L.-H., HERZOG, W., LINDNER, G., MCMAHON, J. A., PETERS, C., LAUSTER, R., MCMAHON, A. P. & PAUS, R. 1999. Noggin is a mesenchymally derived stimulator of hair-follicle induction. *Nat Cell Biol,* 1**,** 158-164.

BOTTCHER-HABERZETH, S., BIEDERMANN, T., PONTIGGIA, L., BRAZIULIS, E., SCHIESTL, C., HENDRIKS, B., EICHHOFF, O. M., WIDMER, D. S., MEULI-SIMMEN, C., MEULI, M. & REICHMANN, E. 2013. Human Eccrine Sweat Gland Cells Turn into Melanin-Uptaking Keratinocytes in Dermo-Epidermal Skin Substitutes. *J Invest Dermatol,* 133**,** 316-324.

BOVELL, D. L., CORBETT, A. D., HOLMES, S., MACDONALD, A. & HARKER, M. 2007. The absence of apoeccrine glands in the human axilla has disease pathogenetic implications, including axillary hyperhidrosis. *British Journal of Dermatology,* 156**,** 1278-1286.

BOVELL, D. L., MACDONALD, A., MEYER, B. A., CORBETT, A. D., MACLAREN, W. M., HOLMES, S. L. & HARKER, M. 2011. The secretory clear cell of the eccrine sweat gland as the probable source of excess sweat production in hyperhidrosis. *Experimental Dermatology,* 20**,** 1017-1020.

BRAKE, D. J. & BATES, G. P. 2003. Fluid losses and hydration status of industrial workers under thermal stress working extended shifts. *Occupational and environmental medicine,* 60**,** 90-96.

BRAND, T. M., IIDA, M., LI, C. & WHEELER, D. L. 2011. The Nuclear Epidermal Growth Factor Receptor Signaling Network and its Role in Cancer. *Discovery Medicine,* 12**,** 419-432.

BRAUN, K. M. & PROWSE, D. M. 2006. Distinct epidermal stem cell compartments are maintained by independent niche microenvironments. *Stem Cell Rev,* 2**,** 221-31.

BRAYMAN, M., THATHIAH, A. & CARSON, D. D. 2004. MUC1: a multifunctional cell surface component of reproductive tissue epithelia. *Reprod Biol Endocrinol,* 2**,** 4.

BREULS, R. G. M., JIYA, T. U. & SMIT, T. H. 2008. Scaffold Stiffness Influences Cell Behavior: Opportunities for Skeletal Tissue Engineering. *The Open Orthopaedics Journal,* 2**,** 103-109.

BROHEM, C. A., DA SILVA CARDEAL, L. B., TIAGO, M., SOENGAS, M. S., DE MORAES BARROS, S. B. & MARIA-ENGLER, S. S. 2011. Artificial skin in perspective: concepts and applications. *Pigment Cell & Melanoma Research,* 24**,** 35-50.

BROWN, J. H. 1989. *The muscarinic receptors,* Clifton, N.J., Humana.

BULLARD, K. M., LONGAKER, M. T. & LORENZ, H. P. 2003. Fetal wound healing: current biology. *World J Surg,* 27**,** 54-61.

BUONO, M. J., GONZALEZ, G., GUEST, S., HARE, A., NUMAN, T., TABOR, B. & WHITE, A. 2010. The role of in vivo β-adrenergic stimulation on sweat production during exercise. *Autonomic Neuroscience,* 155**,** 91-93.

BUONO, M. J., TABOR, B. & WHITE, A. 2011. Localized beta-adrenergic receptor blockade does not affect sweating during exercise. *Am J Physiol Regul Integr Comp Physiol,* 300**,** R1148-51.

BURNS, T., BREATHNACH, S., COX, N. & GRIFFITHS, C. 2010. *Rook's Textbook of Dermatology,* London, Wiley-Blackwell.

CAI, S., PAN, Y., HAN, B., SUN, T. Z., SHENG, Z. Y. & FU, X. B. 2011. Transplantation of human bone marrow-derived mesenchymal stem cells transfected with ectodysplasin for regeneration of sweat glands. *Chin Med J (Engl),* 124**,** 2260-8.

CARLSON, B. M. 2009. *Human embryology and developmental biology,* Edinburgh, Mosby.

CASANOVA ML, B. A., JORCANO JL. 2006. *Simple epithelial keratins: expression, function and disease*, Springer, US.

CAULIN, C., SALVESEN, G. S. & OSHIMA, R. G. 1997. Caspase cleavage of keratin 18 and reorganization of intermediate filaments during epithelial cell apoptosis. *J Cell Biol,* 138**,** 1379-94.

CHAN, B. P. & LEONG, K. W. 2008. Scaffolding in tissue engineering: general approaches and tissue-specific considerations. *European Spine Journal,* 17**,** 467-479.

CHENGWIDDEN, R., CARTER, N. & EDWARDS, Y. 2000. *The Carbonic Anhydrases: New Horizons*, Springer Science.

CHIANG, C., SWAN, R. Z., GRACHTCHOUK, M., BOLINGER, M., LITINGTUNG, Y., ROBERTSON, E. K., COOPER, M. K., GAFFIELD, W., WESTPHAL, H., BEACHY, P. A. & DLUGOSZ, A. A. 1999. Essential role for Sonic hedgehog during hair follicle morphogenesis. *Dev Biol,* 205**,** 1-9.

CHIONI, A. M. & GROSE, R. 2008. Organotypic modelling as a means of investigating epithelial-stromal interactions during tumourigenesis. *Fibrogenesis Tissue Repair,* 1**,** 8.

CHO, G., BRAGIEL, A. M., WANG, D., PIECZONKA, T. D., SKOWRONSKI, M. T., SHONO, M., NIELSEN, S. & ISHIKAWA, Y. 2015. Activation of muscarinic receptors in rat parotid acinar cells induces AQP5 trafficking to nuclei and apical plasma membrane.

CHUONG, C. M., PATEL, N., LIN, J., JUNG, H. S. & WIDELITZ, R. B. 2000. Sonic hedgehog signaling pathway in vertebrate epithelial appendage morphogenesis: perspectives in development and evolution. *Cellular and Molecular Life Sciences CMLS,* 57**,** 1672-1681.

CLAPHAM, D. E. 2007. Calcium signaling. *Cell,* 131**,** 1047-58.

CLAUDINOT, S., NICOLAS, M., OSHIMA, H., ROCHAT, A. & BARRANDON, Y. 2005. Long-term renewal of hair follicles from clonogenic multipotent stem cells. *Proc Natl Acad Sci U S A,* 102**,** 14677-82.

CLUZEAU, C., HADJ-RABIA, S., JAMBOU, M., MANSOUR, S., GUIGUE, P., MASMOUDI, S., BAL, E., CHASSAING, N., VINCENT, M. C., VIOT, G., CLAUSS, F., MANIERE, M. C., TOUPENAY, S., LE MERRER, M., LYONNET, S., CORMIER-DAIRE, V., AMIEL, J., FAIVRE, L., DE PROST, Y., MUNNICH, A., BONNEFONT, J. P., BODEMER, C. & SMAHI, A. 2011. Only four genes (EDA1, EDAR, EDARADD, and WNT10A) account for 90% of hypohidrotic/anhidrotic ectodermal dysplasia cases. *Hum Mutat,* 32**,** 70-2.

COLOMBO, E. S., MENICUCCI, G., MCGUIRE, P. G. & DAS, A. 2007. Hepatocyte growth factor/scatter factor promotes retinal angiogenesis through increased urokinase expression. *Invest Ophthalmol Vis Sci,* 48**,** 1793-800.

CONSTANTINE, V. S. & MOWRY, R. W. 1966. Histochemical Demonstration of Sialomucin in Human Eccrine Sweat Glands1. *The Journal of Investigative Dermatology,* 46**,** 536-541.

COOPER, M. L., HANSBROUGH, J. F., SPIELVOGEL, R. L., COHEN, R., BARTEL, R. L. & NAUGHTON, G. 1991. In vivo optimization of a living dermal substitute employing cultured human fibroblasts on a biodegradable polyglycolic acid or polyglactin mesh. *Biomaterials,* 12**,** 243-8.

COTSARELIS, G., SUN, T. T. & LAVKER, R. M. 1990. Label-retaining cells reside in the bulge area of pilosebaceous unit: implications for follicular stem cells, hair cycle, and skin carcinogenesis. *Cell,* 61**,** 1329-37.

COULSON, I. H. 2010. Disorders of Sweat Glands. *Rook's Textbook of Dermatology*. Wiley-Blackwell.

CRAPO, P. M., GILBERT, T. W. & BADYLAK, S. F. 2011. An overview of tissue and whole organ decellularization processes. *Biomaterials,* 32**,** 3233-43.

CUI, C.-Y., CHILDRESS, V., PIAO, Y., MICHEL, M., JOHNSON, A. A., KUNISADA, M., KO, M. S. H., KAESTNER, K. H., MARMORSTEIN, A. D. & SCHLESSINGER, D. 2012. Forkhead transcription factor FoxA1 regulates sweat secretion through Bestrophin 2 anion channel and Na-K-Cl cotransporter 1. *Proceedings of the National Academy of Sciences,* 109**,** 1199-1203.

CUI, C.-Y., KUNISADA, M., ESIBIZIONE, D., DOUGLASS, E. G. & SCHLESSINGER, D. 2008. Analysis of the Temporal Requirement for Eda in Hair and Sweat Gland Development. *J Invest Dermatol,* 129**,** 984-993.

CUI, C. Y. & SCHLESSINGER, D. 2006. EDA signaling and skin appendage development. *Cell Cycle,* 5**,** 2477-83.

CUI, C. Y. & SCHLESSINGER, D. 2015. Eccrine sweat gland development and sweat secretion. *Exp Dermatol,* 24**,** 644-50.

CUI, C. Y., YIN, M., SIMA, J., CHILDRESS, V., MICHEL, M., PIAO, Y. & SCHLESSINGER, D. 2014. Involvement of Wnt, Eda and Shh at defined stages of sweat gland development. *Development,* 141**,** 3752-60.

CUNHA, G. 2010. Urogenital development: a four-part story of mesenchymal-epithelial interactions. *Differentiation,* 80**,** 79-80.

CVEKL, A. & PIATIGORSKY, J. 1996. Lens development and crystallin gene expression: many roles for Pax-6. *Bioessays,* 18**,** 621-30.

DAMIANO, R. & CICIONE, A. 2011. The role of sodium hyaluronate and sodium chondroitin sulphate in the management of bladder disease. *Ther Adv Urol,* 3**,** 223-32.

DANN, E. J. & BERKMAN, N. 1992. Chronic idiopathic anhydrosis--a rare cause of heat stroke. *Postgraduate Medical Journal,* 68**,** 750-752.

DARBY, I. A., LAVERDET, B., BONTE, F. & DESMOULIERE, A. 2014. Fibroblasts and myofibroblasts in wound healing. *Clin Cosmet Investig Dermatol,* 7**,** 301-11.

DAVIS, P. K., HO, A. & DOWDY, S. F. 2001. Biological methods for cell-cycle synchronization of mammalian cells. *Biotechniques,* 30**,** 1322-6, 1328, 1330-1.

DE VIRAGH, P. A., SZEIMIES, R. M. & ECKERT, F. 1997. Apocrine cystadenoma, apocrine hidrocystoma, and eccrine hidrocystoma: three distinct tumors defined by expression of keratins and human milk fat globulin 1. *J Cutan Pathol,* 24**,** 249-55.

DEAK, A. T., BLASS, S., KHAN, M. J., GROSCHNER, L. N., WALDECK-WEIERMAIR, M., HALLSTRÖM, S., GRAIER, W. F. & MALLI, R. 2014. Inositol-1,4,5-trisphosphate (IP3)-mediated STIM1 oligomerization requires intact mitochondrial Ca2+ uptake. *Journal of Cell Science*.

DHOUAILLY, D. 1975. Formation of cutaneous appendages in dermo-epidermal recombinations between reptiles, birds and mammals. *Wilhelm Roux's archives of developmental biology,* 177**,** 323-340.

DHOUAILLY, D. 1977. Regional specification of cutaneous appendages in mammals. *Wilhelm Roux's archives of developmental biology,* 181**,** 3-10.

DHOUAILLY, D., HARDY, M. H. & SENGEL, P. 1980. Formation of feathers on chick foot scales: a stage-dependent morphogenetic response to retinoic acid. *J Embryol Exp Morphol,* 58**,** 63-78.

DOFT, M. A., HARDY, K. L. & ASCHERMAN, J. A. 2012. Treatment of Hyperhidrosis With Botulinum Toxin. *Aesthetic Surgery Journal,* 32**,** 238-244.

DU, W., STIBER, J. A., ROSENBERG, P. B., MEISSNER, G. & EU, J. P. 2005. Ryanodine receptors in muscarinic receptor-mediated bronchoconstriction. *J Biol Chem,* 280**,** 26287-94.

EGLES, C., GARLICK, J. A. & SHAMIS, Y. 2010. Three-dimensional human tissue models of wounded skin. *Methods Mol Biol,* 585**,** 345-59.

EIRAKU, M., TAKATA, N., ISHIBASHI, H., KAWADA, M., SAKAKURA, E., OKUDA, S., SEKIGUCHI, K., ADACHI, T. & SASAI, Y. 2011. Self-organizing optic-cup morphogenesis in three-dimensional culture. *Nature,* 472**,** 51-6.

EL-GHALBZOURI, A., GIBBS, S., LAMME, E., VAN BLITTERSWIJK, C. A. & PONEC, M. 2002. Effect of fibroblasts on epidermal regeneration. *Br J Dermatol,* 147**,** 230-43.

FARAGE, M., MILLER, K. & MAIBACH, H. 2010. Degenerative Changes in Aging Skin. *In:* FARAGE, M., MILLER, K. & MAIBACH, H. (eds.) *Textbook of Aging Skin.* Springer Berlin Heidelberg.

FEINBERG, R. & BEEBE, D. 1983. Hyaluronate in vasculogenesis. *Science,* 220**,** 1177-1179.

FERRARI, S., BATTINI, R., KACZMAREK, L., RITTLING, S., CALABRETTA, B., DE RIEL, J. K., PHILIPONIS, V., WEI, J. F. & BASERGA, R. 1986. Coding sequence and growth regulation of the human vimentin gene. *Mol Cell Biol,* 6**,** 3614-20.

FERRARIS, C., CHEVALIER, G., FAVIER, B., JAHODA, C. A. & DHOUAILLY, D. 2000. Adult corneal epithelium basal cells possess the capacity to activate epidermal, pilosebaceous and sweat gland genetic programs in response to embryonic dermal stimuli. *Development,* 127**,** 5487-95.

FESKE, S. & PRAKRIYA, M. 2013. Conformational dynamics of STIM1 activation. *Nat Struct Mol Biol,* 20**,** 918-919.

FILL, M. & COPELLO, J. A. 2002. Ryanodine receptor calcium release channels. *Physiol Rev,* 82**,** 893-922.

FISHER, K. E., SACHARIDOU, A., STRATMAN, A. N., MAYO, A. M., FISHER, S. B., MAHAN, R. D., DAVIS, M. J. & DAVIS, G. E. 2009. MT1-MMP- and Cdc42-dependent signaling co-regulate cell invasion and tunnel formation in 3D collagen matrices. *Journal of Cell Science,* 122**,** 4558-4569.

FREINKEL, R. K. & WOODLEY, D. T. 2001. *Biology of the skin*, Parthenon publishing group.

FREUND, A., LABERGE, R. M., DEMARIA, M. & CAMPISI, J. 2012. Lamin B1 loss is a senescence-associated biomarker. *Mol Biol Cell,* 23**,** 2066-75.

FROJDMAN, K., PELLINIEMI, L. J., LENDAHL, U., VIRTANEN, I. & ERIKSSON, J. E. 1997. The intermediate filament protein nestin occurs transiently in differentiating testis of rat and mouse. *Differentiation,* 61**,** 243-9.

FUCHS, E. 1990. Epidermal differentiation: the bare essentials.

FUCHS, E. 2007. Scratching the surface of skin development. *Nature,* 445**,** 834-842.

FUCHS, E. 2008. Skin stem cells: rising to the surface. *J Cell Biol,* 180**,** 273-84.

FUCHS, E. & RAGHAVAN, S. 2002. Getting under the skin of epidermal morphogenesis. *Nat Rev Genet,* 3**,** 199-209.

GANGATIRKAR, P., PAQUET-FIFIELD, S., LI, A., ROSSI, R. & KAUR, P. 2007. Establishment of 3D organotypic cultures using human neonatal epidermal cells. *Nat. Protocols,* 2**,** 178-186.

GAWKRODGER, D. J. 2002. *Dermatology : An Illustrated Colour Text*, Churchill Livingstone.

GHOSH, S., GHOSH, E. & DAYAL, S. 2014. Autosomal recessive anhidrotic ectodermal dysplasia: A rare entity.

GILBERT, S. F. 2003. *Developmental biology,* Sunderland, Mass., Sinauer Associates.

GINIS, I., LUO, Y., MIURA, T., THIES, S., BRANDENBERGER, R., GERECHT-NIR, S., AMIT, M., HOKE, A., CARPENTER, M. K., ITSKOVITZ-ELDOR, J. & RAO, M. S. 2004. Differences between human and mouse embryonic stem cells. *Developmental Biology,* 269**,** 360-380.

GJOREVSKI, N., RANGA, A. & LUTOLF, M. P. 2014. Bioengineering approaches to guide stem cell-based organogenesis. *Development,* 141**,** 1794-804.

GLASS, C., CULLEN, J., ROZTOCIL, E., DOAN, C., AUGUSTIN, G., ILLIG, K., SINGH, M. & GILLESPIE, D. 2010. Neonatal and Adult Dermal Fibroblasts Show Differences in Transforming Growth Factor (TGF-β) Secretion and TGF-β Type II Receptor Expression at Baseline and Under Constant Stretch Conditions. *Journal of Vascular Surgery,* 51**,** 795-796.

GOODISON, S., URQUIDI, V. & TARIN, D. 1999. CD44 cell adhesion molecules. *Molecular Pathology,* 52**,** 189-196.

GOSIEWSKA, A., YI, C. F., BROWN, L. J., CULLEN, B., SILCOCK, D. & GEESIN, J. C. 2001. Differential expression and regulation of extracellular matrix-associated genes in fetal and neonatal fibroblasts. *Wound Repair Regen,* 9**,** 213-22.

GRANT, M. P., LANDIS, S. C. & SIEGEL, R. E. 1991. The molecular and pharmacological properties of muscarinic cholinergic receptors expressed by rat sweat glands are unaltered by denervation. *J Neurosci,* 11**,** 3763-71.

GRINNELL, F. 2008. Fibroblast mechanics in three-dimensional collagen matrices. *J Bodyw Mov Ther,* 12**,** 191-3.

GROEBER, F., HOLEITER, M., HAMPEL, M., HINDERER, S. & SCHENKE-LAYLAND, K. 2011. Skin tissue engineering -- In vivo and in vitro applications. *Advanced Drug Delivery Reviews,* 63**,** 352-366.

GUNTHERT, U., HOFMANN, M., RUDY, W., REBER, S., ZOLLER, M., HAUSSMANN, I., MATZKU, S., WENZEL, A., PONTA, H. & HERRLICH, P. 1991. A new variant of glycoprotein CD44 confers metastatic potential to rat carcinoma cells. *Cell,* 65**,** 13-24.

HAKAMATA, Y., NAKAI, J., TAKESHIMA, H. & IMOTO, K. 1992. Primary structure and distribution of a novel ryanodine receptor/calcium release channel from rabbit brain. *FEBS Letters,* 312**,** 229-235.

HAMADA, T., MATSUKITA, S., GOTO, M., KITAJIMA, S., BATRA, S. K., IRIMURA, T., SUEYOSHI, K., SUGIHARA, K. & YONEZAWA, S. 2004. Mucin expression in pleomorphic adenoma of salivary gland: a potential role for MUC1 as a marker to predict recurrence. *J Clin Pathol,* 57**,** 813-21.

HARKER, M. 2013. Psychological sweating: a systematic review focused on aetiology and cutaneous response. *Skin Pharmacol Physiol,* 26**,** 92-100.

HAWLEY-NELSON, P., STANLEY, J. R., SCHMIDT, J., GULLINO, M. & YUSPA, S. H. 1982. The tumor promoter, 12-O-tetradecanoylphorbol-13-acetate accelerates keratinocyte differentiation and stimulates growth of an unidentified cell type in cultured human epidermis. *Exp Cell Res,* 137**,** 155-67.

HEADINGTON, J. T. 1986. The dermal dendrocyte. *Adv Dermatol,* 1**,** 159-71.
HEADON, D. J. 2009. Ectodysplasin signaling in cutaneous appendage development: dose, duration, and diversity. *J Invest Dermatol,* 129**,** 817-9.
HEADON, D. J., EMMAL, S. A., FERGUSON, B. M., TUCKER, A. S., JUSTICE, M. J., SHARPE, P. T., ZONANA, J. & OVERBEEK, P. A. 2001. Gene defect in ectodermal dysplasia implicates a death domain adapter in development. *Nature,* 414**,** 913-6.
HELDIN, C.-H., MIYAZONO, K. & TEN DIJKE, P. 1997. TGF-[beta] signalling from cell membrane to nucleus through SMAD proteins. *Nature,* 390**,** 465-471.
HENKE, N., ALBRECHT, P., BOUCHACHIA, I., RYAZANTSEVA, M., KNOLL, K., LEWERENZ, J., KAZNACHEYEVA, E., MAHER, P. & METHNER, A. 2013. The plasma membrane channel ORAI1 mediates detrimental calcium influx caused by endogenous oxidative stress. *Cell Death & Disease,* 4**,** e470.
HILGEMANN, D. W., FENG, S. & NASUHOGLU, C. 2001. The Complex and Intriguing Lives of PIP2 with Ion Channels and Transporters. *Sci. STKE,* 2001**,** re19-.
HOANG, M. P., KEADY, M. & MAHALINGAM, M. 2009. Stem cell markers (cytokeratin 15, CD34 and nestin) in primary scarring and nonscarring alopecia. *British Journal of Dermatology,* 160**,** 609-615.
HUANG, S., XU, Y., WU, C., SHA, D. & FU, X. 2010. In vitro constitution and in vivo implantation of engineered skin constructs with sweat glands. *Biomaterials,* 31**,** 5520-5525.
HUGHES, C. S., POSTOVIT, L. M. & LAJOIE, G. A. 2010. Matrigel: A complex protein mixture required for optimal growth of cell culture. *PROTEOMICS,* 10**,** 1886-1890.
HUMPHREY, R. K., BUCAY, N., BEATTIE, G. M., LOPEZ, A., MESSAM, C. A., CIRULLI, V. & HAYEK, A. 2003. Characterization and isolation of promoter-defined nestin-positive cells from the human fetal pancreas. *Diabetes,* 52**,** 2519-25.
HYNES, N. E. & WATSON, C. J. 2010. Mammary Gland Growth Factors: Roles in Normal Development and in Cancer. *Cold Spring Harbor Perspectives in Biology,* 2.
IOZZO, R. V. 2005. Basement membrane proteoglycans: from cellar to ceiling. *Nat Rev Mol Cell Biol,* 6**,** 646-56.
ISHIKAWA, Y. & ISHIDA, H. 2000. Aquaporin Water Channel in Salivary Glands. *The Japanese Journal of Pharmacology,* 83**,** 95-101.
ISHIWATA, T., KUDO, M., ONDA, M., FUJII, T., TEDUKA, K., SUZUKI, T., KORC, M. & NAITO, Z. 2006. Defined localization of nestin-expressing cells in L-arginine-induced acute pancreatitis. *Pancreas,* 32**,** 360-8.
ITO, M., LIU, Y., YANG, Z., NGUYEN, J., LIANG, F., MORRIS, R. J. & COTSARELIS, G. 2005. Stem cells in the hair follicle bulge contribute to wound repair but not to homeostasis of the epidermis. *Nat Med,* 11**,** 1351-1354.
JASKOLL, T., LEO, T., WITCHER, D., ORMESTAD, M., ASTORGA, J., BRINGAS, P., JR., CARLSSON, P. & MELNICK, M. 2004. Sonic hedgehog signaling plays an essential role during embryonic salivary gland epithelial branching morphogenesis. *Developmental dynamics : an*

official publication of the American Association of Anatomists, 229**,** 722-32.

JONES, P. H. & WATT, F. M. 1993. Separation of human epidermal stem cells from transit amplifying cells on the basis of differences in integrin function and expression. *Cell,* 73**,** 713-724.

JORIS, L., KROUSE, M. E., HAGIWARA, G., BELL, C. L. & WINE, J. J. 1989. Patch-clamp study of cultured human sweat duct cells: amiloride-blockable Na+ channel. *Pflugers Arch,* 414**,** 369-72.

JUNG, S., KIM, H. W., LEE, J. H., KANG, S. S., RHU, H. H., JEONG, Y. I., YANG, S. Y., CHUNG, H. Y., BAE, C. S., CHOI, C., SHIN, B. A., KIM, K. K. & AHN, K. Y. 2002. Brain tumor invasion model system using organotypic brain-slice culture as an alternative to in vivo model. *J Cancer Res Clin Oncol,* 128**,** 469-76.

KAJAHN, J., GORJUP, E., TIEDE, S., VON BRIESEN, H., PAUS, R., KRUSE, C. & DANNER, S. 2008. Skin-derived human adult stem cells surprisingly share many features with human pancreatic stem cells. *European Journal of Cell Biology,* 87**,** 39-46.

KALLURI, R. & ZEISBERG, M. 2006. Fibroblasts in cancer. *Nat Rev Cancer,* 6**,** 392-401.

KARHUMAA, P., KAUNISTO, K., PARKKILA, S., WAHEED, A., PASTOREKOVÁ, S., PASTOREK, J., SLY, W. S. & RAJANIEMI, H. 2001. Expression of the transmembrane carbonic anhydrases, CA IX and CA XII, in the human male excurrent ducts. *Molecular Human Reproduction,* 7**,** 611-616.

KEALEY, T. 1983. The metabolism and hormonal responses of human eccrine sweat glands isolated by collagenase digestion.

KERE, J., SRIVASTAVA, A. K., MONTONEN, O., ZONANA, J., THOMAS, N., FERGUSON, B., MUNOZ, F., MORGAN, D., CLARKE, A., BAYBAYAN, P., CHEN, E. Y., EZER, S., SAARIALHO-KERE, U., DE LA CHAPELLE, A. & SCHLESSINGER, D. 1996. X-linked anhidrotic (hypohidrotic) ectodermal dysplasia is caused by mutation in a novel transmembrane protein. *Nature genetics,* 13**,** 409-16.

KHAVARI, P. A. 2006. Modelling cancer in human skin tissue. *Nat Rev Cancer,* 6**,** 270-80.

KIM DO, Y., CHO, S. B., CHUNG, K. Y. & KIM, Y. C. 2006. Clear cell basal cell carcinoma with sialomucin deposition. *Yonsei Med J,* 47**,** 870-2.

KOBIELAK, K., KOBIELAK, A., LIMON, J. & TRZECIAK, W. H. 1998. Mutation in the regulatory region of the EDA gene coincides with the symptoms of anhidrotic ectodermal dysplasia. *Acta Biochim Pol,* 45**,** 245-50.

KORPELAINEN, J. T., SOTANIEMI, K. A. & MYLLYLA, V. V. 1993. Asymmetric sweating in stroke: a prospective quantitative study of patients with hemispheral brain infarction. *Neurology,* 43**,** 1211-4.

KRAUSE, S., MAFFINI, M. V., SOTO, A. M. & SONNENSCHEIN, C. 2008. A novel 3D in vitro culture model to study stromal-epithelial interactions in the mammary gland. *Tissue Eng Part C Methods,* 14**,** 261-71.

KRUSE, C., BODÓ, E., PETSCHNIK, A. E., DANNER, S., TIEDE, S. & PAUS, R. 2006. Towards the development of a pragmatic technique for isolating and differentiating nestin-positive cells from human scalp skin into

neuronal and glial cell populations: generating neurons from human skin? *Experimental Dermatology,* 15**,** 794-800.

KU, N.-O., ZHOU, X., TOIVOLA, D. M. & OMARY, M. B. 1999. The cytoskeleton of digestive epithelia in health and disease. *American Journal of Physiology - Gastrointestinal and Liver Physiology,* 277**,** G1108-G1137.

KUFE, D. W. 2009. Functional targeting of the MUC1 oncogene in human cancers. *Cancer biology & therapy,* 8**,** 1197-1203.

KUMAR, P., GOSAI, A., MONDAL, A. K., LAL, N. R. & GHARAMI, R. C. 2012. Granulosis rubra nasi: a rare condition treated successfully with topical tacrolimus. *Dermatology Reports,* 4**,** e5.

KURATA, R., FUTAKI, S., NAKANO, I., TANEMURA, A., MUROTA, H., KATAYAMA, I. & SEKIGUCHI, K. 2014. Isolation and Characterization of Sweat Gland Myoepithelial Cells from Human Skin. *Cell Structure and Function,* 39**,** 101-112.

LAJTHA, L. G. 1979. Stem cell concepts. *Differentiation,* 14**,** 23-34.

LANCASTER, M. A. & KNOBLICH, J. A. 2014. Generation of Cerebral Organoids from Human Pluripotent Stem Cells. *Nature protocols,* 9**,** 2329-2340.

LANGBEIN, L., ROGERS, M., PRAETZEL, S., CRIBIER, B., PELTRE, B., GASSLER, N. & SCHWEIZER, J. 2005. Characterization of a novel human type II epithelial keratin K1b, specifically expressed in eccrine sweat glands. *J Invest Dermatol,* 125**,** 428-44.

LANNER, J. T., GEORGIOU, D. K., JOSHI, A. D. & HAMILTON, S. L. 2010. Ryanodine receptors: structure, expression, molecular details, and function in calcium release. *Cold Spring Harb Perspect Biol,* 2**,** a003996.

LAVKER, R. M. & SUN, T. T. 2000. Epidermal stem cells: properties, markers, and location. *Proc Natl Acad Sci U S A,* 97**,** 13473-5.

LEE, C. M. & DESSI, J. 1989. NCL-SG3: a human eccrine sweat gland cell line that retains the capacity for transepithelial ion transport. *Journal of cell science,* 92 (Pt 2)**,** 241-9.

LEE, C. M., JONES, C. J. & KEALEY, T. 1984. Biochemical and ultrastructural studies of human eccrine sweat glands isolated by shearing and maintained for seven days. *Journal of Cell Science,* 72**,** 259-274.

LEI, X., LIU, B., WU, J., LU, Y. & YANG, Y. 2011. Matrigel-Induced Tubular Morphogenesis of Human Eccrine Sweat Gland Epithelial Cells. LID - 10.1002/ar.21459 [doi].

LEI, X., WU J FAU - LIU, B., LIU B FAU - LU, Y. & LU, Y. 2012a. Hepatocyte growth factor promoting the proliferation of human eccrine sweat gland epithelial cells is relative to AKT signal channel and beta-catenin.

LEI, X., WU, J., LIU, B. & LU, Y. 2012b. Hepatocyte growth factor promoting the proliferation of human eccrine sweat gland epithelial cells is relative to AKT signal channel and beta-catenin. *Archives of dermatological research,* 304**,** 23-9.

LEI, X., WU, J., LU, Y. & ZHU, T. 2008. Effects of acetylcholine chloride on intracellular calcium concentration of cultured sweat gland epithelial cells. *Arch Dermatol Res,* 300**,** 335-41.

LEIGH, I. M., LANE, E. B. & WATT, F. M. 1994. *The Keratinocyte Handbook,* Cambridge, Cambridge Universitty Press.

LENDAHL, U., ZIMMERMAN, L. B. & MCKAY, R. D. 1990. CNS stem cells express a new class of intermediate filament protein. *Cell,* 60**,** 585-95.

LEPOCK, J. R. 2003. Cellular effects of hyperthermia: relevance to the minimum dose for thermal damage. *International Journal of Hyperthermia,* 19**,** 252-266.

LEVY, V., LINDON, C., HARFE, B. D. & MORGAN, B. A. 2005. Distinct stem cell populations regenerate the follicle and interfollicular epidermis. *Dev Cell,* 9**,** 855-61.

LEWIS, M. P., LYGOE, K. A., NYSTROM, M. L., ANDERSON, W. P., SPEIGHT, P. M., MARSHALL, J. F. & THOMAS, G. J. 2004. Tumour-derived TGF-beta1 modulates myofibroblast differentiation and promotes HGF/SF-dependent invasion of squamous carcinoma cells. *Br J Cancer,* 90**,** 822-32.

LEWIS, R. S. 2011. Store-operated calcium channels: new perspectives on mechanism and function. LID - 10.1101/cshperspect.a003970 [doi] LID - a003970 [pii].

LI, A. G., KOSTER, M. I. & WANG, X.-J. 2003. Roles of TGFβ signaling in epidermal/appendage development. *Cytokine & Growth Factor Reviews,* 14**,** 99-111.

LI, H., CHEN, L., ZENG, S., LI, X., ZHANG, X., LIN, C., ZHANG, M., XIE, S., HE, Y., SHU, S., YANG, L., TANG, S. & FU, X. 2015. Matrigel basement membrane matrix induces eccrine sweat gland cells to reconstitute sweat gland-like structures in nude mice. *Experimental Cell Research,* 332**,** 67-77.

LI, H. H., ZHOU, G., FU, X. B. & ZHANG, L. 2009. Antigen expression of human eccrine sweat glands. *J Cutan Pathol,* 36**,** 318-24.

LI, J., FU, X., SUN, X., SUN, T. & SHENG, Z. 2002. The Interaction between Epidermal Growth Factor and Matrix Metalloproteinases Induces the Development of Sweat Glands in Human Fetal Skin. *Journal of Surgical Research,* 106**,** 258-263.

LIND, G. J. & CAVANAGH, H. D. 1995. Identification and subcellular distribution of muscarinic acetylcholine receptor-related proteins in rabbit corneal and Chinese hamster ovary cells. *Investigative Ophthalmology & Visual Science,* 36**,** 1492-507.

LINDFORS, P. H., VOUTILAINEN, M. & MIKKOLA, M. L. 2013. Ectodysplasin/NF-kappaB signaling in embryonic mammary gland development. *J Mammary Gland Biol Neoplasia,* 18**,** 165-9.

LINDSKOG, S. 1997. Structure and mechanism of carbonic anhydrase. *Pharmacology & Therapeutics,* 74**,** 1-20.

LIOU, J., KIM, M. L., DO HEO, W., JONES, J. T., MYERS, J. W., FERRELL JR, J. E. & MEYER, T. 2005. STIM Is a Ca2+ Sensor Essential for Ca2+-Store-Depletion-Triggered Ca2+ Influx. *Current Biology,* 15**,** 1235-1241.

LO, A., MORI, H., MOTT, J. & BISSELL, M. 2012. Constructing Three-Dimensional Models to Study Mammary Gland Branching Morphogenesis and Functional Differentiation. *Journal of Mammary Gland Biology and Neoplasia***,** 1-8.

LOCKE, M., HEYWOOD, M., FAWELL, S. & MACKENZIE, I. C. 2005. Retention of intrinsic stem cell hierarchies in carcinoma-derived cell lines. *Cancer Res,* 65**,** 8944-50.

LOPEZ, J. I., CAMENISCH, T. D., STEVENS, M. V., SANDS, B. J., MCDONALD, J. & SCHROEDER, J. A. 2005. CD44 attenuates metastatic invasion during breast cancer progression. *Cancer Res,* 65**,** 6755-63.

LOUDERBOUGH, J. M. V. & SCHROEDER, J. A. 2011. Understanding the Dual Nature of CD44 in Breast Cancer Progression. *Molecular Cancer Research,* 9**,** 1573-1586.

LU, C. & FUCHS, E. 2014. Sweat gland progenitors in development, homeostasis, and wound repair. *Cold Spring Harb Perspect Med,* 4.

LU, C. P., POLAK, L., ROCHA, A. S., PASOLLI, H. A., CHEN, S.-C., SHARMA, N., BLANPAIN, C. & FUCHS, E. 2012. Identification of stem cell populations in sweat glands and ducts reveals roles in homeostasis and wound repair. *Cell,* 150**,** 136-50.

MA, H.-T., PATTERSON, R. L., VAN, D. B., ROSSUM, BIRNBAUMER, L., MIKOSHIBA, K. & GILL, D. L. 2000. Requirement of the Inositol Trisphosphate Receptor for Activation of Store-Operated Ca2+ Channels. *Science,* 287**,** 1647-1651.

MA, L., HUANG, Y.-G., DENG, Y.-C., TIAN, J.-Y., RAO, Z.-R., CHE, H.-L., ZHANG, H.-F. & ZHAO, G. 2007. Topiramate reduced sweat secretion and aquaporin-5 expression in sweat glands of mice. *Life Sciences,* 80**,** 2461-2468.

MACK, G. W. S. L. M. N. E. R. 1986. Influence of beta-adrenergic blockade on the control of sweating in humans. *Journal of Applied Physiology,* 61**,** 1701-1705.

MARTINEZ, R., JONES, D., HODGE, D. & BUONO, M. J. 2012. Blocking the beta-adrenergic system does not affect sweat gland function during heat acclimation. *Autonomic Neuroscience,* 169**,** 113-115.

MASSAOUS, J. & HATA, A. 1997. TGF-beta signalling through the Smad pathway. *Trends Cell Biol,* 7**,** 187-92.

MATSUDA, Y., HAGIO, M. & ISHIWATA, T. 2013. Nestin: a novel angiogenesis marker and possible target for tumor angiogenesis. *World J Gastroenterol,* 19**,** 42-8.

MCCARL, C. A., PICARD, C., KHALIL, S., KAWASAKI, T., ROTHER, J., PAPOLOS, A., KUTOK, J., HIVROZ, C., LEDEIST, F., PLOGMANN, K., EHL, S., NOTHEIS, G., ALBERT, M. H., BELOHRADSKY, B. H., KIRSCHNER, J., RAO, A., FISCHER, A. & FESKE, S. 2009. ORAI1 deficiency and lack of store-operated Ca2+ entry cause immunodeficiency, myopathy, and ectodermal dysplasia. *J Allergy Clin Immunol,* 124**,** 1311-1318 e7.

MCGRATH, J. A., EADY, R. A. J. & POPE, F. M. 2004. Anatomy and Organization of Human Skin. *Rook's Textbook of Dermatology.* Blackwell Publishing, Inc.

MCGRATH, J. A., EADY, R. A. J. & POPE, F. M. 2008. Anatomy and Organization of Human Skin. *Rook's Textbook of Dermatology.* Blackwell Publishing, Inc.

MERRILL, A. E., EAMES, B. F., WESTON, S. J., HEATH, T. & SCHNEIDER, R. A. 2008. Mesenchyme-dependent BMP signaling directs the timing of mandibular osteogenesis. *Development (Cambridge, England),* 135**,** 1223-1234.

MIKKOLA, M. L. 2007. Genetic basis of skin appendage development. *Semin Cell Dev Biol,* 18**,** 225-36.
MIKKOLA, M. L. 2009. Molecular aspects of hypohidrotic ectodermal dysplasia. *American Journal of Medical Genetics Part A,* 149A**,** 2031-2036.
MIKKOLA, M. L. & THESLEFF, I. 2003. Ectodysplasin signaling in development. *Cytokine & Growth Factor Reviews,* 14**,** 211-224.
MIKOSHIBA, K. 2007. IP3 receptor/Ca2+ channel: from discovery to new signaling concepts. *Journal of Neurochemistry,* 102**,** 1426-1446.
MOLL, I. & MOLL, R. 1992. Changes of expression of intermediate filament proteins during ontogenesis of eccrine sweat glands. *J Invest Dermatol,* 98**,** 777-85.
MORGAN, A. J. & JACOB, R. 1994. Ionomycin enhances Ca2+ influx by stimulating store-regulated cation entry and not by a direct action at the plasma membrane. *Biochem J,* 300 (Pt 3)**,** 665-72.
NAGEL, S., ROHR, F., WEBER, C., KIER, J., SIEMERS, F., KRUSE, C., DANNER, S., BRANDENBURGER, M. & MATTHIESSEN, A. E. 2013. Multipotent nestin-positive stem cells reside in the stroma of human eccrine and apocrine sweat glands and can be propagated robustly in vitro. *PLoS One,* 8**,** e78365.
NAJAFZADEH, N., ESMAEILZADE, B. & DASTAN IMCHEH, M. 2015. Hair follicle stem cells: In vitro and in vivo neural differentiation. *World J Stem Cells,* 7**,** 866-72.
NAKAGAWA, H., AKITA, S., FUKUI, M., FUJII, T. & AKINO, K. 2005. Human mesenchymal stem cells successfully improve skin-substitute wound healing. *British Journal of Dermatology,* 153**,** 29-36.
NAKASHIMA, Y., NISHIMURA, S., MAEDA, A., BARSOUMIAN, E. L., HAKAMATA, Y., NAKAI, J., ALLEN, P. D., IMOTO, K. & KITA, T. 1997. Molecular cloning and characterization of a human brain ryanodine receptor 1. *FEBS Letters,* 417**,** 157-162.
NAVSARIA, H. A., MYERS, S. R., LEIGH, I. M. & MCKAY, I. A. 1995. Culturing skin in vitro for wound therapy. *Trends Biotechnol,* 13**,** 91-100.
NEJSUM, L. N., KWON, T.-H., JENSEN, U. B., FUMAGALLI, O., FRØKIAER, J., KRANE, C. M., MENON, A. G., KING, L. S., AGRE, P. C. & NIELSEN, S. 2002. Functional requirement of aquaporin-5 in plasma membranes of sweat glands. *Proceedings of the National Academy of Sciences,* 99**,** 511-516.
NEJSUM, L. N., PRAETORIUS, J. & NIELSEN, S. 2005. NKCC1 and NHE1 are abundantly expressed in the basolateral plasma membrane of secretory coil cells in rat, mouse, and human sweat glands. *Am J Physiol Cell Physiol,* 289**,** C333-40.
NG, Y. Z., POURREYRON, C., SALAS-ALANIS, J. C., DAYAL, J. H., CEPEDA-VALDES, R., YAN, W., WRIGHT, S., CHEN, M., FINE, J. D., HOGG, F. J., MCGRATH, J. A., MURRELL, D. F., LEIGH, I. M., LANE, E. B. & SOUTH, A. P. 2012. Fibroblast-derived dermal matrix drives development of aggressive cutaneous squamous cell carcinoma in patients with recessive dystrophic epidermolysis bullosa. *Cancer Res,* 72**,** 3522-34.
O'TOOLE, E. A. 2001. Extracellular matrix and keratinocyte migration. *Clin Exp Dermatol,* 26**,** 525-30.

OGAWA, T. 1975. Thermal influence on palmar sweating and mental influence on generalized sweating in man. *Jpn J Physiol,* 25**,** 525-36.

OGINO, H. & YASUDA, K. 1998. Induction of Lens Differentiation by Activation of a bZIP Transcription Factor, L-Maf. *Science,* 280**,** 115-118.

OH, J. W., HSI, T. C., GUERRERO-JUAREZ, C. F., RAMOS, R. & PLIKUS, M. V. 2013. Organotypic skin culture. *J Invest Dermatol,* 133**,** e14.

OHARA, K., MORITA, Y. & OKUDA, N. 1984. Significance of adrenergic transmission in thermal sweating in man. *Journal of Thermal Biology,* 9**,** 127-132.

OHYAMA, M. 2007. Hair follicle bulge: A fascinating reservoir of epithelial stem cells. *Journal of Dermatological Science,* 46**,** 81-89.

OOTTAMASATHIEN, S., WANG, Y., WILLIAMS, K., FRANCO, O. E., WILLS, M. L., THOMAS, J. C., SABA, K., SHARIF-AFSHAR, A.-R., MAKARI, J. H., BHOWMICK, N. A., DEMARCO, R. T., HIPKENS, S., MAGNUSON, M., BROCK III, J. W., HAYWARD, S. W., POPE IV, J. C. & MATUSIK, R. J. 2007. Directed differentiation of embryonic stem cells into bladder tissue. *Developmental Biology,* 304**,** 556-566.

OSHIMA, R. G. 2002. Apoptosis and keratin intermediate filaments. *Cell Death Differ,* 9**,** 486-92.

OWENS, D. M. & WATT, F. M. 2003. Contribution of stem cells and differentiated cells to epidermal tumours. *Nat Rev Cancer,* 3**,** 444-51.

PAPAKONSTANTINOU, E., ROTH, M. & KARAKIULAKIS, G. 2012. Hyaluronic acid: A key molecule in skin aging. *Dermatoendocrinol,* 4**,** 253-8.

PAREKH, A. B. 2008. Store-operated channels: mechanisms and function. *J Physiol,* 586**,** 3033.

PARTANEN, A. M. & THESLEFF, I. 1989. Growth factors and tooth development. *Int J Dev Biol,* 33**,** 165-72.

PENA-DIAZ, J., HEGRE, S. A., ANDERSSEN, E., AAS, P. A., MJELLE, R., GILFILLAN, G. D., LYLE, R., DRABLOS, F., KROKAN, H. E. & SAETROM, P. 2013. Transcription profiling during the cell cycle shows that a subset of Polycomb-targeted genes is upregulated during DNA replication. *Nucleic Acids Res,* 41**,** 2846-56.

PENNEYS, N. S. 1993. CD44 expression in normal and inflamed skin. *J Cutan Pathol,* 20**,** 250-3.

PETSCHNIK, A., KLATTE, J., EVERS, L., KRUSE, C., PAUS, R. & DANNER, S. 2010a. Phenotypic indications that human sweat glands are a rich source of nestin-positive stem cell populations. *Br J Dermatol,* 162**,** 380-3.

PETSCHNIK, A. E., KLATTE, J. E., EVERS, L. H., KRUSE, C., PAUS, R. & DANNER, S. 2010b. Phenotypic indications that human sweat glands are a rich source of nestin-positive stem cell populations. *Br J Dermatol,* 162**,** 380-3.

PLANKO, L., BOHSE, K., HOHFELD, J., BETZ, R. C., HANNEKEN, S., EIGELSHOVEN, S., KRUSE, R., NOTHEN, M. M. & MAGIN, T. M. 2007. Identification of a keratin-associated protein with a putative role in vesicle transport. *Eur J Cell Biol,* 86**,** 827-39.

PLIKUS, M., WANG, W. P., LIU, J., WANG, X., JIANG, T. X. & CHUONG, C. M. 2004. Morpho-regulation of ectodermal organs: integument pathology and phenotypic variations in K14-Noggin engineered mice through

modulation of bone morphogenic protein pathway. *Am J Pathol,* 164**,** 1099-114.

PLISKO, A. & GILCHREST, B. A. 1983. Growth Factor Responsiveness of Cultured Human Fibroblasts Declines with Age. *Journal of Gerontology,* 38**,** 513-518.

PONTA, H., SHERMAN, L. & HERRLICH, P. A. 2003. CD44: From adhesion molecules to signalling regulators. *Nat Rev Mol Cell Biol,* 4**,** 33-45.

PONTIER, S. M. & MULLER, W. J. 2009. Integrins in mammary-stem-cell biology and breast-cancer progression--a role in cancer stem cells? *J Cell Sci,* 122**,** 207-14.

PONTIGGIA, L., BIEDERMANN, T., BOTTCHER-HABERZETH, S., OLIVEIRA, C., BRAZIULIS, E., KLAR, A. S., MEULI-SIMMEN, C., MEULI, M. & REICHMANN, E. 2014. De Novo Epidermal Regeneration Using Human Eccrine Sweat Gland Cells: Higher Competence of Secretory over Absorptive Cells. *J Invest Dermatol,* 134**,** 1735-1742.

PRAKRIYA, M., FESKE, S., GWACK, Y., SRIKANTH, S., RAO, A. & HOGAN, P. G. 2006. Orai1 is an essential pore subunit of the CRAC channel. *Nature,* 443**,** 230-3.

PRIESTLEY, G. C. 1988. Urinary excretion of glycosaminoglycans in psoriasis. *Arch Dermatol Res,* 280**,** 77-82.

PRUNIERAS, M., REGNIER, M. & WOODLEY, D. 1983. Methods for Cultivation of Keratinocytes with an Air-Liquid Interface. *J Investig Dermatol,* 81**,** 28s-33s.

PUTNEY, J. W. 2010. Pharmacology of store-operated calcium channels. *Mol Interv,* 10**,** 209-18.

QUINTON, P. M. 1983. Sweating and its disorders. *Annu Rev Med,* 34**,** 429-52.

QUINTON, P. M. 1990. Cystic fibrosis: a disease in electrolyte transport. *The FASEB Journal,* 4**,** 2709-17.

QUINTON, P. M. 2007. Cystic fibrosis: lessons from the sweat gland. *Physiology (Bethesda),* 22**,** 212-25.

RANG, H. P. & DALE, M. M. 2007. *Rang & Dale's pharmacology,* [Edinburgh], Churchill Livingstone.

REDDI, A. H. 1998. Role of morphogenetic proteins in skeletal tissue engineering and regeneration. *Nat Biotechnol,* 16**,** 247-52.

REDDY, M. M. & BELL, C. L. 1996. Distinct cellular mechanisms of cholinergic and beta-adrenergic sweat secretion. *Am J Physiol,* 271**,** C486-94.

REIMER, R., HELMBOLD, H., SZALAY, B., HAGEL, C., HOHENBERG, H., DEPPERT, W. & BOHN, W. 2009. Nestin modulates glucocorticoid receptor function by cytoplasmic anchoring. *PLoS One,* 4**,** e6084.

REISFELD, R. 2007. The importance of classification in sympathetic surgery and a proposed mechanism for compensatory hyperhidrosis: experience with 464 cases. *Surgical Endoscopy,* 21**,** 1249-1250.

RHEINWALD, J. G. & GREEN, H. 1975. Serial cultivation of strains of human epidermal keratinocytes: the formation of keratinizing colonies from single cells. *Cell,* 6**,** 331-43.

RICHARDSON, G. D., BAZZI, H., FANTAUZZO, K. A., WATERS, J. M., CRAWFORD, H., HYND, P., CHRISTIANO, A. M. & JAHODA, C. A. B. 2009. KGF and EGF signalling block hair follicle induction and promote interfollicular epidermal fate in developing mouse skin. *Development,* 136**,** 2153-2164.

RITTIE, L., SACHS, D. L., ORRINGER, J. S., VOORHEES, J. J. & FISHER, G. J. 2013. Eccrine Sweat Glands are Major Contributors to Reepithelialization of Human Wounds. *Am J Pathol,* 182**,** 163-71.

ROBERTSHAW, D. 1979. Hyperhidrosis and the sympatho-adrenal system. *Med Hypotheses,* 5**,** 317-22.

ROBERTSON, J. & BOVELL, D. 2014. Pharmacological blockers of STIM1 inhibit increases in intracellular calcium in horse sweat gland cells (650.2). *The FASEB Journal,* 28.

ROOMANS, G. M. 1999. 10 - X-ray microanalytical studies of epithelial cells with reference to cystic fibrosis. *In:* INGRAM, P., SHELBURNE, J. D., ROGGLI, V. L. & LEFURGEY, A. (eds.) *Biomedical Applications of Microprobe Analysis.* San Diego: Academic Press.

RYER, H. I., KATZ, S. E. & SERBY, M. 1995. Muscarinic receptors on human eccrine sweat gland in aging and Alzheimer's disease. *Biological Psychiatry,* 37**,** 259-264.

SAGA, K. 2001. Histochemical and Immunohistochemical Markers for Human Eccrine and Apocrine Sweat Glands: An Aid for Histopathologic Differentiation of Sweat Gland Tumors. *J Investig Dermatol Symp Proc,* 6**,** 49-53.

SAGA, K. 2002. Structure and function of human sweat glands studied with histochemistry and cytochemistry. *Prog Histochem Cytochem,* 37**,** 323-86.

SAGA, K. & JIMBOW, K. 2001. Immunohistochemical Localization of Activated EGF Receptor in Human Eccrine and Apocrine Sweat Glands. *Journal of Histochemistry & Cytochemistry,* 49**,** 597-601.

SAGA, K., SATO, F. & SATO, K. 1988. K+ efflux from the monkey eccrine secretory coil during the transient of stimulation with agonists. *The Journal of Physiology,* 405**,** 205-217.

SALBACH, J., RACHNER, T. D., RAUNER, M., HEMPEL, U., ANDEREGG, U., FRANZ, S., SIMON, J. C. & HOFBAUER, L. C. 2011. Regenerative potential of glycosaminoglycans for skin and bone.

SARGUNAM, C., THOMAS, J. & AHMED, N. A. 2013. Granulosis rubra nasi. *Indian Dermatol Online J,* 4**,** 208-9.

SATO, F., OWEN, M., MATTHES, R., SATO, K. & GISOLFI, C. V. 1990. Functional and morphological changes in the eccrine sweat gland with heat acclimation. *J Appl Physiol (1985),* 69**,** 232-6.

SATO, K., KANG, W. H., SAGA, K. & SATO, K. T. 1989. Biology of sweat glands and their disorders. I. Normal sweat gland function. *Journal of the American Academy of Dermatology,* 20**,** 537-563.

SATO, K., OHTSUYAMA, M. & SAMMAN, G. 1991. Eccrine sweat gland disorders. *Journal of the American Academy of Dermatology,* 24**,** 1010-1014.

SATO, K. & SATO, F. 1981a. Pharmacologic responsiveness of isolated single eccrine sweat glands. *American Journal of Physiology - Regulatory, Integrative and Comparative Physiology,* 240**,** R44-R51.

SATO, K. & SATO, F. 1981b. Role of calcium in cholinergic and adrenergic mechanisms of eccrine sweat secretion. *Am J Physiol,* 241**,** C113-20.

SATO, K. & SATO, F. 1983a. Cholinergic potentiation of isoproterenol-induced cAMP level in sweat gland. *Am J Physiol,* 245**,** C189-95.

SATO, K. & SATO, F. 1983b. Individual variations in structure and function of human eccrine sweat gland. *Am J Physiol,* 245**,** R203-8.

SATO, T. & CLEVERS, H. 2013. Growing self-organizing mini-guts from a single intestinal stem cell: mechanism and applications. *Science,* 340**,** 1190-4.

SATO, T., VRIES, R. G., SNIPPERT, H. J., VAN DE WETERING, M., BARKER, N., STANGE, D. E., VAN ES, J. H., ABO, A., KUJALA, P., PETERS, P. J. & CLEVERS, H. 2009. Single Lgr5 stem cells build crypt-villus structures in vitro without a mesenchymal niche. *Nature,* 459**,** 262-5.

SCHIAVONE, A. & BRAMBILLA, A. 1991. Muscarinic M3 receptors mediate secretion from sweat glands in the rat. *Pharmacol Res,* 23**,** 233-9.

SCHLERETH, T. 2009. Hyperhidrosis—Causes and Treatment of Enhanced Sweating. *Dtsch Arztebl International,* 106**,** 32-37.

SELLHEYER, K., NELSON, P. & PATEL, R. M. 2011. Expression of embryonic stem cell markers SOX2 and nestin in dermatofibrosarcoma protuberans and dermatofibroma. *J Cutan Pathol*.

SHAMSUDDIN, A. K. M., REDDY, M. M. & QUINTON, P. M. 2008. Iontophoretic β-adrenergic stimulation of human sweat glands: possible assay for cystic fibrosis transmembrane conductance regulator activity in vivo. *Experimental Physiology,* 93**,** 969-981.

SHERMAN, T. A., RONGALI, S., MATTHEWS, T. A., PFEIFFER, J. & NEHRKE, K. 2012. Identification of a Nuclear Carbonic Anhydrase in Caenorhabditis elegans. *Biochim Biophys Acta,* 1823**,** 808-817.

SHIBASAKI, M., WILSON, T. E. & CRANDALL, C. G. 2006. Neural control and mechanisms of eccrine sweating during heat stress and exercise. *J Appl Physiol,* 100**,** 1692-701.

SHIKIJI, T., MINAMI, M., INOUE, T., HIROSE, K., OURA, H. & ARASE, S. 2003. Keratinocytes can differentiate into eccrine sweat ducts in vitro: involvement of epidermal growth factor and fetal bovine serum. *Journal of Dermatological Science,* 33**,** 141-150.

SHINOHARA, T., AVARBOCK, M. R. & BRINSTER, R. L. 1999. β1- and α6-integrin are surface markers on mouse spermatogonial stem cells. *Proceedings of the National Academy of Sciences,* 96**,** 5504-5509.

SINGH, R. & BANDYOPADHYAY, D. 2007. MUC1: a target molecule for cancer therapy. *Cancer Biol Ther,* 6**,** 481-6.

SMITH, K. L. & DEAN, S. J. 1998. Tissue repair of the epidermis and dermis. *J Hand Ther,* 11**,** 95-104.

SOBOLOFF, J., ROTHBERG, B. S., MADESH, M. & GILL, D. L. 2012. STIM proteins: dynamic calcium signal transducers. *Nat Rev Mol Cell Biol,* 13**,** 549-65.

SONTHALIA, S., SINGAL, A. & SHARMA, R. 2012. Hyperhidrosis, vesicles, and papules over the nose: granulosis rubra nasi. *Indian J Dermatol Venereol Leprol,* 78**,** 97-8.

SORRENTINO, V. 1995. The ryanodine receptor family of intracellular calcium release channels. *Adv Pharmacol,* 33**,** 67-90.

SRIKANTH, S. & GWACK, Y. 2012. Orai1, STIM1, and their associating partners. *The Journal of Physiology,* 590**,** 4169-4177.

SRIVASTAVA, A. K., DURMOWICZ, M. C., HARTUNG, A. J., HUDSON, J., OUZTS, L. V., DONOVAN, D. M., CUI, C.-Y. & SCHLESSINGER, D. 2001. Ectodysplasin-A1 is sufficient to rescue both hair growth and sweat glands in Tabby mice. *Human Molecular Genetics,* 10**,** 2973-2981.

STARK, H. J., BOEHNKE, K., MIRANCEA, N., WILLHAUCK, M. J., PAVESIO, A., FUSENIG, N. E. & BOUKAMP, P. 2006. Epidermal homeostasis in long-term scaffold-enforced skin equivalents. *J Investig Dermatol Symp Proc,* 11**,** 93-105.

STEVEN, A. C. & STEINERT, P. M. 1994. Protein composition of cornified cell envelopes of epidermal keratinocytes. *J Cell Sci,* 107 (Pt 2)**,** 693-700.

STOREY, A., PIM, D., MURRAY, A., OSBORN, K., BANKS, L. & CRAWFORD, L. 1988. Comparison of the in vitro transforming activities of human papillomavirus types. *EMBO J,* 7**,** 1815-20.

SUGAHARA, K. N., MURAI, T., NISHINAKAMURA, H., KAWASHIMA, H., SAYA, H. & MIYASAKA, M. 2003. Hyaluronan oligosaccharides induce CD44 cleavage and promote cell migration in CD44-expressing tumor cells. *J Biol Chem,* 278**,** 32259-65.

SUNABORI, T., TOKUNAGA, A., NAGAI, T., SAWAMOTO, K., OKABE, M., MIYAWAKI, A., MATSUZAKI, Y., MIYATA, T. & OKANO, H. 2008. Cell-cycle-specific nestin expression coordinates with morphological changes in embryonic cortical neural progenitors. *J Cell Sci,* 121**,** 1204-1212.

TADEVOSYAN, A., VANIOTIS, G., ALLEN, B. G., HEBERT, T. E. & NATTEL, S. 2012. G protein-coupled receptor signalling in the cardiac nuclear membrane: evidence and possible roles in physiological and pathophysiological function. *J Physiol,* 590**,** 1313-30.

TAKASATO, M., ER, P. X., BECROFT, M., VANSLAMBROUCK, J. M., STANLEY, E. G., ELEFANTY, A. G. & LITTLE, M. H. 2014. Directing human embryonic stem cell differentiation towards a renal lineage generates a self-organizing kidney. *Nat Cell Biol,* 16**,** 118-126.

TAO, R., HAN, Y., CHAI, J., LI, D. & SUN, T. 2010. Isolation, culture, and verification of human sweat gland epithelial cells. *Cytotechnology*.

TAYLOR, D. K., BUBIER, J. A., SILVA, K. A. & SUNDBERG, J. P. 2012. Development, Structure, and Keratin Expression in C57BL/6J Mouse Eccrine Glands. *Veterinary Pathology,* 49**,** 146-154.

TAYLOR, R., WANG, H., WILKINSON, S., RICHARDS, M., BRITT, K., VAILLANT, F., LINDEMAN, G., VISVADER, J., CUNHA, G., ST JOHN, J. & RISBRIDGER, G. 2009. Lineage enforcement by inductive mesenchyme on adult epithelial stem cells across developmental germ layers. *Stem Cells,* 27**,** 3032-42.

THIEL, M., LIS, A. & PENNER, R. 2013. STIM2 drives Ca2+ oscillations through store-operated Ca2+ entry caused by mild store depletion. *The Journal of Physiology,* 591**,** 1433-1445.

THOMAS, I., BROWN, J., VAFAIE, J. & SCHWARTZ, R. A. 2004. Palmoplantar hyperhidrosis: a therapeutic challenge. *Am Fam Physician,* 69**,** 1117-20.

TIEDE, S., KLOEPPER, J. E., BODO, E., TIWARI, S., KRUSE, C. & PAUS, R. 2007. Hair follicle stem cells: walking the maze. *Eur J Cell Biol,* 86**,** 355-76.

TIEDE, S., KLOEPPER, J. E., ERNST, N., POEGGELER, B., KRUSE, C. & PAUS, R. 2009. Nestin in Human Skin: Exclusive Expression in Intramesenchymal Skin Compartments and Regulation by Leptin. *J Invest Dermatol,* 129**,** 2711-2720.

TODARO, G. J. & GREEN, H. 1963. Quantitative studies of the growth of mouse embryo cells in culture and their development into established lines. *J Cell Biol,* 17**,** 299-313.

TOIVOLA, D. M., ZHOU, Q., ENGLISH, L. S. & OMARY, M. B. 2002. Type II Keratins Are Phosphorylated on a Unique Motif during Stress and Mitosis in Tissues and Cultured Cells. *Molecular Biology of the Cell,* 13**,** 1857-1870.

TORTORA, G. J. & GRABOWSKI, S. R. 2003. *Principles of Anatomy and Physiology*, John Wiley and Sons, Inc.

TSUJIMURA, T., MAKIISHI-SHIMOBAYASHI, C., LUNDKVIST, J., LENDAHL, U., NAKASHO, K., SUGIHARA, A., IWASAKI, T., MANO, M., YAMADA, N., YAMASHITA, K., TOYOSAKA, A. & TERADA, N. 2001. Expression of the intermediate filament nestin in gastrointestinal stromal tumors and interstitial cells of Cajal. *Am J Pathol,* 158**,** 817-23.

TUCKER, A. S., HEADON, D. J., SCHNEIDER, P., FERGUSON, B. M., OVERBEEK, P., TSCHOPP, J. & SHARPE, P. T. 2000. Edar/Eda interactions regulate enamel knot formation in tooth morphogenesis. *Development,* 127**,** 4691-700.

VIALLET, J. P. & DHOUAILLY, D. 1994. Retinoic acid and mouse skin morphogenesis. I. Expression pattern of retinoic acid receptor genes during hair vibrissa follicle, plantar, and nasal gland development. *J Invest Dermatol,* 103**,** 116-21.

VUKICEVIC, S., KLEINMAN, H. K., LUYTEN, F. P., ROBERTS, A. B., ROCHE, N. S. & REDDI, A. H. 1992. Identification of multiple active growth factors in basement membrane matrigel suggests caution in interpretation of cellular activity related to extracellular matrix components. *Experimental Cell Research,* 202**,** 1-8.

WANG, B., LI, L., DU, S., LIU, C., LIN, X., CHEN, Y. & ZHANG, Y. 2010a. Induction of human keratinocytes into enamel-secreting ameloblasts. *Dev Biol,* 344**,** 795-9.

WANG, B. & LI, Y. 2006. Evidence for the direct involvement of {beta}TrCP in Gli3 protein processing. *Proc Natl Acad Sci U S A,* 103**,** 33-8.

WANG, Y. N., YAMAGUCHI, H., HSU, J. M. & HUNG, M. C. 2010b. Nuclear trafficking of the epidermal growth factor receptor family membrane proteins. *Oncogene,* 29**,** 3997-4006.

WATT, F. M. 1998. Epidermal stem cells: markers, patterning and the control of stem cell fate. *Philos Trans R Soc Lond B Biol Sci,* 353**,** 831-7.

WATT, F. M. 2001. Stem cell fate and patterning in mammalian epidermis. *Curr Opin Genet Dev,* 11**,** 410-7.

WATT, F. M. 2002. Role of integrins in regulating epidermal adhesion, growth and differentiation. *Embo J,* 21**,** 3919-26.

WATT, F. M. & HUCK, W. T. 2013. Role of the extracellular matrix in regulating stem cell fate. *Nat Rev Mol Cell Biol,* 14**,** 467-73.

WATT, F. M., LO CELSO, C. & SILVA-VARGAS, V. 2006. Epidermal stem cells: an update. *Curr Opin Genet Dev,* 16**,** 518-24.

WEST, D., HAMPSON, I., ARNOLD, F. & KUMAR, S. 1985. Angiogenesis induced by degradation products of hyaluronic acid. *Science,* 228**,** 1324-1326.

WIDELITZ, R. B. & CHUONG, C. M. 1999. Early events in skin appendage formation: induction of epithelial placodes and condensation of dermal mesenchyme. *J Investig Dermatol Symp Proc,* 4**,** 302-6.

WILKE, K., MARTIN, A., TERSTEGEN, L. & BIEL, S. S. 2007. A short history of sweat gland biology. *International Journal of Cosmetic Science,* 29**,** 169-179.

WILKE, K., WEPF, R., KEIL, F. J., WITTERN, K. P., WENCK, H. & BIEL, S. S. 2006. Are Sweat Glands an Alternate Penetration Pathway? Understanding the Morphological Complexity of the Axillary Sweat Gland Apparatus. *Skin Pharmacology and Physiology,* 19**,** 38-49.

WILSON, S. E., HE, Y. G., WENG, J., ZIESKE, J. D., JESTER, J. V. & SCHULTZ, G. S. 1994. Effect of epidermal growth factor, hepatocyte growth factor, and keratinocyte growth factor, on proliferation, motility and differentiation of human corneal epithelial cells. *Exp Eye Res,* 59**,** 665-78.

WOLFF, K. & FITZPATRICK, T. B. D. I. G. M. 2008. *Fitzpatrick's dermatology in general medicine,* New York ; London, McGraw-Hill.

WOLLINA, U., LANGE, D., TEN DIJKE, P., HELDIN, C. H. & FUNA, K. 1999. Eccrine sweat glands: expression of transforming growth factor-beta and bone morphogenetic protein type I receptors and their intracellular signalling Smad proteins. *Acta Derm Venereol,* 79**,** 183-6.

WOLPERT, L. 2006. *Principles of development,* Oxford, Oxford University Press.

YAMADA, K. M. & CUKIERMAN, E. 2007a. Modeling tissue morphogenesis and cancer in 3D. *Cell,* 130**,** 601-10.

YAMADA, K. M. & CUKIERMAN, E. 2007b. Modeling Tissue Morphogenesis and Cancer in 3D. *Cell,* 130**,** 601-610.

YAMAGUCHI, Y., HEARING, V., ITAMI, S., YOSHIKAWA, K. & KATAYAMA, I. 2005. Mesenchymal-epithelial interactions in the skin: aiming for site-specific tissue regeneration. *J Dermatol Sci,* 40**,** 1-9.

YAMAMOTO, H., MASTERS, J. R., DASGUPTA, P., CHANDRA, A., POPERT, R., FREEMAN, A. & AHMED, A. 2012. CD49f Is an Efficient Marker of Monolayer- and Spheroid Colony-Forming Cells of the Benign and Malignant Human Prostate. *PLoS One,* 7**,** e46979.

YOSHIDA, S. & PLANT, S. 1992. Mechanism of release of Ca2+ from intracellular stores in response to ionomycin in oocytes of the frog Xenopus laevis. *The Journal of Physiology,* 458**,** 307-18.

YOSHII, N., KITAJIMA, S., YONEZAWA, S., MATSUKITA, S., SETOYAMA, M. & KANZAKI, T. 2002. Expression of mucin core proteins in extramammary Paget's disease. *Pathology International,* 52**,** 390-399.

YU, K. R., YANG, S. R., JUNG, J. W., KIM, H., KO, K., HAN, D. W., PARK, S. B., CHOI, S. W., KANG, S. K., SCHOLER, H. & KANG, K. S. 2012. CD49f enhances multipotency and maintains stemness through the direct regulation of OCT4 and SOX2. *Stem Cells,* 30**,** 876-87.

YU, Q. & TOOLE, B. P. 1997. Common pattern of CD44 isoforms is expressed in morphogenetically active epithelia. *Dev Dyn,* 208**,** 1-10.

YU, X., SHARMA, K. D., TAKAHASHI, T., IWAMOTO, R. & MEKADA, E. 2002. Ligand-independent dimer formation of epidermal growth factor receptor (EGFR) is a step separable from ligand-induced EGFR signaling. *Mol Biol Cell,* 13**,** 2547-57.

ZHOU, Q. & MELTON, D. A. 2008. Extreme Makeover: Converting One Cell into Another. *Cell Stem Cell,* 3**,** 382-388.

ZHOU, Y., SRINIVASAN, P., RAZAVI, S., SEYMOUR, S., MERANER, P., GUDLUR, A., STATHOPULOS, P. B., IKURA, M., RAO, A. & HOGAN, P. G. 2013. Initial activation of STIM1, the regulator of store-operated calcium entry. *Nat Struct Mol Biol,* 20**,** 973-981.

ZÖLLER, M. 2011. CD44: can a cancer-initiating cell profit from an abundantly expressed molecule? *Nat Rev Cancer,* 11**,** 254-267.

ZYGAR, C. A., COOK, T. L. & GRAINGER, R. M., JR. 1998. Gene activation during early stages of lens induction in Xenopus. *Development,* 125**,** 3509-19.